

**DEVELOPMENT AND EVALUATION OF NOVEL MOLECULARLY
IMPRINTED THIN-FILMS FOR PHENOL AND APPLICATION OF DIRECT
SPECTROSCOPIC DETECTION FOR PETROGENIC CONTAMINANTS
ADSORBED TO MOLECULARLY IMPRINTED FILMS**

by

© Andriy O. Gryshchenko

A dissertation submitted to the

School of Graduate Studies

in partial fulfillment of the requirements for the degree of

Doctor of Philosophy

Department of Chemistry

Faculty of Science

Memorial University of Newfoundland

October, 2014

St. John's, Newfoundland, Canada

ABSTRACT

Phenol and alkylphenols are priority water pollutants from oil extraction, pyrolysis, and industry. The adsorption of phenols is required for the separations in analytical chemistry and industry. Molecularly imprinted polymers (MIPs) are novel adsorbents with the template shaped binding sites. A MIP has to be prepared in film format to be combined with an analytical technique to accomplish rapid and direct detection of phenols and other water pollutants. Films from MIP particles and monolithic films, having 20 and 100 μm thicknesses and bound to a glass slide, were fabricated by UV-initiated radical polymerization between two inert surfaces. The morphology, thickness, and porosity of MIP films were studied by scanning electron microscopy and gravimetric analysis. Porosity was rendered using alcohol-water mixtures as a solvent and, in some instances, polyethyleneglycol and polyvinylacetate as solvent modifiers. Many MIPs for phenol were synthesized through non-covalent imprinting by hydrogen bonding and hydrophobic interactions. The MIP components included functional monomer (itaconic acid, 4-vinylpyridine, and styrene) and solvent, cross-linker (ethylene glycol dimethacrylate, triethylene glycol dimethacrylate, divinylbenzene, pentaerythritol triacrylate—PETA), and template (phenol, xylene). The binding and imprinting properties of the MIPs were assessed based on adsorption capacities and cross-binding towards other phenolics and polycyclic aromatic hydrocarbons (PAHs). A MIP with increased styrene content and xylene along with a copolymer of divinylbenzene and PETA, both acting by hydrophobic interactions, can be recommended for practical applications. The higher content of styrene and/or more hydrophobic monomers such as divinylbenzene increased the binding capacity. The hydrophilicity of PETA rendered water compatibility to the films. The modest imprinting effect is attributed to a tight polymer network formed with PETA as well as xylene as a hydrophobic template. Alcohol-water mixtures promoted the imprinting by hydrophobic interactions and, concurrently, lead to homogeneous, porous, and rigid morphology of the films. Surface enhanced Raman spectroscopy with silver nanoparticles, and fluorimetry, were unsuccessfully attempted for the direct detection of phenol on MIP films because of the low sensitivity and MIP background issues. The direct fluorimetric detection of light PAHs, as another group of pollutants from oil, was shown to be sensitive and selective, when front-face illumination geometry, 100 μm thick films, and synchronous scanning were used.

ACKNOWLEDGEMENTS

I would like to acknowledge a number of people for their support in my graduate studies. First of all, I am grateful to my supervisor, Christina Bottaro, for granting me a position of PhD student, obtaining funds for my scholarship and conferences, creating conditions for my experimental work, guiding me through the complexity of the academic life, helping to improve the quality of my thesis, and trusting me to follow my own approach to complete the research work. I am also thankful to the following people, who gave me their time and attention, in facilitating or even making possible my experimental work. Brent Myron, for teaching me to use the fluorimeter and solve both instrumental and theoretical problems connected with fluorescence spectroscopy. David Thompson, for addressing my numerous questions about solid-phase fluorimetry. Linda Winsor, Liqiu Men, Sandra Estevez, Julie Collins, and other CREAT staff, for training me on how to use research equipment and troubleshooting. Graduate students in our group, M. Pappoe, S. Egli, A. Beaton, K. Burton, E. Butler and others, for sharing and maintaining the laboratory and office space. My supervisory committee, Dr. Travis Fridgen and Yuming Zhao, for their supervision during my study program and the revision of my thesis. I also want to thank professors, who taught me Chemistry courses and raised my science proficiency, P. Pickup, R. Helleur, J. Banoub, and C. Bottaro. Laboratory instructors and teaching fellows, for example, G. Kennedy and K. Devaine, with whom I shared the remarkable experience of teaching assistance. I will always remember Newfoundland, which I called home for almost 5 years. I especially love the very attentive local people, and the picturesque countryside with its many free natural foods.

This research project was undertaken and completed with the financial assistance of Petroleum Research Newfoundland & Labrador, Research and Development Corporation (RDC); Natural Science and Engineering Research Council of Canada (NSERC); School of Graduate Studies at Memorial University of Newfoundland; Atlantic Innovation Fund (AIF) program by Atlantic Canada Opportunities Agency (ACOA).

CO-AUTHORSHIP STATEMENT

The candidate, hereby, declares that he made a major contribution to this thesis in the research and writing phases, in particular, the design of research, experimental work, data analysis, and the preparation of this manuscript. Section 1.2.5 (Chemical analysis of phenol and alkylphenols in waters) includes materials written by the author in the following publication: K. Hawboldt, B. Chen, W. Thanyamanta, S. Egli, A. Gryshchenko. Review of Produced Water Management and Challenges in Harsh/Arctic Environments. Faculty of Engineering and Applied Science of Memorial University of Newfoundland to the American Bureau of Shipping, 2010. 129 p.

Table of Contents

ABSTRACT	ii
ACKNOWLEDGEMENTS	iii
CO-AUTHORSHIP STATEMENT	v
Table of Contents	vi
List of Tables	xi
List of Symbols, Nomenclature or Abbreviations	xvi

Chapter 1. Introduction and Overview

1.1 INTRODUCTION	2
1.2 LITERATURE REVIEW	6
1.2.1 Phenol and alkylphenols as water pollutants	6
1.2.1.1 Physico-chemical properties of phenol and alkylphenols	6
1.2.1.2 Common sources of water contamination with phenols	7
1.2.1.3 Toxicity-related properties of phenol and alkylphenols	10
1.2.2 Synthesis of molecularly imprinted polymers	11
1.2.2.1 The general principle of molecular imprinting	11
1.2.2.2 Approaches to MIP synthesis	13
1.2.2.3 Selection of MIP components	15
1.2.3 Effect of monomer-template interactions on imprinting effect	20
1.2.4 Study of MIP binding properties	22
1.2.4.1 Determination of MIP binding capacity	22
1.2.4.2 Analysis of binding isotherms	25
1.2.4.3 Chromatographic studies of imprinting effect	27
1.2.5 Chemical analysis of petrogenic contaminants in waters	30
1.2.5.1 Common methods of chemical analysis of phenols	30
1.2.5.2 Methods of direct detection of phenols	34
1.2.5.3 Methods of chemical analysis of polycyclic hydrocarbons	39
1.2.6 Research objectives	41
1.3 CONCLUSIONS	41
1.4 REFERENCES	42

Chapter 2. Development of Procedures to Fabricate MIP Films

2.1 INTRODUCTION	52
2.2 MATERIALS AND METHODS.....	56
2.2.1 Precipitation polymerization.....	56
2.2.2 Fabrication of MIP films.....	57
2.2.2.1 The derivatization of glass slides.....	57
2.2.2.2 Sandwich technique.....	58
2.2.2.3 Sandwich technique in a “well”.....	59
2.2.2.4 Sandwich technique to bind MIP particles within a film	59
2.2.2.5 Sandwich technique with the application of a membrane frame.....	60
2.3 RESULTS AND DISCUSSION.....	62
2.3.1 MIP particles by precipitation polymerization	62
2.3.2 MIP film fabrication	63
2.3.2.1 The characterization of sandwich technique	63
2.3.2.2 Sandwich technique to bind MIP particles within a film	66
2.3.2.3 Sandwich technique with the application of a membrane frame.....	67
2.3.3 The morphology of fabricated films	68
2.4 CONCLUSIONS.....	72
2.5 REFERENCES	74

Chapter 3. Study of Functional Monomer-Template Interactions

3.1 INTRODUCTION	78
3.2 MATERIALS AND METHODS.....	81
3.2.1 Raman spectroscopic measurements for liquid samples.....	82
3.2.2 UV-absorbance measurements.....	82
3.3 RESULTS AND DISCUSSIONS.....	83
3.3.1 Study of monomer-template interactions.....	83
3.3.1.1 Raman spectroscopy	83
3.3.1.2 UV-absorbance spectrometry	86
3.4 CONCLUSIONS.....	91
3.5 REFERENCES	92

Chapter 4. Development of Molecularly Imprinted Polymer in Porous Film Format for Binding of Phenol and Alkylphenols from Water

4.1 INTRODUCTION	95
4.2 MATERIALS AND METHODS.....	97
4.2.1 Fabrication of MIP films by sandwich technique	97
4.2.2 Gravimetical analysis of porosity	99
4.2.3 SEM imaging and thickness measurements.....	100
4.2.4 Adsorbate binding studies.....	100
4.3 RESULTS AND DISCUSSION	102
4.3.1 MIP films prepared by sandwich technique.....	102
4.3.2 Choice of monomer and solvent	106
4.3.3 Phenol binding studies in water for MIPs prepared on selected monomers and solvents.....	108
4.3.4 Choice of cross-linker	111
4.3.5 Characterization of styrene/PETA MIP (MIP 5)	114
4.3.5.1 Binding properties study.....	114
4.3.5.2 Cross-binding study.....	117
4.4 CONCLUSIONS AND FUTURE WORK	119
4.5 REFERENCES	121

Chapter 5. Development of MIPs Acting by Hydrophobic Interactions to Bind Phenol

5.1 INTRODUCTION	126
5.2 MATERIALS AND METHODS.....	127
5.2.1 Synthesis of MIPs	128
5.2.2 Study of the binding properties of MIP films	129
5.3 RESULTS AND DISCUSSION	130
5.3.1 Rationale for the choice of components for MIPs and novel adsorbent	130
5.3.2 The physical quality of fabricated films	134
5.3.3 Study of binding and imprinting properties for MIPs imprinted with phenol and xylene	134
5.3.4 Comparison of binding and imprinting properties.....	138
5.4 CONCLUSIONS AND FUTURE WORK	141
5.5 REFERENCES	142

Chapter 6. Application of Surface Enhanced Raman Spectroscopy for Detection of Water Contaminants on Molecularly Imprinted Polymeric Films

6.1 INTRODUCTION	145
6.2 MATERIALS AND METHODS.....	149
6.2.1 Preparation of silver nanoparticles.....	150
6.2.2 Treatment of silver nanoparticles.....	151
6.2.3 Preparation of samples for SERS/Raman measurements	152
6.3 RESULTS AND DISCUSSION	153
6.3.1 The rationale for choice of methods for synthesis and post-treatment of silver nanoparticles.....	153
6.3.2 SERS measurements with a 532 nm laser.....	155
6.3.3 SERS measurements with a 830 nm laser.....	160
6.3.4 MIP as a matrix for SERS detection	166
6.4 CONCLUSIONS AND FUTURE WORK.....	168
6.5 REFERENCES	170

Chapter 7. Application of Fluorimetry for Detection of Water Contaminants on Molecularly Imprinted Polymeric Films

7.1 INTRODUCTION	174
7.2 MATERIALS AND METHODS.....	179
7.2.1 Fluorimetric measurements.....	179
7.2.2 Fabrication of MIP films and analyte adsorption to these films.....	180
7.2.3 Synthesis of coumarin-6-sulfonyl chloride and the derivatization of phenol	182
7.3 RESULTS AND DISCUSSION	183
7.3.1 Illumination geometries to excite fluorescence	183
7.3.2 Effect of MIP composition on the background of fluorescence spectra.....	187
7.3.3 Effect of film thickness.....	189
7.3.4 Comparison of emission and synchronous scan measurement modes.....	190
7.3.5 Fluorescence measurements for different analytes loaded on a MIP film.....	193
7.3.5.1 Phenol	193
7.3.5.2 The derivatization of phenol by coumarin-6-sulfonyl chloride.....	194
7.3.5.3 Caffeine	196
7.3.5.4 Polycyclic aromatic hydrocarbons.....	199
7.4 CONCLUSIONS.....	203
7.5 REFERENCES	204

Chapter 8. Fluorimetric Detection of PAHs on Molecularly Imprinted Polymeric Films

8.1 INTRODUCTION	209
8.2 MATERIALS AND METHODS.....	211
8.2.1 Loading of MIP films with PAHs.....	211
8.2.2 Fluorescence measurement from a MIP film.....	212
8.2.3 Estimation of performances of quantitative detection	214
8.3 RESULTS AND DISCUSSION	215
8.3.1 Comparison of fluorescence measurement modes to identify PAHs in their mixture	215
8.3.1.1 Emission measurement mode	215
8.3.1.2 Synchronous scanning measurement mode.....	219
8.3.2 Preliminary characterization of quantitative fluorimetric detection	221
8.4 CONCLUSIONS.....	225
8.5 REFERENCES	226
Chapter 9. Conclusions and Future Work	227

Appendices

APPENDIX A. Procedures to Determine Adsorption Capacities of MIPs to bind Phenol.....	238
APPENDIX B. Supporting Information for Chapter 4.....	250
APPENDIX C. Electrospray Ionization of Phenol facilitated with Basic Reagents.....	254
APPENDIX D. Attempts for Direct Detection of Phenol on MIP Films using Colorimetry, Resonance Raman Spectroscopy, and Matrix-Assisted Laser Desorption/Ionization-Mass Spectrometry.....	259

List of Tables

Table 1-1. Physical, acidic, and hydrophobic properties of phenol and alkylphenols.....	7
Table 1-2. Imprinting factors achieved by MIPs for different phenols	21
Table 1-3. Main attributes of Langmuir, Freundlich, and Langmuir-Freundlich isotherm binding models	26
Table 2-1. Visual characterization of selected films prepared by sandwich technique	71
Table 4-1. Composition of MIP prepolymerization mixtures.....	98
Table 4-2. Elution and UV-detection conditions for chromatographic analysis of phenols.....	102
Table 4-3. Thickness (by SEM) and porosity (gravimetric method) of films fabricated by sandwich technique.	105
Table 4-4. Imprinting factors for MIP formulations prepared on different monomers. ...	108
Table 4-5. Data for binding isotherms for MIP/NIP 5 (PETA) at low phenol concentrations (0.1 – 40 mg L ⁻¹).....	115
Table 4-6. Parameters for fitting to Freundlich isotherm model and calculated binding parameters.....	117
Table 5-1. Composition of prepolymerization mixtures for phenol and xylene imprinted polymers, and novel adsorbent based on divinylbenzene and PETA.	129
Table 6-1. Measurement and experimental parameters to obtain data for Chapter 6.	153
Table 7-1. Measurement and experimental parameters to obtain data for Chapter 7.	181
Table 8-1. Estimation of fluorimetric quantitative detection of PAHs on MIP films in the synchronous scanning mode.....	224

List of Figures

Figure 1-1. The general scheme of MIP synthesis.....	13
Figure 1-2. Examples of functional monomers, cross-linkers, and initiators	16
Figure 1-3. The derivatization of phenol with N,O-bis(trimethylsilyl) trifluoroacetamide for GC-MS analysis	31
Figure 1-4. The derivatization of phenol with 4-aminoantipyrine for colorimetric detection	33
Figure 2-1. The general scheme of fabrication of MIP films by sandwich technique.....	59
Figure 2-2. Application of sandwich technique to produce ~100 μm thick MIP film by means of a membrane frame.	61
Figure 2-3. Photo pictures for the main steps to prepare MIP films by sandwich technique	63
Figure 3-1. Raman spectra (532 nm) measured for methanol/water (4:1) as solvent, and solutions of styrene, phenol, and phenol and styrene (1:1).	85
Figure 3-2. UV-absorbance spectrum of phenol (0.5 mM) in MeOH:H ₂ O (4:1).	87
Figure 3-3. Effect of styrene on E2-band of phenol in MeOH:H ₂ O (4:1); phenol concentration – 0.100 mM; styrene concentrations: 0; 0.100; 0.200; 0.400 mM.....	88
Figure 3-4. Effect of itaconic acid on E2-band of phenol in MeOH/H ₂ O (4:1); phenol concentration – 0.100 mM; itaconic acid concentrations: 0; 0.400; 0.800 mM.....	89

Figure 4-1. Top-down SEM images of MIP cross-sections.....	103
Figure 4-2. Structures of cross-linkers used in Chapter 4.....	112
Figure 4-3. Binding isotherms for Sty-based MIP/NIP on different cross-linkers: EGDMA, TEGDMA, and PETA from 15 to 300 mg L ⁻¹ phenol in water...113	113
Figure 4-4. Phenol adsorption isotherms for MIP 5 and NIP in Log-Log format and fitting to Freundlich isotherm binding model	116
Figure 4-5. Cross-binding of MIP 5 and NIP towards other phenols and 3-octanone.....	119
Figure 5-1. Comparison of binding capacities and imprinting factors for MIPs 5, 7 and 8 at three phenol concentrations: 0.500, 15.00, 300.0 mg L ⁻¹	135
Figure 5-2. Cross-binding of polymer imprinted with xylene (MIP 8) towards phenol, naphthalene, fluorene, phenanthrene, and anthracene.	138
Figure 5-3. Comparison of phenol binding capacities and imprinting effects at C _i (phenol)=15.00 mg L ⁻¹ for MIPs/NIPs studied in Chapters 4 and 5.	139
Figure 6-1. SERS spectra (532 nm laser) of Rhodamine 6G adsorbed on silver nanostars and nanospheres.	156
Figure 6-2. SERS spectra (532 nm laser) of phenol on nanostars.	158
Figure 6-3. Raman and SERS spectra of L-phenylalanine; 2,4,6-trimethylphenol; dibenzothiophene (~100 µg each) loaded on silica..	161
Figure 6-4. Raman and SERS spectra of dibenzothiophene (~1.33 µg) loaded on silica.....	164
Figure 6-5. Raman spectra for MIP matrices based on EGDMA and different monomers: itaconic acid; styrene; 4-vinylpyridine; scans with 830 nm and 532 nm lasers.....	167

Figure 7-1. Reactions for synthesis of coumarin-6-sulfonyl chloride and derivatization of phenol.....	183
Figure 7-2. Back-surface and front-face illumination geometries to excite fluorescence from a polymeric film bound to the quartz slide.....	184
Figure 7-3. Effect of back-surface and front-face illumination geometries on emission spectrum ($\lambda_{\text{ex}}=298$ nm) of phenanthrene adsorbed on the MIP film.....	186
Figure 7-4. Background of fluorescence spectra ($\lambda_{\text{ex}}=270$ nm) originated from MIP matrices based on EGDMA and styrene; no monomer; methacrylic acid; and 4-vinylpyridine.	188
Figure 7-5. Emission ($\lambda_{\text{ex}}=298$ nm) and synchronous scan ($\Delta\lambda=63$ nm) spectra of phenanthrene adsorbed from $400 \mu\text{g L}^{-1}$ solution on the MIP film.	191
Figure 7-6. Emission spectrum of phenol ($\lambda_{\text{ex}}=269$ nm) adsorbed on the MIP film	193
Figure 7-7. Emission ($\lambda_{\text{ex}}=360$ nm) and synchronous scan ($\Delta\lambda=100$ nm) spectra of phenol tagged with coumarin-6-sulfonyl chloride	195
Figure 7-8. Excitation ($\lambda_{\text{em}}=391$ nm), emission ($\lambda_{\text{ex}}=275$ nm), and synchronous scan ($\Delta\lambda=53$ nm) spectra of caffeine adsorbed on the MIP film	198
Figure 7-9. Emission ($\lambda_{\text{ex}}=270$ nm) and synchronous scan ($\Delta\lambda=50$ nm) spectra of naphthalene adsorbed on the MIP film.	200
Figure 7-10. Excitation ($\lambda_{\text{em}}=361$ nm), emission ($\lambda_{\text{ex}}=298$ nm), and synchronous scan ($\Delta\lambda=63$ nm) spectra of phenanthrene adsorbed on the MIP film.	201
Figure 7-11. Function of fluorescence intensity from phenanthrene concentration in solutions for loading MIP films. The fluorescence was detected in synchronous scanning mode ($\Delta\lambda=63$ nm).....	202

Figure 8-1. Experimental set-up for front-face illumination of MIP films to excite fluorescence.....	213
Figure 8-2. Excitation and emission spectra of naphthalene, phenanthrene, fluorene, and anthracene individually loaded on the MIP film.	217
Figure 8-3. Emission spectra for the mixture of naphthalene, phenanthrene, fluorene, and anthracene loaded on the MIP film at $\lambda_{ex} = 290$ nm and $\lambda_{ex} = 358$ nm.	218
Figure 8-4. Synchronous scan spectra at different $\Delta\lambda$ for individual PAHs and their mixture loaded on the MIP films	220
Figure 8-5. Function of fluorescence intensity (A) from phenanthrene concentration in solutions for loading MIP films and Log-Log plot of this function (B). Fluorescence was detected in synchronous scanning mode ($\Delta\lambda=69$ nm).	222

List of Symbols, Nomenclature or Abbreviations

- a.u. – arbitrary units
- BTEX – benzene, toluene, ethylbenzene, and xylenes
- 2,4-DM – 2,4-dimethylphenol
- 3-oct – octanone
- 4-MP – methylphenol
- 4-PP – 4-propylphenol
- 4-VP – 4-vinylpyridine
- ACS – American Chemical Society
- AIBN – azobisisobutyronitrile
- Ant – anthracene
- BET – Brunauer-Emmett-Teller
- BSTFA – N,O-bis(trimethylsilyl) trifluoroacetamide
- C18 – octadecyl
- C – concentration
- C_i – initial concentration (before adsorption)
- C_f – final concentration (after adsorption)
- DESI – desorption electrospray ionization
- DMF – dimethylformamide
- DMPA – 2,2-dimethoxy-2-phenylacetophenone
- DMSO – dimethyl sulfoxide
- DVB – divinylbenzene
- EGDMA – ethyleneglycol dimethacrylate
- EG – ethylene glycol
- EPA US – United States Environmental Protection Agency
- ESI – electrospray ionization
- EVB – ethylvinylbenzenes
- f – degree of freedom
- FI – Freundlich isotherm
- Flu – fluorene

GC – gas chromatography
HPLC – high-performance liquid chromatography
IA – itaconic acid
IF – imprinting factor
IR – infrared
K – affinity constant
LC – liquid chromatography
LoD – the limit of detection
Log P_{ow} – the octanol-water partition coefficient
LoQ – the limit of quantitation
MALDI – matrix assisted laser desorption ionization
MeOH – methanol
MIP – molecularly imprinted polymers
MSD – mass detector
MS – mass spectrometry
Mw – molecular weight
N.A. – not available
Naph – naphthalene
NIP – non-imprinted polymer
NIR – near infra-red
NMR – nuclear magnetic resonance
n – the number of parallel measurements
NPD – naphthalene, phenanthrene, and dibenzothiophene
PEG – polyethylene glycol
PETA – pentaerythritol triacrylate
Phe – phenanthrene
ph-1 – phenol
PrOH – 1-propanol
PVA – polyvinyl acetate
Q – adsorption (binding) capacity
 R^2 – the coefficient of determination for linear regression

res-1 – resorcinol
RPD – relative percentage difference
RRS – resonance Raman scattering
rpm – rotation per minute
SD – standard deviation
SERRS – surface-enhanced resonance Raman scattering
SERS – surface enhanced Raman spectroscopy or scattering
SIM – selected ion monitoring mode
SPR – surface-plasmon resonance
 S_r – the coefficient of variance, or relative standard deviation
Sty – styrene
TEA – triethylamine
TEGDMA – triethyleneglycol dimethacrylate
TLC – thin-layer chromatography
TMAH – tetramethylammonium hydroxide
TMP – 2,4,6-trimethylphenol
TRIM – trimethylolpropane trimethacrylate
UV – ultraviolet
UV-Vis – ultraviolet and visible
w/w, % – weight percentage
v/v, % – volume percentage
WC – water compatibility
xyl – xylene
 $\Delta\lambda$ – the spacing for synchronous scan
 λ_{em} – emission wavelength
 λ_{ex} – excitation wavelength

Chapter 1. Introduction and Overview

1.1 Introduction

Phenol and alkylphenols are water contaminants from oil and the waste products from oil treatment and extraction, particularly, produced water [1]. Phenol and alkylphenols (cresols, xylenols, and propylphenols) occur together with aromatic hydrocarbons, PAHs, and thiophenes. Produced water is the oil-contaminated water that is pumped into a well to allow for oil extraction. The discharge of produced water presents an environmental concern for Newfoundland, where offshore oil production is immense [2, 3]. In addition to oil extraction, other sources of phenol and alkylphenols are wood and coal pyrolysis, industrial organic synthesis, and the degradation of pesticides [4]. Phenol and 2,4-dimethylphenol are considered as priority water pollutants [5] because they are abundant and toxic. Phenol changes the smell and taste of water and fish; phenol is chronically toxic; and it is the precursor of chlorophenol that can be formed during the chlorination of water [6, 7]. The Canadian Council of Ministers of the Environment sets $4.0 \mu\text{g L}^{-1}$ of the total of mono- and dihydroxy phenols as the safe level for aquatic biota [8]. Thus, there is a need for monitoring the level of phenol and alkylphenols in environmental waters and produced water [3, 9, 10].

For the monitoring of water contaminants, including phenols, analytical systems and sensors have to be applied. An essential part of many devices is a layer of adsorbent required to separate and preconcentrate an analyte from water [11]. For this purpose, traditional adsorbents, such as octadecyl silica and divinylbenzene-styrene based resins, are used [12, 13]. Alternatively, a novel synthetic material that is designed for the adsorption of specific targets can be used to give the advantage of uptake selectivity and

high binding capacity. This binding medium can be a molecularly imprinted polymer [9]. The term “molecularly imprinted” means that the polymer bears binding sites of particular molecular size that can accommodate certain molecules. In addition to their application in analytical chemistry, MIPs can be used in industrial separations, e.g., for the cleanup of waters and in the food industry [14-17].

A MIP, in the same way as any other polymeric material, can be prepared in a variety of physical forms such as monolith, particles, beads, films, and immobilized layers [18]. A MIP often has to be prepared in film format to be used in sensors, microfluidics, and some analytical testing systems [19-22]. Direct detection from a MIP film immobilized on a substrate provides the following benefits: the convenience of handling the film during the analysis; the preconcentration and separation of an analyte; the circumvention of extraction with a solvent and extract manipulation; the possibility to adapt this detection design for on-line sensing [20, 22].

Many studies about MIPs for phenols have been published. However, the majority of the publications address MIPs for chlorophenols [16, 23], nitrophenols [24-26], dioxhydroxyphenols [20], and bisphenol A [27], and only a few papers are about MIPs for phenol [21, 28, 29], 2,4-dimethylphenol [30], and nonylphenol [31]. In a survey of the works MIPs for phenol- and alkylphenols, a number of limitations can be identified. Very often a MIP of only one composition was studied [29, 32]. When a group of MIPs of different composition was screened, all of them targeted the phenolic compound only by hydrogen bonding, e.g., with functionalities of itaconic acid [21] and 4-vinylpyridine [30], not considering other types of interactions, e.g., hydrophobic and metal-coordination. In

the majority of the publications about MIPs for phenol and alkylphenols [28, 30, 31], the selectivity and binding parameters were evaluated using chromatographic studies in an organic solvent, which is very different from static adsorption in water, which takes place in practice. The selectivity for phenol is likely be much better in organic solvents than in pure water, since recognition through hydrogen bonding is suppressed in water. Sergeyeva et al. [21] only presented the intensity of the MIP-bound dye as detected by densitometry for the evaluation of phenol binding. The detector output cannot be used for the comparison with phenol binding parameters in other works. Some binding experiments [21] were completed at the non-equilibrium condition, which gives different parameters of binding and selectivity than in the equilibrium condition. The fact that the selectivity and binding parameters have been estimated by different approaches makes it difficult to make head-to-head comparisons of the data [33] presented separately in their respective papers. Therefore, it is difficult to compile the whole picture about MIPs for phenols in terms of factors determining the imprinting and binding properties, and more comprehensive, systematic and unified research is required. In addition, in only one work, a MIP for phenol has been prepared as a membrane [21]. Most of the MIPs have been prepared as polymeric particles by grinding a monolith [28, 30, 31], which is now considered outdated and imperfect [18].

Sensors for the direct detection of phenol in water have been constructed based on electrochemical enzymatic facilitated detection [34, 35] and surface enhanced Raman spectroscopic detection with electrochemical preconcentration [36]. With the use of a MIP, only one analytical test system by colorimetric detection with the 4-aminoantipyrine

derivatization of phenol has been designed [21]. Thus, a niche in the analytical systems for phenol and alkylphenols with the use of MIPs in sensors is open for the development.

In this research project, procedures to fabricate MIP films were formulated and the factors influencing the fabrication processes were investigated and discussed (Chapter 2). The morphology of the films in terms of their structure and porosity was studied with scanning electron microscopy and gravimetric analysis (Chapter 4). A number of MIPs for phenol were synthesized through non-covalent imprinting [37] to accomplish binding of phenol through hydrogen bonding or hydrophobic interactions. The choice of the functional monomers and solvents, as the MIP components, was guided by the need to facilitate the interactions between functional monomers and templates (phenol or xylene). Some of the interactions were studied with UV absorbance and Raman spectroscopies (Chapter 3). Methodology was developed to determine MIP adsorption capacities towards phenol and other phenolics in aqueous solutions. The adsorption capacities can be considered as fundamental and reproducible parameters of phenol binding [33]. The binding and imprinting properties were assessed based on the analysis of a set of adsorption capacities, adsorption isotherms, and the MIP cross-binding studied towards other phenolics and PAHs. In the first round of tests of different MIP compositions (Chapter 4), the effect of functional monomers (itaconic acid, 4-vinylpyridine, and styrene) was studied. The properties of MIPs based on styrene, that act by hydrophobic interactions, were further modified by the variation of a cross-linker. In the second round of experiments (Chapter 5), other formulations of MIPs acting by hydrophobic interactions were tested in order to enhance MIP binding capacity, and efforts were made

to adapt the MIPs for the practical applications. Various analytical techniques were attempted for the direct detection of phenol on MIP films. Special attention was given to surface enhanced Raman spectroscopic (SERS) detection, where a suspension of silver nanoparticles was deposited on the MIP film after phenol adsorption (Chapter 6). Fluorimetric detection was tested for phenol with and without derivatization reaction (Chapter 7). Because the detection of phenol with SERS and fluorimetry was problematic, it was decided to detect light PAHs with fluorimetry. The study of the factors influencing the fluorimetric measurements on MIP films, described in Chapter 7, was applied to establish the conditions of the direct detection of light PAHs (Chapter 8).

1.2 Literature review

1.2.1 Phenol and alkylphenols as water pollutants

1.2.1.1 Physico-chemical properties of phenol and alkylphenols

Phenol is the simplest of phenols, where a hydroxyl group is directly attached to a benzene ring. Phenol and its simple alkyl derivatives such as cresols, xylenols, propyl and butyl-phenols are weakly acidic with a pK_a over 10 (Table 1-1). Phenols are present in their unionized forms in the majority of natural waters, including sea water (pH ~8). Phenol, cresols, and xylenols can be considered moderately hydrophobic and noticeably soluble in water. According to $\text{Log } K_{ow}$ values, the hydrophobicity of phenols rises dramatically with the increase of carbon content. Phenols with higher carbon content, such as C6-C9 phenols, are barely soluble in water. This is important for the estimation of the occurrence of C6-C9 phenols in the natural water environment; they mostly partition

in oil drops, e.g., at oil spill, or organic sediments, which diminishes the content of these phenols in water. Phenols, especially those of a lower molecular weight, are volatile with a strong, unpleasant, and very specific smell that is usually described as “phenolic”. Phenols occur not only in water, but also in the atmosphere; therefore they are considered as air pollutants.

Table 1-1. Physical, acidic, and hydrophobic properties of phenol and alkylphenols

	Mw, g mol ⁻¹	Boiling T, °C	pK _a	Log K _{ow}	Solubility in water at 20 – 25 °C, g per 100 g
phenol	94.1	182	9.99	1.48	8.3
4-methylphenol	108.1	202	10.26	1.98	1.9
2,4-dimethylphenol	122.2	212	10.45	2.35	0.8
4-propylphenol	136.2	232		3.20	0.13
butylphenols	150.2	~237	~10.6	~3.7	
nonylphenols	220.4	~295	~10.7		~5·10 ⁻⁴

Note: K_{ow} – octanol-water partition coefficient. Sources of the data are on-line directories [38, 39] and the Material Safety Data Sheets.

1.2.1.2 Common sources of water contamination with phenols

Benzene and phenolic moieties are some of the most widespread building blocks in organic matter of both natural and industrial origin, e.g., oil, coal, lignin, humic acids, pesticides, and dyes. It is possible to expect that processing and oxidation of these materials will yield compounds such as phenol and alkylphenols. Phenol is formed as a result of many natural processes: the decomposition of organic matter including the petrogenic formation of oil; chemical processes in the atmosphere, biosynthesis in plants;

and human metabolism [4]. However, it is not natural processes but human economic activities that are responsible for phenols classified as Priority Pollutants by United States Environmental Protection Agency [5]. The list includes phenol, chloro- and nitrophenols, and 2,4-dimethylphenol as a representative of alkylphenols.

Phenols are released during industrial organic synthesis where they are reagents or products, for example: the production of phenol formaldehyde resins; *p*-nitrophenol as a pesticide; phenolic drugs and dyes; 2,4,6-trinitrophenol (picric acid) as an explosive; and aniline. However, anthropogenic sources are not limited to the chemical industry. Other industries, whose waste waters contain phenols, are oil extraction and processing, coal and wood pyrolysis, and paper milling. Phenols are discharged into the environment when organic matter is not completely burnt, e.g., within vehicle exhaust and tobacco smoke. Another source of phenols is household sewage because many household products contain phenols such as disinfectants, e.g., “lysol” (potassium soap with cresols), and bathing lotions. Phenols can be formed during the degradation of surfactants and pesticides, e.g., nonylphenols from alkylphenol ethoxylates, and 2-methylphenol from 4-chloro-2-methylphenoxyacetic acid, respectively. Phenol has been detected in ground waters under landfill sites; phenol leaks from asphalt, which is based on coal tar, and wood, which is treated with creosote as a preservative; smoked meat can contain up to 70 mg kg⁻¹ of phenol in its outer layer [4, 40].

In pristine surface and ground waters, the concentration of phenol is usually 1 µg L⁻¹ or less while the phenol concentration is approximately 100 µg L⁻¹ in many other environmental waters [40] exceeding the safe level of 4.0 µg L⁻¹ for aquatic life. In

Quebec (Canada), where many textile and wood processing plants were located, drinking water contained on average 0.02 – 2.8, and up to 43 $\mu\text{g L}^{-1}$, of alkylphenols [4].

Environmental issues connected with oil extraction are of special interest to Dr. Christina Bottaro group in Memorial University, which is located in Newfoundland (Canada). In Newfoundland, there are many off-shore oil rigs: Hibernia, Terra Nova, and White Rose. They produce 300,000 barrels of crude oil per day, or 12 percent of the total oil produced in Canada [2]. The content of phenols in crude oil can be up to 7000 mg kg^{-1} . The oil extraction process is based on pumping water into an oil well, which causes the discharge of oil-contaminated water, termed as “produced water”. The volume of produced water discharged into the ocean or inland waters is immense and is in excess of the volume of extracted oil in ratios of 2:1, 5:1, or even 50:1 for older wells. Produced water contains both dispersed oil drops and dissolved oil components. Thus, in places where oil extraction is extensive, it is possible to observe an increased level of phenols.

The content of water-soluble phenols in produced water can reach up to 20 mg L^{-1} , while monoaromatic hydrocarbons, e.g., benzene, toluene, ethylbenzene, and xylenes (BTEX) constitute 24 mg L^{-1} ; two and three ring polycyclic hydrocarbons (PAHs), especially “NPD” group (naphthalene, phenanthrene, and dibenzothiophene) can make up 10 mg L^{-1} . The concentration of other PAHs does not usually exceed 0.13 mg L^{-1} [1]. Hence, phenols constitute one of the important groups of contaminants that originate from oil. In the group of phenols, phenol and cresols constitute the most (each about 40% of all phenolics), xyleneols make up 15%. Following this, the content of phenols continues to

decrease with the degree of alkylation, for example, 3% for C3-phenol, and C6–C9 phenols are rarely detected because they mostly partition into oil drops present in produced water [6].

1.2.1.3 Toxicity-related properties of phenol and alkylphenols

The class of phenols includes many phenol derivatives such as alkylated, halogenated, nitrated, and dihydroxy phenols. Among the variety of phenols, halogenated and nitrated phenols are probably the most toxic and persistent [4]. However, phenol and alkylphenols are the focus of this project because they are more common water pollutants from the oil extraction processes. Phenol and alkylphenols are not considered to be persistent on the long-term in the natural water environment; they readily deplete through oxidation, photo-sensitized oxidation, biodegradation, and slightly by evaporation [3, 8]. In environmental waters, photo-oxidation and biodegradation are mostly responsible for the elimination of phenols. It takes 28 days for phenol and alkylphenols to be completely degraded by bacteria in produced water [3]. The persistence of phenols to oxygen that is present in water increases with the degree of alkylation. For example, in slightly alkaline water (pH 9.0) at room temperature, the oxidation half-life for phenol is 12 days and, for comparison, the half-life is 462 days for *o*-cresol [8].

When the degree of alkylation rises, the extent of accumulation of phenols in lipophilic tissues grows and, therefore, the toxicity of phenols also increases. The levels of *p*-cresol, C2–C3, C4–C5, C6–C8 phenols that led to chronic disorders in fish in terms of reproduction, were 1000, 100, 18, and 1.6 $\mu\text{g L}^{-1}$, respectively [8]. It should be noted

that each set of data was obtained under different experimental conditions, so that care must be taken when they are directly compared. Phenol and C1–C3 phenols do not accumulate in fish tissues to a significant extent. These phenols act as non-specific toxicants through hydrophobic partitioning and radical reactions [4, 6]. Phenols with a longer alkyl chain, e.g., C4–C5, accumulate to a much more significant degree in fish tissue and, in addition, they act as estrogen mimics, which can affect the sexual development of fish. The exposure of premature cod to $20 \mu\text{g L}^{-1}$ of phenol and alkylphenols for 5 weeks caused a delay in spawning and defects in testes of cod [3]. Because of the effect on amphibian reproduction, the Canadian Environmental Council established the limit of $4.0 \mu\text{g L}^{-1}$ total of monohydroxy phenols (phenol, cresols, and xylenols) and dihydroxy phenols (catechol, resorcinol, and hydroquinone) as the safe level for aquatic life [8]. Despite the fact that United States Environmental Protection Agency [41] states that 2 mg L^{-1} of phenol in drinking water can be considered safe, the control of phenol concentration in water becomes much more stringent when the water is to be chlorinated for domestic use. Formed chlorinated phenols are much more toxic and spoil water taste to an even greater extent than their precursor, phenol [7].

1.2.2 Synthesis of molecularly imprinted polymers

1.2.2.1 The general principle of molecular imprinting

The first, or at least one of, the very earliest academic papers about molecularly imprinted polymers (MIPs) used to separate racemates was published by Wulff in 1973. MIPs were presented as new affinity materials based on organic polymer networks for

selective recognition, as alternatives to natural antibodies [42]. Starting from a single work in the 1970s, the field of molecular imprinting has rapidly developed into a broad discipline of MIP technologies, which are practically employed for separations in analytical chemistry, catalysis, medicine, and industry, including water purification [15, 43]. It is interesting to note that to describe this separation phenomenon, a term “host-guest polymerization” was used initially, and the term “molecularly imprinted polymer” was adopted only since 1993 [42, 44].

A MIP is a synthetic material with template-shaped vacant sites of molecular size, which can bind molecules similar to the template in terms of structure, shape and/or functional groups [42, 44]. The nature of MIPs can be understood from the general process of MIP synthesis [37, 43, 44] (Figure 1-1). The first step is the association of a template and functional monomers. It can be achieved through covalent bonding or weak and reversible interactions: ion pairing, metal coordination, hydrogen bonding, and van der Waals interactions, including π - π stacking. Following this, the polymerization of the monomers bound to the template with an excess of a cross-linker yields a solid polymer network with monomers grouped around the template. The cross-linker is a monomer with two to four polymerizable groups, whose purpose is to form a rigid polymer network, which hosts binding sites. The removal of the template is completed through the cleavage of covalent bonds or the disruption of weak interactions between monomers and template. The removal results in a template imprinted binding site, which can uptake the template or a structurally and functionally similar molecule with the same bonding and in the same steric configuration that existed in the monomer-template assembly [44].

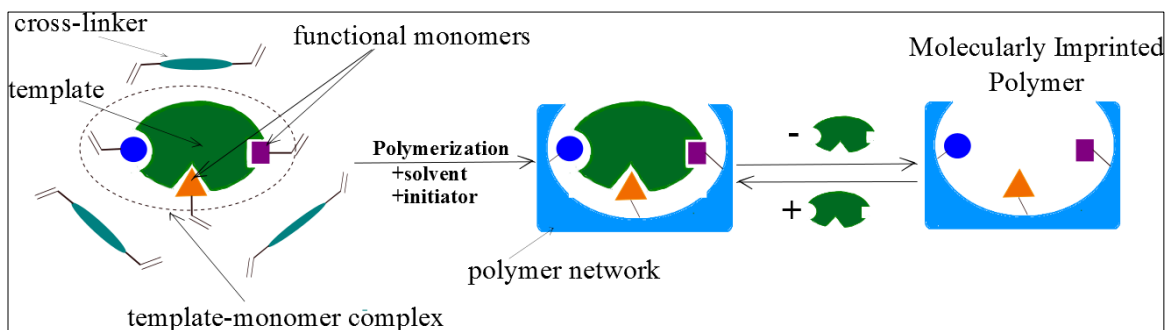


Figure 1-1. The general scheme of MIP synthesis

Not every polymer that is prepared with the intention to be a MIP will exhibit a so called “imprinting effect” [45]. The imprinting effect is the outcome of the formation of binding sites, which results in the enhanced binding properties and selectivity. In practice, the selectivity is observed as the ability to bind a template in the presence of other species, which is assessed using MIP cross-binding studies. For the assessment of the imprinting effect, MIP binding properties, e.g., a binding capacity and association constant, are compared against a control material. The control material is normally a non-imprinted polymer (NIP), which is prepared as a MIP from the same components but without template. Another control material is a MIP imprinted with a compound structurally different to the primary template or a chiral isomer to template [46].

1.2.2.2 Approaches to MIP synthesis

An approach to MIP synthesis, where template and monomers are bound covalently both at the self-assembly and at rebinding experiments, is covalent imprinting. When the self-assembly leads to formation of a covalent bond, but the template is rebound via weak interactions, this is termed semi-covalent imprinting. The non-covalent approach implies

weak interactions are exploited both at the formation of the self-assembled complex and, then, at template rebinding [44]. The first paper about MIPs acting through non-covalent interactions was published by Mosbach et al. in 1981[47].

Use of the non-covalent approach is most widespread, and this approach was applied in this research project. Compared to the covalent and semi-covalent approaches, the non-covalent approach does not require complex and tedious synthesis of a monomer-template adduct before polymerization; simple mixing of MIP components is sufficient. After the polymerization a template can be simply removed by extraction with an organic solvent, which breaks the weak interactions and dissolves the template. Also, imprinting via weak interactions is highly universal; many molecules can be targeted by commercially available monomers through hydrogen bonding and other types of interactions such as ion pairing. The fact that both the template removal and rebinding are reversible allows reusing MIPs [48].

However, the non-covalent approach has limitations. The complexation between monomers and a template is flexible but rarely strong. This explains the fact that after the polymerization a variety of differently organized binding sites are formed. The non-uniform structure of binding sites is observed in rebinding studies as some range of association constants, or binding heterogeneity and as a wide cross-binding towards other species that are structurally or functionally similar to the template. Monomer-template complexes are disrupted during the polymerization, leaving a significant amount of a functional monomer spread in a polymer network outside binding sites, which contributes to non-specific binding with low affinity [37, 44]. A careful selection of MIP components

helps to prepare MIPs with stronger binding, having a reduction in previously described drawbacks.

A MIP polymer network can be formed via a polycondensation reaction, as for MIPs based on polyurethane [49] and silicone xerogel [50], or via vinyl polymerization [43]. The latter kind of polymerization is the most universal, mainly because the wide variety of monomers is commercially available. Also, many methods have been developed to prepare vinyl-MIPs in different physical forms: microparticles, beads, and porous films. Vinyl polymerization was chosen for this research project and will be discussed further.

1.2.2.3 Selection of MIP components

In this section, the choice of components for MIP syntheses by the non-covalent approach is described in general terms. These components are template, functional monomer, solvent, cross-linker, and polymerization initiator (Figure 1-2).

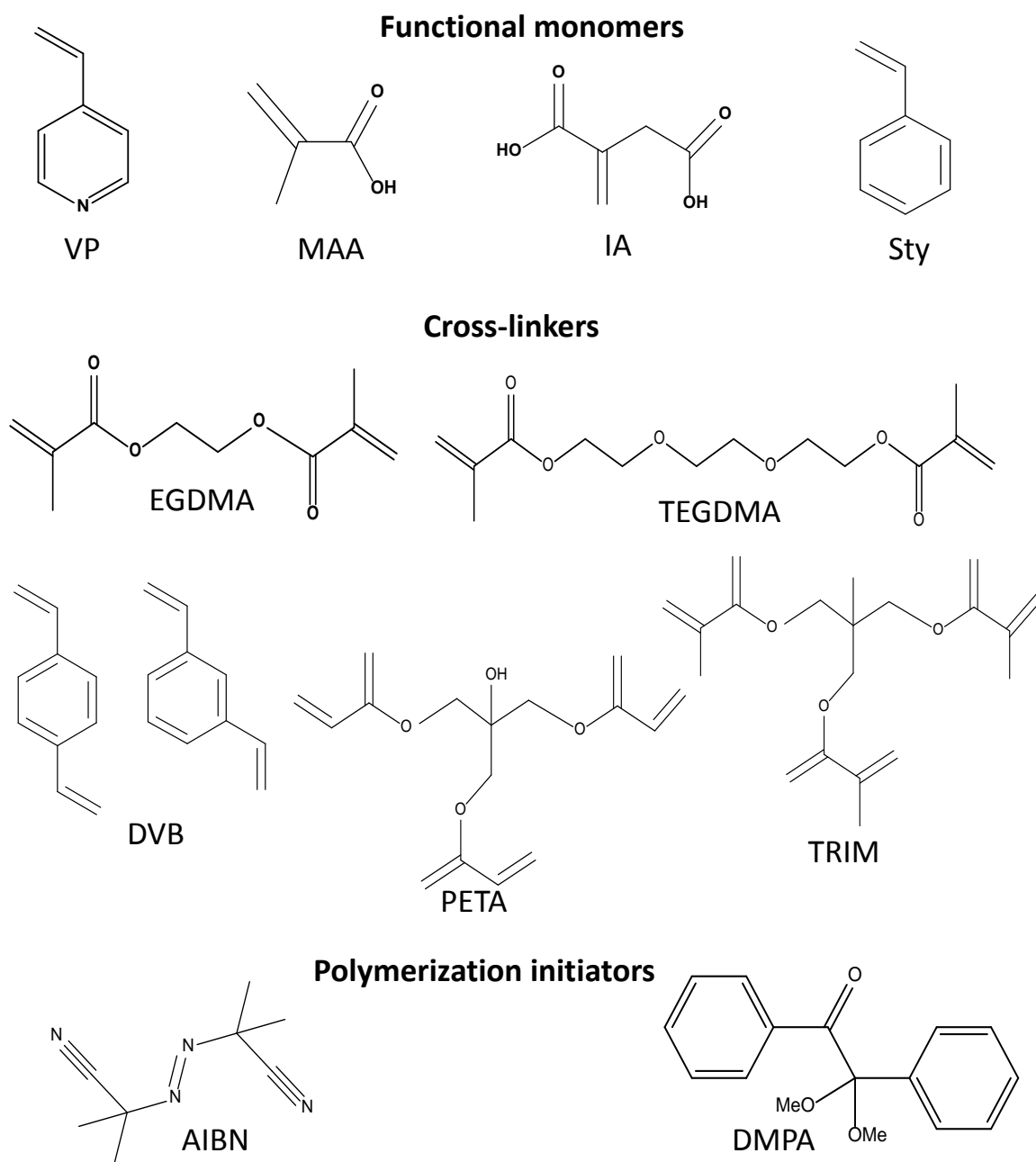


Figure 1-2. Examples of functional monomers, cross-linkers, and initiators.1

Note: VP – 4-vinylpyridine; MAA – methacrylic acid; IA – itaconic acid; Sty – styrene; EGDMA – ethyleneglycol dimethacrylate; TEGDMA – triethyleneglycol dimethacrylate; DVB – m- and p-divinylbenzenes; PETA – pentaerythritol triacrylate; TRIM – trimethylolpropane trimethacrylate; AIBN – azobisisobutyronitrile; DMPA – 2,2-dimethoxy-2-phenylacetophenone.

Template

In most cases the removal of a template following polymerization is not complete; some remains incorporated into the MIP network. When this MIP is used for the preconcentration of analyte in trace chemical analysis, e.g., for solid phase extraction, the residual amount of the template can be responsible for the blank value not to be equal to zero; this is called template bleeding [15, 44]. Therefore, a template is very often chosen to be different from an analyte. This pseudo-template can be a similar compound with a slightly different structure and/or functionalities or be an isotopically labeled analogue. The pseudo-template must be selected so that the corresponding pseudo-MIP is still able to recognize the targeted analyte by recognition cross-binding inherent to the MIP [44].

Functional monomer

A functional monomer is selected based on its ability to bind with a template through weak and reversible interactions. The most efficient and specific non-covalent imprinting is achieved through hydrogen bonding [44]. This kind of bonding is always exploited when a template molecule has a functional group, which can accept or donate protons: -COOH, -COO⁻, -CN, -NO₂, -N=, -Cl, -NH₂, -OH, -SH [37]. Methacrylic acid and 4-vinylpyridine (Figure 1-1) are probably the most universal monomers because they can form hydrogen bonds with many template molecules [37, 44]. The most common molar ratio of a functional monomer to template is 4:1 [22, 28, 30], which is usually enough to “wrap” a template in the polymer network. This ratio can be lower to shift the monomer-template equilibrium to achieve a higher yield of the prepolymerization complex [51].

Solvent

A solvent must be able to dissolve MIP components [44]. For example, 4-vinylpyridine and EGDMA are not soluble in each other, but their mixture in methanol/water is homogeneous. Another reason to use a solvent is to render porosity to the final polymer network. Otherwise, without a solvent, the polymer network would be dense, having low permeability to water or other solvents. Because of its role in creating the porosity of the final polymer, the solvent is also called the “porogen” [48, 50]. A solvent constitutes about half volume, or even more, of a final MIP prepolymerization mixture, therefore it is always an environment for the monomer-template interactions. Thus, another point to consider at the selection of the solvent is that it has to facilitate or at least not to disrupt these interactions [37, 43, 44]. For example, in the case of hydrogen bonding, solvents of low polarity such as toluene and chloroform should be chosen [44, 48]. To facilitate hydrophobic interactions, highly polar and protic solvents such as methanol, methanol/water, and water are preferred. Another factor to take into account in the selection of a solvent is that a stronger imprinting effect is often observed when a solvent used in MIP synthesis and in the template rebinding experiments are the same, or at least similar, in terms of their chemical nature and polarity. For example, when a MIP was prepared with acetonitrile, chromatographic studies showed a higher retention factor for the template when a mobile phase also contained acetonitrile [45]. Although this principle of similarity is a rule of thumb that is often considered in the choice of MIP components, the reasons for this phenomenon have not been clearly elucidated. Probably, in this case the imprinting effect is benefited by the similarity of solvent related

conditions for MIP synthesis and template rebinding in terms of developed monomer-template interactions, solvation and microswelling of polymer network [44].

Cross-linker

A cross-linker constitutes the framework of a polymer network, which carries binding sites. This is the most abundant MIP component, making up over 80% of polymer mass. A cross-linker is a monomer with two, three, or four vinyl groups per molecule (Figure 1-2), so that the cross-linker is called two, three, or four-functional, respectively. Cross-linker moieties build a three-dimensional branched network, within which the incorporated functional monomers form binding sites [37]. The most common cross-linkers are ethylene glycol dimethacrylate, divinylbenzene, and trimethylolpropane trimethacrylate (Figure 1-2). Together with a solvent, a cross-linker determines the morphology of a polymer network. The higher content of cross-linker in MIP prepolymerization mixture and the higher its functionality number, the more cross-linked and rigid polymer network will be formed. Although a cross-linker does not often bear any specific functional groups such as functional monomers, it can still cause non-specific binding to a template by hydrophobic interactions [52]. When a cross-linker bears a functional group, e.g., the hydroxyl group in pentaerythritol triacrylate, a MIP can be prepared only from the cross-linker, and the latter will also serve as the functional monomer [17].

Initiator

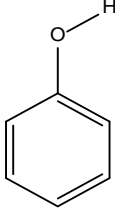
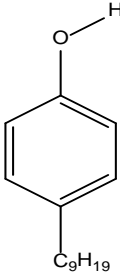
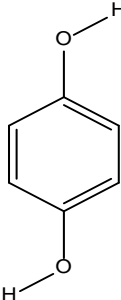
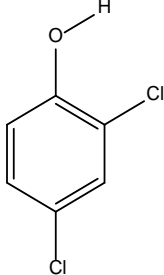
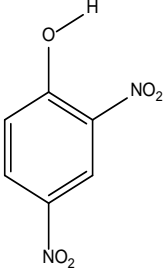
The choice of an initiator is dictated by the type of energy initiating a radical polymerization process. A common thermo-initiator is azobisisobutyronitrile, which breaks into radicals at 60 °C. For initiation with UV light, e.g., 254 nm light produced with a mercury lamp, 2,2-dimethoxy-2-phenylacetophenone is usually employed. The UV induced polymerization, which can be conducted at room and lower temperatures, has an advantage over the thermally induced polymerization that a higher imprinting effect can be achieved. The self-assembly process between a monomer and template becomes less efficient with rising temperatures [53]. MIP films and other in-situ prepared polymeric materials can be conveniently cured with UV light. Polymerization in solutions, to produce MIP particles, e.g., precipitate and suspension polymerization, is usually induced and maintained thermally.

1.2.3 Effect of monomer-template interactions on imprinting effect

Both MIP synthesis and template rebinding are very complex processes. Beside the formation of the self-assembly, the processes include many other steps greatly influencing the MIP imprinting effect. Some of them are the formation of polymer network, template removal, microswelling of binding sites in a solvent for rebinding, and template rebinding. However, if the self-assembly does not take place, it is not possible to expect effective imprinting in a MIP. A rule of thumb is stated “the stronger the binding interaction, the better” [45]. However, the presence of strong interactions in a prepolymerization mixture does not always guarantee a strong imprinting effect for the

final MIP. For example, when allylamine is used as a functional monomer, it forms dimers with itself rather than structured binding sites [51].

Table 1-2. Imprinting factors achieved by MIPs for different phenols

Template					
Monomer/ solvent	itaconic acid/ dimethyl formamide	diethyl amino- ethyl methacrylate/ dimethyl- formamide	methacrylic acid/ acetonitrile and toluene	4-vinyl pyridine/ chloroform	acrylamide/ acetonitrile
Cross-linker	EGDMA	EGDMA	TRIM	EGDMA	EGDMA
IF at high template concentrations	1.0	0.99	2.2	2.1	2.2
Reference	this project	[31]	[20]	[54]	[24]

Another very important factor governing the imprinting effect, which is relevant to MIPs for phenols, is the number of possible interaction points developed between a template molecule and functional monomers [45]. When there is binding between monomers and two or more functional groups of a template, the separate interactions cooperate and build a stronger prepolymerization complex, which results in a better MIP selectivity. This phenomenon can be observed when MIPs for phenols, which contain

other functional groups beside the hydroxyl group, are compared to MIPs for phenol and alkylphenols in terms of an imprinting factor (Table 1-2). Almost no imprinting was observed for MIPs imprinted with phenol and 4-nonylphenol. This could be because phenol and 4-nonylphenol are molecules without much shape specificity and with only one slightly acidic hydroxyl group. For comparison, hydroquinone, dichlorophenol, and dinitrophenol have more specific shapes and at least two functional groups available for “chelation” by hydrogen bonding. Also, chloro- and nitrophenols have more acidic hydroxyl groups, therefore stronger hydrogen bonding can be achieved. All these factors make the prepolymerization complex more stable, which results in better shaped binding sites after the polymerization and, as a consequence, a higher imprinting factor.

1.2.4 Study of MIP binding properties

1.2.4.1 Determination of MIP binding capacity

MIPs, as other adsorbents, can be characterized in terms of morphology (surface area, pore size distribution, pore volume), spectral (IR, NMR), and binding properties [48]. The latter group of properties is of key importance because the main purpose of a MIP is adsorption. MIP binding properties are characterized in binding experiments, where the adsorption of different compounds, or adsorbates, is studied [33, 48]. In these experiments, the MIP is placed in a solution of adsorbate, adsorption equilibrium is established, and the amount of adsorbate bound to the MIP is evaluated. There are two approaches to determine the amount of bound adsorbate. The first approach, which has been very often used in biosorption [55] and fundamental adsorption studies [56], is “by

difference”. The amount of a bound adsorbate is calculated based on a difference between the initial concentration of an adsorbate and its final concentration at the adsorption equilibrium. This approach, due to its simplicity, is one of the most widespread in the study of MIP binding behaviour [48]. Another approach applicable to MIPs is “by extraction” [22, 57], where the bound adsorbate is extracted from the MIP into an aliquot of a solvent, where its amount is quantified. In this case, it is possible to make measurements when the initial and final concentrations of an adsorbate are very close [56], for example, when a negligible fraction of the adsorbate is bound to a MIP or there is a large excess of an adsorbate solution over the adsorbent, which are common circumstances in adsorption studies.

To estimate an adsorption uptake, or a binding capacity, the amount of a bound adsorbate, by mass or moles, can be normalized to the adsorbent mass (very common for practical reasons), volume (e.g., in bed-packed columns), surface area (e.g., for films and immobilized layers), or amount of functional groups (common for biosorption) [55]. A binding capacity (Q) is a fundamental characteristic [45, 55] expressed in conventional terms as the amount of adsorbent per mass of adsorbent material. For example, for a MIP it can be presented as:

$$Q = \frac{m(\text{adsorbate})}{m(\text{MIP})} \quad (1-1)$$

The ratio of the binding capacity (Q) to an adsorbate concentration in a solution (C) measured at equilibrium is a partition coefficient for the adsorbate (D):

$$D = \frac{Q(\text{adsorbate})}{C(\text{adsorbate})} \quad (1-2)$$

This value (D) can be used to approximately assess MIP binding performance in a wide range of applications: elution chromatography, solid-phase extraction, and separation [33]. The partition coefficient is directly connected to the free energy of binding (ΔG) [45]:

$$\Delta G = -RT \ln D \quad (1-3)$$

In the simplest evaluations, a MIP imprinting effect can be evaluated based on an imprinting factor [48]—a ratio of a MIP binding capacity over that of a non-imprinted polymer (NIP).

$$IF = \frac{Q(MIP)}{Q(NIP)} \quad (1-4)$$

A NIP is prepared in the same way and from the same components as the corresponding MIP except no template is used [46]. Thus, the NIP and MIP have approximately similar morphology, chemical composition, and, what is most important, the level of non-specific binding. In this circumstance, when a difference between the MIP and NIP binding capacities is observed, the reason for the increase of the binding by the MIP is probably an imprinting effect.

1.2.4.2 Analysis of binding isotherms

A plot of binding capacities over a wide range of adsorbate concentrations at the same temperature is called a binding isotherm. The binding isotherm itself and its analysis give a comprehensive characterization of the binding behavior of an adsorbent. Experimental isotherms can be modeled with various functions that describe certain binding models. The most common binding models are Langmuir, Freundlich, and their hybrid—Langmuir-Freundlich isotherms [55, 58] (Table 1-3). These isotherms correspond to different patterns of the heterogeneity of binding sites, which are characterized with an affinity distribution function—a graph of the population of binding sites with a certain affinity constant against the value of this affinity constant [59].

Table 1-3. Main attributes of Langmuir, Freundlich, and Langmuir-Freundlich isotherm binding models

	Langmuir	Freundlich	Langmuir-Freundlich
Function	$Q = \frac{Q_t KC}{1 + KC}$	$Q = aC^m$	$Q = \frac{Q_t (KC)^m}{1 + (KC)^m}$
Linearized form of function	$\frac{Q}{C} = -QK + Q_t K$	$\text{Log}Q = \text{Log}a + m\text{Log}C$	none, has to be processed by a three parameter curve fit, e.g., by Mathematica®
Shape of affinity distribution	peak of Gaussian distribution	an asymptotically decaying tail	a peak of a Gaussian distribution (Langmuir part) with asymptotically decaying tail towards higher affinities (Freundlich part)
Binding parameters	K–slope; $Q_t = \frac{\text{intercept}}{K}$	Formulas in the Appendix B	Q_t , K, m are the fitting parameters, where K relates to the maximum of the affinity distribution peak
Special notes	often observed at high adsorbate concentrations; corresponds to a homogeneous distribution of binding sites	often observed at low adsorbate concentrations; corresponds to a heterogeneous distribution of binding sites	often used for isotherms built over a wide range of adsorbent concentrations; it is also applicable to model Langmuir-Langmuir isotherms
Examples	[58]	[60, 61]	[58, 62]

Note: Q – adsorption (binding) capacity; Q_t – total adsorption capacity; C – equilibrium concentration; K – affinity constant; a – the Freundlich isotherm fitting constant; m – the heterogeneity index.

It is important to note that the Langmuir and Langmuir-Freundlich isotherm binding models extrapolate the total number of binding sites (Q_t) based on theoretical assumptions. The Freundlich isotherm model can be considered empirical: an apparent, or observed, number of binding sites and an average affinity constant over the affinity distribution are directly related to experimental data [60]. A more comprehensive way to characterize an imprinting effect is to compare the MIP and NIP fundamental binding parameters: affinity constants, total binding capacities, and the trends of an affinity distribution, which is also determined based on the isotherm analysis [53, 63].

1.2.4.3 Chromatographic studies of imprinting effect

Besides adsorption studies, another widespread approach to study MIP binding, especially the imprinting effect and selectivity, is liquid chromatography. A HPLC column is packed with MIP (or NIP) particles and is used to separate the template and other structurally related compounds in reverse phase conditions. A capacity factor is related to an association constant as [45, 48]:

$$K = \frac{k'}{\phi} \quad (1-5)$$

$$k' = \frac{(R_t - D_t)}{D_t} \quad (1-6)$$

where k' – a capacity factor, R_t – the retention time of adsorbate, D_t – a dead time, and ϕ – the ratio of volumes of stationary and mobile phases.

An imprinting factor for the same compound can be expressed as a ratio of capacity factors for a MIP and NIP.

$$IF = \frac{k'(MIP)}{k'(NIP)} \quad (1-7)$$

The chromatographic studies are very convenient to assess MIP cross-binding, which can be done based on a pair of chromatograms for a MIP and NIP; the IFs for sequentially eluted template and other compounds are compared [28, 30]. The chromatographic method was applied to study the imprinting effect of MIPs for phenol [28]; 2,4-dimethylphenol [30]; 4-nonylphenol [31]; 4-nitrophenols [63], 2,4,6-trichlorophenol [23]. Unfortunately, this is the only method that has been used comprehensively to study the imprinting properties for phenol and alkylphenols MIPs. The chromatographic evaluation has substantial drawbacks such as: the derived characteristics of the binding and imprinting behavior greatly depend on experimental conditions, e.g., packing pressure, particle size, the column length and diameter; the dynamic nature of the chromatographic separation differs from a static adsorption in the batch rebinding experiments; the evaluation of the MIP binding takes place in a very limited concentration range [33]. Also, the partition in a mobile phase, with an organic modifier, is significantly different from the adsorption in water, which is an environment for real binding of phenol and alkylphenols, for example, sensor work in sea water.

In water, the recognition of an adsorbate by hydrogen bonding in a binding site is greatly suppressed, while this recognition is facilitated in the presence of an organic solvent in a mobile phase. Also, in water and in a mobile phase with an organic modifier

it is possible to expect a different degree of microswelling of the polymer network, including binding sites; therefore, the size and geometry of the binding sites can vary from water to the mobile phase. The same MIP formulation can exhibit a much higher imprinting effect in chromatographic studies than in adsorption experiments with aqueous solutions. For example, the HPLC method gave an imprinting factor of 3.02 for a MIP for 4-nonylphenol based on diethylaminoethyl methacrylate as a functional monomer. Almost no difference in the performances of this MIP and its NIP was observed in solid phase extraction of 4-nonylphenol from its aqueous solution [31]. The difference in the results can be also explained by the well-known fact that higher imprinting is observed when the chemical natures of the solvent for rebinding (e.g., water-acetonitrile mobile phase) and solvent, e.g., dimethylformamide, used in the MIP prepolymerization mixture are close [45], which is always a common circumstance for the chromatographic evaluations. Probably, the similarity of conditions in terms of the nature of interactions and MIP micro-swelling during a course of MIP synthesis and template rebinding benefits the imprinting effect. Thus, it is not completely adequate to transfer the results of chromatographic evaluations to characterize binding of phenols from water. Therefore, the chromatographic methodology was not chosen to study MIP binding in this research project despite the fact that the chromatographic evaluations are prompt and much less labor consuming than the construction of binding isotherms. Nevertheless, a MIP porous monolith could be conveniently fabricated inside a chromatographic column, and this is an optional format for MIP characterization.

1.2.5 Chemical analysis of petrogenic contaminants in waters

1.2.5.1 Common methods of chemical analysis of phenols

The majority of methods for the analysis of phenol and alkylphenols in water, including produced water, employ gas chromatography with the detection by mass spectrometry (GC–MS) with or without derivatization of phenols. The main reason to use GC is that it is compatible with organic solvents such as hexane and chlorohydrocarbons, which are used for liquid-liquid and solid-phase extractions. Also, the combination of GC and MS with electron ionization provides high sensitivity and selectivity of the detection. In addition, the high resolution of GC and narrow peaks makes this method applicable for the analysis of samples with a complex composition. Many GC-MS procedures for the analysis of produced water have been developed for the regulatory purposes in the field of the safety of the disposal of produced water. These procedures can also be used for the analysis of phenol and alkylphenols in any kind of waters.

The Norwegian Oil Industry Association sets gas chromatography coupled with mass-spectrometry as a standard method for the analysis of phenols in produced water [64]. The procedure uses liquid-liquid extraction of phenols with dichloromethane from water adjusted to pH 2 as a preconcentration step. The extract is purified with gel permeation chromatography to remove benzoic acids and other compounds, which can render host peaks and background noise during the GC–MS analysis. A non–polar or weakly polar capillary column can be used to separate phenols. The chromatograms are recorded in a selected ion monitoring mode (SIM). The quantitative analysis is based on internal standardization with deuterated phenols. The recovery of phenols determined by

the analysis of standard samples must be within 70 – 130%. A similar GC-MS procedure that targets phenols, hydrocarbons, and fatty acids ($C > 8$) was used to study an environmental effect of produced water in the North Sea [65]. Phenols and other species were extracted with dichloromethane and the volume of the extract was reduced by rotary evaporation. The residue was reconstituted in methanol and loaded onto a $\text{SiO}_2\text{-C18}$ phase contained in a cartridge. Phenols were eluted with methanol and analyzed with GC-MS in SIM mode. A derivatization procedure for the determination of alkylphenols in crude oils [66] can be adapted for the analysis of produced water. The extract of phenols in dichloromethane is evaporated, and phenols are derivatized with N,O-bis(trimethylsilyl) trifluoroacetamide (BSTFA) (Figure 1-3) to the corresponding trimethylsilyl ethers for ease of GC separation and MS detection.

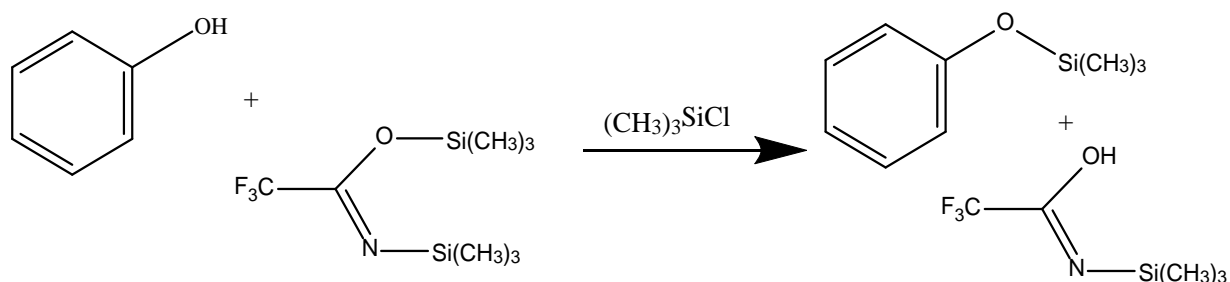


Figure 1-3. The derivatization of phenol with N,O-bis(trimethylsilyl) trifluoroacetamide for GC-MS analysis

The analysis of a large number of alkylphenols including para-substituted long-chain alkylphenols and their different positional isomers, altogether 52 phenolics, was shown to be possible by Boitsov et al. [10]. Gel permeation and normal phase

chromatographies were used for the clean-up and fractionation of phenols. Phenols were separated in GC conditions and detected with the mass spectrometry detector equipped with electron ionization and negative chemical ionization sources. For identification, the retention indices of alkylphenols were calculated based on the retention times and chemical structures of phenols.

A reversed phase LC has been coupled with the preconcentration of phenols by solid phase extraction on N-vinylpyrrolidane-divinylbenzene, divinylbenzene, graphitised carbons, polypyrrole, and octadecyl silica (C18-SiO₂) sorbents using acetonitrile and methanol-based solvents for the elution of phenols [67]. The preconcentration step can be conveniently completed online in a column packed with the adsorbents, which is directly connected to a LC column [68, 69]. After chromatographic separation, detection by UV-absorbance [68, 70], electrochemistry (amperometry) [68], or atmospheric-pressure chemical ionization-mass spectrometry (APCI-MS) [71-73] are often applied. APCI in negative mode exploits the property of phenols to be ionized through the deprotonation of phenolic hydroxyl group under the action of an ionized gas. A conflict was observed when acetic acid, which is needed to reduce the dissociation of acidic nitro- and chlorophenols in a mobile phase, suppressed the ionization process. When the ionization by an electrospray source (ESI-MS) was applied, phenol and 2,4-dimethylphenol exhibited poor signal [71] probably because of their low susceptibility to ionization under standard ESI-MS conditions.

Derivatization of phenols to produce strongly fluorescing species imparts high selectivity and sensitivity to LC with fluorimetric detection, which makes it possible to

omit a preconcentration step by solid-phase or liquid-liquid extractions. Not only natural waters [74], but also other samples with complex matrixes such as urine [75] and serum [76], have been analyzed by this approach without a pre-separation step. Typical fluorescence labelling agents are 4-(4,5-diphenyl-1H-imidazol-2-yl)benzoyl chloride [75]; 2-(4-carboxyphenyl)-5,6-dimethylbenzimidazole [76]; and coumarin-6-sulfonyl chloride using ion-pairing of the product with cetyltrimethylammonium bromide, following a reversed phase chromatographic separation [74]. EPA US method 420.4 [77] for phenols analysis in waters is based on spectrophotometry and the derivatization reaction of phenols with 4-aminoantipyrine in the presence of potassium ferricyanide in moderately alkaline media (pH=7.5 – 10.5) (Emerson reaction, Figure 1-4).

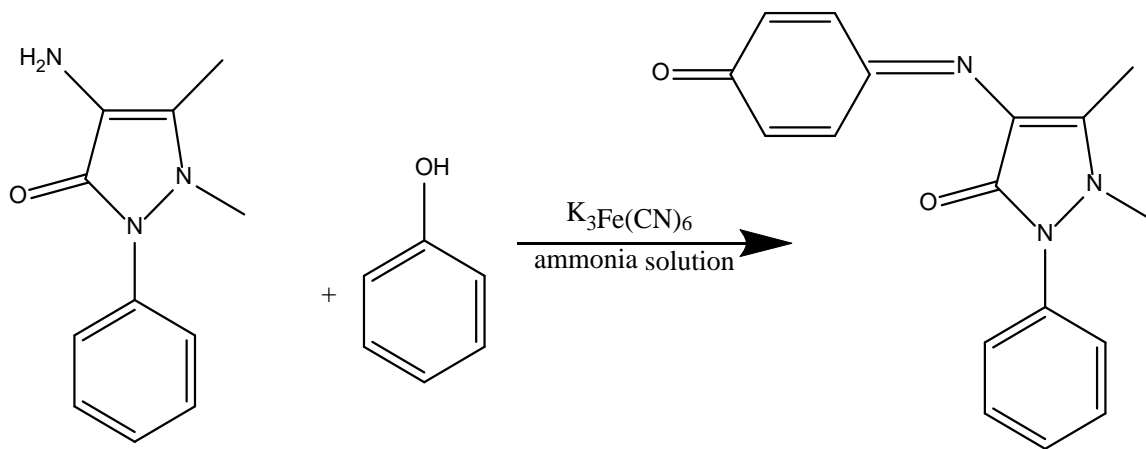


Figure 1-4. The derivatization of phenol with 4-aminoantipyrine for colorimetric detection [78]

This color reaction and the conditions of the quantification procedure, e.g., the dye spectral properties, reagent concentrations, and interferences are well studied factors [78-

80]. The method does not require expensive equipment such as a chromatograph and is very specific and sensitive. The analytical procedure can detect several $\mu\text{g L}^{-1}$ of phenol in water when a preconcentration step is applied such as the distillation of phenols [77] or their extraction with chloroform [79]. However, the colorimetric reaction is affected by the presence of oxidants (H_2O_2 , ClO^-) [80]; the reaction has cross-binding towards aromatic amines and cannot target para-substituted alkyl phenols [81]. Phenols give red coloration, so that intensity of red color is expressed as the absorbance at 505 – 520 nm [79]. Separate phenols cannot be distinguished in their mixture. The total concentration of the phenolics is enumerated in the concentration of phenol that would give the same analytical signal.

1.2.5.2 Methods of direct detection of phenols

Traditionally, chemical analysis includes the following steps: the concentration and separation of an analyte, e.g., with a solid-phase extraction; the analyte extraction with an organic solvent; the treatment of the extract, e.g., evaporation, purification, and filtration; and, finally, a chromatographic analysis and/or instrumental detection, e.g., fluorimetric; as described in the previous section. The simplest method would be to omit the extraction step and subsequent manipulations with the extract. The simplification of the analysis can be achieved when an analyte is bound on the layer of an adsorbent material, and the subsequent detection (e.g., fluorimetric, mass-spectrometric) of the analyte is made directly within the layer of the adsorbent or on its surface [11, 13, 22]. This direct approach has the following benefits: reduction of the uncertainty of final results because

of less sample handling; saving reagents, solvents, labor; and shortening the analysis time; this approach also could allow for continuous and on-site chemical sensing.

It is reasonable to use a MIP as an adsorbent material due to the possible higher adsorption efficiency and binding selectivity, compared to traditional adsorbents, such as divinylbenzene, octadecyl silica stationary phase, and ion-exchange resins [31, 43, 82]. Also, many methods have been developed for the fabrication of MIPs in a variety of formats, e.g., membranes, particles, recognition layers, films, MIP coated walls [18, 21], for incorporation into analytical systems like sensors, microfluidics, and test systems.

Direct detection on a MIP film can also be used as a fast technique to study MIP binding properties. Binding capacities for different MIPs can be compared based on the values of an analytical signal, which are often proportional to the amount of analyte loaded on the MIP. The colorimetric detection of phenol with the step of direct derivatization with 4-aminoantipyrine on a MIP membrane was used to compare phenol binding by MIPs of different formulations and to build MIP and NIP binding isotherms [21]. Cross-binding of a MIP for 2,4-dichlorophenoxyacetic acid towards structurally similar compounds was studied with desorption electrospray ionization mass spectrometry (DESI-MS) [22].

A MIP used as a recognition layer with a bound analyte can participate in a detection process in the three following ways [83]. First, upon the binding event a MIP property, e.g. mass, electrical capacitance or conductivity, is changed causing a specific output of the transducer, e.g., a piezoelectric crystal or an electrode that contacts the MIP.

A very common example of this kind of detection is a MIP mass sensitive sensor, where the change of the resonance frequency of a quartz piezoelectric crystal is observed when a MIP mass is increased due to an adsorption event. The selectivity of this technique is limited by the specificity of MIP binding towards a target in the presence of other species [11]. The second way is when the MIP itself is a signal transducer; its property, very often spectral, is changed during the binding event. An example is the quenching of the fluorescence of quantum dots incorporated in binding sites within a MIP network when 2,4-dinitrotoluene was taken up into the binding sites [84]. Third, an analyte generates a signal because of its spectral, e.g., spectral [85], electrochemical properties [35], or ability to be desorbed and ionized with mass-spectrometry [22]. In this case, the role of a MIP in the detection process is to trap an analyte from water media on the adsorbent surface and to make the analyte available for the production of an analytical signal. In this research project, detection techniques, working mostly by the third approach, were developed and studied, where phenols or PAHs were loaded on thin and porous MIP films, and detection directly on the film was attempted, for example, with fluorimetry, SERS, or mass-spectrometry.

The author believes that the knowledge of the hyphenation of different analytical methods with thin-layer chromatography should be exploited for detection on MIP films. The main reason for this is that the detection takes place on planar and porous films in both cases; a silica stationary phase bound to a plastic or alumina sheet and the polymeric film immobilized on a glass slide. Many experimental procedures have been developed to perform derivatization reactions in the TLC format. Also the designs of detection by UV-

Vis absorbance spectrometry (densitometry), fluorescence, infrared, Raman, and mass spectrometry were comprehensively described [86]. The principles of hyphenation with the analytical techniques and troubleshooting approaches can be transferred to the MIP films. For example, colorimetric detection [21] has a potential to suit the MIP films because they also can hold a dye within their porous structure and have white and opaque background for color measurements in the reflectance mode, as in the case of a TLC layer. When fluorescence is measured for MIP films, which are opaque, it is also possible to expect a high level of stray light in the measured spectra [19] because of prominent light scattering by MIP films, as also occur with TLC plates.

A group of ionization techniques for mass spectrometric detection, that work by desorption principle, includes [87]: secondary ions mass spectrometry (SIMS), direct analysis in real time (DART), matrix and surface assisted laser desorption ionization (MALDI and SALDI), desorption electrospray and atmospheric pressure chemical ionization (DESI and APCI), electrospray-assisted laser desorption ionization (ELDI), and desorption atmospheric pressure photoionization (DAPPI). The techniques that operate at atmospheric pressure (atmospheric pressure-MALDI, DART, DESI, ELDI, DAPPI) are especially convenient for the detection from planar surfaces. Within this group, special attention should be given to those techniques that do not require the application of any reagents: DART, DESI, and DAPPI.

In the context of analytical chemistry, phenol and alkylphenols can be targeted as monoaromatic species with a phenolic hydroxyl group. The aromatic nature allows for detection with UV absorbance [30], fluorescence, infrared, and Raman spectroscopies

[88]. The wide range of mass spectrometric techniques can also be applied because of the ionizable nature of the phenolic hydroxyl group [71-73]. A phenolate ion may be produced under the action of soft ionization agents, for example: excited metastable atoms (DART), charged droplets (DESI), or gas (APCI) [72]. Light absorbative and fluorescent properties of phenolics can be greatly enhanced and modified by the derivatization reactions via the phenolic hydroxyl group [21, 54].

So far, several test systems and chemical sensors have been developed for monitoring phenol in water. The majority of the systems work based on an electrochemical principle, for example: chronoamperometric enzyme-facilitated detection [34] and amperometric detection within tubules, which are filled with an enzyme and are made of a conductive polymer [35]. Highly sensitive and portable sensing of phenol and other phenolics was achieved with SERS on a silver electrode combined with an electrostatic preconcentration step [36]. The production of phenol SERS was demonstrated in a sandwich configuration, where phenol molecules were entrapped between a smooth gold surface and tips of gold nanostars [88]. A noticeable interference from phenol fluorescence was observed during fluorescence detection of monoaromatic hydrocarbons on MIP particles in the flow-injection analysis of waters [89]. Thus, similar fluorimetric detection of phenol on a MIP is probably possible. A test system based on the colorimetric detection of phenol with 4-aminoantipyrine derivatization on a MIP membrane was developed for analysis of phenol in natural waters [21].

1.2.5.3 Methods of chemical analysis of polycyclic hydrocarbons

Along with phenols and monoaromatic hydrocarbons, polycyclic hydrocarbons (PAHs) constitute another important group of petrogenic contaminants in water [3, 65]. PAHs are made of fused benzene rings with a ring number from two to six. The lighter PAHs, with two and three rings, are more soluble in water and thus found more commonly in produced water. The average concentrations of naphthalene and phenanthrene, including their alkylated forms, are 4900 and 560 $\mu\text{g L}^{-1}$, respectively, in produced water from oil extraction in the North Sea. The higher molecular weight of PAHs, the lower their solubility in water; therefore, the concentration of four- and five-ring PAHs rapidly drops to 4 $\mu\text{g L}^{-1}$ for pyrene and 0.6 $\mu\text{g L}^{-1}$ for benzo[a]pyrene in the produced water in the North Sea [1]. PAHs have narcotic, mutagenic, teratogenic, and carcinogenic action [6], which can be greatly enhanced under sunlight [90]. Acute and chronic toxicity of PAHs are observed in $\mu\text{g L}^{-1}$ and sub $\mu\text{g L}^{-1}$ range [91]. For example, “no-observed-effect concentrations” for naphthalene and anthracene are 1.5 and 0.095 $\mu\text{g L}^{-1}$, respectively [6]. Toxicity of PAHs increases with their molecular weight due to higher bioaccumulation in lipophilic tissues. According to Ambient Water Quality Criteria by the Ministry of Environment (BC, Canada), marine and fresh waters can be considered safe for aquatic life at levels below 1.0, 0.30, and 4.0 $\mu\text{g L}^{-1}$ for naphthalene, phenanthrene, and anthracene, respectively [91].

To ensure water safety, PAHs have to be detected at trace levels. Similar to the analysis of phenols, the most common analytical methods are based on chromatography. Gas chromatography is hyphenated with mass spectrometry using electron ionization

source [92]. Approximate limits of quantitation for ground waters are $10 \mu\text{g L}^{-1}$ for both phenanthrene and anthracene. Liquid chromatography uses UV/fluorescence detection. UV detection is a choice for naphthalene and fluorene, while fluorescence detection is used for anthracene, phenanthrene, and larger PAHs, which are relatively strong fluorophores [93]. In the absence of interferences, the limits of quantitation are around $7 \mu\text{g L}^{-1}$ for both phenanthrene and anthracene. Although these two analytical procedures have been comprehensively validated and used for the compliance with environmental regulations, these procedures are very lengthy and require large volume of solvents. Both GC and LC procedures include the liquid-liquid extraction of PAHs with methylene chloride from water samples, the purification of extract by silica gel, and extract evaporation [94].

Analytical systems for solvent-free and fast monitoring of PAHs in water are based on the principle of direct detection of PAHs after they partition in a layer of adsorbent from a water sample. The detection has been completed with a quartz-crystal microbalance device [49] and surface-enhanced Raman spectroscopy on functionalized gold nanoparticles [13]. Another common detection technique is fluorimetry, which exploits the unique ability of PAHs to emit strong fluorescence. The fluorescence of PAHs was measured directly from an adsorbent, such as divinyl-based resin, packed in a flow-through cell of flow-injection device on resins [12]. Also, fluorescence was measured from molecularly imprinted polymeric films [11, 85]. Although many studies have been completed to develop the design of direct fluorimetric detection, they mostly target four- and five-ring polycyclic hydrocarbons, not considering two- and three-ring

polycyclic hydrocarbons that are also present in produced water. For example, a 30 ng L⁻¹ detection limit in water was achieved for pyrene [11].

1.2.6 Research objectives

Objectives for this research project can be summarized as the following:

- a. to develop uncomplicated methods to fabricate high quality MIP films suitable for applications in analytical chemistry;
- b. to synthesize MIPs effective towards phenol and alkylphenols in terms of binding and imprinting performances;
- c. to determine factors that influence the binding, imprinting, and morphological properties of MIPs, and establish principles to prepare efficient MIPs for phenols;
- d. to apply various analytical techniques for direct chemical analysis of phenols or other oil related contaminants adsorbed on MIP films to achieve rapid, sensitive, and solvent free detection.

1.3 Conclusions

The preceding sections described the preparation of MIPs in general and specifically for phenol and alkylphenols, and application of the MIPs for direct detection. Phenol and alkylphenols were set as the target for adsorption and chemical analysis because they constitute a fraction of water contaminants, together with PAHs and BTEX, from oil and produced water. Phenols were characterized as water pollutants in terms of sources, physico-chemical, and toxicological properties. Non-covalent imprinting and vinyl polymerization were discussed on the basis of synthesis of MIPs, where monomer-

template interactions have a key effect on the imprinting effect by the MIPs. Phenol binding from aqueous solutions and chromatographic separations, as approaches to study MIP binding properties, were characterized and compared. The former constitutes an important part of this research project methodology because binding studies allow for the calculation of the adsorption capacity and construction of adsorption isotherms, which are fundamental characteristics of the binding behavior. Traditional analytical methods for the analysis of phenols in waters based on preconcentration, chromatographic separation, derivatization reactions, and different kinds of instrumental detection were reviewed. Next, it was shown how the derivatization reactions and instrumental detection could be hyphenated with preconcentration on a MIP to achieve fast and direct detection. It can be seen that more development work in the area of the direct detection of phenol is of current importance.

1.4 References

1. *Report 1.20/324. Aromatics in produced water - occurrence, fate and effects, and treatment*; International Oil and Gas Producers Association: London, UK, 2002; p 30.
2. Build a career in oil & gas. <http://www.careersinoilandgas.com/build-your-career/working-in-oil-gas-/oil-gas-locations/oil-gas-locations-newfoundland-labrador.aspx#.UszJkLG9zmQ> (accessed 18.12.2013).
3. Hawboldt, K.; Chen, B.; Thanyamanta, W.; Egli, S.; Gryshchenko., A., Review of produced water management and challenges in harsh/arctic environments. Faculty of Engineering and Applied Science of Memorial University of Newfoundland to the American Bureau of Shipping: 2010; p 129.
4. Michałowicz J., D. W., Phenols – sources and toxicity. *Polish Journal of Environmental Studies* **2007**, *16* (3), 347-362.

5. Water: CWA Methods. Priority Pollutants. <http://water.epa.gov/scitech/methods/cwa/pollutants.cfm> (accessed 17.12.2013).
6. *Report 364. Fate and effects of naturally occurring substances in produced water on the marine environment*; International Oil and Gas Producers Association: London, UK, 2005; p 42.
7. EPA440/5-80-066, Ambient water quality criteria for phenol. US Government Printing Office: 1980.
8. Canadian water quality guidelines for the protection of aquatic life. In Phenols — mono- and dihydric phenols, Canadian Council of Ministers of the Environment: Winnipeg, 1999; p 5.
9. Locke, J. Protecting our oceans, one polymer at a time. Faculty of Engineering and Applied Science. <http://www.engr.mun.ca/news.php?id=1226> (accessed 05.09.2014).
10. Boitsov, S.; Mjøs, S. A.; Meier, S., Identification of estrogen-like alkylphenols in produced water from offshore oil installations. *Marine Environmental Research* **2007**, *64* (5), 651-665.
11. Lieberzeit, P. A.; Halikias, K.; Afzal, A.; Dickert, F. L., Polymers imprinted with PAH mixtures—comparing fluorescence and QCM sensors. *Analytical and Bioanalytical Chemistry* **2008**, *392* (7-8), 1405-10.
12. Fernandezsanchez, J., The development of solid-surface fluorescence characterization of polycyclic aromatic hydrocarbons for potential screening tests in environmental samples. *Talanta* **2003**, *60* (2-3), 287-293.
13. Peron, O.; Rinnert, E.; Toury, T.; Lamy de la Chapelle, M.; Compere, C., Quantitative SERS sensors for environmental analysis of naphthalene. *The Analyst* **2011**, *136* (5), 1018-22.
14. Shen, X.; Xu, C.; Ye, L., Molecularly imprinted polymers for clean water: analysis and purification. *Industrial & Engineering Chemistry Research* **2013**, *52* (39), 13890-99.
15. Murray, A.; Ormeci, B., Application of molecularly imprinted and non-imprinted polymers for removal of emerging contaminants in water and wastewater treatment: a review. *Environmental Science and Pollution Research International* **2012**, *19* (9), 3820-30.
16. Shiraishi, Y.; Suzuki, T.; Hirai, T., Selective photooxidation of chlorophenols with molecularly imprinted polymers containing a photosensitizer. *New Journal of Chemistry* **2010**, *34* (4), 714-717.

17. Manesiotis, P.; Borrelli, C.; Aureliano, C. S. A.; Svensson, C.; Sellergren, B., Water-compatible imprinted polymers for selective depletion of riboflavine from beverages. *Journal of Materials Chemistry* **2009**, *19* (34), 6185-6193.
18. Pérez-Moral, N.; Mayes, A., Novel MIP formats. *Bioseparation* **2001**, *10* (6), 287-299.
19. Harz, S.; Schimmelpfennig, M.; Tse Sum Bui, B.; Marchyk, N.; Haupt, K.; Feller, K.-H., Fluorescence optical spectrally resolved sensor based on molecularly imprinted polymers and microfluidics. *Engineering in Life Sciences* **2011**, *11* (6), 559-565.
20. Kan, X.; Zhao, Q.; Zhang, Z.; Wang, Z.; Zhu, J. J., Molecularly imprinted polymers microsphere prepared by precipitation polymerization for hydroquinone recognition. *Talanta* **2008**, *75* (1), 22-26.
21. Sergeeva, T. A.; Gorbach, L. A.; Slinchenko, O. A.; Goncharova, L. A.; Piletska, O. V.; Brovko, O. O.; Sergeeva, L. M.; Elska, G. V., Towards development of colorimetric test-systems for phenols detection based on computationally-designed molecularly imprinted polymer membranes. *Materials Science and Engineering: C* **2010**, *30* (3), 431-436.
22. Van Biesen, G.; Wiseman, J. M.; Li, J.; Bottaro, C. S., Desorption electrospray ionization-mass spectrometry for the detection of analytes extracted by thin-film molecularly imprinted polymers. *The Analyst* **2010**, *135* (9), 2237-40.
23. Feng, Q. Z.; Zhao, L. X.; Yan, W.; Lin, J. M.; Zheng, Z. X., Molecularly imprinted solid-phase extraction combined with high performance liquid chromatography for analysis of phenolic compounds from environmental water samples. *Journal of Hazardous Materials* **2009**, *167* (1-3), 282-8.
24. Zakaria, N. D.; Yusof, N. A.; Haron, J.; Abdullah, A. H., Synthesis and evaluation of a molecularly imprinted polymer for 2,4-dinitrophenol. *International Journal of Molecular Sciences* **2009**, *10* (1), 354-65.
25. An, F. Q.; Gao, B. J.; Feng, X. Q., Binding and recognition ability of molecularly imprinted polymer toward p-nitrophenol. *Journal of Applied Polymer Science* **2012**, *125* (4), 2549-2555.
26. Caro, E.; Marcé, R. M.; Cormack, P. A. G.; Sherrington, D. C.; Borrull, F., On-line solid-phase extraction with molecularly imprinted polymers to selectively extract substituted 4-chlorophenols and 4-nitrophenol from water. *Journal of Chromatography A* **2003**, *995* (1-2), 233-238.
27. Cela-Perez, M. C.; Castro-Lopez, M. M.; Lasagabaster-Latorre, A.; Lopez-Vilarino, J. M.; Gonzalez-Rodriguez, M. V.; Barral-Losada, L. F., Synthesis and characterization of

bisphenol-A imprinted polymer as a selective recognition receptor. *Analytica Chimica Acta* **2011**, 706 (2), 275-84.

28. Lv, Y.Q.; Lin, Z.; Feng, W.; Tan, T., Evaluation of the polymerization and recognition mechanism for phenol imprinting SPE. *Chromatographia* **2007**, 66 (5-6), 339-347.

29. An, F.; Gao, B., Adsorption of phenol on a novel adsorption material PEI/SiO₂. *Journal of Hazardous Materials* **2008**, 152 (3), 1186-91.

30. Qi, P.; Wang, J.; Jin, J.; Su, F.; Chen, J., 2,4-Dimethylphenol imprinted polymers as a solid-phase extraction sorbent for class-selective extraction of phenolic compounds from environmental water. *Talanta* **2010**, 81 (4-5), 1630-5.

31. Guerreiro, A.; Soares, A.; Piletska, E.; Mattiasson, B.; Piletsky, S., Preliminary evaluation of new polymer matrix for solid-phase extraction of nonylphenol from water samples. *Analytica Chimica Acta* **2008**, 612 (1), 99-104.

32. Yin, X. Y.; Zhong, Y. Q.; Jiang, Y. F.; Luo, Y. M., The spectroscopy analysis of intermolecular interaction between the template molecule and functional monomer before polymerization. *Guang Pu Xue Yu Guang Pu Fen Xi* **2010**, 30 (8), 2211-4.

33. Toth, B.; Pap, T.; Horvath, V.; Horvai, G., Which molecularly imprinted polymer is better? *Analytica Chimica Acta* **2007**, 591 (1), 17-21.

34. Adamski, J.; Nowak, P.; Kochana, J., Simple sensor for the determination of phenol and its derivatives in water based on enzyme tyrosinase. *Electrochimica Acta* **2010**, 55 (7), 2363-2367.

35. Baek, S.; Lee, Y.; Son, Y., Amperometric phenol sensors employing conducting polymer microtubule structure. *Molecular Crystals and Liquid Crystals* **2010**, 519 (1), 69-76.

36. Li, D.; Li, D.-W.; Fossey, J. S.; Long, Y.-T., Portable surface-enhanced raman scattering sensor for rapid detection of aniline and phenol derivatives by on-site electrostatic preconcentration. *Analytical Chemistry* **2010**, 82 (22), 9299-9305.

37. Yan, H.; Row, K., Characteristic and synthetic approach of molecularly imprinted polymer. *International Journal of Molecular Sciences* **2006**, 7 (5), 155-178.

38. Welcome to the Handbook of Chemistry & Physics Online. <http://www.hbcnetbase.com> (accessed 07.10.13).

39. Australian Government. National Pollutant Inventory. Phenol. <http://www.npi.gov.au/resource/phenol> (accessed 18.12.2013).

40. Phenol. <http://www.eco-usa.net/toxics/chemicals/phenol.shtml> (accessed 18.12.2013).
41. Toxicological profile for phenol. U.S. Department of Health and Human Services: Atlanta, USA, 2008; p 27.
42. Mayes, A. G., A Brief History of the "New Era" of molecular imprinting. In *Molecularly Imprinted Materials: Science and Technology*, Mingdi, Y.; Ramström, O., Eds. Marcel Dekker: New York, USA, 2005; pp 13-19.
43. Li, W.; Li, S., Molecular imprinting: a versatile tool for separation, sensors and catalysis. In *Oligomers - Polymer Composites - Molecular Imprinting*, Springer Berlin Heidelberg: 2007; Vol. 206, pp 191-210.
44. Mayes, A. G.; Whitcombe, M. J., Synthetic strategies for the generation of molecularly imprinted organic polymers. *Advanced Drug Delivery Reviews* **2005**, *57* (12), 1742-78.
45. Spivak, D. A., Selectivity in molecularly imprinted matrices. In *Molecularly Imprinted Materials: Science and Technology*, Mingdi, Y.; Ramström, O., Eds. Marcel Dekker: New York, USA, 2005; pp 395-419.
46. Ramstrom, O.; Mingdi, Y., Molecular Imprinting. An Introduction. In *Molecularly Imprinted Materials: Science and Technology*, Mingdi, Y.; Ramström, O., Eds. Marcel Dekker: New York, USA, 2005; pp 6-9.
47. Arshady, R.; Mosbach, K., Synthesis of substrate-selective polymers by host-guest polymerization. *Die Makromolekulare Chemie* **1981**, *182* (2), 687-692.
48. Spivak, D. A., Optimization, evaluation, and characterization of molecularly imprinted polymers. *Advanced Drug Delivery Reviews* **2005**, *57* (12), 1779-94.
49. Dickert, F. L.; Tortschanoff, M.; Bulst, W. E.; Fischerauer, G., Molecularly imprinted sensor layers for the detection of polycyclic aromatic hydrocarbons in water. *Analytical Chemistry* **1999**, *71* (20), 4559-4563.
50. Holthoff, E. L.; Stratis-Cullum, D. N.; Hankus, M. E., A nanosensor for TNT detection based on molecularly imprinted polymers and surface enhanced Raman scattering. *Sensors* **2011**, *11* (3), 2700-14.
51. Karim, K.; Breton, F.; Rouillon, R.; Piletska, E. V.; Guerreiro, A.; Chianella, I.; Piletsky, S. A., How to find effective functional monomers for effective molecularly imprinted polymers? *Advanced Drug Delivery Reviews* **2005**, *57* (12), 1795-808.

52. Muhammad, T.; Nur, Z.; Piletska, E. V.; Yimit, O.; Piletsky, S. A., Rational design of molecularly imprinted polymer: the choice of cross-linker. *The Analyst* **2012**, *137* (11), 2623-8.
53. Rampey, A. M.; Umpleby, R. J.; Rushton, G. T.; Iseman, J. C.; Shah, R. N.; Shimizu, K. D., Characterization of the imprint effect and the influence of imprinting conditions on affinity, capacity, and heterogeneity in molecularly imprinted polymers using the freundlich isotherm-affinity distribution analysis. *Analytical Chemistry* **2004**, *76* (4), 1123-1133.
54. Feng, Q. Z.; Zhao, L. X.; Yan, W.; Ji, F.; Wei, Y. L.; Lin, J. M., Molecularly imprinted solid-phase extraction and flow-injection chemiluminescence for trace analysis of 2,4-dichlorophenol in water samples. *Analytical and Bioanalytical Chemistry* **2008**, *391* (3), 1073-9.
55. Volesky, B., Equilibrium (bio-)sorption. In *Sorption and Biosorption*, BV-Sorbex, Inc.; Montreal, Canada, 2004; pp 103-116.
56. Chapter 7. Theory of binding data analysis. In *Technical Resource Guide. Fluorescence Polarization.*, Invitrogen Corporation: 2006; p 18.
57. Feng, Q.; Zhao, L.; Lin, J. M., Molecularly imprinted polymer as micro-solid phase extraction combined with high performance liquid chromatography to determine phenolic compounds in environmental water samples. *Analytica Chimica Acta* **2009**, *650* (1), 70-76.
58. Umpleby, R. J.; Baxter, S. C.; Chen, Y.; Shah, R. N.; Shimizu, K. D., Characterization of molecularly imprinted polymers with the Langmuir–Freundlich isotherm. *Analytical Chemistry* **2001**, *73* (19), 4584-4591.
59. Umpleby, R. J.; Bode, M.; Shimizu, K. D., Measurement of the continuous distribution of binding sites in molecularly imprinted polymers. *The Analyst* **2000**, *125* (7), 1261-1265.
60. Umpleby, R. J.; Baxter, S. C.; Bode, M.; Berch Jr, J. K.; Shah, R. N.; Shimizu, K. D., Application of the Freundlich adsorption isotherm in the characterization of molecularly imprinted polymers. *Analytica Chimica Acta* **2001**, *435* (1), 35-42.
61. Corton, E.; García-Calzón, J. A.; Díaz-García, M. E., Kinetics and binding properties of cloramphenicol imprinted polymers. *Journal of Non-Crystalline Solids* **2007**, *353* (8-10), 974-980.
62. Holland, N.; Frisby, J.; Owens, E.; Hughes, H.; Duggan, P.; McLoughlin, P., The influence of polymer morphology on the performance of molecularly imprinted polymers. *Polymer* **2010**, *51* (7), 1578-1584.

63. Masqué, N.; Marcé, R. M.; Borrull, F.; Cormack, P. A. G.; Sherrington, D. C., Synthesis and evaluation of a molecularly imprinted polymer for selective on-line solid-phase extraction of 4-nitrophenol from environmental water. *Analytical Chemistry* **2000**, 72 (17), 4122-4126.
64. OLF 085:2003. Recommended guidelines for the sampling and analysis of produced water. Norwegian Oil Industry Association: 2003; p 14.
65. Strømgren, T.; Sørstrøm, S. E.; Schou, L.; Kaarstad, I.; Aunaas, T.; Brakstad, O. G.; Johansen, Ø., Acute toxic effects of produced water in relation to chemical composition and dispersion. *Marine Environmental Research* **1995**, 40 (2), 147-169.
66. Bennett, B.; Noke, K. J.; Bowler, B. F. J.; Larter, S. R., The accurate determination of C0-C3 alkylphenol concentrations in crude oils. *International Journal of Environmental Analytical Chemistry* **2007**, 87 (5), 307-320.
67. Mahugo Santana, C.; Sosa Ferrera, Z.; Esther Torres Padron, M.; Juan Santana Rodriguez, J., Methodologies for the extraction of phenolic compounds from environmental samples: new approaches. *Molecules* **2009**, 14 (1), 298-320.
68. Puig, D.; Barceló, D., Comparative study of on-line solid phase extraction followed by UV and electrochemical detection in liquid chromatography for the determination of priority phenols in river water samples. *Analytica Chimica Acta* **1995**, 311 (1), 63-69.
69. Application Note 191. Determination of phenols in drinking and bottled mineral waters using online solid-phase extraction followed by hplc with uv detection. Dionex Corporation: 2008; p 12.
70. Marko-Varga, G.; Barceló, D., Liquid chromatographic retention and separation of phenols and related aromatic compounds on reversed phase columns. *Chromatographia* **1992**, 34 (3-4), 146-154.
71. Martinez Vidal, J. L.; Belmonte Vega, A.; Garrido Frenich, A.; Egea Gonzalez, F. J.; Arrebola Liebanas, F. J., Determination of fifteen priority phenolic compounds in environmental samples from Andalusia (Spain) by liquid chromatography-mass spectrometry. *Analytical and Bioanalytical Chemistry* **2004**, 379 (1), 125-30.
72. Jauregui, O.; Moyano, E.; Galceran, M. T., Liquid chromatography-atmospheric pressure ionization mass spectrometry for the determination of chloro- and nitrophenolic compounds in tap water and sea water. *Journal of Chromatography A* **1997**, 787 (1-2), 79-89.
73. Puig, D.; Silgoner, I.; Grasserbauer, M.; Barceló, D., Part-per-Trillion Level Determination of priority methyl-, nitro-, and chlorophenols in river water samples by automated on-line liquid/solid extraction followed by liquid chromatography/mass

spectrometry using atmospheric pressure chemical ionization and ion spray interfaces. *Analytical Chemistry* **1997**, *69* (14), 2756-2761.

74. Suliman, F. E.; Al-Kindi, S. S.; Al-Kindy, S. M.; Al-Lawati, H. A., Analysis of phenols in water by high-performance liquid chromatography using coumarin-6-sulfonyl chloride as a fluorogenic precolumn label. *Journal of Chromatography A* **2006**, *1101* (1-2), 179-84.

75. Nakashima, K.; Kinoshita, S.; Wada, M.; Kuroda, N.; R. G. Baeyens, W., HPLC with fluorescence detection of urinary phenol, cresols and xylenols using 4-(4,5-diphenyl-1H-imidazol-2-yl)benzoyl chloride as a fluorescence labeling reagent. *The Analyst* **1998**, *123* (11), 2281-2284.

76. Katayama, M.; Sasaki, T.; Matsuda, Y.; Kaneko, S.; Iwamoto, T.; Tanaka, M., Sensitive determination of bisphenol A and alkylphenols by high performance liquid chromatography with pre-column derivatization with 2-(4-carboxyphenyl)-5,6-dimethylbenzimidazole. *Biomedical Chromatography* **2001**, *15* (6), 403-7.

77. Method 420.4. Determination of total recoverable phenolics by semi-automated colorimetry. U.S. Environmental Protection Agency: Cincinnati, Ohio 1993; p 14.

78. Fiamegos, Y.; Stalikas, C.; Pilidis, G., 4-Aminoantipyrine spectrophotometric method of phenol analysis: Study of the reaction products via liquid chromatography with diode-array and mass spectrometric detection. *Analytica Chimica Acta* **2002**, *467* (1-2), 105-114.

79. Ettinger, M.; Ruchhoft, C.; Lishka, R., Sensitive 4-Aminoantipyrine Method for Phenolic Compounds. *Analytical Chemistry* **1951**, *23* (12), 1783-1788.

80. Norwitz, G.; Farino, J.; Keliher, P. N., Interference of oxidants in the determination of phenol by the 4-aminoantipyrine and ultraviolet ratio spectrophotometric methods. *Analytical Chemistry* **1979**, *51* (11), 1632-1637.

81. Svobodová, D.; Gasparič, J., Investigation of the colour reaction of phenols with 4-aminoantipyrine. *Mikrochimica Acta* **1971**, *59* (2), 384-390.

82. Pichon, V.; Chapuis-Hugon, F., Role of molecularly imprinted polymers for selective determination of environmental pollutants—a review. *Analytica Chimica Acta* **2008**, *622* (1-2), 48-61.

83. Haupt, K., Molecularly imprinted polymers as recognition elements in sensors: mass and electrochemical sensors. In *Molecularly imprinted materials: Science and Technology*, Mingdi, Y.; Ramström, O., Eds. Marcel Dekker: New York, USA, 2005; pp 687-690.

84. Stringer, R. C.; Gangopadhyay, S.; Grant, S. A., Detection of nitroaromatic explosives using a fluorescent-labeled imprinted polymer. *Analytical Chemistry* **2010**, *82* (10), 4015-4019.
85. Lieberzeit, P. A.; Dickert, F. L., Sensor technology and its application in environmental analysis. *Analytical and Bioanalytical Chemistry* **2007**, *387* (1), 237-47.
86. Bernd, S.; Poole, C. F.; Weins, C., Chapter 7. Specific staining reactions. In *Quantitative Thin-Layer Chromatography. A Practical Survey*, Springer: 2011; pp 155-200.
87. Morlock, G.; Schwack, W., Hyphenations in planar chromatography. *Journal of Chromatography A* **2010**, *1217* (43), 6600-9.
88. Rodríguez-Lorenzo, L.; Álvarez-Puebla, R. n. A.; de Abajo, F. J. G. a.; Liz-Marzán, L. M., Surface enhanced raman scattering using star-shaped gold colloidal nanoparticles. *The Journal of Physical Chemistry C* **2009**, *114* (16), 7336-7340.
89. Sainz-Gonzalo, F. J.; Medina-Castillo, A. L.; Fernandez-Sanchez, J. F.; Fernandez-Gutierrez, A., Synthesis and characterization of a molecularly imprinted polymer optosensor for TEXs-screening in drinking water. *Biosensors & Bioelectronics* **2011**, *26* (7), 3331-8.
90. Pelletier, M. C.; Burgess, R. M.; Ho, K. T.; Kuhn, A.; McKinney, R. A.; Ryba, S. A., Phototoxicity of individual polycyclic aromatic hydrocarbons and petroleum to marine invertebrate larvae and juveniles. *Environmental Toxicology and Chemistry* **1997**, *16* (10), 2190-2199.
91. Ambient water quality criteria for polycyclic aromatic hydrocarbons Ministry of Environment, Lands and Parks. Province of British Columbia. <http://www.env.gov.bc.ca/wat/wq/BCguidelines/pahs/> (accessed 09.09.2014).
92. Method 8270D. Semivolatile organic compounds by gas chromatography/mass spectrometry (GC/MS). US Environmental Protection Agency: 2007; pp 72.
93. Method 8310. Polynuclear aromatic hydrocarbons. US Environmental Protection Agency.1986; pp 13.
94. Method 3510C. Separatory funnel liquid-liquid extraction. US Environmental Protection Agency: 1996; p 8.

Chapter 2. Development of Procedures to Fabricate MIP Films

2.1 Introduction

Since the 1970s, MIP technologies have received extensive study and almost developed into a discipline in its own right. Aside from the synthesis of MIPs [1], this new field of knowledge includes: fabrication of MIPs in different physical forms, e.g. beads, nano-layers, monolithic micro-columns [2, 3]; methodologies for study of MIP properties, e.g., binding, swelling, light-scattering [4]; and application of MIPs in separation science and analytical chemistry [5]. MIPs in different physical formats have specific advantages, limitations, and applications. MIPs in the form of particles can be used as adsorbents for solid-phase extraction [6], stationary phases in liquid chromatography [7, 8], or for fabrication of films. A MIP fabricated in a film format can be exploited for microextraction in miniaturized analytical systems, sensors, and analytical test systems [2].

The simplest way to prepare a MIP is by polymerization in a vessel, which results in a bulk monolith. This monolith is rarely used without any further modifications; it is usually mechanically crushed into particles of an irregular shape [9]. The crushed particles, whose size falls in a certain range, are sieved out. These particles can be used further, as a sample of a MIP, to study its adsorption properties, as adsorbent for solid-phase extraction, or the particles can be bound with glue to form a film. However, crushing and sieving steps make this method laborious, resulting in the low yield of particles for use. Also, the MIP network can partially lose its recognition properties due to the mechanical stress. Unfortunately, bulk polymerization is still a widespread format for the synthesis of MIPs, and this polymerization is chosen by many scientists due to its

simplicity. However, bulk polymerization is of low practical importance because of the drawbacks discussed above; and the format is mainly used only for research purposes [2]. More efficient and rational methods of MIP particles and films fabrication have been developed.

One of the methods to prepare MIP particles is precipitation polymerization. Monomers and the initiator are dissolved in a solvent to form a dilute solution (<5%); upon growth of a polymer network, the polymer precipitates into spheres of a sub-micron size. This technique has an advantage that it is simple and one-step, has a high yield of particles (>80%), and does not require any polymerization stabilizers like emulsifiers [9]. Precipitation polymerization has found a wide application in MIP technologies to prepare MIP particles. These particles have been used to form a recognition layer for an electrochemical sensor [10], and in a microfluidic device coupled with fluorimetric detection [11], to fabricate micro SPE devices for a chromatographic analysis [12], and as an HPLC stationary phase for enantioselective separations [8].

Traditionally, MIP films are fabricated with spin-coating, sandwiching, affixing MIP particles, or by polymerization based on a network of another film [2]. In a spin-coating method a prepolymerization mixture is spread on a planar substrate at high spinning velocities and UV cured into a thin film. The main advantage of this method is the fabrication of films with a controlled thickness ranging from ~0.1 to 10 μm [13]. However, this method requires the prepolymerization mixture to be of a certain viscosity and of significantly low volatility. The latter requirement is in conflict with the fact that the majority of solvents used for MIP synthesis, generally and in this research project, are

too volatile for this purpose, e.g., chloroform, methanol, acetonitrile, and dimethylformamide. Also, the spin-coating technique requires some specialized equipment such as a spin-coater equipped with a UV-light source and a chamber filled with an inert gas. Only one film at a time can be fabricated, which does not allow the production of many MIP samples to conveniently study various aspects of MIPs. Thus, this technique was not used in this research project, and a preference was given to different variations of sandwich technique.

The sandwich technique can be considered as a bulk polymerization completed in a thin layer [13]. A blend of MIP components in a solvent, a prepolymerization mixture, is polymerized between two planar surfaces. On the bottom surface, for example, a derivatized glass slide or metal surface, a polymer film is immobilized covalently. The upper surface is not treated and should be easily detached from the polymer film after polymerization. Also, the surface has to be able to transmit the UV-light. Therefore, a thin microscope cover glass is mostly used as the top surface. In addition to the simple polymerization on a glass slide surface [14], the sandwich technique has been employed to form a MIP recognition layer directly on a transducer of a chemical sensor, for example, on a quartz crystal microbalance surface for mass-sensitive detection [15], and on the surface of a ZnSe crystal (total reflection wave guide) for infrared spectroscopic detection [16]. The thickness of the resulting films was several μm . The sandwich technique is also a format to fabricate sections of MIP membrane that are free of any substrate [17]. The sandwiching approach was used for imprinting with macromolecules;

protein was deposited on the contact surface of a cover glass to imprint the surface of a polymeric film [18].

MIP particles prepared by any method such as precipitation polymerization or by crushing a MIP monolith can be adapted for the fabrication of films by binding these particles with glue. For example, MIP particles prepared with precipitation polymerization were adhered onto a layer of polyethyleneimine immobilized on a glass slide surface to produce ~1 μm thick film of MIP particles [11]. However, such films appeared to be easily destroyed under a fluid flow and it is possible to expect that a fraction of MIP binding sites would be blocked with the polymeric binder.

A MIP composite film can be produced when a porous material, e.g., a membrane, filter paper [19], or another filter material such as an alumina membrane filter [20, 21] is soaked with a prepolymerization mixture, which is polymerized directly within the porous network. These films are permeable to fluids and are used for different kinds of selective separations, or as MIP membranes. The carrying matrix dictates the porosity and network structure of the final film. At the same time, the mechanical strength of the films is increased due to the extra “gluing” of the matrix network with the formed polymer.

In this project, attempts were made to develop procedures to produce high quality films based on the sandwiching principle. MIP particles were prepared by precipitation polymerization and incorporated into films. These particles were mixed with another MIP prepolymerization mixture, and the resulting suspension was UV cured to form a composite film. Such “gluing” by polymerization solved the problem of the mechanical

stability of films prepared from MIP particles. Thick films were produced by polymerization in a membrane frame, where the frame controlled the thickness of the final MIP film. These thick films can be useful for spectrometric detection, where it is important to have the high loading of adsorbate per area of the film.

2.2 Materials and methods

The following chemicals were purchased from Sigma-Aldrich (Oakville, ON, Canada). Phenol, 2,2-dimethoxy-2-phenylacetophenone (DMPA), itaconic acid, and styrene were 99% pure. 3-(Trimethoxysilyl)propyl methacrylate and ethylene glycol dimethacrylate were 98% pure. Triethylene glycol dimethacrylate and 4-vinylpyridine were 95% pure. Polyethyleneglycol and polyvinylacetate had average Mw of 20,000 and 100,000, respectively. *N, N*-Dimethylformamide (DMF) was of ACS reagent grade with <0.005% water. Chloroform (stabilized with amylenes), methanol, dimethyl sulfoxide, acetic acid, hydrochloric acid (37% w/w) were of ACS reagent grade and were purchased from ACP Chemicals (Montreal, QC, Canada). Hydrophilic polypropylene membrane GHP-200, 0.2 μm pore size, 76.2–127.0 μm thickness, was from Pall Corporation (Mississauga, ON, Canada). Micro cover glasses $25 \times 25 \text{ mm}^2$ and plain glass microscope slides $75 \times 25 \text{ mm}^2$ were from Fisher Scientific (Ottawa, ON, Canada).

2.2.1 Precipitation polymerization

The MIP particles based on divinylbenzene were prepared according to a method adapted from previous work [22]. 2,4,6-Trimethylphenol was used as a template. The MIP components were mixed in a 100 mL-tube keeping the same ratio as in the original

work: 0.214 mmol of 2,4,6-trimethylphenol; 1.71 mmol of MAA; 8.56 mmol of DVB; 0.145 mmol of AIBN; and 15.0 mL of acetonitrile/toluene (3:1). The reaction mixture was degassed by purging with nitrogen gas, heated at 60 °C and shaken (60 rotations per minute) in an Innova 4230 Incubator Shaker (New Brunswick Scientific, Enfield, CT, USA) for 20 h. The prepared MIP particles were stirred in methanol/acetic acid (9:1) and, then, centrifuged. Altogether 3 cycles of stirring/centrifugation were completed to remove the template. The divinylbenzene is commercially available in technical grade; this reagent contained 80% (v/v) of *m*- and *p*-divinylbenzenes and 20% (v/v) of ethylstyrenes. Thus, ethylstyrenes also acted as functional monomers in the MIP synthesis. MIPs based on other cross-linkers (TRIM and EGDMA) and itaconic acid were prepared in a similar way. The washed particles were enclosed between two square sheets (15×15 mm²) of polypropylene membrane, which were sealed by gentle ironing to form a micro-envelope [22].

2.2.2 Fabrication of MIP films

2.2.2.1 The derivatization of glass slides

To insure fabricated films adhered to glass substrates, prior to the application of the pre-polymerization mixture, the glass surface was derivatized with the moieties of methacrylic acid [14, 23]. This was achieved in the following procedure. The cut pieces of glass slides (25×25 mm²) were soaked in methanol/hydrochloric acid (1:1) for 2 h. Next, the slides were washed with tap and deionized water, and finally air-dried. The clean slides were soaked in a 3% (v/v) solution of 3-(trimethoxysilyl)propyl methacrylate in toluene overnight. Finally, the slides were washed with methanol, air-dried, and stored

in a fridge before use. No deterioration of the quality of the slides was observed over several months of storage.

2.2.2.2 Sandwich technique

First, a prepolymerization mixture is prepared in a vial by mixing 0.400 mmol of template (phenol), 0.800 mmol of functional monomer, e.g, itaconic acid, 0.060 mmol of 2,2-dimethoxy-2-phenylacetophenone, 4.00 mmol of cross-linker, e.g, ethyleneglycol dimethacrylate, and 1000 μ L of solvent, e.g, methanol:water (3/1). The mixture was sonicated for 5 min under nitrogen. Next, a 16- μ L aliquot of prepolymerization mixture was delivered with a displacement pipette onto the glass slide and quickly covered with a cover glass before illumination with the UV light (UVG-54, 6W, 254 nm, VWR, Mississauga, ON, Canada) for 30 min. A scheme of the procedure is presented in Figure 2-1. The cover glass was removed immediately following the polymerization. The template, labile linear polymers, and unreacted species were removed in methanol/acetic acid (9:1, v/v) with stirring. The total time of the washing was 19 h 30 min using three fresh portions of the methanol/acetic mixture. Polymerization at the slide edges (~2–3 mm in width) was affected by oxygen in air and solvent evaporation; these parts were trimmed with a razor to yield a film with completely homogeneous texture. Care was taken not to scratch the glass. Finally, the films were stirred in methanol for 30 min and air dried.

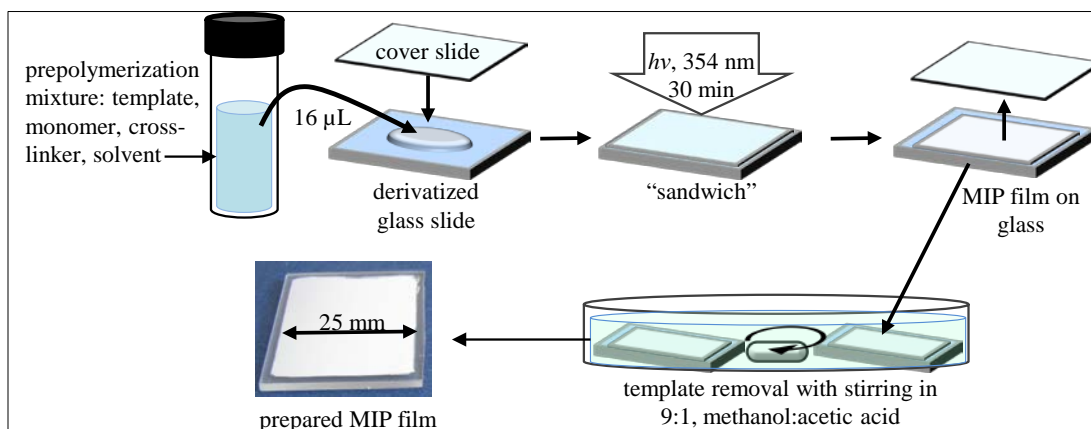


Figure 2-1. The general scheme of fabrication of MIP films by sandwich technique

2.2.2.3 Sandwich technique in a “well”

The square frame was cut with a fine razor from a polyethylene plastic film (a regular food wrap film). The frame had thickness $\sim 10 \mu\text{m}$, $25 \times 25 \text{ mm}^2$ and $15 \times 15 \text{ mm}^2$ outside and inside sizes, respectively. The frame was placed on a glass slide ($25 \times 25 \text{ mm}^2$). A prepolymerization mixture ($20 \mu\text{L}$) was pipetted inside the well and covered with the cover glass ($25 \times 25 \text{ mm}^2$). The subsequent treatment was completed according to the sandwich technique.

2.2.2.4 Sandwich technique to bind MIP particles within a film

Divinylbenzene based MIP particles (30 mg) prepared by precipitation polymerization (Section 2.2.1.) were mixed with $100 \mu\text{L}$ of a viscous MIP prepolymerization mixture to form a stable suspension. The mixture contained phenol (0.200 mmol); 2,2-dimethoxy-2-phenylacetophenone (0.060 mmol); itaconic acid (0.800 mmol); ethylene glycol dimethacrylate (4.00 mmol); 1.00 mL of methanol/water (4:1)

and 0.200 g of polyethylene glycol. An aliquot of the suspension (15.4 μL) was pipetted onto the glass slide and after the polymerization the film was treated according to the sandwich technique (Section 2.2.2.2).

2.2.2.5 Sandwich technique with the application of a membrane frame

This procedure (Figure 2-2) is similar to the production of a film in a “well” with one important difference that the frame is cut from a porous and relatively thick polypropylene membrane. A square frame (25 \times 25 mm² outside and 15 \times 15 mm² inside sizes) was cut (Figure 2-2a) from the membrane and (b) placed onto the derivatized glass (25 \times 25 mm²) to make a square hollow. This frame was soaked with a prepolymerization mixture (~40 μL), then, the mixture drop (~40 μL) was pipetted onto the center of the hollow (c). A cover glass (25 \times 25 mm²) was put onto the mixture above (d) squeezing the excess of the liquid with air bubbles. The film was UV cured (e) and, next, treated according to the primary sandwich technique with one additional step; after polymerization, the membrane frame, which was filled with the polymer, was scratched away with a razor (f) leaving a thick free standing MIP polymer film.

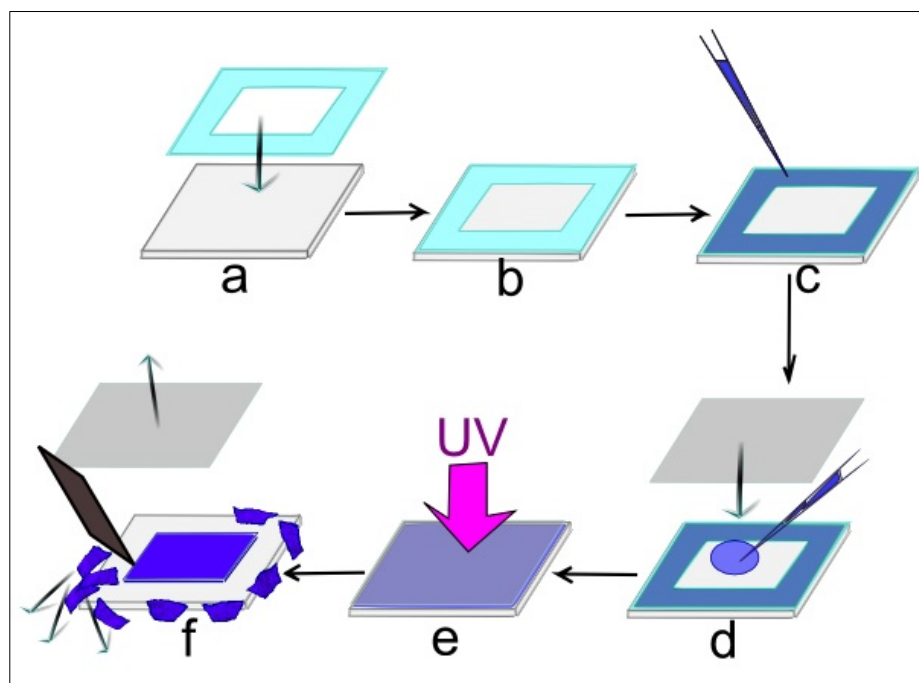


Figure 2-2. Application of sandwich technique to produce ~100 μm thick MIP film by means of a membrane frame.

Note: Steps (a – f) are described in the text: (a, b) the membrane frame was placed on the derivatized glass slide; (c) the membrane frame was soaked with the prepolymerization mixture; (d) the hollow in the membrane frame was filled with the prepolymerization mixture, and the cover glass was placed; (e) UV curing; (f) the cover glass is detached, and the membrane frame is removed with a razor.

2.3 Results and discussion

2.3.1 MIP particles by precipitation polymerization

The same procedure used for MIP synthesis with 2,4,6-trichlorophenol as a template by precipitation polymerization [22] was used for the preparation of MIP particles for phenol and alkylphenols with an alternative template—2,4,6-trimethylphenol. The MIP particles were treated and packed in membrane micro-envelopes for solid-phase extraction, according to the primary work [22]. Originally toluene/acetonitrile (1:3), methacrylic acid, and divinylbenzene were used as a solvent, monomer, and a cross-linker, respectively. When acetonitrile, itaconic acid, and other cross-linkers, such as EGDMA and TRIM, were tested in the synthesis of MIP particles by this procedure, a low yield of particles was observed. Very small particles were formed, almost colloidal in nature; they could easily pass through a 0.2 μm nylon syringe filter. Thus, it was concluded that precipitation polymerization was found to be unsuitable to test a variety of MIP compositions in this project. The content of monomers and thermal initiator have to be optimized for each MIP composition to yield MIP particles, which can be practically used [24]. It would be reasonable to complete such time-consuming experiments for only one most promising MIP formulation in order to apply the MIP for micro solid-phase extraction.

2.3.2 MIP film fabrication

2.3.2.1 The characterization of sandwich technique

According to the sandwich principle, a procedure to fabricate MIP films was compiled. The fabrication process (Section 2.2.2.2) can be broken into three main steps. Photographs of some stages of the fabrication process are presented in Figure 2-3. The steps are the following: deposition of a fixed volume of a prepolymerization mixture on a glass slide, and the placement of a cover glass above the mixture; polymer UV curing and detachment of the cover glass; the removal of the template and unreacted species from MIP films with methanol:acetic acid (9/1), and cutting the film edges with a razor.

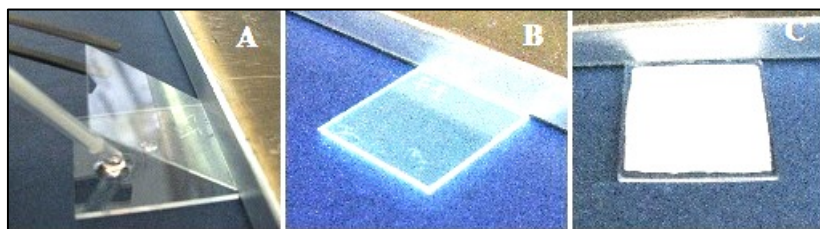


Figure 2-3. Photo pictures for the main steps to prepare MIP films by sandwich technique: (A) deposition of prepolymerization mixture; (B) UV-curing; (C) slide/film after washing step and trimming film edges.

It has been stated previously by Schmidt that the main disadvantages of the sandwich approach are the production of films lacking homogeneity and a narrow range of thicknesses [25]. In the procedure of film preparation in this project, these issues are addressed by controlling the volume of prepolymerization mixture and its viscosity, by using polymeric porogens and removal of the film edges.

Following the sandwich approach, it was decided to control the thickness of the final films by the application of a controlled volume of prepolymerization mixture, which would evenly spread between the glass slide and cover glass without significant leakage over the glass slide borders. In this case, the thickness of the film is the height of a rectangular parallelepiped, whose bases are the glass slide and cover glass. Therefore, the specific volumes of prepolymerization mixture were precisely and quickly delivered with a positive displacement pipette, which is especially suitable for the viscous liquids. As the sandwich assembly is a system with unconstrained sides, large volumes of the liquid mixture cannot be applied because they can leak out the border of the glass slide. It was found that prepolymerization mixture volumes of 13–17 μL could be entrapped without a significant leakage. When the volume of the prepolymerization mixture was less (5 – 10 μL), the produced films had visible non-uniformity in terms of the thickness, with voids. Such uneven spreading of the polymer on the glass slide can be due to the erratic shrinkage of the polymer network of the small volume during the course of polymerization. Also, the variance of film thickness can be caused by the limited planarity of the glass slide/cover glass affects the uniformity of coating of the glass slide with the prepolymerization mixture when small volumes are used. When volumes larger than 18 μL were applied, the prepolymerization mixture leaked significantly, and the thickness of the final film could not be increased, as estimated visually. The films had a smooth and uniform surface, as estimated by the human eye. The thickness of the film may not be a crucial factor when these films are coupled with a detection technique where the analytical signal is formed mostly on a film surface, for example, desorption mass

spectrometry (DESI, MALDI) and surface enhanced Raman spectrometry (SERS). The fact that the thickness of the fabricated films was only tens of microns (discussed in Chapter 4¹) can ensure a relatively fast absorption rate within the whole depth of polymer networks of the films.

A liquid has to be of a sufficient viscosity [16] not to be squeezed under the weight of a cover glass and to be retained in the sandwich even when a moderate volume of liquid is applied. For this reason, too thin films with surface defects were produced when a significantly fluidic prepolymerization mixture was used. Components that decreased the viscosity of a prepolymerization mixture were styrene, divinylbenzene, chloroform, and other low polarity liquids. Conversely, the mixture could be made more viscous with the addition of high molecular weight linear polymers [13, 17, 25] such as polyvinyl acetate (PVA) and polyethylene glycol (PEG). In this project, these polymers were preferred because they contain the same functional groups and moieties as most of cross-linkers: a glycol chain, alkyl chain, and ester linkage. Therefore, they should mostly change rheological properties of the prepolymerization mixture, but not its chemical composition to a significant extent. Another very crucial effect of the linear polymers is to influence the porosity of films, which is discussed below (Section 2.3.3).

When volatile solvents such as acetonitrile, methanol/water, and chloroform were used; they evaporated from the reaction mixture situated close to the edges of a glass slide during the course of the polymerization process. It was very important to pipet the prepolymerization mixture and apply the cover glass quickly and accurately to reduce the

¹ the thickness and morphology of the films will be studied in Chapter 4

exposure of the mixture to air. Also, close to the edges of a glass slide, polymerization is quenched by oxygen in air. These factors yielded a film with glassy and/or flaky edges. In order to eliminate these problematic spots around the film, it was decided to use as large as possible cover glass (25×25 mm²), which completely covers the glass slide. Afterward, film edges of poor quality, which were close to the edges of the slide, were scraped off with a razor, leaving a large area of uniform film. Thus, when in-situ fabrication was of interest, initially a larger cover glass was applied, taking into account that after polymerization the area of the film would be reduced by trimming.

To avoid solvent evaporation, quenching by oxygen, and to produce films of controlled thickness, attempts were made to fabricate a polymer film by sandwiching in a “well”, where the reaction mixture was better isolated from air and the film thickness would be determined by the thickness of the frame placed in between the glass slide and cover glass. However, it was difficult to avoid air bubbles being trapped in the “well”. Therefore, larger volumes of a prepolymerization mixture were deposited into the “well” to squeeze the bubbles out with the excess of prepolymerization mixture when the cover glass was applied. However, the produced films showed visible voids on the surface. Probably, the fixed volume of the well prevented the polymer contracting without voids when the polymer volume was naturally decreasing during the polymerization [25].

2.3.2.2 Sandwich technique to bind MIP particles within a film

When MIP particles are glued to a surface to form a film, the durability of such films is poor [11]. In this work this problem was solved when the particles were “glued” by polymerization. MIP particles were initially prepared by the precipitation

polymerization; then, were mixed with a MIP prepolymerization mixture, which was highly viscous, to form a stable suspension. Polymerization through sandwiching on the glass slide yielded a porous composite material, which was similar to concrete, where sand particles are bound within the cement. This film was stable under stirring in aqueous solutions, having the same mechanical stability as other films made by the sandwich technique. Later (Chapter 5), it will be shown that the use of divinylbenzene and other aromatic functional monomers for the MIP synthesis benefits the binding capacity of the MIP films towards phenol. However, it was observed (Section 2.3.2.1) that it was hard to produce films from prepolymerization mixtures that contained a high content of divinylbenzene or styrene. Alternatively, the films were easily fabricated to incorporate divinylbenzene-MIP particles; thus, the fabrication of films with a significant content of divinylbenzene can be possible.

2.3.2.3 Sandwich technique with the application of a membrane frame

The sandwich technique, with a free standing or unsupported layer of a prepolymerization mixture, could produce relatively thin films. As was mentioned earlier, thicker films can be required to achieve higher sensitivity of detection by the increase of the amount of loaded analyte per area, as needed for solid-surface fluorimetry (Chapters 7 and 8). Thicker films can be produced by polymerization within a host porous film, for example, membrane or filter paper [2, 20, 21]. The final film would render not only the thickness from the host film, but also the final adsorbent material of the film will contain the host matrix of the substrate film. The procedure to make a composite film [20, 21] was modified in order to produce a homogenous thicker MIP film using a membrane

frame with a square hollow (Figure 2-2). The membrane substrate determined the thickness of the film, here $\sim 100 \mu\text{m}$; at the end of the fabrication process the frame was removed, leaving a MIP film of a defined thickness. An important finding was that the material of the frame needed to be porous and soaked with the prepolymerization mixture. This lets the polymer network shrink at the edges of the frame, which avoids the non-uniformity of the film thickness in the hollow. Also, the soaked membrane provided a very tight seal between the junctions of glass slide/the membrane frame/the cover glass. This isolates a polymerization mixture in the hollow from the air and inhibits solvent evaporation. Such sealing cannot be achieved between smooth and hard surfaces, e.g., of photoresist or glass. A monolithic frame, made in a photoresist film, or a well, etched in the glass slide, are probably less suitable for the production of thick and uniform films.

2.3.3 The morphology of fabricated films

When common organic solvents (such as dimethylformamide, chloroform, dimethylsulfoxide, acetonitrile, toluene, and chloroform) were used as solvents in MIP prepolymerization mixtures, non-porous or low porosity films were obtained. Photos and electron microscope images for such films are shown in Appendix B. The polymer network of these films shrinks upon the evaporation of the solvents [26] and, as a result, the films flake from a glass slide. These films also had many surface defects such as cracks and variable coloration. Adsorption by these non-porous films probably takes place on the surface and in pores close to the surface, while the deeper MIP layers do not participate in the adsorption, which limits the adsorption capacity. Therefore, one goal of this work was set to fabricate highly porous films.

The porosity of the fabricated films was assessed on the basis of the permeability with solvent, and opaqueness. The porous films appeared to be mechanically stable and uniform. Protic solvents and the linear polymers used as co-porogens have an important role in the formation of porous networks. The processes occurring in the formation of the polymer network are very complex, and they can be only approximated. In brief [26, 27], as a polymer network grows in a solvent, the growing oligomers reach a solubility limit and precipitate into nuclei. When the solvent solvates the polymer network efficiently, the nuclei are swollen better with the solvent rather than with a monomer. Such solvent is called “good”. Consequently, a large number of small polymeric globules form a network with small pores. All aforementioned solvents, like dimethylformamide, dimethylsulfoxide, and toluene, can be classified as “good” solvents. The films prepared with these solvents are visually dense and glassy or slightly opaque, or non-porous. When the solvent is “poor” having low solvation ability, e.g. methanol/water, the nuclei are swollen preferably with a monomer. As a result, a limited number of the nuclei grow into large globules, which precipitate out of the reaction mixture, forming a polymer network with a granular and porous structure. Another way to produce a porous network is the use of an additional polymer. If another polymer is added into a solvent, e.g., dimethylformamide, the solubility of growing polymer chains can be reduced. As a result, the chains precipitate into nuclei at an early stage of the polymerization [13, 25]. In order to reduce the surface energy of the formed nuclei, they will grow into large globules [27], which will also form the granular and porous morphology of the films.

A large number and variety of MIP compositions were tested for their ability to produce porous films. It was observed that the porosity of the films depended mostly on macro components such as solvent and cross-linker. At the same time, the porous morphology was very sensitive to the content of the linear polymers (PVA and PEG). A content of PVA and PEG that can produce a sufficiently porous network was determined for various MIP formulations, for examples see Table 2-1. The nature and proportion of functional monomer, e.g., itaconic acid and styrene, altogether with template, e.g, phenol and dihydroquinone, did not appear to have a dramatic effect on the morphology. However, the functionality of a monomer affected the wettability of the film with water. For example, styrene and 4-vinylpyridine made films of low wettability; while itaconic acid had the opposite effect because of the highly polar and protic nature of itaconic acid (Table 2-1).

Table 2-1. Visual characterization of selected films prepared by sandwich technique

<i>Compositions of the prepolymerization mixtures</i>	<i>phenol DMPA Sty EGDMA 6% (w/w) PVA in DMSO</i>	<i>phenol DMPA Sty TEGDMA methanol:water (3/1)</i>	<i>phenol DMPA IA EGDMA 15% (w/w) PEG in DMF</i>	<i>phenol DMPA IA EGDMA 10% (w/w) PVA in DMF</i>	<i>phenol DMPA 4-VP EGDMA 10% (w/w) PVA in CHCl₃</i>
Visual appearance of film surface	smooth and fine-grained	smooth and slightly glossy	smooth and fine-grained	smooth and medium-grained	smooth and large-grained, slightly opalescent
Wettability with water	slow	good	good	good	very poor unless prewetted with acetonitrile
Special notes	pre-polymerization mixture is of very low volatility and can be used for spin-coating	the highest observed resistance to scratching; further characterization in Chapter 4	further characterization in Chapter 4	further characterization in Chapter 4	further characterization in Chapter 4

Note: DMPA – 2,2-dimethoxy-2-phenylacetophenone; EGDMA – ethyleneglycol dimethacrylate; TEGDMA – triethyleneglycol dimethacrylate; Sty – styrene, IA – itaconic acid, 4-VP – 4-vinylpyridine, DMF – dimethylformamide, DMSO – dimethyl sulfoxide, PEG – polyethylene glycol, PVA – polyvinyl acetate

Although the majority of fabricated films were porous and white, they were different in their texture and, what is practically important, in their mechanical durability, e.g., resistance to scratching. It is not exactly clear how the components of a prepolymerization mixture determine the specific features and properties of film morphology. The formation of the morphology is very complex and influenced by many factors. Some films were porous but they still had a slightly glossy texture and brittle, while other films were of a spongy texture and were prone to crumble. Among the variety of prepared films, some of them (Table 2-1) can be highlighted for their high mechanical durability, optimal porosity, and perfect uniform texture, in other words, a superior quality of film morphology. The high mechanical durability for the film made from TEGDMA (Table 2-1) can be explained by the fact that TEGDMA molecule is long and highly flexible, forming an elastic structure. Though, the MIP films of these compositions appeared to have weak or no imprinting towards phenol, which will be shown in Chapter 4, their NIP films still could be used as adsorbent layers for phenols and other hydrophobic species. These compositions (Table 2-1) can be varied in terms of a template and monomer to fabricate other MIP films with a high quality of morphology.

2.4 Conclusions

Based on the sandwich principle, polymerization between two planar surfaces, procedures were developed to fabricate various MIP films: ~20 μm thin films, films from MIP particles, and ~100 μm thick films with the help of a membrane frame. Care was taken to fabricate uniform, durable, and porous films. In the fabrication process, it was crucial to have a free standing layer of the prepolymerization mixture, which reduced the

detrimental effect of polymer network shrinkage on the evenness of film surface. The use of a large cover glass and trimming film edges, eliminated the effect of solvent evaporation and quenching of polymerization with oxygen from air. An important requirement for the prepolymerization mixture was to be viscous, so that it was not squeezed under the weight of the cover glass. In the simplest case, films of limited thickness in the range of tens microns were produced, and the thickness of the films was mostly determined by the volume of prepolymerization mixture that could be freely entrapped between the two surfaces. In order to produce thicker films, the sandwich technique was modified with the use of a porous membrane frame, whose thickness determined the thickness of the final film. Although low-polar and low viscous monomers did not work well for the production of films, films were also able to be fabricated from divinylbenzene-based particles by their incorporation into a composite MIP film. The porous morphology of fabricated films was necessary not only for the high surface area available for mass transfer, but also for the uniformity and mechanical stability of these films. The morphology of the films was influenced by many factors in a complex way and, therefore, the MIP compositions that produced good quality films were investigated mostly empirically; in particular, varying solvent system. A porous morphology was formed by the use of protic solvent, or apolar and low-polar solvents with the addition of polymeric additives (PEG and PVA).

2.5 References

1. Lanza, F.; Sellergren, B., Method for synthesis and screening of large groups of molecularly imprinted polymers. *Analytical Chemistry* **1999**, *71* (11), 2092-2096.
2. Pérez-Moral, N.; Mayes, A., Novel MIP formats. *Bioseparation* **2001**, *10* (6), 287-299.
3. Mayes, A. G.; Whitcombe, M. J., Synthetic strategies for the generation of molecularly imprinted organic polymers. *Advanced Drug Delivery Reviews* **2005**, *57* (12), 1742-78.
4. Spivak, D. A., Optimization, evaluation, and characterization of molecularly imprinted polymers. *Advanced Drug Delivery Reviews* **2005**, *57* (12), 1779-94.
5. Pichon, V.; Chapuis-Hugon, F., Role of molecularly imprinted polymers for selective determination of environmental pollutants—a review. *Analytica Chimica Acta* **2008**, *622* (1-2), 48-61.
6. Lasakova, M.; Jandera, P., Molecularly imprinted polymers and their application in solid phase extraction. *Journal of Separation Science* **2009**, *32* (5-6), 799-812.
7. Schweitz, L.; Andersson, L. I.; Nilsson, S., Molecular imprint-based stationary phases for capillary electrochromatography. *Journal of Chromatography A* **1998**, *817* (1-2), 5-13.
8. Sambe, H.; Hoshina, K.; Moaddel, R.; Wainer, I. W.; Haginaka, J., Uniformly-sized, molecularly imprinted polymers for nicotine by precipitation polymerization. *Journal of Chromatography A* **2006**, *1134* (1-2), 88-94.
9. Wang, D.; Hong, S.; Yang, G.; Row, K., Caffeine Molecular Imprinted Microgel Spheres by Precipitation Polymerization. *Korean Journal of Chemical Engineering* **2003**, *20* (6), 1073-1076.
10. Kan, X.; Zhao, Q.; Zhang, Z.; Wang, Z.; Zhu, J. J., Molecularly imprinted polymers microsphere prepared by precipitation polymerization for hydroquinone recognition. *Talanta* **2008**, *75* (1), 22-6.
11. Harz, S.; Schimmelpfennig, M.; Tse Sum Bui, B.; Marchyk, N.; Haupt, K.; Feller, K.-H., Fluorescence optical spectrally resolved sensor based on molecularly imprinted polymers and microfluidics. *Engineering in Life Sciences* **2011**, *11* (6), 559-565.

12. Feng, Q.; Zhao, L.; Lin, J. M., Molecularly imprinted polymer as micro-solid phase extraction combined with high performance liquid chromatography to determine phenolic compounds in environmental water samples. *Analytica Chimica Acta* **2009**, *650* (1), 70-76.
13. Schmidt, R. H.; Mosbach, K.; Haupt, K., A Simple Method for Spin-Coating Molecularly Imprinted Polymer Films of Controlled Thickness and Porosity. *Advanced Materials* **2004**, *16* (8), 719-722.
14. Van Biesen, G.; Wiseman, J. M.; Li, J.; Bottaro, C. S., Desorption electrospray ionization-mass spectrometry for the detection of analytes extracted by thin-film molecularly imprinted polymers. *The Analyst* **2010**, *135* (9), 2237-40.
15. Haupt, K.; Noworyta, K.; Kutner, W., Imprinted polymer-based enantioselective acoustic sensor using a quartz crystal microbalance. *Analytical Communications* **1999**, *36* (11-12), 391-393.
16. Jakusch, M.; Janotta, M.; Mizaikoff, B.; Mosbach, K.; Haupt, K., Molecularly imprinted polymers and infrared evanescent wave spectroscopy. a chemical sensors approach. *Analytical Chemistry* **1999**, *71* (20), 4786-4791.
17. Sergeyeva, T. A.; Gorbach, L. A.; Slinchenko, O. A.; Goncharova, L. A.; Piletska, O. V.; Brovko, O. O.; Sergeeva, L. M.; Elska, G. V., Towards development of colorimetric test-systems for phenols detection based on computationally-designed molecularly imprinted polymer membranes. *Materials Science and Engineering: C* **2010**, *30* (3), 431-436.
18. Kryscio, D. R.; Peppas, N. A., Surface imprinted thin polymer film systems with selective recognition for bovine serum albumin. *Analytica Chimica Acta* **2012**, *718*, 109-15.
19. Singh, K. P., Use of isoproturon imprinted polymer membranes as a selective recognition platform in a resistance based electrochemical sensor. *Open Journal of Applied Biosensor* **2013**, *02* (01), 20-28.
20. Hong, J. M., Separation of Chemically Similar Molecules by Molecular Recognition. *Journal of Industrial and Engineering Chemistry* **1998**, *4* (3), 226-230.

21. Ballarin, B.; Brumlik, C. J.; Lawson, D. R.; Liang, W.; Van Dyke, L. S.; Martin, C. R., Chemical sensors based on ultrathin-film composite membranes – a new concept in sensor design. *Analytical Chemistry* **1992**, *64* (21), 2647-2651.
22. Feng, Q.; Zhao, L.; Lin, J. M., Molecularly imprinted polymer as micro-solid phase extraction combined with high performance liquid chromatography to determine phenolic compounds in environmental water samples. *Analytica Chimica Acta* **2009**, *650* (1), 70-76.
23. Cras, J. J.; Rowe-Taitt, C. A.; Nivens, D. A.; Ligler, F. S., Comparison of chemical cleaning methods of glass in preparation for silanization. *Biosensors and Bioelectronics* **1999**, *14* (8–9), 683-688.
24. Shim, S. E.; Yang, S.; Jin, M.-J.; Chang, Y. H.; Choe, S., Effect of the polymerization parameters on the morphology and spherical particle size of poly(styrene-co-divinylbenzene) prepared by precipitation polymerization. *Colloid and Polymer Science* **2004**, *283* (1), 41-48.
25. Schmidt, R. H.; Haupt, K., Molecularly imprinted polymer films with binding properties enhanced by the reaction-induced phase separation of a sacrificial polymeric porogen. *Chemistry of Materials* **2005**, *17* (5), 1007-1016.
26. Vendamme, R.; Eevers, W.; Kaneto, M.; Minamizaki, Y., Influence of polymer morphology on the capacity of molecularly imprinted resins to release or to retain their template. *Polymer Journal* **2009**, *41* (12), 1055-1066.
27. Brazier, J. J.; Mingdi, Y., Micromonoliths and microfabricated molecularly imprinted polymers. In *Molecularly Imprinted Materials: Science and Technology*, Mingdi, Y.; Ramström, O., Eds. Marcel Dekker: New York, USA, 2005; pp 492-494.

Chapter 3. Study of Functional Monomer-Template Interactions

3.1 Introduction

To develop a MIP with a pronounced imprinting effect, MIP components need to be carefully selected in terms of a functional monomer, solvent, and cross-linker. This screening task can be completed by computer simulations of the functional monomer-template interactions [1]. Another common approach is combinatorial screening [2], where a large number of MIPs of different compositions are synthesized in micro-scale and studied at template rebinding studies with a semi-automated system [3]. The results are treated with chemometrics to assess the effect of each experimental factor, e.g., the nature of a component and its content. The initial choice of functional monomers can be guided by the chemistry of the monomer-template interactions. These interactions should be studied with a spectroscopic technique, e.g, fluorimetry and UV spectrophotometry [4, 5]. This method does not require complex equipment, such as the combinatorial approach, and promises to give realistic results because they are based on experimental measurements, and not computer simulations. Thus, spectroscopic studies were applied in this research project.

The key step in the MIP synthesis by a non-covalent approach is the formation of the prepolymerization complex between a template and monomer, and the strength of this complexation determines the MIP imprinting effect [1, 4]. A wide variety of vinyl monomers are available to be selected for complexation with almost any template [1, 6]. A solvent in the polymerization mixture plays an important role in facilitating the complexation with template. The solvent has to be matched according to the monomer used and the type of interaction to be developed. Thus, there is a need to screen a wide

range of monomers and solvents to invent an efficient MIP. It is obvious that the best way for such screening is template rebinding studies. However, these experiments are multi-step, complex, and laborious. It would be reasonable to select several functional monomers if they can interact strongly with a template in a certain solvent. This limited number of monomers should be used to prepare MIPs, which can be tested in more elaborate rebinding experiments. This selection can be accomplished based on the monomer-template interactions. These experiments can reveal not only the presence of the interactions, but also their relative strength, for example, for monomers bound to the same template [4-6]. The stoichiometry also can be studied for better understanding the imprinting process [4].

Methods to study monomer-template interactions can be divided into two groups: computational and spectroscopic [7]. A computational method estimates the free energy of binding between a template and a monomer in simulated annealing experiments, e.g., with the LeapfrogTM algorithm [6, 8]. As a result, a limited number of monomers with a high energy of binding can be selected from a wide library of monomers. However, the effect of a solvent, as the environment for these interactions, is not estimated because the addition of the solvent to the computational model will make this model too complex.

The following spectroscopic techniques have been applied to study monomer-template interactions. Nuclear magnetic resonance (NMR) spectroscopy is often used to study hydrogen bonding based on a change of a chemical shift for proton participating in the bond formation [9, 10]. It is a very common technique used in MIP studies, but this technique requires expensive equipment and deuterated solvents. A NMR titration is used

for the determination of association constants [11]. Absorbance spectrometry can be applied not only to study hydrogen bonding, but also other kinds of interactions, e.g., metal coordination, electrostatic interactions, π - π stacking [1, 12, 13], and others that influence molecular electron density. Thus, this technique can play an important role in the study of a wide range of interactions employed for MIP synthesis. Only solvents that are sufficiently transparent in the UV region can be used; aromatic solvents, such as toluene, and acetone are not normally used in the UV range. The interaction can result in a change of peak shape, shift of the peak maximum, and/or in a rise or drop of the maximum absorbance value [13]. Absorbance spectrometry is a classical method used to determine the complexation stoichiometry and association constants. The straightforward calculation of association constant can be performed for systems where spectral changes are observed in a large excess of a monomer [11]. Absorbance spectrometry has been used in the selection of monomers [4, 11, 13] and solvents [5]. The association constant of a prepolymerization complex was successfully correlated with the MIP binding and imprinting properties [4, 14]. Infrared spectroscopy is used to observe the alteration of the vibrational frequency of a specific bond upon a binding event due to the change of bond length. The most convenient way to observe hydrogen bonding is to probe the vibrational frequency of a carbonyl group at 1600 – 1700 cm^{-1} [5, 7], but not the frequency of amino and hydroxyl groups. The bands from amino and hydroxyl groups, which are around 3000 cm^{-1} and over, are too broad because they exist in a variety of solvation and binding conditions [15]. IR spectra are usually highly populated, and they can be easily analyzed only for simple mixtures in terms of a variety of functional groups and moieties. Also,

protic and highly polar solvents make IR spectra difficult to interpret with respect to monomer-template interactions. IR spectroscopy has been used for the following systems: monomer-template mixtures based on chloroform [9] and hexane [16] with a simple IR background; mixtures of template with a monomer without solvent [17]; and the dry MIP networks with a loaded adsorbate [7]. The last two approaches have the drawback that the crucial role of the solvent is not accounted for and the interaction is too simplified.

To synthesize a MIP that targets phenol and alkylphenols, initially phenol was chosen as a template. In this work, characterization of interactions between phenol and various functional monomers in a series of solvents was attempted with Raman spectroscopy and UV-absorbance spectrometry. Raman spectroscopy was applied as an alternative to IR absorbance spectroscopy to probe complexation with phenol. The main advantage to using Raman spectroscopy is that it has the potential to be applicable to complex mixtures based on polar and protic solvents, where the IR technique is not suitable. To the best of my knowledge, Raman spectroscopy has not been applied to study monomer-template interactions before. UV-absorbance spectroscopy was selected as a second technique to exploit the fact that phenol is an aromatic compound with strong absorbance peaks in the UV region, which may be sensitive to the presence of the interactions with monomers. Also, this technique is attractive due to its simplicity, universality, and equipment availability.

3.2 Materials and methods

Phenol (98%), itaconic acid (99%), styrene (99%), and 4-vinylpyridine (95%), *N,N*-dimethylformamide (DMF) (ACS reagent, <0.005% water), 1-octanol ($\geq 99\%$), ethylamine

(70% in water), allylamine (98%) were purchased from Sigma-Aldrich (Oakville, ON, Canada). Chloroform (stabilized with amylenes), acetic acid, diglyme, acetonitrile, and dimethylsulfoxide (DMSO) that are all of the ACS reagent grade were purchased from ACP Chemicals (Montreal, QC, Canada).

3.2.1 Raman spectroscopic measurements for liquid samples

Raman spectra were measured for relatively highly concentrated solutions of phenol (1.20 mmol g⁻¹), monomer (1.20 mmol g⁻¹), and phenol and monomer mixture (1.20 mmol g⁻¹ of each solute) to assure intense Raman bands from the solutes. These solutions were prepared by weighing the solutes and solvents (DMSO, DMF, methanol/water (4:1)), and the molal concentration is shown. The solutions were filled in 2 mL-glass vials made of ordinary glass. A Raman microscope (LabRAM, Jobin Yvon Horiba, 532 nm 70 mW laser, the confocal geometry) was adapted to measure Raman scattering from solutions through the vial walls. The laser beam was tightly focused with 10×objective at the surface of the vial wall. Measurement parameters were the following: no beam attenuation; hole and slits were 300 and 150 μm, respectively; scanning from 200 – 3500 cm⁻¹ at 60 s acquisition; two scans for each measurement were run at the same focusing, and each spectrum is an average of the two measurements.

3.2.2 UV-absorbance measurements

Absorbance spectra of phenol solutions with various monomers were measured with a Thermo Scientific Evolution 600 UV-Vis Spectrophotometer (Thermo Scientific, Ottawa, ON, Canada) against a reference solution with the same concentrations of the monomer. The concentration of phenol was set at 0.3 mM when the B-band (~270 nm)

was investigated and 0.1 mM in the case of the E2-band (~220 nm). Various ratios of phenol to a monomer were probed with the highest ratio at 1:4. A phenol absorbance spectrum can be seriously affected by the imbalance of monomer concentrations in the sample and reference solutions, especially, when this monomer significantly absorbs in UV region, as does styrene. In order to have the equality of the monomer concentrations, a stock phenol solution or a solvent (if to prepare the reference solution) were reconstituted with the same solution of the monomer in calibrated volumetric flasks. The absolute absorbance (not relative) of the solutions was over 1.5 mainly due to the high absorbance of the solvent itself in the UV region (e.g. for DMSO, DMF, and diglyme). Therefore, a wide bandwidth (4 nm) and slow scan rate (10 nm min^{-1}) were set to diminish the level of the noise in the measurements.

3.3 Results and discussions

3.3.1 Study of monomer-template interactions

3.3.1.1 Raman spectroscopy

The interaction between a monomer and template can be inferred from shifts of vibrational bands associated with Raman scattering. To assign bands to a monomer, template, and solvent, individual Raman spectra for solvent, monomer solution, and template solution were recorded (Figure 3-1). Phenol-styrene solution in methanol/water (4:1) is a complex system from a spectroscopic point of view; its spectrum is populated with bands from the two aromatic species and the binary solvent. However, it is possible to distinguish bands from phenol and styrene, which do not overlap with each other and the solvent. These bands are mainly attributed to aromatic ring breathing modes: 812 cm^{-1}

for phenol and 773, 1182, 1204, 1416; and CH stretching at 3013 cm^{-1} for styrene. No significant shifts of these bands were observed when spectra for the solution of phenol and the phenol-styrene solution were compared (Figure 3-1). A similar situation was observed for phenol-styrene solution in DMSO. The fact that no band shifts were observed can be explained by either limited susceptibility of ring-breathing vibrations to the hydrophobic interactions and/or such highly concentrated solutions were not suitable for the study of these interactions.

The presence of hydrogen bonding was evaluated in phenol and itaconic acid solutions in two solvents: DMF and DMSO. These solvents, as proton acceptors, can promote the dissociation of itaconic acid with the production of the anion, which can readily bind with the phenolic hydroxyl group. A phenol vibration at 1167 cm^{-1} involves hydroxyl moiety, therefore -OH band may be affected by hydrogen bonding. This band can be assigned to “CH and OH bending coupled to CC stretching” [18]. Although many phenol bands can be distinguishable for the studied solutions, this phenol band at 1167 cm^{-1} , which was relevant to the study, was hidden by other bands from the solvents (DMF and DMSO) and itaconic acid.

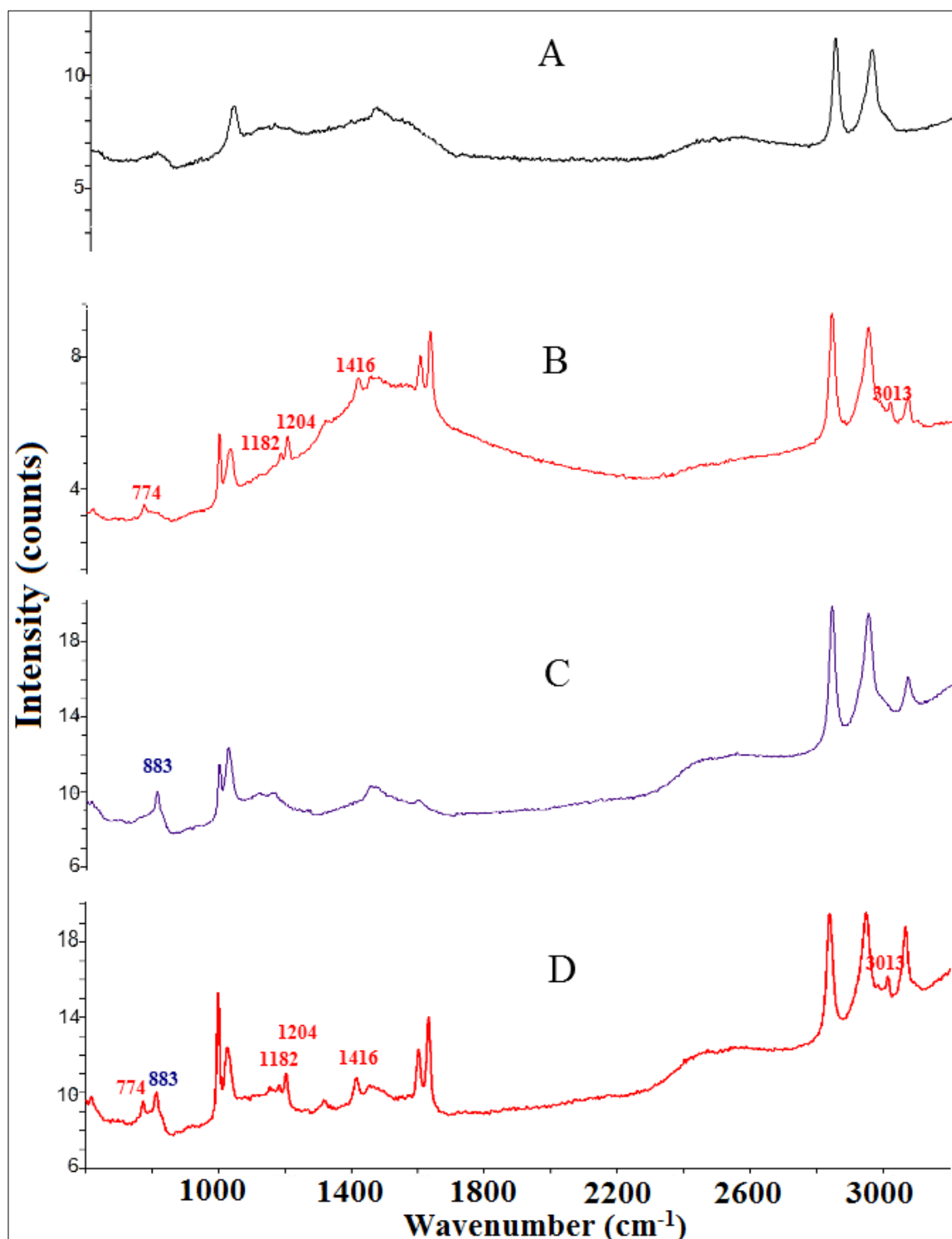


Figure 3-1. Raman spectra (532 nm) measured for (A) methanol/water (4:1) as solvent, and solutions of (B) styrene, (C) phenol, and (D) phenol and styrene (1:1).

3.3.1.2 UV-absorbance spectrometry

The UV-absorbance spectrum of monoaromatics, including phenol, consists of wide and featured E2 and B bands (Figure 3-2), which are attributed to π - π^* transitions in benzene rings and can be shifted upon a change of the solvation environment [19]. Thus, UV-absorbance spectrometry was used to probe possible interactions between phenol and itaconic acid, 4-vinylpyridine, and styrene based on spectral changes of the phenol spectrum. A wide variety of solvents were tested as a medium to promote the complexation between phenol and a certain monomer: acetonitrile, DMSO, DMF, and methanol/water (4:1) with itaconic acid; DMF, diglyme, DMSO, methanol/water (4:1) with styrene; DMSO, chloroform, and methanol/water (4:1) with 4-vinylpyridine. The majority of solvents, such as DMSO, chloroform, DMF, diglyme have limited transparency in the UV region, which makes it possible to probe only the part of the phenol spectrum, which is over 260 nm, i.e., B-band. In the solvents tested, all three selected monomers caused no, or very little, spectral change in the B-band of phenol centered at ~270 nm.

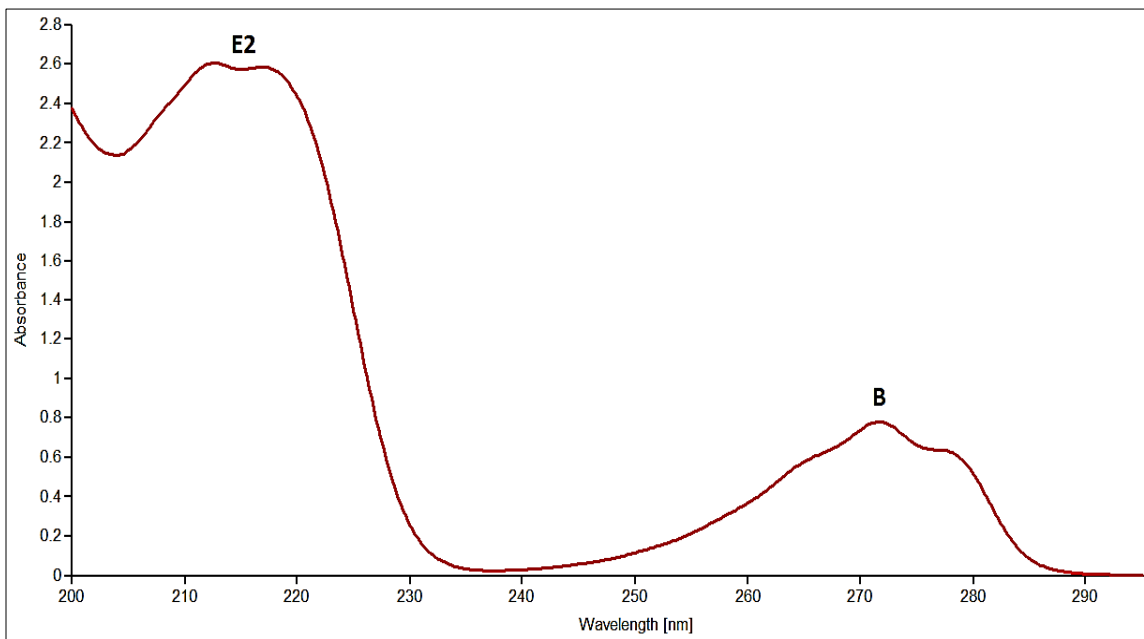


Figure 3-2. UV-absorbance spectrum of phenol (0.5 mM) in MeOH:H₂O (4:1).

Methanol/water has UV a cutoff at 200 nm, therefore, the phenol E2 band can be monitored in this solvent system. It was found that styrene had a dramatic effect on this band in terms of band narrowing (Figure 3-3), but no changes of the B-band were observed. Spectral changes in the E2 band were tracked in a much dilute phenol solution (0.1 mM), where solute molecules do not interact significantly with each other because of the low concentration. Thus, an association between styrene and phenol was shown.

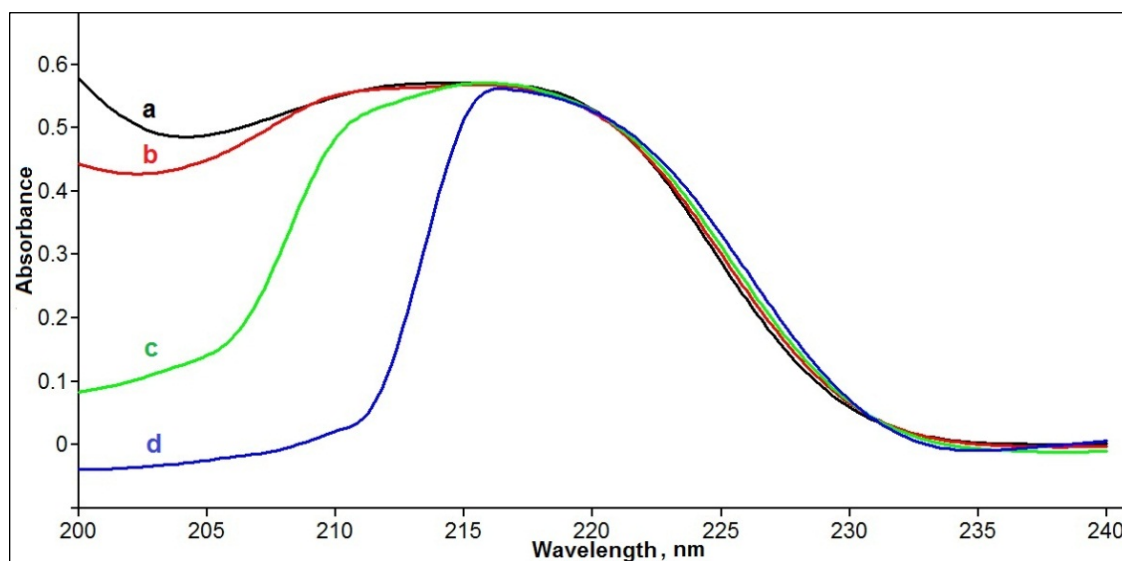


Figure 3-3. Effect of styrene on E2-band of phenol in MeOH:H₂O (4:1); phenol concentration – 0.100 mM; styrene concentrations: (a) 0; (b) 0.100; (c) 0.200; (d) 0.400 mM.

An interesting observation was that the E2 band of phenol displayed a hyperchromic effect with band narrowing upon the addition of itaconic acid (Figure 3-4). Although methanol/water is not the best media to assess hydrogen bonding, it is possible that this solvent facilitates the dissociation of itaconic acid by the effective solvation of its anion, which can interact with the phenolic hydroxyl group through the two carboxyl groups.

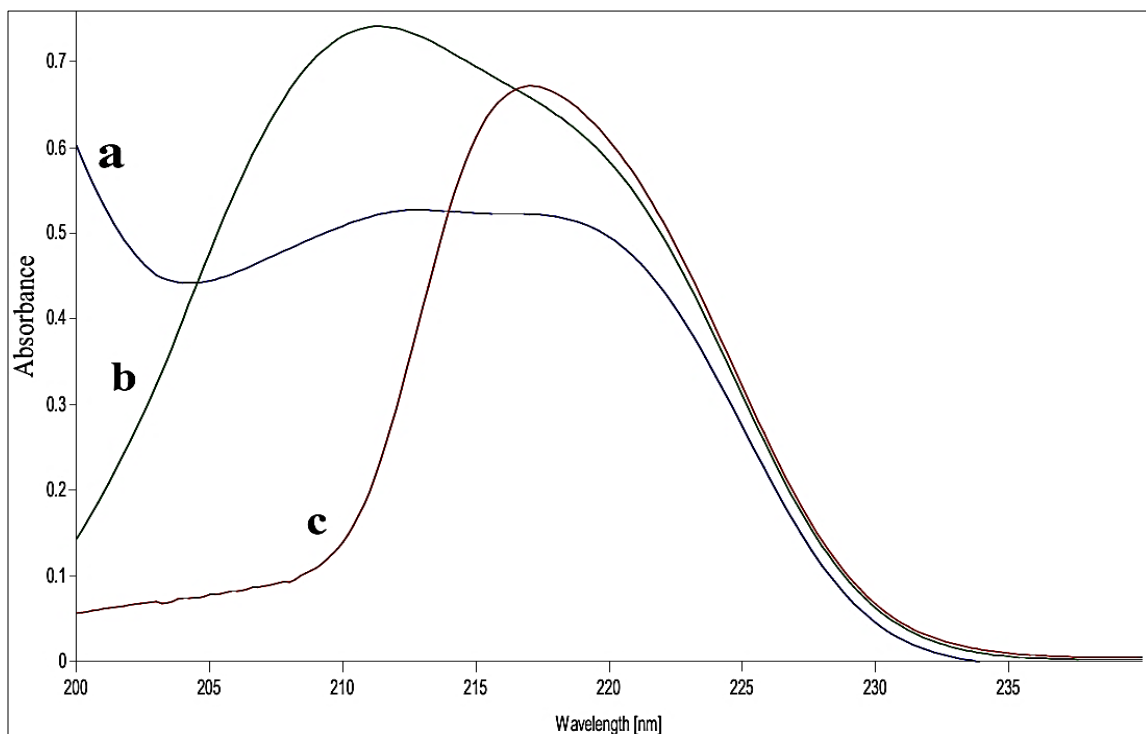


Figure 3-4. Effect of itaconic acid on E2-band of phenol in MeOH/H₂O (4:1); phenol concentration – 0.100 mM; itaconic acid concentrations: (a) 0; (b) 0.400; (c) 0.800 mM.

The effect of 1-octanol, acetic acid (or acetate anion after the dissociation), ethylamine, and allylamine on the E2-band of phenol was also studied. These agents did not cause any spectral changes for phenol. The comparison of the effects of styrene and 1-octanol suggested that the complexation between phenol and styrene can be attributed to the aromatic nature of styrene. The comparison of the effects of itaconic acid and other proton acceptors (acetic acid, ethylamine, and allylamine) suggested that itaconic acid ($pK_a=3.85, 5.45$) induced the phenol spectral changes, and they are not only because it is a carboxylic acid and it has a vinyl group. The fact that itaconic acid has two carboxyl

groups and/or itaconic acid is highly polar plays an important role in the complexation with phenol.

It might be concluded that there was no complexation between a monomer and template based on the lack of spectral changes according to one method, for example, monitoring the B band of phenol. However, it can be assumed that the B-band is not very sensitive to the interactions. The same interactions described in this section that did not undergo spectral changes of the B-band of phenol, were confirmed by other scientists: phenol and 4-vinylpyridine in chloroform with NMR [9]; phenol and the anion from itaconic acid computationally with the LeapfrogTM algorithm [6]. The fact that changes in the phenol B-band are negligible may serve as an evidence that the interactions developed between phenol and the monomers are not strong. For comparison, dramatic spectral changes were observed by Feng et al. for 2,4-dichlorophenol at 295 nm upon the addition of 4-vinylpyridine in the low-polar environment of chloroform [20]. The same spectral changes could not be observed in the case of phenol. It is possible to expect that much stronger hydrogen bonding is formed between the pyridinium nitrogen and the more acidic phenolic hydroxyl group in 2,4-dichlorophenol. The subtle nature of the interactions between phenol and the studied monomers probably can be one of reasons why phenol imprinted polymers showed little or no imprinting effect towards phenol in the binding studies, described in the next chapter (Chapter 4).

3.4 Conclusions

The presence of interactions between phenol and itaconic acid and styrene in a variety of solvents were studied with Raman and UV-absorbance spectroscopies. Although in the case of the phenol systems, Raman spectroscopy is not applicable, the technique has a potential to be applied for other templates whose key bands do not overlap and/or are satisfactorily intense. It was demonstrated that Raman spectroscopy can resolve a few vibrational bands in complex mixtures based on highly polar and water containing solvents; the cases where IR spectroscopy is not suitable. The application of UV-absorbance spectrometry is limited by solvent transparency, which makes it possible to observe only the phenol B-band for the majority of organic solvents. The fact that the phenol B-band was not sensitive to the presence of the monomers can indicate that the complexation between phenol and these monomers is either absent or weak. However, the E2 phenol band was sensitive to styrene and itaconic acid in methanol/water (4:1), which proves that some interactions occur in these systems. If the spectral changes cannot be observed with one technique, it does not necessarily mean that the interaction is absent. Two or even more techniques should be employed and their results compared to make the final conclusion. The fact that it is generally hard to observe the complexation of phenol with the Raman and UV spectroscopic techniques could be because the bonding between phenol and studied monomers is not strong or distinctive.

3.5 References

1. Mayes, A. G.; Whitcombe, M. J., Synthetic strategies for the generation of molecularly imprinted organic polymers. *Advanced Drug Delivery Reviews* **2005**, *57* (12), 1742-78.
2. Takeuchi, T.; Fukuma, D.; Matsui, J., Combinatorial molecular imprinting: an approach to synthetic polymer receptors. *Analytical Chemistry* **1998**, *71* (2), 285-290.
3. Lanza, F.; Hall, A. J.; Sellergren, B.; Berczki, A.; Horvai, G.; Bayouth, S.; Cormack, P. A. G.; Sherrington, D. C., Development of a semiautomated procedure for the synthesis and evaluation of molecularly imprinted polymers applied to the search for functional monomers for phenytoin and nifedipine. *Analytica Chimica Acta* **2001**, *435* (1), 91-106.
4. Wang, G.; Cao, Q.; Ding, Z.; Wang, Y.; Yang, M., Preparation and characteristics of esculin-imprinted polymers. *Helvetica Chimica Acta* **2007**, *90* (6), 1179-1189.
5. Wang, G.; Cao, Q.; Zhu, X.; Yang, X.; Yang, M.; Ding, Z., Molecular imprinted solid-phase extraction of huperzine A from *Huperzia Serrata*. *Journal of Applied Polymer Science* **2009**, *113* (5), 3049-3058.
6. Sergeeva, T. A.; Gorbach, L. A.; Slinchenko, O. A.; Goncharova, L. A.; Piletska, O. V.; Brovko, O. O.; Sergeeva, L. M.; Elska, G. V., Towards development of colorimetric test-systems for phenols detection based on computationally-designed molecularly imprinted polymer membranes. *Materials Science and Engineering: C* **2010**, *30* (3), 431-436.
7. Karim, K.; Breton, F.; Rouillon, R.; Piletska, E. V.; Guerreiro, A.; Chianella, I.; Piletsky, S. A., How to find effective functional monomers for effective molecularly imprinted polymers? *Advanced Drug Delivery Reviews* **2005**, *57* (12), 1795-808.
8. Guerreiro, A.; Soares, A.; Piletska, E.; Mattiasson, B.; Piletsky, S., Preliminary evaluation of new polymer matrix for solid-phase extraction of nonylphenol from water samples. *Analytica Chimica Acta* **2008**, *612* (1), 99-104.
9. Lv, Y.Q.; Lin, Z.; Feng, W.; Tan, T., Evaluation of the polymerization and recognition mechanism for phenol imprinting SPE. *Chromatographia* **2007**, *66* (5-6), 339-347.
10. Vendamme, R.; Eevers, W.; Kaneto, M.; Minamizaki, Y., Influence of polymer morphology on the capacity of molecularly imprinted resins to release or to retain their template. *Polymer Journal* **2009**, *41* (12), 1055-1066.

11. Lu, Y.; Li, C.; Zhang, H.; Liu, X., Study on the mechanism of chiral recognition with molecularly imprinted polymers. *Analytica Chimica Acta* **2003**, *489* (1), 33-43.
12. Lasagabáster-Latorre, A.; Cela-Pérez, M. C.; Fernández-Fernández, S.; López-Vilariño, J. M.; González-Rodríguez, M. V.; Abad, M. J.; Barral-Losada, L. F. Insight into BPA-4-vinylpyridine interactions in molecularly imprinted polymers using complementary spectroscopy techniques. *Materials Chemistry and Physics* **2013**, *141* (1), 461-476.
13. Muhammad, T.; Cui, L.; Jide, W.; Piletska, E. V.; Guerreiro, A. R.; Piletsky, S. A., Rational design and synthesis of water-compatible molecularly imprinted polymers for selective solid phase extraction of amiodarone. *Analytica Chimica Acta* **2012**, *709*, 98-104.
14. Rong, F.; Fu, D. G.; Wu, W., Study on the effect of functional monomer on the binding characteristics of molecularly imprinted polymer. *Advanced Materials Research* **2011**, *239 - 242*, 821-824.
15. Li, J.; Jiang, F., A Chlortoluron sensor based on molecularly imprinted sensitive membranes. *Chemistry Letters* **2010**, *39* (5), 478-479.
16. Brune, B. J.; Koehler, J. A.; Smith, P. J.; Payne, G. F., Correlation between adsorption and small molecule hydrogen bonding. *Langmuir* **1999**, *15* (11), 3987-3992.
17. Zakaria, N. D.; Yusof, N. A.; Haron, J.; Abdullah, A. H., Synthesis and evaluation of a molecularly imprinted polymer for 2,4-dinitrophenol. *International Journal of Molecular Sciences* **2009**, *10* (1), 354-65.
18. Rodríguez-Lorenzo, L.; Álvarez-Puebla, R. n. A.; de Abajo, F. J. G. a.; Liz-Marzán, L. M., Surface enhanced raman scattering using star-shaped gold colloidal nanoparticles. *The Journal of Physical Chemistry C* **2009**, *114* (16), 7336-7340.
19. Ungnade, H. E., The effect of solvents on the absorption spectra of aromatic compounds. *Journal of the American Chemical Society* **1953**, *75* (2), 432-434.
20. Feng, Q. Z.; Zhao, L. X.; Yan, W.; Ji, F.; Wei, Y. L.; Lin, J. M., Molecularly imprinted solid-phase extraction and flow-injection chemiluminescence for trace analysis of 2,4-dichlorophenol in water samples. *Analytical and Bioanalytical Chemistry* **2008**, *391* (3), 1073-9.

Chapter 4. Development of Molecularly Imprinted Polymer in Porous Film Format for Binding of Phenol and Alkylphenols from Water

This chapter was published as a research paper: Gryshchenko, A.; Bottaro, C. International Journal of Molecular Sciences 2014, 15 (1), 1338-135

4.1 Introduction

Phenol and other phenolics are water pollutants that originate from various sources, such as oil extraction and treatment, wood and coal pyrolysis, and industrial organic synthesis [1]. Due to its toxicity and abundance, the United States Environmental Protection Agency (US EPA) has placed phenol on their list of Priority Pollutants, which specifies a safe level of 2 mg L^{-1} in drinking water [2] and 0.001 mg L^{-1} in water to be chlorinated [3], for example, in drinking water treatment. Materials for adsorption of phenol and other phenolics are widely used in wastewater clean-up, solid-phase extraction for chromatographic analysis, and sensors. In all these cases, adsorption can be effectively completed with molecularly imprinted polymers (MIPs) [4–6]. A MIP is a synthetic material with template-shaped vacant sites, which can bind molecules of specific structure and/or functionality. MIPs can be synthesized by different types of imprinting approaches (covalent, semi and non-covalent, with sacrificial spacer, and metal ion-mediation) in a variety of formats (monolith, film, powder, beads, a layer grafted onto surfaces) [7].

Many MIPs have been synthesized for a range of phenols: chlorophenols [4,8,9], nitrophenols [5, 10, 11], dixydroxyphenols [6, 12], nonylphenol [13], and bisphenol A [14], though only a few of them target phenol and simple alkylphenols. MIPs for phenol have been prepared by the non-covalent imprinting approach in the form of crushed monolith [15], a recognition layer immobilized on silica particles [16], and as a membrane [17].

To employ MIPs in miniaturized analysis systems [18], sensors [6], and analytical test systems [17, 19], they should be fabricated in a film format. This can be done by

spin-coating, sandwiching, mixing of MIP particles with a polymer binder, and polymerization within a porous structure of another film [20].

In this work, a non-covalent approach was applied to MIP synthesis because of its simplicity and versatility. The core of this approach is formation of a prepolymerization complex between a template and functional monomer (in solvent) through relatively weak interactions: van der Waals, ionic, and hydrogen bonding. After polymerization and template removal, an imprinted site is formed, which can rebind a template with similar non-covalent interactions and in the same configuration that existed in the prepolymerization complex [7]. Here, the polymerization step was completed by sandwiching the prepolymerization solution between two glass surfaces to form a thin continuous polymer film.

The goal of this project has been to fabricate and study MIP porous films for phenol using different compositions of monomer, solvent and cross-linker. The morphology of the films was studied with scanning electron microscopy (SEM) and gravimetric analysis. MIP binding properties were characterized using adsorption isotherms of phenol rebinding from aqueous phenol solutions. The imprinting effects of these MIPs were evaluated based on analysis of the phenol binding isotherms, and cross-binding towards other compounds.

4.2 Materials and methods

All chemicals were purchased from Sigma-Aldrich (Oakville, ON, Canada) unless otherwise indicated. Phenol (ph-1), resorcinol (res-1), 4-methylphenol (4-MP), 4-propylphenol (4-PP), 2,2-dimethoxy-2-phenylacetophenone (DMPA), itaconic acid (IA) and styrene (Sty) were 99% pure. 2,4-Dimethylphenol (2,4-DM), 3-(trimethoxysilyl)propyl methacrylate, ethylene glycol dimethacrylate (EGDMA), 3-octanone (3-oct), 1-decanol were 98% pure. Triethylene glycol dimethacrylate (TEGDMA) and 4-vinylpyridine (4-VP) were at 95%; pentaerythritol triacrylate (PETA) was technical grade. Polyethyleneglycol (PEG) and polyvinylacetate (PVA) had average Mw 20,000 and 100,000, respectively. *N,N*-Dimethylformamide (DMF) was of ACS reagent (Sigma-Aldrich, Oakville, ON, Canada) grade with <0.005% water, phenol-2,3,4,5,6-d5, was 98% deuterated. Chloroform (stabilized with amylenes), methanol, acetic acid, hydrochloric acid (37% w/w) were of ACS reagent grade and were purchased from ACP Chemicals (Montreal, QC, Canada). Hydrophilic polypropylene membrane GHP-200, 0.2 μm were from Pall Corporation (Mississauga, ON, Canada); micro cover glasses $25 \times 25 \text{ mm}^2$ and plain glass microscope slides $75 \times 25 \text{ mm}^2$ were from Fisher Scientific (Ottawa, ON, Canada). All solutions were prepared with 18.2 M Ω ·cm water from a Barnstead NanoPure Diamond (18 M Ω) water purification system (Barnstead Nanopure Water Systems, Lake Balboa, CA, USA).

4.2.1 Fabrication of MIP films by sandwich technique

In a vial, phenol (the template), monomer, and cross-linker were mixed in 1:2:10 molar ratio except MIP 5 where PETA (a trifunctional cross-linker) was used in a lower

molar ratio (1:2:6.67) to maintain the same ratio of vinyl groups in the reaction mixture. Then, the UV-initiator (DMPA) and solvent (1 mL for all mixtures) were added according to Table 4-1.

Table 4-1. Composition of MIP prepolymerization mixtures.

	MIP 1	MIP 2	MIP 3	MIP 4	MIP 5
template	phenol 0.4 mmol (37.6 mg)				
monomer	IA 0.8 mmol (104 mg)	VP 0.8 mmol (85.4 μ L)	Sty 0.8 mmol (92.0 μ L)		
cross-linker	EGDMA 4 mmol 755 μ L			TEGDMA 4 mmol 1049 μ L	PETA 2.67 mmol 674 μ L
photoinitiator	DMPA 0.06 mmol (15.4 mg)				
solvent (1000 μL)	15% (w/w) PEG in DMF	10% (w/w) PVA in CHCl ₃	20% (w/w) PEG in MeOH:H ₂ O 4:1	MeOH:H ₂ O 3:1	MeOH:H ₂ O 5:1

Note: MIP 1 (no PEG) and MIP 2 (no PVAc) were prepared using pure dimethylformamide and chloroform (1000 μ L), respectively.

The mixture was sonicated for 5 min under nitrogen. Glass slides were cut in 3 pieces $25 \times 25 \text{ mm}^2$, soaked in MeOH:HCl_{37%} (1:1) and silanized with 3-(trimethoxysilyl) propylmethacrylate [19] (Chapter 2). The same procedure, by sandwich technique, as in Chapter 2, was used for the fabrication of films. The non-imprinted polymer (NIP) was prepared simultaneously without phenol, using the same procedure.

4.2.2 Gravimetric analysis of porosity

The volume of liquid absorbed into the porous structure of a MIP film bound to glass was determined using the mass difference between the MIP film soaked with 1-decanol (m_l) at room temperature and the initial dry MIP film, and accounting for the density of 1-decanol (ρ_l , e.g., 0.829 g mL⁻¹ at 25 °C). Normalization of this volume to film mass (m) gives specific pore volume (v):

$$v = \frac{m_l}{\rho_l m} \quad (4-1)$$

The MIP film mass (m) was obtained by subtraction of the glass slide mass before polymerization from mass of the slide with bound MIP (as in Section 4.2.4). Mettler Toledo XS 105 (Mettler Toledo, Mississauga, ON, Canada) analytical balances, with accuracy to 0.01 mg, were used for mass measurements. 1-Decanol was chosen because of its low volatility and non-hydroscopic properties to ensure minimal uncontrolled mass change for the soaked films. A MIP film/slide was placed film-down on several layers of GHP-200 membrane (with smooth surface), which were moistened with 1-decanol, and the slide was slightly pressed onto the membrane to completely soak the porous film; this was assessed visually. Excess of 1-decanol was removed by gentle contact with a section of membrane. Porosity values for four films of the same kind were averaged. No statistically significant difference between the specific pore volumes of MIPs and their NIPs was observed.

4.2.3 SEM imaging and thickness measurements

An edge of the MIP films on glass was removed using a razor and the film was coated with sputtered gold. An FEI Quanta 650F field emission scanning electron microscope (FEI, Hillsboro, OR, USA) was used for imaging of the MIP film section with secondary electrons at a 70° tilt and 10 kV acceleration potential. A thickness of film (H) was estimated based on average height of seeming 90° section measured on SEM image (H') and the tilt angle:

$$H = \frac{H'}{\sin 70^\circ} \quad (4-2)$$

Thickness values for three films of the same kind were averaged.

4.2.4 Adsorbate binding studies

Procedures to determine MIP adsorption capacities of phenol are discussed in details in Appendix A. In this chapter, the “by difference” method is employed. Adsorption by the MIP was completed until binding equilibrium was reached. For calculation of binding capacity for adsorbate (Q), the amount of bound adsorbate (mg) was found based on a difference between an initial adsorbate concentration (C_i) and a concentration at equilibrium (C_f). The mass of MIP film (m_{film} , ~4 mg) was measured as was described in Section 4.2.2, and Q was calculated as follows:

$$Q = \frac{V(C_i - C_f)}{m_{\text{film}}} \quad (4-3)$$

MIPs 2 and 3 together with corresponding NIPs were firstly pre-wetted with acetonitrile:water (1:1) while other films were used directly. A 50-mL beaker with a MIP

film on a glass slide and aqueous adsorbate solution was sealed with paraffin film and was shaken at 150 rpm (rotations per minute) at 20.0 °C for 4 h 30 min in an Innova 4230 Incubator Shaker (New Brunswick Scientific, Enfield, CT, USA). The volume of the adsorbate solution (V) was proportional to the mass of MIP film. This ratio was chosen to be 0.44 mL mg⁻¹ for resorcinol and 3-octanone and 0.714 mL mg⁻¹ for other compounds to have an optimal difference $C_i - C_f$ for determination of Q .

Quantitation of the free adsorbate concentrations was completed with an Agilent 1100 Series LC-MS equipped with a diode array detector (Agilent Technologies Canada Inc., Mississauga, ON, Canada). Chromatographic parameters were the following: Phenomenex Synergi Fusion-RP column (150 × 4.6 mm; particle size 4 μm, Phenomenex, Torrance, CA, USA); isocratic elution with acetonitrile/water mobile phase (Table 4-2); injection volume varied from 100 to 10 μL depending on analyte concentration. Calibration solutions were the same as used for rebinding experiments and were prepared by their dilution to bracket measured concentrations.

More sensitive quantification of solutions with phenol concentration around 0.1 mg L⁻¹ was achieved with mass spectrometry using APCI (atmospheric pressure chemical ionization), and internal standardization with phenol-d5. A small correction for phenol template bleeding from the MIP was applied in determination of the adsorption capacities and the imprinting effect using the concentration of phenol extracted with pure water. The detector was operated in standard settings, fragmentation voltage was 50 V, negative mode with intensities acquired for ions at m/z 93 and 98 (C₆H₅O⁻ and C₆D₅O⁻), isocratic mobile phase was MeOH/pure H₂O (70/30 v/v) at 1.2 mL min⁻¹, injection volume was 100 μL.

Table 4-2. Elution and UV-detection conditions for chromatographic analysis of phenols.

Analyzed species	Mobile phase (v/v)		Detection wavelength, nm
	CH ₃ CN	H ₂ O with 5% CH ₃ CN (v/v)	
phenol	55	45	195 *; 216 *; 272
4-methylphenol	55	45	279
resorcinol	35	65	276
2,4-dimethylphenol	65	35	280
4-propylphenol	65	35	278
3-octanone	85	15	279

*: detection at 195 and 216 nm was used for solution with low phenol concentration ($\leq 5 \text{ mg L}^{-1}$).

4.3 Results and discussion

4.3.1 MIP films prepared by sandwich technique

Different methods for fabrication of MIP films have been discussed elsewhere [7, 21, 22]. Among them, a spin-coating method has been identified as having the advantage to produce films of controlled and uniform thickness, but it usually requires a low volatility prepolymerization mixture [21]. When more volatile solvents or monomers are used, MIP films can be prepared by sandwich technique, which was applied in this work. MIP films were prepared based on the following components. The monomers selected were: itaconic acid (IA), 4-vinylpyridine (VP), and styrene (Sty); cross-linkers: ethylene glycol dimethacrylate (EGDMA), triethylene glycol dimethacrylate (TEGDMA), and pentaerythritol triacrylate (PETA). The solvents used were: *N,N*-dimethylformamide (DMF), chloroform (CHCl₃), methanol/water (MeOH:H₂O). Polyvinylacetate (PVA) and

polyethyleneglycol (PEG) were also added to these solvent. All fabricated films (MIP 1–5, Figure 4-1) have been characterized and the morphological details are discussed below. Binding properties will be discussed in the subsequent sections.

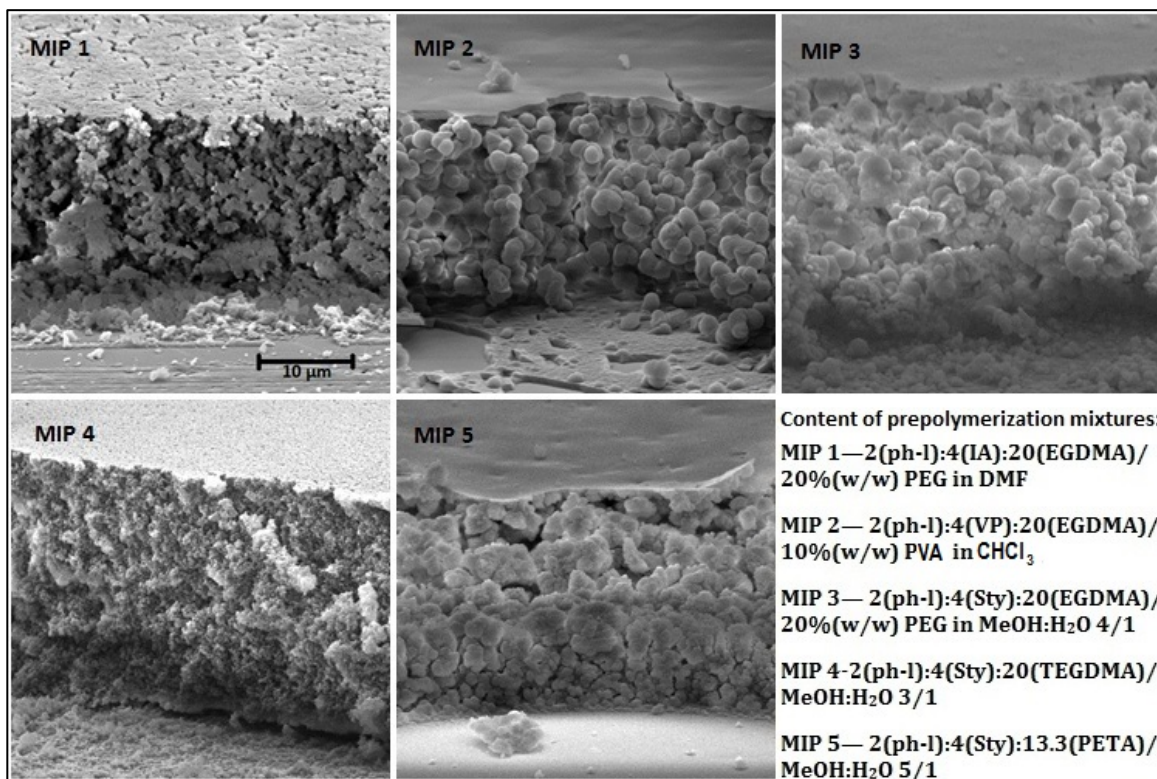


Figure 4-1. Top-down SEM images of MIP cross-sections

The films, covalently bound to the chemically modified surface of the glass slide, were white and opaque with a visually uniform and even surface. SEM imaging of film cross-sections (Figure 4-1) showed that the films had a flat surface, which was shaped by the cover glass and the film body had a porous and granular structure. In order to obtain films of this structure, a so called “poor” solvent that causes “reaction-induced phase separation” during polymerization [21] was applied. Also, linear polymers (PVA and

PEG) were added into solvents to aid in the formation of a stable porous/granular MIP (Figure 4-1); PEG was added to DMF to produce MIP 1 and PVA to CHCl_3 to give MIP 2 (Table 4-1). PEG and PVA have been used previously as solvent modifiers to render a high porosity to the MIP network, where PEG has been used for membranes [17] and PVA for spin-coated films [21]. For comparison, MIP 1 and 2 formulations were also prepared without these polymeric additives; this resulted in only slightly opaque films of low porosity (Figure B1). These films also shrank with air-drying and became very brittle, flaking from the glass slide. This suggests that the porous structure is a significant factor in the mechanical stability of the film. MeOH:H₂O is a “poor” solvent system itself without any polymeric additives and it was used for production of porous MIP networks previously [19, 23]. MeOH:H₂O was used in preparation of MIPs 3, 4, 5 producing highly porous films. Though the use of PEG to render porosity to MIP 3 films is not necessary, it was added to increase viscosity of the prepolymerization mixture in order to reduce its leakage beyond the cover glass boundary, making fabrication of films more facile and reproducible.

The thickness of fabricated films depends mostly on the volume of prepolymerization mixture deposited onto the glass slide and the area the liquid mixture spreads on under the cover glass ($25 \times 25 \text{ mm}^2$). The average thickness for all films was estimated to be about 20 μm (Table 4-3) using SEM. This value is less than the initial thickness calculated (a height, or thickness, of 16 μL liquid enclosed between two $25 \times 25 \text{ mm}^2$ surfaces of glass slide and cover glass should be approximately 26 μm) for the applied volume of the prepolymerization mixture, but the difference is not problematic and can be attributed to the leakage of fluid beyond the cover glass, as well

as shrinkage of the polymer network during polymerization. For comparison, mechanical pressure with spring clamps has been applied onto the cover glass to control film thickness during similar fabrication by sandwiching [23].

Table 4-3. Thickness (by SEM) and porosity (gravimetric method) of films fabricated by sandwich technique (SD – standard deviation).

Characteristic determined	MIP				
	1	2	3	4	5
H (SD, $n = 3$), μm	24.1 (2.5)	23.4 (3.5)	18.5 (3.1)	21.5 (5.2)	20.6 (2.5)
v (SD, $n = 4$), $\text{mL}\cdot\text{g}^{-1}$	1.22 (0.04)	1.08 (0.08)	1.46 (0.05)	0.76 (0.07)	0.91 (0.04)

Degree of porosity is an important morphological feature, however, a conventional nitrogen BET analyzer cannot be used to study porosity of these MIP films because each film only weighs a few mg and they are bound to a glass slide. Therefore, quantitative analysis of bulk porosity has been suggested to measure porosity gravimetrically, where specific pore volume (v) is calculated from the volume of absorbed liquid in the film pores normalized to polymer mass. Although it is acknowledged that this method cannot give an indication of pore size distribution, it is easy and does not require any special equipment.

From the data given in Table 4-3, it can be seen that films have a significant porosity—about 1 mL of pores per gram of polymer network. A comparison of morphologies for MIPs 3, 4 and 5, which use different cross-linkers (Section 4.3.4),

shows that the lowest porosity was observed for MIP 4 with TEGDMA. This reflects what is observed in the SEM images (Figure 4-1) that shows a dense packing of small granules for the TEGDMA MIP. There are at least two potential explanations for this effect. One is that because the composition of the MIPs was based on mole ratios and a fixed volume of solvent (the compositions are described in the experimental section), the MIPs based on TEGDMA had a higher mass concentration in the prepolymerization solution and resulted in a more dense material. The other is related to the length of the spacer in the cross-linker, which in principle allows for formation of a more complexly cross-linked polymeric structure. The higher porosity for MIP 3 (EGDMA) than that for MIP 5 (PETA) is likely due to the trifunctionality of PETA, which should render a higher degree of cross-linking, forming a denser polymer network (Section 4.3.4). The high porosity and the granular film structure suggest that it is possible for the adsorbate (e.g., phenol) to be adsorbed not only at the surface of MIP film but also within film bulk. For this reason, the amount of bound adsorbate ($m_{\text{adsorbate}}$) was normalized against film mass (m_{film}) rather than the film surface to get binding capacity (Q):

$$Q = \frac{m_{\text{adsorbate}}}{m_{\text{film}}}, \text{mg} \cdot \text{g}^{-1} \quad (4-4)$$

4.3.2 Choice of monomer and solvent

In development of these MIPs towards phenol, it was decided to use phenol as the template rather than a pseudo-template for simplicity. In future work, the use of an alkylated phenol or other monoaromatic species as the template would be useful. IA, VP, and Sty were chosen as monomers based on their ability to interact with phenol in

different ways, such as hydrogen bonding and π - π interactions. In the choice of solvent, along with to be a relatively “poor” solvent for the polymer components, a condition of not significantly disrupt the monomer-template interactions in prepolymerization mixture were also considered [24].

Computational studies carried out during the development of MIP membranes selective to phenol have shown that anion of itaconic acid (IA) binds phenolic hydroxyl group via hydrogen bonding [17]. In that work, DMF was used as the solvent, probably due to its ability to act as a proton acceptor and, thereby, facilitate itaconic acid dissociation. Thus, the IA/DMF pair was also used in this work. The other pairing of VP and CHCl_3 was based on the capacity for hydrogen bonding between the basic nitrogen of VP and the phenolic hydroxyl group, which has been observed in low-polar solvent systems such as CHCl_3 by various techniques (NMR, IR) [15]. Between styrene and phenol, hydrophobic interactions including π - π stacking can be developed. A solvent to promote interactions of this kind should be highly polar and protic like the MeOH:H₂O mixture. UV absorbance spectrometry is a common technique to study monomer-template interactions by hydrogen bonding [25]. It can be applied to study the hydrophobic interactions in protic solvents, where NMR and IR spectroscopy are not applicable. The complexation of phenol and styrene was concluded from changes in the phenol spectrum (E_2 -band) upon addition of styrene, which were observed for very dilute phenol solutions (0.100 mM) (Chapter 3).

4.3.3 Phenol binding studies in water for MIPs prepared on selected monomers and solvents

MIP films based on IA, VP, and Sty (MIP 1, 2, 3 in Table 4-1) were prepared and tested in phenol rebinding from aqueous solutions. For this study, the concentrations used are described as moderate phenol concentrations (10 and 15 mg L⁻¹) and high phenol concentrations (100 and 300 mg L⁻¹). At each concentration range, the average imprinting factor (*IF*) was calculated (Table 4-4).

$$IF = \frac{Q_{MIP}}{Q_{NIP}} \quad (4-5)$$

IF characterizes MIP binding capacity (Q_{MIP}) over that for non-imprinted polymer (Q_{NIP}), and it is the simplest estimation of imprinting effect.

Table 4-4. Imprinting factors for MIP formulations prepared on different monomers.

MIP (composition)	C_i (phenol), mg L ⁻¹			
	10	15	100	300
	<i>IF</i> (SD, $n = 4$)			
MIP 1 (IA/DMF)	1.04 (0.008)		1.00 (0.019)	
MIP 2 (VP/CHCl ₃)	0.99 (0.038)		1.00 (0.017)	
MIP 3 [Sty/(MeOH:H ₂ O)]	1.00 (0.015)		1.04 (0.018)	

Note: C_i – phenol concentration before the binding studies; SD – standard deviation.

For MIP 1 (IA/DMF), IFs at moderate concentrations (10 – 15 mg L⁻¹) are slightly higher than those at high concentrations (100 – 300 mg L⁻¹). This suggests the presence of higher energy MIP binding sites, which are occupied at low phenol concentrations. However, efficiency of the MIP over the NIP is very modest; and maybe because

recognition of phenol through hydrogen bonding is suppressed in the aqueous environment. For similar reasons, in case of MIP 2 (VP/CHCl₃) and the corresponding NIP, the binding capacities are about the same for all phenol concentration range taking the variability into account ($IF \approx 1.0$). A further factor at play in this system is the mismatch between the highly hydrophobic solvent in prepolymerization mixture (CHCl₃) and the highly polar and protic water as environment for binding. It has been noted previously that the imprinting effect is more pronounced when the solvent used during the formation of prepolymerization complex has similar properties to the solvent for rebinding [26]. The MeOH/H₂O solvent system, used for MIP 3 based on styrene, is probably the closest solvent to the water from which phenol rebinding takes place. Although the hydrophobic interactions between styrene and phenol should be strong in this solvent, it seems that the non-selective hydrophobic interactions dominate over selective interactions associated with imprinted cavities. It was observed that only the IF for the higher phenol concentrations is higher than unity, and only marginally so.

Generally, it is a challenging task to prepare effective MIPs for phenol because it is a small molecule without many special features in terms of shape and functionality. Thus far, MIPs for binding phenol from water have been prepared with only modest imprinting effect, for example, ca 1.25 [17], or even less than unity in the case of MIP towards nonylphenol [13]². Phenol has only one hydroxyl group, therefore, it can be retained in a binding site only by one hydrogen bond. In contrast to phenol, MIPs with higher imprinting factors have been prepared for 2,4-dichlorophenol (2.1) [9], 2,4-dinitrophenol

² in both cases the imprinting factors were estimated based on MIP and NIP binding behavior at high adsorbate concentrations.

(2.2) [10], bisphenol A [14], hydroquinone (2.2) [12]. These species used as templates have more specific shape and at least two functional groups available for bonding (e.g., two $-\text{NO}_2$ and one $-\text{OH}$ in dinitrophenol). Furthermore, the hydroxyl protons for chloro- and nitrophenol are more acidic than the proton in phenol, which can yield stronger hydrogen bonding with proton accepting monomers. All these factors make the prepolymerization complex more stable, which results in more selective binding sites in the final MIP network, and, consequently, a stronger imprinting effect.

Although these MIPs did not give satisfactory imprinting effects, other factors with a potential to influence the selectivity of the MIPs, such as the effect of cross-linker are of interest and are useful to study. Based on the somewhat promising results for the imprinting factors, the styrene/MeOH:H₂O system was chosen for the study of cross-linkers to improve imprinting effect towards phenol; this system also should maximize the hydrophobic interactions that dominate in aqueous environments and these systems have not been studied for phenol imprinting previously.

4.3.4 Choice of cross-linker

The cross-linker constitutes most of the MIP by mass (in this work 88–93% *w/w*); therefore, it dictates the structure and tightness of the polymer network [24], and potentially contributes to a significant amount of the non-specific binding [27]. In addition to the styrene MIPs with EDGMA, styrene based MIPs were prepared with two other cross-linkers, TEGDMA and PETA (Figure 4-2). TEGDMA has been used for synthesis of a variety of resins and MIP membranes [17], and has a long flexible glycol chain. Due to its hydroxyl group, PETA has been used for preparation of hydrophilic MIPs [27]. Also, as a trifunctional cross-linker it is expected to produce a greater degree of cross-linking and a tighter polymer network. These cross-linkers were dissolved in MeOH/H₂O with the highest possible water content that can still produce homogeneous prepolymerization mixtures. It is believed that higher water content in the solvent allows for stronger phenol-styrene interaction in a prepolymerization complex. PETA is soluble in 5:1 MeOH:H₂O in contrast to the widely used trifunctional cross-linker trimethylolpropane trimethacrylate (TRIM), which cannot be dissolved in such polar solvent systems, even acetonitrile. TEGDMA tolerates the highest amount of water, and is soluble in 3:1 MeOH:H₂O (the composition for EDGMA is 4:1); better TEGDMA solubility is due to a higher number of ethereal oxygen in TEGDMA than EDGMA.

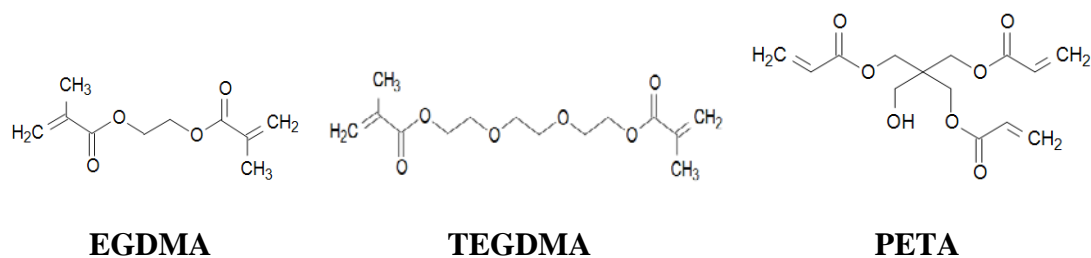


Figure 4-2. Structures of cross-linkers used in Chapter 4.

For MIP 3 (EGDMA), the IF rises from 1.00 at 15 mg L⁻¹ to 1.04 at 300 mg L⁻¹ (Figure 4-3 with data in Table B1). In case of MIP 4 (TEGDMA), IF increases from 1.04 to 1.06, within the studied concentration range. For MIP 5 (PETA) IF improves from 1.04 at 40 mg L⁻¹ to 1.12 at 300 mg L⁻¹; below 40 mg L⁻¹ there is a slight increase in IFs as the phenol concentration diminishes (see next Section 4.3.5). Comparison of IFs in the region 150 – 300 mg L⁻¹, where the IFs for each MIP exhibit little variation over the range of phenol concentrations, shows that the highest IFs are observed for MIP 5 (PETA). It can be explained by the tighter and more rigid structure of binding sites, which better fit phenol as a small molecule. An average IF for TEGDMA-MIP is slightly higher than that for EGDMA-MIP, probably due to higher water content (Section 4.3.1) in the solvent combined with tighter structure of the TEGDMA-MIP. Generally, the extent of non-specific binding by an MIP can be assessed based on binding capacity for its NIP. Comparison of the NIP binding capacities (Figure 4-3 and Table B1) for all studied phenol concentrations demonstrates that non-specific hydrophobic binding towards phenol is lower for MIPs on TEGDMA and especially on PETA.

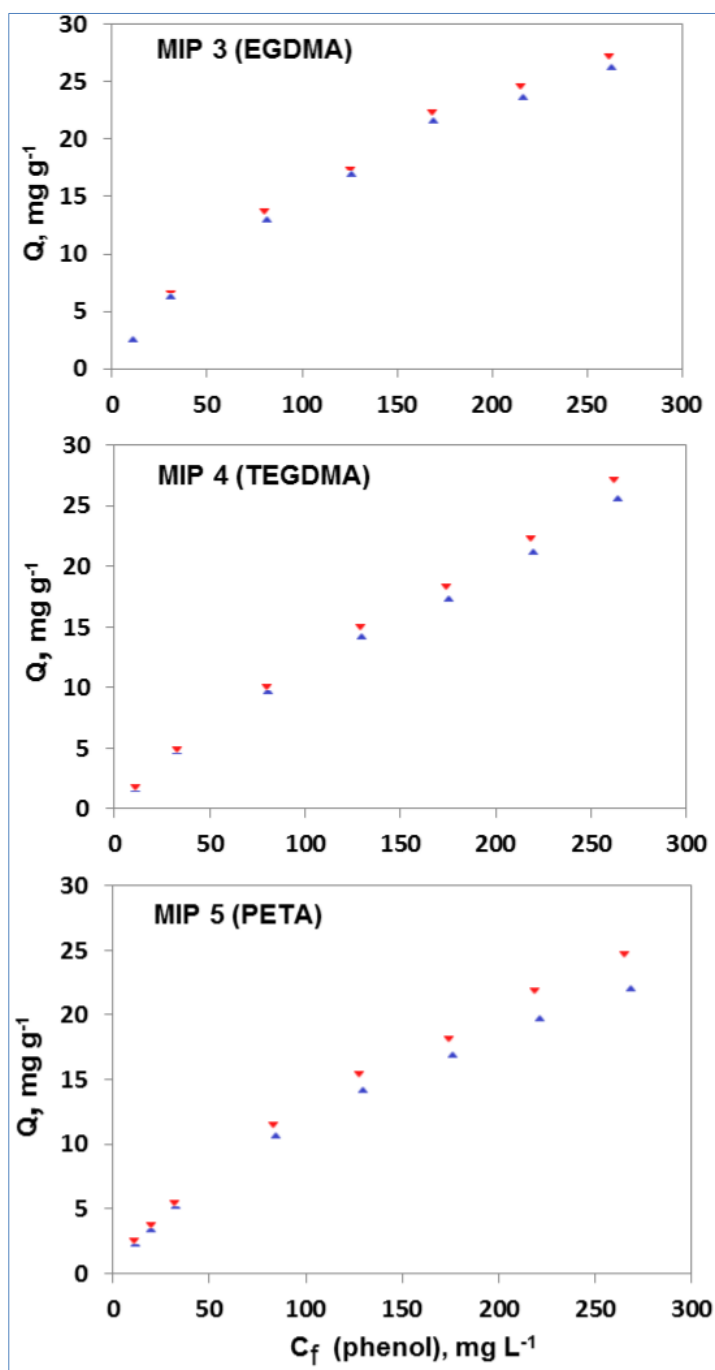


Figure 4-3. Binding isotherms for Sty-based MIP/NIP on different cross-linkers: EGDMA, TEGDMA, and PETA from 15 to 300 mg L^{-1} phenol in water.

Note: \blacktriangledown – MIP, \blacktriangle – NIP, C_f – phenol concentration at binding equilibrium.

Another feature of the MIP films based on PETA and TEGDMA is that they were easily wetted with water; whereas the Sty-MIP film with EGDMA had to be conditioned in acetonitrile:water (1:1). This dependence of wetting and non-specific binding on the cross-linker type can be explained by the higher hydrophilicities of TEGDMA and PETA when compared to EGDMA; TEGDMA has long hydrophilic glycol chain, and PETA possesses a hydroxyl group and lower carbon content due to acrylic moieties instead of methacrylate. Thus, TEGDMA and PETA can be recommended as cross-linkers for water-compatible MIPs with less non-specific binding in water towards hydrophobic species. In light of the highest imprinting factor and water compatibility, the PETA-MIP was chosen for more detailed study of binding characteristics, which is presented in the next section.

4.3.5 Characterization of styrene/PETA MIP (MIP 5)

4.3.5.1 Binding properties study

It was mentioned previously (Section 4.3.4) that there is a breakpoint in the isotherm for MIP 5 around 40 mg L^{-1} , where the MIP 5 isotherm begins to diverge from the NIP isotherm with rising IFs towards both high and low phenol concentrations (Tables 4-5 and B1). It is known that lack of uniformity in MIP binding behavior can occur because the MIP shows different binding site distributions depending on adsorbate concentration range [25, 28, 29].

Table 4-5. Data for binding isotherms for MIP/NIP 5 (PETA) at low phenol concentrations (0.1 – 40 mg L⁻¹)

$C_i(\text{phenol}), \text{mg}\cdot\text{L}^{-1}$	0.1	0.5	1	5	15	25	40
$Q(\text{NIP}), \text{mg}\cdot\text{g}^{-1}$	0.0168 (0.0043)	0.0865 (0.0008)	0.192 (0.009)	0.882 (0.007)	2.31 (0.011)	3.45 (0.13)	5.20 (0.28)
$Q(\text{MIP}), \text{mg}\cdot\text{g}^{-1}$	0.0202 (0.0051)	0.1004 (0.0011)	0.212 (0.0001)	0.957 (0.025)	2.52 (0.020)	3.70 (0.11)	5.41 (0.32)
IF	1.20 (0.023)	1.16 (0.016)	1.11 (0.0044)	1.09 (0.0200)	1.09 (0.0037)	1.07 (0.0060)	1.04 (0.0080)

Note: SD (standard deviation) in parenthesis: $n = 2$ for 1, 5, 15 mg L⁻¹; $n = 3$ for 25, 40 and $n = 4$ for 0.1, 0.5 mg L⁻¹.

In practice, the concentration of phenol in natural and sewage waters is in the $\mu\text{g L}^{-1}$ to mg L^{-1} range, therefore, it is appropriate to study MIP binding behavior, including binding sites distribution, in a low phenol concentration region. Thus, NIP and MIP 5 isotherms were built from 0.1 to 40 mg L⁻¹ (Table 4-5 and Figure 4-4). The imprinting factors, reflecting the efficiency of the MIP over its NIP, showed a steady increase with decreasing phenol concentration (Table 4-5): $IF = 1.04$ at 40 mg L⁻¹, 1.07 at 25 mg L⁻¹, 1.16 at 0.5 mg L⁻¹ and 1.20 at 0.1 mg L⁻¹. In this concentration window, the MIP and NIP isotherms can be linearized on a logarithmic scale (Figure 4-4), which means that they are described well by the Freundlich isotherm (FI) binding model. For comparison, linearization with the Langmuir binding model [25,30], which corresponds to the unimodal affinity distribution, gives a worse fit with R^2 values of 0.9474 (MIP) and 0.8608 (NIP) (Figure B2).

According to the FI, the amount of bound adsorbate, expressed as binding capacity (Q), depends on free adsorbate concentration (C) in a power of m as:

$$Q = a C^m \quad (4-6)$$

or in a linearized form

$$\text{Log } Q = m \text{ Log } C + \text{Log } a \quad (4-7)$$

where m and a are fitting parameters connected with adsorbent binding properties.

The FI pattern corresponds to the asymptotic decay region of the affinity distribution (Figure B3), which usually takes place within a limited interval of adsorbate concentrations at low levels [30, 31].

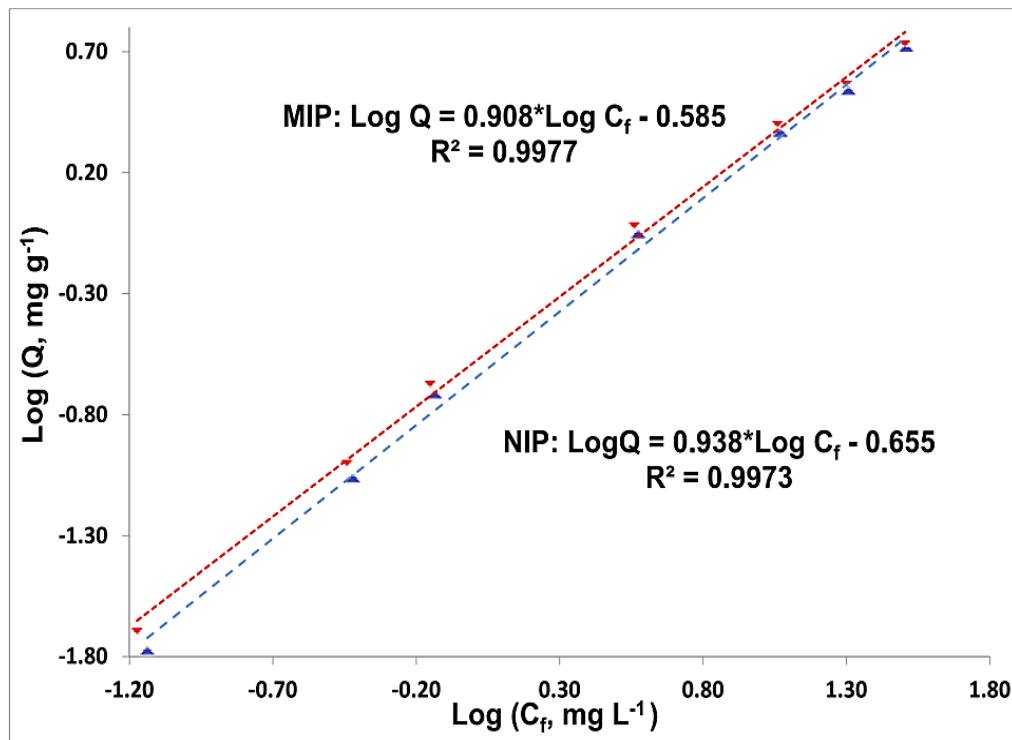


Figure 4-4. Phenol adsorption isotherms for MIP 5 and NIP in Log-Log format and fitting to Freundlich isotherm binding model: ▼ MIP, ▲ NIP.

The heterogeneity index, m , is a value between 0 and 1 that characterizes the “ratio of high-to-low affinity sites”. The lower the m value, the higher heterogeneity, meaning there is a greater proportion of high affinity binding sites in the affinity distribution [31], which is the case for MIP 5 compared to its NIP (Table 4-6). Based on fitting parameters m and a , the apparent number of binding sites, N_{K1-K2} , and apparent weighted average affinity, K_{K1-K2} , were calculated (formulas in Appendix B) for the range of affinity constants, K_1-K_2 , set by the concentration limits of these experimental isotherms (Table 4-5). Relative to the NIP, the MIP has higher N_{K1-K2} , and greater degree of heterogeneity (m) resulting in slightly higher average affinity K_{K1-K2} , which all prove a modest imprinting effect [31].

Table 4-6. Parameters for fitting to Freundlich isotherm model and calculated binding parameters.

Adsorbent	R^2	$a, \text{mg g}^{-1}$ $(\text{mg L}^{-1})^{-m}$	m	$N_{K1-K2},$ mmol g^{-1}	$K_{K1-K2},$ L mg^{-1}
MIP 5	0.9977	0.260 (0.012)	0.908 (0.020)	0.0112 (0.0018)	0.237 (0.011)
NIP 5	0.9973	0.221 (0.012)	0.938 (0.022)	0.0073 (0.0022)	0.221 (0.010)

Notes: $K_1 = 0.0313$; $K_2 = 14.9 (\text{L mg}^{-1})$; SD for $\log a$ and m values were calculated in Excel with LINEST function and on their base SD for a , N_{K1-K2} , K_{K1-K2} were calculated by the uncertainty propagation and presented in parenthesis.

4.3.5.2 Cross-binding study

Cross-binding of the PETA MIP was evaluated based on a comparison between binding for phenol (ph-l) and structurally-related phenols: resorcinol (res-l);

4-methylphenol (4-MP); 2,4-dimethylphenol (2,4-DM), 4-propylphenol (4-PP), and 3-octanone (3-oct). Figure 4-5 shows that this MIP has comparable cross-binding in terms of IFs towards other phenols, which are different from phenol by one or two substituents on the aromatic ring. This is consistent with the low specificity associated with binding by hydrophobic interactions, which has been discussed previously [32]. Both MIP and NIP binding capacities rise with adsorbate hydrophobicity. For example, the octanol-water partition coefficients ($\log K_{ow}$), e.g., 1.48, 1.97, 2.35 for phenol, 4-methylphenol, and 2,4-dimethylphenol, respectively [33], increase with alkyl substitution which parallels the trend in binding capacities. Virtually no difference is observed for MIP and NIP binding capacities of 3-octanone, which is non-aromatic in nature and significantly different from phenol structurally. Thus, the modestly higher uptake of phenols is likely due to some molecular recognition capability of MIP 5 and the aromatic nature of phenols. Such wide cross-adsorption, characteristic to this MIP acting by hydrophobic interactions, can be advantageous for separation of a whole class of phenols including alkylphenols, which are all of environmental importance.

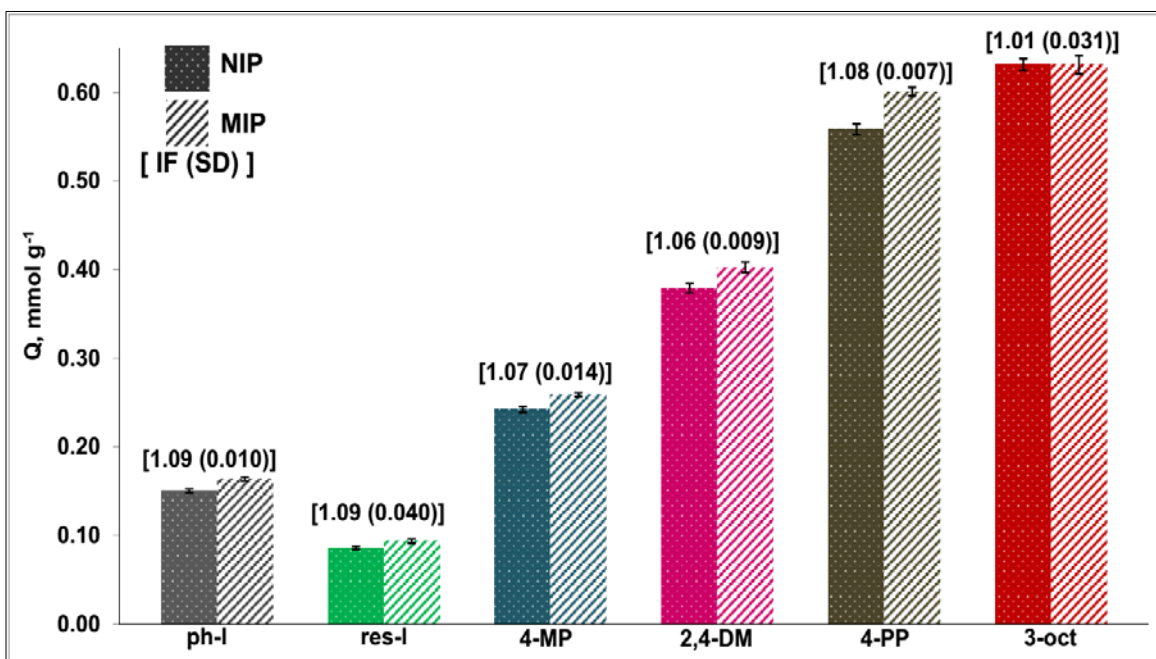


Figure 4-5. Cross-binding of MIP 5 and NIP towards other phenols and 3-octanone, $C_i(\text{adsorbate}) = 1.594 \text{ mM}$.

Note: IF is an average of ratios of Q_{MIP} to Q_{NIP} ($n = 4$, SD in parenthesis); $Q_{\text{MIP(NIP)}}$ is an average of values corresponding to different batches ($n = 4$, SD error bars).

4.4 Conclusions and future work

The sandwich technique can be used for simple fabrication of $\sim 20 \mu\text{m}$ thick MIP films with a smooth surface from a wide variety of prepolymerization mixtures. These films can be rendered porous by use of “poor” solvents such as methanol-water mixtures or dimethylformamide and chloroform with addition of linear polymers (PEG and PVA). The fabricated MIP films are suitable for use as adsorptive layers in sensors and as a phase for microextraction, e.g. in microfluidics, given their reproducible and consistent porous morphology. Also, the described sandwich technique is recommended as a format for screening of MIP formulations in MIP synthesis because of convenience of handling

MIPs bound to glass slides, labor and material savings, and applicability to a wide variety of MIP formulations.

MIP films were prepared based on various monomers to bind phenol through hydrogen bonding (itaconic acid and 4-vinylpyridine) and hydrophobic effect (styrene). The binding properties and selectivity of the MIPs were characterized based on phenol adsorption capacities from aqueous solutions studied at equilibrium. It is challenging to develop high affinity MIPs with high selectivity for phenol due to phenol's small size, simple shape and the fact it has only one weakly acidic hydroxyl group. In aqueous environments, selective binding of phenol via hydrogen bonding is suppressed, while binding with a MIP made with styrene is not significantly specific because binding is mainly through hydrophobic and π - π interactions associated with the aromatic structures of the monomer and phenols. The denser more rigid structure of styrene-based MIPs achieved with trifunctional PETA is beneficial for phenol recognition. Also, the high hydrophilicity of this cross-linker makes MIP films water-compatible and reduces the non-specific binding. Binding isotherms for phenol uptake at low concentrations by styrene and PETA based MIPs showed that the imprinting factors are higher for lower phenol concentrations. The MIP and NIP isotherms follow the Freundlich binding model. The analysis of the isotherms conveys moderately better binding parameters for the MIP over its NIP, and a limited number of selective imprinted sites that are mostly occupied at low phenol concentrations. Although the selectivity is not exceptional, MIPs with this composition can be used for binding other structurally similar phenols.

The authors believe that this work is a beginning step in the development of more efficient systems for binding of phenol and alkylphenols in water, and the basic

components for these MIPs or non-imprinted simple adsorbent phases can be styrene, PETA, and methanol/water as monomer, cross-linker and solvent, respectively. A number of approaches can be used in efforts to improve the imprinting effect, for example, use of higher monomer and template content, polymerization at lower temperatures [31], and the addition of a proton accepting monomer with styrene to develop extra hydrogen bonding [7]. Studies of phenol rebinding over shorter intervals, *i.e.*, before adsorption equilibrium is reached, may also yield better imprinting factors.

4.5 References

1. Michałowicz, J.; Duda, W. Phenols—Sources and toxicity. *Polish Journal of Environmental Studies* **2007**, *16*, 347-362.
2. *Toxicological Profile for Phenol*; U.S. Department of Health and Human Services: Atlanta, GA, USA, 2008; p. 27.
3. *Ambient Water Quality Criteria for Phenol*; U.S. Environmental Protection Agency: Washington, DC, USA, 1980; EPA440/5-80-066.
4. Shiraishi, Y.; Suzuki, T.; Hirai, T. Selective photooxidation of chlorophenols with molecularly imprinted polymers containing a photosensitizer. *New Journal of Chemistry* **2010**, *34*, 714–717.
5. Caro, E.; Marcé, R.M.; Cormack, P.A.G.; Sherrington, D.C.; Borrull, F. On-line solid-phase extraction with molecularly imprinted polymers to selectively extract substituted 4-chlorophenols and 4-nitrophenol from water. *Journal of Chromatography A* **2003**, *995*, 233–238.
6. Lakshmi, D.; Whitcombe, M.J.; Davis, F.; Chianella, I.; Piletska, E.V.; Guerreiro, A.; Subrahmanyam, S.; Brito, P.S.; Fowler, S.A.; Piletsky, S.A. Chimeric polymers formed from a monomer capable of free radical, oxidative and electrochemical polymerisation. *Chemical Communications* **2009**, 2759–2761.
7. Mayes, A.G.; Whitcombe, M.J. Synthetic strategies for the generation of molecularly imprinted organic polymers. *Advanced Drug Delivery Reviews* **2005**, *57*, 1742–1778.

8. Feng, Q.; Zhao, L.; Lin, J.M. Molecularly imprinted polymer as micro-solid phase extraction combined with high performance liquid chromatography to determine phenolic compounds in environmental water samples. *Analytica Chimica Acta* **2009**, *650*, 70–76.
9. Feng, Q.Z.; Zhao, L.X.; Yan, W.; Ji, F.; Wei, Y.L.; Lin, J.M. Molecularly imprinted solid-phase extraction and flow-injection chemiluminescence for trace analysis of 2,4-dichlorophenol in water samples. *Analytical and Bioanalytical Chemistry* **2008**, *391*, 1073–1079.
10. Zakaria, N.D.; Yusof, N.A.; Haron, J.; Abdullah, A.H. Synthesis and evaluation of a molecularly imprinted polymer for 2,4-dinitrophenol. *International Journal of Molecular Sciences* **2009**, *10*, 354–365.
11. An, F.Q.; Gao, B.J.; Feng, X.Q. Binding and recognition ability of molecularly imprinted polymer toward p-nitrophenol. *Journal of Applied Polymer Science* **2012**, *125*, 2549–2555.
12. Kan, X.; Zhao, Q.; Zhang, Z.; Wang, Z.; Zhu, J.J. Molecularly imprinted polymers microsphere prepared by precipitation polymerization for hydroquinone recognition. *Talanta* **2008**, *75*, 22–26.
13. Guerreiro, A.; Soares, A.; Piletska, E.; Mattiasson, B.; Piletsky, S. Preliminary evaluation of new polymer matrix for solid-phase extraction of nonylphenol from water samples. *Analytica Chimica Acta* **2008**, *612*, 99–104.
14. Cela-Perez, M.C.; Castro-Lopez, M.M.; Lasagabaster-Latorre, A.; Lopez-Vilarino, J.M.; Gonzalez-Rodriguez, M.V.; Barral-Losada, L.F. Synthesis and characterization of bisphenol-a imprinted polymer as a selective recognition receptor. *Analytica Chimica Acta* **2011**, *706*, 275–284.
15. Lv, Y. Q.; Lin, Z.; Feng, W.; Tan, T. Evaluation of the polymerization and recognition mechanism for phenol imprinting SPE. *Chromatographia* **2007**, *66*, 339–347.
16. An, F.; Gao, B. Adsorption of phenol on a novel adsorption material PEI/SiO₂. *Journal of Hazardous Materials* **2008**, *152*, 1186–1191.
17. Sergeeva, T.A.; Gorbach, L.A.; Slinchenko, O.A.; Goncharova, L.A.; Piletska, O.V.; Brovko, O.O.; Sergeeva, L.M.; Elska, G.V. Towards development of colorimetric test-systems for phenols detection based on computationally-designed molecularly imprinted polymer membranes. *Materials Science and Engineering: C* **2010**, *30*, 431–436.

18. Harz, S.; Schimmelpfennig, M.; Tse Sum Bui, B.; Marchyk, N.; Haupt, K.; Feller, K.-H. Fluorescence optical spectrally resolved sensor based on molecularly imprinted polymers and microfluidics. *Engineering in Life Sciences* **2011**, *11*, 559–565.
19. Van Biesen, G.; Wiseman, J.M.; Li, J.; Bottaro, C.S. Desorption electrospray ionization-mass spectrometry for the detection of analytes extracted by thin-film molecularly imprinted polymers. *Analyst* **2010**, *135*, 2237–2240.
20. Pérez-Moral, N.; Mayes, A. Novel MIP formats. *Bioseparation* **2001**, *10*, 287–299.
21. Schmidt, R.H.; Haupt, K. Molecularly imprinted polymer films with binding properties enhanced by the reaction-induced phase separation of a sacrificial polymeric porogen. *Chemistry of Materials* **2005**, *17*, 1007–1016.
22. Ulbricht, M. Molecularly imprinted polymer films and membranes. In *Molecularly Imprinted Materials: Science and Technology*; Yan, M., Ramström, O., Eds.; Marcel Dekker: New York, NY, USA, 2005; pp. 455–491.
23. Jakusch, M.; Janotta, M.; Mizaikoff, B.; Mosbach, K.; Haupt, K. Molecularly imprinted polymers and infrared evanescent wave spectroscopy. A chemical sensors approach. *Analytical Chemistry* **1999**, *71*, 4786–4791.
24. Yan, H.; Row, K. Characteristic and synthetic approach of molecularly imprinted polymer. *International Journal of Molecular Sciences* **2006**, *7*, 155–178.
25. Lulinski, P.; Maciejewska, D. Examination of imprinting process with molsidomine as a template. *Molecules* **2009**, *14*, 2212–2225.
26. Spivak, D.A. Selectivity in molecularly imprinted matrices. In *Molecularly Imprinted Materials: Science and Technology*; Yan, M., Ramström, O., Eds.; Marcel Dekker: New York, NY, USA, 2005; p. 413.
27. Manesiotis, P.; Borrelli, C.; Aureliano, C.S.A.; Svensson, C.; Sellergren, B. Water-compatible imprinted polymers for selective depletion of riboflavine from beverages. *Journal of Materials Chemistry* **2009**, *19*, 6185–6193.
28. Turner, N.W.; Holdsworth, C.I.; Donne, S.W.; McCluskey, A.; Bowyer, M.C. Microwave induced MIP synthesis: Comparative analysis of thermal and microwave induced polymerisation of caffeine imprinted polymers. *New Journal of Chemistry* **2010**, *34*, 686–692.

29. Corton, E.; García-Calzón, J.A.; Díaz-García, M.E. Kinetics and binding properties of cloramphenicol imprinted polymers. *Journal of Non-Crystalline Solids* **2007**, *353*, 974–980.
30. Umpleby, R.J.; Baxter, S.C.; Chen, Y.; Shah, R.N.; Shimizu, K.D. Characterization of molecularly imprinted polymers with the Langmuir–Freundlich isotherm. *Analytical Chemistry* **2001**, *73*, 4584–4591.
31. Rampey, A.M.; Umpleby, R.J.; Rushton, G.T.; Iseman, J.C.; Shah, R.N.; Shimizu, K.D. Characterization of the imprint effect and the influence of imprinting conditions on affinity, capacity, and heterogeneity in molecularly imprinted polymers using the freundlich isotherm-affinity distribution analysis. *Analytical Chemistry* **2004**, *76*, 1123–1133.
32. Haupt, K.; Dzgoev, A.; Mosbach, K. Assay system for the herbicide 2,4-dichlorophenoxyacetic acid using a molecularly imprinted polymer as an artificial recognition element. *Analytical Chemistry* **1998**, *70*, 628–631.
33. The Handbook of Chemistry and Physics. Available online: <http://www.hbcernetbase.com> (accessed on 7 October 2013).

**Chapter 5. Development of MIPs Acting by Hydrophobic Interactions
to Bind Phenol**

5.1 Introduction

The majority of MIPs are synthesized through non-covalent imprinting based on the formation of hydrogen bonding between a template and functional monomers [1]. However, there are many adsorbates that cannot form strong hydrogen bonds and some adsorbates do not have the necessary functional groups to participate in hydrogen bonding or electrostatic interactions. Many of those adsorbates are of environmental importance, e.g., phenol and PAHs are water contaminants from oil extraction. The adsorption of phenol on MIPs via hydrogen bonding is suppressed in an aqueous environment [2, 3], and PAHs can participate only in non-polar interactions, including π - π stacking. Thus, the development of MIPs acting by the hydrophobic interactions to bind non-polar or low-polarity analytes in water is a task of current importance. Few papers have been published about the imprinting by hydrophobic interactions; these report MIPs based on aromatic polyurethane to bind PAHs [4], styrene and EGDMA for 1-hydroxypyrene [5], and amylose for bisphenol A [6].

In the previous chapter, a MIP was developed to bind phenol and alkylphenols by hydrophobic interactions and some selectivity was reported. The main components used to synthesize this MIP were styrene as a functional monomer to bind phenols, MeOH/H₂O as a solvent to promote interactions between a template and styrene in the prepolymerization mixture, and a trifunctional cross-linker, PETA, to form a tight polymer network of binding sites. This work builds on the results of the previous chapter; in particular, ways to prepare more effective binding media in the film format are addressed here. The effect of a pseudotemplate as the fourth main component in the MIP synthesis was studied. The content of styrene in MIPs was increased, and how this

influenced the binding capacity and imprinting for MIPs was investigated. MIP cross-binding towards two and three ring PAHs was assessed. A copolymer of divinylbenzene, ethylvinylbenzene, and PETA was synthesized as an alternative material for the adsorption of phenol according to the future work discussed in Chapter 4. The binding and imprinting performances of the MIP films towards phenol, prepared in the current and previous chapters, were compared and some principles to prepare modern and effective MIPs were derived.

5.2 Materials and methods

Technical grade divinylbenzene was purchased from Sigma-Aldrich (Oakville, ON, Canada). The divinylbenzene reagent consisted of *m*- and *p*-divinylbenzenes (DVB, 80%), along with a large fraction of ethylvinylbenzenes (EVB, 20 %). 1-Propanol (>99%, PrOH) was supplied by Eastman Chemical Company (Kingsport, TN, USA). Xylene (xyl) as a mixture of ortho-, meta-, and para-isomers, was ACS grade solvent supplied by Fisher Chemical (Ottawa, ON, Canada). Ethylene glycol (99.5%, EG), naphthalene (99%, Naph), phenanthrene (99.5%, Phe), fluorene (99%, Flu), and anthracene (99.0%, Ant) were produced by Fluka Analytical and purchased from Sigma-Aldrich (Oakville, ON, Canada). Acetone and hexane of ACS reagent grade were purchased from ACP Chemicals (Montreal, QC, Canada). All other used reagents and materials were the same as in Chapter 4.

5.2.1 Synthesis of MIPs

Two MIP films imprinted with phenol (MIP 7) and xylene (MIP 8), their corresponding NIP 6 (common for MIP 7 and 8), and an adsorbent film made of a copolymer of PETA and divinylbenzene were prepared according to the sandwich technique (Chapters 2 and 4). The composition of the prepolymerization mixtures for these MIPs is described in Table 5-1. The only difference from the fabrication procedure described earlier (Chapter 2) is that after the polymerization, to remove the template the films were washed with acetone:hexane (1:1, v/v) at stirring for 3 hours, using three fresh portions of the solvent. The acetone and hexane mixture was chosen because it has been used before to remove toluene, as template, for a MIP towards toluene, ethylbenzene, and xylene [7].

Table 5-1. Composition of prepolymerization mixtures for phenol and xylene imprinted polymers, and novel adsorbent based on divinylbenzene and PETA.

Polymer components	NIP 6	MIP 7	MIP 8	Ads
The abbreviation of the composition	8(Sty):13.3(PETA)/PrOH:EG:H ₂ O 4/1/1	4(ph-l):8(Sty):13.3(PETA)/PrOH:EG:H ₂ O 4/1/1	4(xyl):8(Sty):13.3(PETA)/PrOH:EG:H ₂ O 4/1/1	2.4(EVB):9.6(DVB):13.3(PETA)/PrOH:EG 5/1
template	NA	phenol 1.6 mmol (151 mg)	xylene 1.6 mmol (198 μL)	NA
functional monomer	Sty 3.2 mmol (368 μL)			DVB-EVB 4.8 mmol (684 μL) and PETA 5.33 mmol (1590 mg)
cross-linker	PETA, 5.33 mmol (1590 mg)			
photoinitiator (DMPA)	0.131 mmol (34.0 mg)			0.1747 mmol (45.0 mg)
solvent (2000 μL)	1-propanol:ethylene glycol:water (4:1:1 v/v)			1-propanol:ethylene glycol (5:1 v/v)

5.2.2 Study of the binding properties of MIP films

Binding towards phenol was studied in the same way as phenol binding in the previous chapter (Chapter 4), which allows the phenol adsorption capacity (Q , mg g⁻¹) to be determined. $Q_{\text{MIP(NIP)}}$ is an average of at least three values corresponding to separate batches (Figure 5-1). Presented IFs are averages of at least three ratios of Q_{MIP} to Q_{NIP} from the same batch, as films fabricated and studied together. In Figure 5-3, at least two values of $Q_{\text{MIP(NIP)}}$ are averaged, and IFs are averages of at least two ratios of Q_{MIP} to Q_{NIP} . In the cross-binding studies (Figure 5-2), the imprinting effect towards PAHs was studied using the measurement procedure for the direct fluorimetric detection on a MIP film,

described in details in Chapter 8. In brief, MIP 8/NIP 6 films were prepared as 100 μm thick films and exposed to an aqueous solution (750 mL) of PAHs: naphthalene ($60.0 \mu\text{g L}^{-1}$), fluorene ($8.00 \mu\text{g L}^{-1}$), phenanthrene ($4.00 \mu\text{g L}^{-1}$), and anthracene ($4.00 \mu\text{g L}^{-1}$). For each PAH, its fluorescence intensity was measured in the synchronous scanning mode at the optimal spacing for each PAH. The intensities for the MIP and NIP, were compared as peak intensities (I) to calculate the IF:

$$IF(PAH) = \frac{I_{MIP}(PAH)}{I_{NIP}(PAH)} \quad (5-1)$$

In Figure 5-2, presented IFs are averages of four ratios of I_{MIP} to I_{NIP} ; each ratio was measured for a pair of MIP 8 and NIP 6 from the same batch.

5.3 Results and discussion

5.3.1 Rationale for the choice of components for MIPs and novel adsorbent

Template

It was mentioned before that a polymer imprinted with phenol may release phenol into the sample solution at the phenol rebinding (Chapter 4). Phenol bleed means that the template removal is not 100% complete. The false positive may be detected when this type of MIP is applied for the analysis of phenol. Therefore, the use of a pseudotemplate, a template that is different from the targets for the binding and detection [8], can surmount the problem of leakage. Xylene, a mixture of *o*, *m*, *p*-dimethylbenzene isomers, was chosen as the template (MIP 8) because it is a monoaromatic compound, similar to

phenol. An important property of dimethylbenzenes is that they are highly hydrophobic compounds, and relatively strong complexation with styrene can be expected. The Log K_{ow} values of dimethylbenzenes and styrene are very close (3.1 – 3.2) [9]. This proximity suggests that, along with the formation of the dimethylbenzene dimers, dimethylbenzenes can actively associate with styrene, participating in the imprinting. The MIP imprinted with phenol (MIP 7) was also synthesized for the comparison with MIP 8, so that the effect of the change in template could be evaluated.

Functional monomer

As suggested in Chapter 4, styrene was used because of its ability to bind phenol through hydrophobic interactions. Compared to MIP 5 (Chapter 4), the content of styrene in the final polymer network (w/w) on dry weight basis was nearly doubled from 9% (MIP 5) to 16% (MIP 7 and 8). The amount of the template, phenol or xylene, was also scaled accordingly to keep the ratio of 1:2, the same as for MIP 5. The reason for the increase of the content of styrene, relative to the amount of cross-linker, is to form more binding sites, both selective and non-selective, in order to increase the overall binding capacity towards phenol.

Solvent

There are a number of factors that influence the choice of a solvent system. First, styrene and xylene are components of low viscosity, and an increase of their content in the prepolymerization mixture requires the use of a viscous solvent. Second, methanol and water mixtures, previously used in Chapter 4, are volatile, which requires the delivery

of the prepolymerization mixture to make the sandwich to be very fast (Chapter 2). Third, to produce the porous network, the solvent must be “poor” in terms of swellability of the polymer network (Chapter 4). Lastly, the solvent still must solubilize all MIP components. By the trial and error method, PrOH:EG:H₂O (4/1/1) was found to meet all these solvent requirements for fabrication of films by the sandwich approach. In addition, this solvent is highly protic and polar due to the high content of the hydroxyl functionality; a solvent of this nature can promote the hydrophobic interactions between xylene and styrene.

Cross-linker

PETA was used as a cross-linker because it was found (Chapter 4) that the highly cross-linked polymeric network is beneficial for the imprinting effect. Compared to EGDMA and TEGDMA, PETA is highly viscous and greatly contributes to the overall viscosity of the prepolymerization mixtures. PETA contains a hydroxyl group, which enhances the wettability of the films with water.

Composition of a novel adsorbent based on divinylbenzene and PETA

So far MIPs/NIPs acting by hydrophobic interactions had been synthesized using styrene as a functional monomer. It seemed interesting and useful to test other non-polar functional monomers, for example, divinylbenzene, which is a widely available industrial reagent. As a starting point in this direction, a copolymer (Ads in Table 5-1) of technical divinylbenzene and PETA was synthesized. For the simplicity of these preliminary experiments, the polymer was synthesized without any template, therefore Ads can be

called non-imprinted polymer. Similar to MIP 8, Ads does not contain phenol, therefore, it can be freely used for the chemical analysis. The binding is expected to be only due to the non-specific interactions and this polymer should be considered as a simple adsorbent medium, or an adsorbent. The main reasons for the selection of the components were the same as for the MIP 8: ethylvinylbenzenes (EVB) and divinylbenzenes (DVB) as aromatic functional monomers, PETA cross-linker, along with 1-propanol and ethylene glycol mixture—a protic and relatively low volatile solvent (Table 5-1). EVBs act as functional monomers while DVBS can serve both as functional monomers and cross-linkers, therefore, Ads contains more aromatic moieties than MIP 8. In order to homogenize highly hydrophobic EVB and DVB together with PETA in the prepolymerization mixture, water was excluded from the solvent mixture.

5.3.2 The physical quality of fabricated films

All fabricated films (NIP 6, MIP 7, MIP 8, Ads) were opaque white and had a fine granular morphology. The quality of the films was good in terms of mechanical stability and homogeneity, which is comparable to the quality of other films (Table 2-1). All films were easily wetted with water. Especially mechanically durable were “Ads” films. This resistance to scratching and mechanical stress can be explained by the use of only cross-linkers as the building blocks for the polymer, which increase the overall degree of crosslinking in the polymer network.

5.3.3 Study of binding and imprinting properties for MIPs imprinted with phenol and xylene

The binding capacities and imprinting factors for MIP 7 and 8 were determined at three phenol concentrations, 0.500, 15.00, 300.0 mg L⁻¹ (Figure 5-1), representing relatively low, average, and high concentration ranges for the phenol binding isotherms. These data are also compared with those for MIP 5/NIP 5 (Chapter 4) in order to study the effect of the increase of styrene content in a MIP.

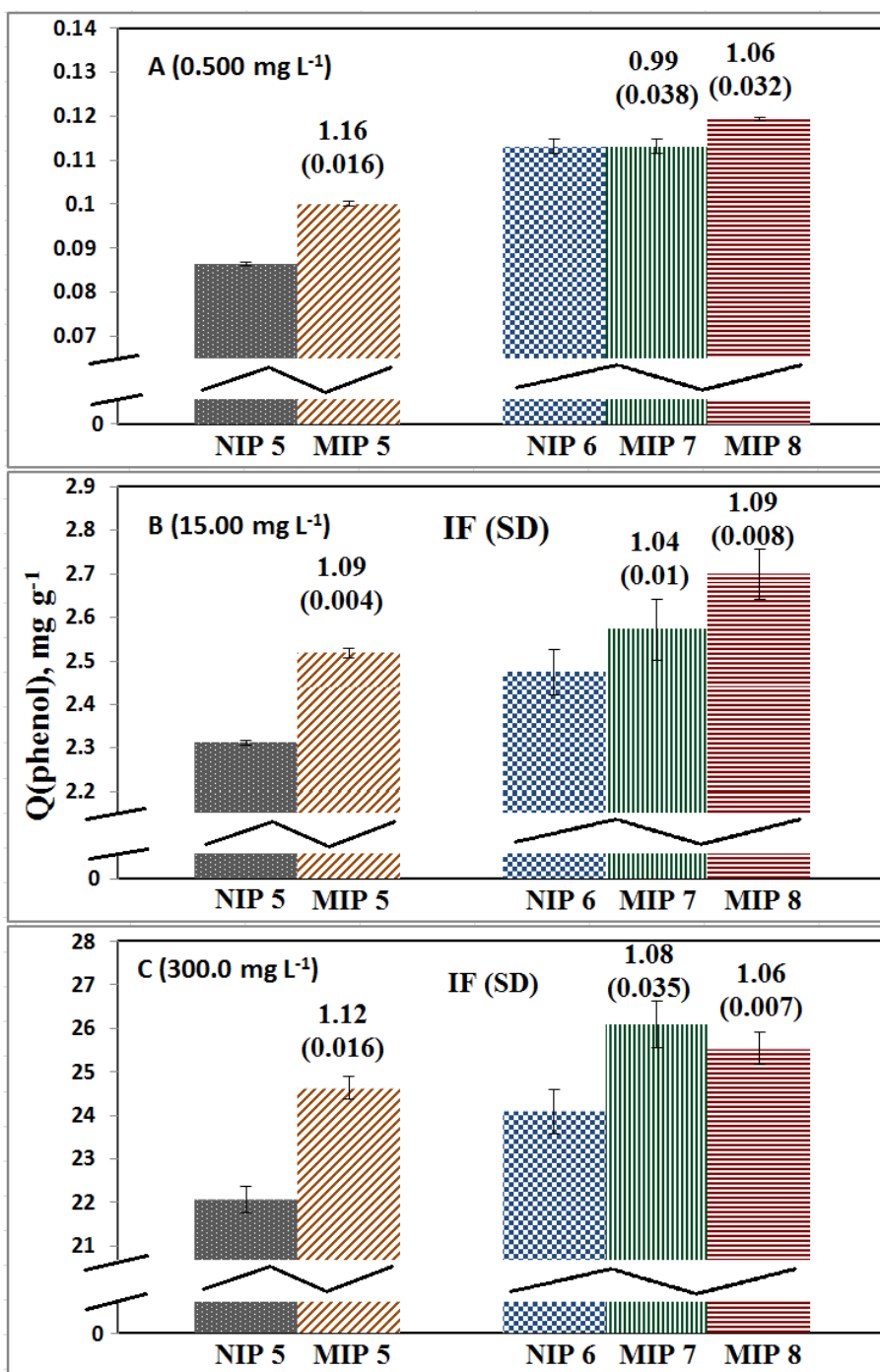


Figure 5-1. Comparison of binding capacities and imprinting factors for MIPs 5, 7 and 8 at three phenol concentrations: A (0.500 mg L^{-1}), B (15.00 mg L^{-1}), and C (300.0 mg L^{-1}).

Note: Standard deviations for IFs ($n=3$) are in parenthesis; $Q_{\text{MIP(NIP)}}$ is an average of values corresponding to different batches ($n = 3$, SDs are error bars).

The general picture is that the increase of styrene content results in the higher binding capacity towards phenol for MIP 7, 8/NIP 6 compared to MIP 5/NIP. For example, the binding capacities for NIP 6 are higher than that for NIP 5 by about 8 % at 15.00 and 300.0 mg L⁻¹. The increase of the binding capacity becomes much more dramatic (27 %) at 0.500 mg L⁻¹. The better performance of MIP 8 to bind phenol at lower concentrations is very relevant for the adsorption of phenol in environmental waters. The fact that the higher styrene content causes the rise of MIP binding capacity at lower phenol concentrations can be explained as not only the number of binding sites is increased, but also the energy of the binding, when MIP 8 and 5 are compared. It is likely that the higher content of styrene results in the formation of more structured and higher affinity binding sites in the polymer network, which are preferably filled at lower phenol concentrations [10].

It was observed that MIP 5 had higher imprinting factors than either new MIPs (MIP 7 and 8); the difference is notable, especially at 0.500 mg L⁻¹ (1.16, 0.99, and 1.06, respectively). It is possible that the increase of styrene content results in the reduction of tightness or rigidity of the polymer network and, consequently, stability of binding sites, which leads to the reduction of imprinting effect. A similar trend was observed for MIPs based on MAA/EGDMA for L-phenylalanine anilide [11].

The imprinting factors for xylene imprinted polymer (MIP 8) are higher than that of phenol imprinted polymer (MIP 7) in the low and moderate concentration ranges by about 6% at 0.500 and 15.00 mg L⁻¹. At the high concentration range, 300 mg L⁻¹, both imprinting factors become about equal (~1.07). With the increase of phenol concentration, the rise in IF from unity to 1.07 is observed for MIP 7, similar to MIP 3

and 4 (Chapter 4), while the IF for MIP 8 decreases, suggesting the heterogeneity of binding sites as with for MIP 5. Thus, at lower concentration ranges, 0.500 and 15.00 mg L⁻¹, the binding capacity of MIP 8 is higher than that for MIP 7. This increase of binding capacity is probably because xylene template associates more strongly with styrene than less hydrophobic phenol, forming more structured binding sites. When a template was different from a target, a significant reduction of recognition is usually observed, such as in the case of binding of 4-chlorophenoxyacetic acid with 2,4-dichlorophenoxyacetic acid imprinted polymer [12]. However, it is likely that when the interactions between a template and functional monomer are hydrophobic and targets are simply shaped molecules, such as phenol, the strength of less sterically defined interactions plays more important role in the imprinting effect than the similarity of template and target.

MIP 8 imprinted with xylene recognizes phenol by cross-binding. Cross-binding in terms of an imprinting factor for MIP 8 was also studied towards other aromatic compounds such as two and three ring PAHs (Figure 5-2). It was found that IFs are higher for the PAHs than for phenol and the IFs for the PAHs gradually decrease with the size of PAHs: 1.30, 1.19, 1.15, 1.12 for naphthalene, fluorene, phenanthrene, and anthracene, respectively. The fact that the IF of phenol is less than that of naphthalene can be explained in terms of the size of binding sites formed by xylene. These sites can be larger relative to the small and not alkylated molecule of phenol, which reduces phenol fitting into the binding site. One reason why IFs of PAHs are higher than that of phenol can be the fact that PAHs are much more hydrophobic and, therefore, interact with styrene moieties more strongly in the binding sites. A clear effect of the size of PAHs on

their IFs was observed. The highest IF was observed for the smallest PAH, naphthalene, and the lowest for the largest PAHs, phenanthrene and anthracene. This trend can be related to how well the PAHs fit the binding sites formed by xylene, which is smaller sized than any of the PAHs. Another possible contribution to this trend is that the conformational flexibility increases as the PAHs rises in size [13]. The flexibility of adsorbate molecule may reduce its tight fitting to the binding sites.

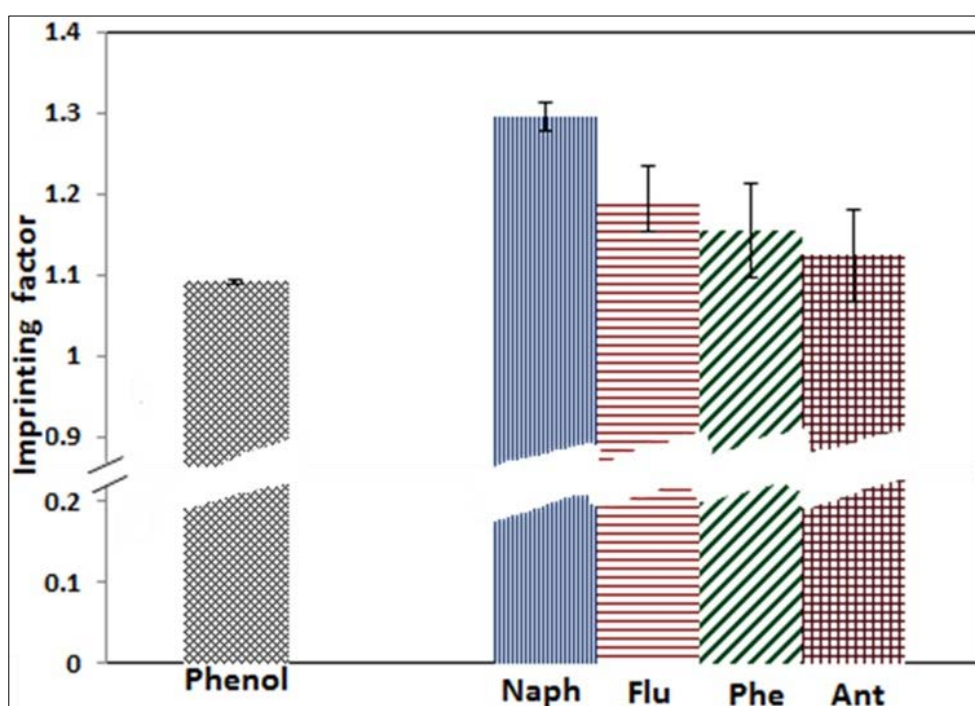


Figure 5-2. Cross-binding of polymer imprinted with xylene (MIP 8) towards phenol, naphthalene, fluorene, phenanthrene, and anthracene. Error bars are SD, n=4.

5.3.4 Comparison of binding and imprinting properties

The binding capacities and imprinting factors for MIPs/NIPs, which have been studied in this chapter (Figure 5-1) and Chapter 4 (Table 4-4, Figure 4-3, Table B1), together with a novel DVB based adsorbent (Ads), were compared at one phenol concentration in the middle range, 15.00 mg L⁻¹ to demonstrate typical binding behavior

observed for these MIPs/NIPs. This concentration is of a practical importance and corresponds to the average concentration of phenol and alkylphenols in produced water [14]. All main polymer components, such as the monomer/solvent, cross-linker along with template, were varied (Figure 5-3) to deduce the effect of the polymer composition on the binding capacity, imprinting effect, and water compatibility. As can be concluded from the data presented in Figure 5-3, higher imprinting factors were observed for MIPs based on styrene and PETA (MIP 5, 7, 8) than for other MIPs, for example, based on EGDMA and IA (MIP 1), VP (MIP 2), and Sty (MIP 3). It shows that hydrophobic interactions with styrene in the combination with the more cross-linked network by PETA polymer are beneficial for the imprinting effect.

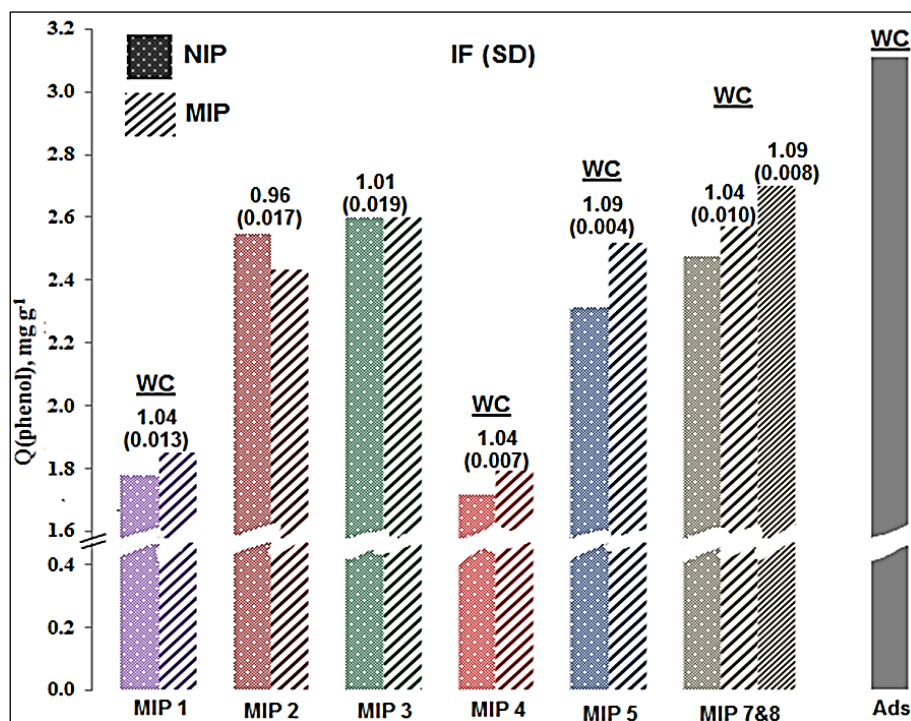


Figure 5-3. Comparison of phenol binding capacities and imprinting effects at $C_i(\text{phenol})=15.00 \text{ mg L}^{-1}$ for MIPs/NIPs studied in Chapters 4 and 5.

Note:., $S_r(Q) \sim 3\%$, $n=2$; SD for IFs are in parenthesis, $n=2$. WC – water compatibility.

The trade-off between water-compatibility and binding capacity can also be observed. Polymers based on VP with EGDMA (MIP 2) and Sty with EGDMA (MIP 3) have some of the highest binding capacities because of the strong hydrophobic effect of VP and Sty. However, they must be prewetted with acetonitrile to facilitate a complete contact with water as necessary in the adsorption process (Chapter 4); therefore, MIPs 2 and 3 can be classified as only conditionally water compatible. Sty-PETA polymers (MIPs 5–8) and “Ads” still have a comparatively high binding capacity and are fully water-compatible. The binding capacities for other water-compatible polymers (MIPs 1 and 4) are significantly lower because they contain carboxyls from itaconic acid and etheric oxygens from TEGDMA that reduce the hydrophobic effect needed for the adsorption in water. In the Sty-PETA polymers and the novel adsorbent (Ads), the hydroxyl groups in PETA moieties offset the water repelling effect of hydrophobic functional monomers, which makes it possible to combine the water compatibility and the high binding capacity towards phenol.

In addition to the increase of the styrene content (MIPs 5, 7, 8), an even more effective tool to increase the binding capacity was to use more hydrophobic functional monomers, such as EVB and DVB. The moieties of DVB and EVB are more hydrophobic than less alkylated styrene moieties, therefore, co-PETA-EVB-DVB adsorbent (Ads) had the highest binding capacity. Because, co-PETA-EVB-DVB was prepared based on protic solvent, it also had a potential to be imprinted, e.g., with xylene, in order to increase the binding capacity even more.

5.4 Conclusions and future work

In this work, the concept of molecular imprinting and binding of phenol by hydrophobic interactions, initially studied in Chapter 4, is further developed and studied. The solvent, cross-linker, and functional monomers proved to have a crucial role. A unique solvent system was based on 1-propanol, ethylene glycol, and water. This solvent system gave the high quality and porous films because it is protic and highly polar, relatively viscous, and not very volatile. In addition, it also promotes hydrophobic interactions between a template and styrene. The PETA cross-linker has an advantage that its hydrophilic nature can compensate for the hydrophobic effect from aromatic monomers, making MIPs with a high adsorption capacity that are still water-compatible. The increase of functional monomer content and the use of more hydrophobic monomers than styrene, such as DVB and EVB, are reliable tools to increase binding of phenol. The change of the template from phenol to xylene brings some improvement of the imprinting effect towards phenol probably because the strength of the complexation between the template and styrene plays a more important role than the similarity between the template and target.

Xylene-Sty-PETA-MIP and co-PETA-EVB-DVB films can be recommended for the practical applications because of their high binding capacities. The xylene-MIP shows selectivity not only towards phenol but also towards other aromatic compounds such as PAHs, for which the imprinting effect is diminished with the increase of their molecular size. With more resources and time, principles derived in this chapter can be employed to develop even more advanced MIPs by hydrophobic interactions, for example, based on co-PETA-EVB-DVB platform.

5.5 References

1. Mayes, A. G.; Whitcombe, M. J., Synthetic strategies for the generation of molecularly imprinted organic polymers. *Advanced Drug Delivery Reviews* **2005**, *57* (12), 1742-78.
2. Lv, Y.Q.; Lin, Z.; Feng, W.; Tan, T., Evaluation of the polymerization and recognition mechanism for phenol imprinting SPE. *Chromatographia* **2007**, *66* (5-6), 339-347.
3. Gryshchenko, A.; Bottaro, C., Development of molecularly imprinted polymer in porous film format for binding of phenol and alkylphenols from water. *International Journal of Molecular Sciences* **2014**, *15* (1), 1338-1357.
4. Dickert, F. L.; Tortschanoff, M.; Bulst, W. E.; Fischerauer, G., Molecularly imprinted sensor layers for the detection of polycyclic aromatic hydrocarbons in water. *Analytical Chemistry* **1999**, *71* (20), 4559-4563.
5. Kirsch, N.; Hart, J. P.; Bird, D. J.; Luxton, R. W.; McCalley, D. V., Towards the development of molecularly imprinted polymer based screen-printed sensors for metabolites of PAHs. *The Analyst* **2001**, *126* (11), 1936-1941.
6. Kanekiyo, Y.; Naganawa, R.; Tao, H., Molecular imprinting of bisphenol A and alkylphenols using amylose as a host matrix. *Chemical communications* **2002**, (22), 2698-2699.
7. Sainz-Gonzalo, F. J.; Medina-Castillo, A. L.; Fernandez-Sanchez, J. F.; Fernandez-Gutierrez, A., Synthesis and characterization of a molecularly imprinted polymer optosensor for TEXs-screening in drinking water. *Biosensors & Bioelectronics* **2011**, *26* (7), 3331-8.
8. Wang, X.; Fang, Q.; Liu, S.; Chen, L., The application of pseudo template molecularly imprinted polymer to the solid-phase extraction of cyromazine and its metabolic melamine from egg and milk. *Journal of Separation Science* **2012**, *35* (12), 1432-1438.
9. Handbook of Chemistry & Physics Online, 94th edition. <http://www.hbcnetbase.com> (accessed 18.12.2013).

10. Rampey, A. M.; Umpleby, R. J.; Rushton, G. T.; Iseman, J. C.; Shah, R. N.; Shimizu, K. D., Characterization of the imprint effect and the influence of imprinting conditions on affinity, capacity, and heterogeneity in molecularly imprinted polymers using the freundlich isotherm-affinity distribution analysis. *Analytical Chemistry* **2004**, *76* (4), 1123-1133.
11. Spivak, D. A., Optimization, evaluation, and characterization of molecularly imprinted polymers. *Advanced Drug Delivery Reviews* **2005**, *57* (12), 1779-94.
12. Van Biesen, G.; Wiseman, J. M.; Li, J.; Bottaro, C. S., Desorption electrospray ionization-mass spectrometry for the detection of analytes extracted by thin-film molecularly imprinted polymers. *The Analyst* **2010**, *135* (9), 2237-40.
13. Zhigalko, M. V.; Shishkin, O. V.; Gorb, L.; Leszczynski, J., Out-of-plane deformability of aromatic systems in naphthalene, anthracene and phenanthrene. *Journal of Molecular Structure* **2004**, *693* (1-3), 153-159.
14. Report 364. Fate and effects of naturally occurring substances in produced water on the marine environment; International Oil and Gas Producers Association: London, UK, 2005; p 42.

**Chapter 6. Application of Surface Enhanced Raman Spectroscopy for
Detection of Water Contaminants on Molecularly Imprinted Polymeric
Films**

6.1 Introduction

Surface enhanced Raman spectroscopy (SERS) is a powerful analytical method that can provide highly sensitive and selective chemical analysis. Raman scattering is inelastic in its nature, where an incident photon loses a part of its energy to a molecule through vibrational or rotational excitation. This scattering is a very weak process where only $10^{-6} - 10^{-8}$ of incident photons constitute Raman scattering [1]. Raman scattering can be greatly enhanced, up to $10^4 - 10^6$ times, when a molecule is located in the electrical field of surface-plasmon resonance (SPR). SPR is induced on a metal surface in contact with incident light. For SPR to occur, the metal surface has to be rough at the nano-level; this can be accomplished with metal nanoparticles or in planar format as the nano-patterned metal surface. When Raman scattering is enhanced due to SPR on the metal surface, it is called surface enhanced Raman scattering³. SERS is one of the most sensitive techniques, with detection limits comparable to those achieved with fluorimetry. At the same time, the narrow bandwidth of Raman peaks gives a measure of selectivity [2, 3]. For the SERS phenomenon to occur, the contact between an analyte and the roughened metal surface, or a SERS substrate, is essential, though, SPR can influence molecules at a distance of several nanometers from the surface [3]. Initially, the analyte moves freely in the aqueous environment. In order to hold the analyte close to the metal surface, a polymeric film of adsorbent can be used. In this case, the detection will also benefit from the analyte preconcentration and separation. Such film can be made of a MIP as an effective and selective adsorbent that targets a certain analyte.

³ also abbreviate as SERS, the same as surface enhanced Raman spectroscopy (SERS)

MIPs can be combined with a metal substrate for the SERS detection in a variety of ways. A MIP film can be immobilized directly on the surface of a planar SERS substrate, so that the MIP will become the mediator between the metal surface and the adsorbed analyte. This approach has been used for the development of an on-line SERS sensor [4, 5]. Initially, a vinyl based MIP was spin coated on a silver surface [4]. The drawback of this work was the detachment of the polymer film after the immobilization. Later this problem was solved by using molecularly imprinted xerogels coated on a commercial gold substrate, and a detection system for explosives such as nitro-aromatics was developed [5]. Another way to combine MIP and a SERS substrate is to apply metal nanoparticles on a MIP film with a loaded analyte. A similar detection approach has been applied in thin-layer chromatography (TLC) not only for identification but also for quantitation, where a metal colloid is pipetted onto an analyte spot on a TLC plate [6, 7]. Thus, it would be reasonable to do the same on a MIP film in the development of analytical test-systems. The development and characterization of this approach constitute a main subject of this research project, where special attention is given to the metal nanoparticles.

Nanoparticles have the advantage that they can be easily prepared in bulk with “wet” chemistry methods and divided into aliquots, where differences between individual particles are averaged. Such dispersions of nanoparticles can be easily applied on any sample, including biological materials for chemical characterization. Also, nanoparticles can be immobilized to a flat surface to form a planar SERS substrate, which can be used for the SERS detection [8].

Metal nanoparticles are usually prepared through the reduction of silver nitrate or gold chloride, forming dispersions of these metals in a liquid phase, either as a colloid or suspension [6, 8]. Sodium citrate, sodium borohydride, and hydroxylamine hydrochloride are common reduction agents. SERS nanoparticles are mostly prepared from silver and gold due to their unique light absorption properties [9]. In this work, silver nanoparticles were applied mainly because they constitute the most widespread and studied group of SERS substrates. The most common method to prepare silver nanoparticles is from Lee and Meisel [6, 10], where silver nitrate is reduced with sodium citrate forming a colloidal solution. Nanoparticles can be prepared as spheres, rods, cubes, prisms, or stars in different sizes typically ranging in 1 – 100 nm [11]. The size and shape depends on the reduction conditions and the use of capping agents, e.g., sodium dodecyl sulphate, polyvinylpyrrolidone, which regulate and direct the growth of nanoparticles. The size and shape of metal nanoparticles determines SERS enhancement efficiency and the region of light wavelengths at which SPR occurs. For example, for gold and larger sized silver nanoparticles including clusters of single nanoparticles, SPR is observed at a broad range of wavelengths that also covers visible red and near IR regions [12]. Thus, there is a variety of different metal nanoparticles and some of them should be chosen as SERS substrates in this work.

Another important SERS measurement parameter is the wavelength of laser used. Commercially available lasers emit green (514.5, 532 nm), red (633 nm), and infrared radiation (785, 833, and 1064 nm). Usually, SPR for different nanoparticles is observed in a wide wavelength interval including visible and near-IR range making many lasers

applicable in terms of inducing SPR [12]. However, there are also other factors that determine what lasers should be used. The laser wavelength greatly determines the intensity of Raman scattering. The lower the wavelength, the higher the fraction of the Raman scattered light, but there is a higher probability of sample photo-degradation. Also, fluorescence, a well-known interference in Raman measurements, can be increased or avoided depending on the laser wavelength used [7, 13].

Not all analytes can give intense SERS. In many publications, SERS is often measured for dyes. These dyes have functionalities to interact strongly with a negatively charged silver surface, e.g., through positively charged nitrogen. Also, they absorb light in the visible region. Therefore, when lasers with wavelengths within this absorption region are used, SERS takes place at resonance, or surface-enhanced resonance Raman scattering (SERRS) is observed. This leads to additional enhancement of Raman scattering, 10^5 – 10^6 higher than SERS [14], with very intense and distinctive peaks from these dye. However, the detection of the dyes is hardly important in chemical analysis, particularly, in environmental monitoring, due to their limited occurrence. Dyes are mainly used as model compounds to study properties of nanoparticles and their treatment [15]. However, the SERS detection of the dyes in ancient artefacts has been applied in archaeology [16]. Other compounds that can be successfully detected with SERS on nanoparticles are those that can chemisorb on the nanoparticle surface. Compounds that contain quaternary nitrogens, hydrosulfide groups, and carboxyl groups can participate in the chemisorption, e.g., aminoacids and some pharmaceuticals [7, 17, 18]. However, the majority of water pollutants from oil extraction, e.g., phenols and PAHs, whose analysis

is the object of this thesis, cannot adsorb strongly on the metal surface. The most important challenge associated with the SERS detection of such compounds is that they do not strongly interact with a surface of a SERS substrate. Despite this challenge, the successful detection of phenols with a semi-aggregated colloid on a TLC plate has been demonstrated by Li et al. [6].

There silver nanospheres and nanostars were made and treated by different methods to induce SERS of phenols, dibenzothiophene, and other species. SERS measurements with a 532 nm laser were compared to those with a 830 nm laser in terms of how sample photodegradation and fluorescence excitation can be minimized or eliminated. Initially, these measurements were completed on silica (TLC plates) for simplicity because this matrix has a relatively low Raman/SERS background. Problems associated with the use of MIP as the matrix for the detection were revealed, and solutions were proposed.

6.2 Materials and methods

Silver nitrate (99.9999%), sodium citrate tribasic dihydrate ($\geq 99\%$), polyvinylpyrrolidone (average Mw 10 000), polyvinylpyrrolidone with average Mw 10 000 and polyvinylpyrrolidone with average Mw 40 000, sodium L-ascorbate ($\geq 99.0\%$), sodium dodecylsulphate ($\geq 98.5\%$), Rhodamine 6G (95 %), L-phenylalanine ($\geq 98\%$), dibenzothiophene ($\geq 98.0\%$) were purchased from Sigma-Aldrich (Oakville, ON, Canada). Tetraethylammonium chloride was supplied with Eastman Chemical Company (Kingsport, TN, USA) and sodium chloride (ACS reagent) with A&C American

Chemicals (Saint-Laurent, QC, Canada). 2,4,6-Trimethylphenol (98%) was from Alfa Aesar (Ward Hill, MA, USA).

Two Raman spectrometers were used to acquire data: a confocal LabRam (Horiba Jobin Yvon, Edison, NJ, USA) equipped with Olympus BX41 microscope, 532 nm 70 mW solid diode laser, CCD detector with a 1024 pixel chip, and 1800 lines/mm grating; and a Renishaw in Via Raman system (Mississauga, ON, Canada) equipped with Leica DM2500M microscope, 830 nm 500 mW diode laser, CCD detector, and 1200 lines/mm grating. Absorbance spectra of silver nanoparticles were measured with Thermo Scientific Evolution 600 UV-Vis Spectrophotometer (Thermo Scientific, Ottawa, ON, Canada) against pure water in the reference cuvette. Spectra were acquired from 300 to 800 nm at a 240 nm min⁻¹ scanning rate with the monochromator slit set 4 nm. Prior to the measurements, freshly prepared silver dispersions were diluted with water so that the absorbance was below 1.5; the dilution was 1:10 for the nanospheres and 3:50 for the nanostars.

6.2.1 Preparation of silver nanoparticles

A colloidal solution of silver nanospheres was prepared according to the modified Lee-Meisel procedure [6]. Silver nitrate (19.0 mg), 2.00 mL of the aqueous solution containing trisodium citrate (1.00% w/w) and polyvinylpyrrolidone (Mw 10 000, 0.02% w/w) were added into 100 mL of deionized water. The resulting solution was mixed and reacted during the course of boiling for 30 min. The resulting nanoparticles were isolated from the prepared colloid by centrifugation (8000 rpm). Finally, the nanoparticles were redispersed with water to make the 1.0 mM silver colloid.

The suspension of silver nanostars was prepared according to the previous procedure by Shen et al. [15]. Briefly, in 5.00 mL of deionized water, 0.0490 g of polyvinylpyrrolidone (Mw 40 000), 100 μ L of 12.5 mM sodium dodecyl sulphate aqueous solution, 3.0 mL of aqueous solution containing 0.0239 g of silver nitrate, 3.0 mL of aqueous solution containing 0.0099 g of sodium ascorbate were reacted at 30 °C for 5 min. The nanoparticles were centrifuged (2000 rpm) and resuspended in water three times to make the final volume of the suspension up to 1.10 mL.

6.2.2 Treatment of silver nanoparticles

Before the use in SERS enhancement experiments, silver nanoparticles were treated in the following ways. Nanostars were washed with 10 mM solution of NaCl or 10 mM solution of $[(\text{C}_2\text{H}_5)_4\text{N}]\text{Cl}$. In a micro-centrifugation vial (1.2 mL), 50 μ L of the initial silver nanostar suspension was redispersed at sonication in 1 mL of NaCl (10 mM) solution in ethanol:water (1:1) (or the same concentration of $[(\text{C}_2\text{H}_5)_4\text{N}]\text{Cl}$ in ethanol/water). The resulting suspension was left standing for 5 min. Next, particles were completely precipitated with centrifugation (6400 rpm, 2 min) and again redispersed with ethanol:water (1:1) at sonication to about 50 μ L volume. In the case of $[(\text{C}_2\text{H}_5)_4\text{N}]\text{Cl}$, one extra cycle of redispersion with ethanol:water (1:1) and the subsequent centrifugation was completed to remove $[(\text{C}_2\text{H}_5)_4\text{N}]\text{Cl}$. The final suspensions were prepared immediately before use. Silver nanospheres (1.0 mM) were semi-aggregated in the recommended conditions: NaCl (20 mM) and 1 – 2 min duration [6]. Therefore, for the semi-aggregation, 20 μ L of NaCl (0.5 M) aqueous solution was pipetted into 0.500 mL of the

silver colloid, mixed, and let standing for 1 min before pipetting this semi-aggregated colloid on silica spots or a MIP film.

6.2.3 Preparation of samples for SERS/Raman measurements

For experiments with Rhodamine 6G, the nanostars were deposited on a silicon wafer and treated with aqueous solution of Rhodamine 6G (1 μM) exactly as in the original work [15]. Other analytes were deposited on the silica plates (Polygram Sil G/UV254 from Macherey-Nagel, Germany) according to the following procedure. On the plates, excess silica was removed to leave 4-5 mm diameter silica spots. A 5- μL aliquot of an analyte (18.75 g L^{-1}) solution in acetonitrile or acetonitrile:water (1:1) was pipetted onto the spot and let dry. In this way, $\sim 100 \mu\text{g}$ of L-phenylalanine, 2,4,6-trimethylphenol, and dibenzothiophene were deposited per spot. To deliver lower masses of these analytes, $\sim 1.3 \mu\text{g}$ per spot, solutions at 0.250 g L^{-1} was pipetted onto the silica spots. Finally, 6 μL of the silver nanoparticle dispersion was pipetted onto the analyte spot and let dry before SERS measurements. MIP films bound to glass slides synthesized from EGDMA as cross-linker, itaconic acid, 4-vinylpyridine, and styrene as monomers were prepared in the same way as in Chapter 4, and treated with the nanoparticles in the same way as the TLC plate. Some specific details of spectroscopic measurements are described in Table 6-1.

Table 6-1. Measurement and experimental parameters to obtain data for Chapter 6.

	Micro- scope objective	Beam power, mW	Integration time, sec	Base for nanoparticles
Figure 6-1	50×	35	4	Silicon wafer
Figure 6-2	50×	0.7	5	Silica TLC plate
Figures 6-3 and 6-4	20×	250	15	Silica TLC plate
Figure 6-5 (830 nm)	20×	250	15	1 – 4(IA):20(EGDMA) 2 – 4(Sty):20(EGDMA) 3 – 4(VP):20(EGDMA)
Figure 6-5 (532 nm)	50×	7	40	films prepared as in Chapter 4

6.3 Results and discussion

6.3.1 *The rationale for choice of methods for synthesis and post-treatment of silver nanoparticles*

To perform SERS measurements, it is always necessary to select an effective SERS substrate. The two kinds of nanoparticles chosen for this purpose were smaller sized silver nanospheres (~60 nm) and much bigger sized nanostars (~500 nm). The nanospheres were prepared via the reduction of silver nitrate with sodium citrate in the presence of polyvinylpyrrolidone. The role of polyvinylpyrrolidone in the preparation of the nanospheres was to regulate the size and uniformity [6]. Semi-aggregation of these nanoparticles into their clusters is required to achieve higher SERS enhancement and to shift SPR into the visible and IR regions. One way to achieve the increase in SERS

enhancement is a so called gap-plasmon effect, which is observed when an analyte molecule is located between two or several metal surfaces. The gap-plasmon effect can be achieved with silver colloid applied and dried on any surface, e.g., MIP films or TLC plates. In this case, the nanoparticles become closely spaced entrapping analyte molecules [12]. The achievement of the gap-plasmon effect as a result of simple drying of the dispersion is another advantage of using metal nanoparticles as a SERS substrate. The semi-aggregation of nanoparticles is induced with the addition of electrolytes into the colloid. For example, sodium chloride, nitric acid, or even an analyte itself, such as pyridine and alkaloids, can induce the aggregation. However, semi-aggregated colloids are highly unstable after being aggregated and, as a result, their ability to enhance SERS rapidly diminishes with time; this greatly affects the robustness of SERS measurements especially for quantitative analysis [19]. Therefore, beside semi-aggregated nanospheres, other nanoparticles were also investigated, which could be used without the semi-aggregation step.

Silver nanostars with sharp tips were synthesized through the reduction of silver nitrate with sodium ascorbate [15]. In this process, sodium dodecylsulfate and polyvinylpyrrolidone directed the growth of the nanoparticles into the nanostars. The nanostars were used directly without semi-aggregation and exhibited a strong enhancement effect for Rhodamine 6G. Therefore, they were also tried in this project as an alternative to the clusters of nanospheres. The procedure of the nanostars synthesis is especially attractive because it only requires mixing of the reagents, and the synthesis takes only 5 min.

When nanoparticles are synthesized with “wet” chemistry methods, SERS spectra can be populated with so called “anomalous” peaks. These originate from reducing agents, e.g. citrate anion, products of their oxidation, and surfactants, which are chemisorbed on the metal surface [17, 20]. These chemisorbed species carry the charge of the dispersed nanoparticles, preventing their coagulation. When silver colloid is semi-aggregated with chloride, it is suggested that the SERS signal is enhanced not only because of the semi-aggregation but also due to “chloride activation” [21]. Treatment of colloids with Cl^- has numerous effects. First, the substitution of polyvalent anions with Cl^- removes the charge from the surface of nanoparticles, which leads to the formation of the clusters of nanoparticles, i.e., semi-aggregation. Second, due to the small size of Cl^- , closer contact between analyte and the metal surface becomes possible, which facilitates the SERS enhancement by the metal surface, or in other words “chloride activation” takes place. In addition to “chloride activation”, the substitution of polyatomic anions, e.g., ascorbate, with Cl^- leads to the suppression of anomalous bands because no Raman bands originate from Cl^- [12]. Washing of prepared silver nanostars with chloride solutions was also carried out to cause “chloride” activation without the semi-aggregation.

6.3.2 SERS measurements with a 532 nm laser

SERS experiments were completed with a Raman system equipped with a 532 nm laser. The first step was to ensure that both silver nanostars and nanospheres were working SERS substrates. The nanoparticles were tested as SERS substrates using a model dye, Rhodamine 6G, in a same procedure reported along with the synthesis of the nanostars [15]. The UV-Vis absorbance spectra of the synthesized nanoparticles were

measured to confirm that the nanoparticles prepared in this work resembled the nanoparticles prepared by others [6, 15]. It was found that both nanostars and nanospheres induced strong SERS of Rhodamine 6G with characteristic and intense bands: 1129, 1183, 1312, 1363, 1509, 1574, and 1651 cm^{-1} [15] (Figure 6-1). This proved that the nanoparticles prepared in this work were functional SERS substrates. It is interesting to note that Rhodamine 6G is a strong fluorescent dye, but its fluorescence was quenched at SPR and no fluorescence background was detected (Figure 6-1). A similar phenomenon was observed for graphene deposited on gold nanoparticles [22].

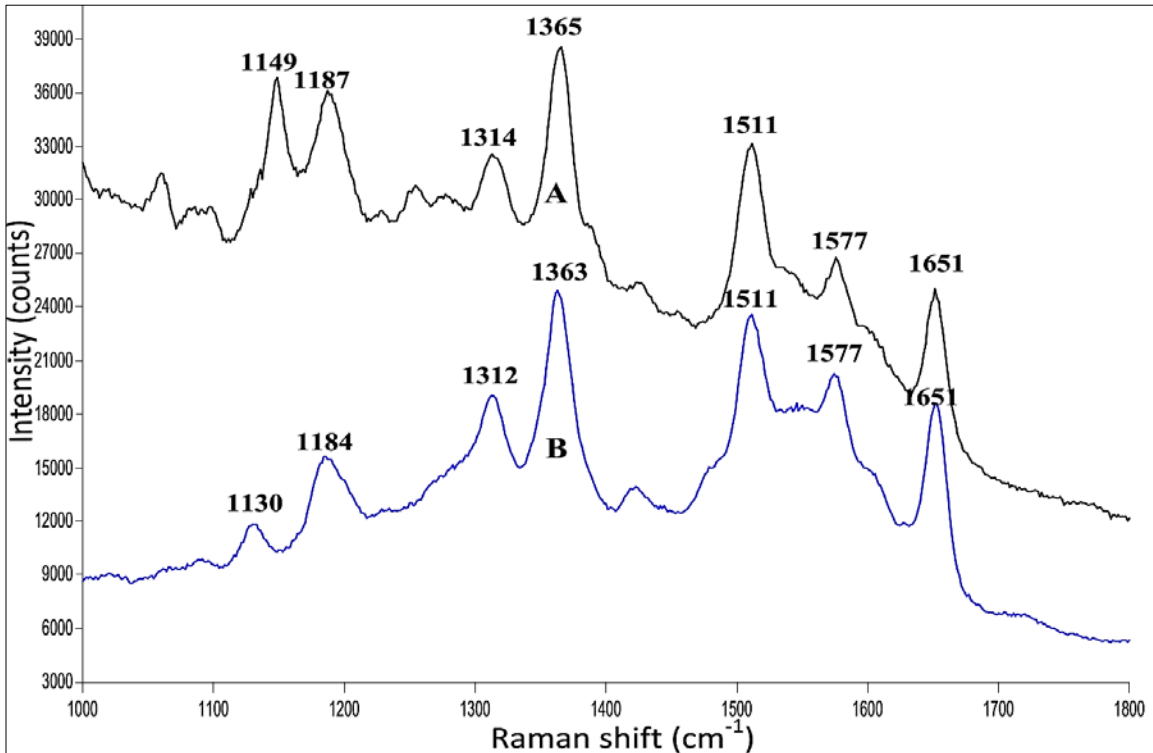


Figure 6-1. SERS spectra (532 nm laser) of Rhodamine 6G adsorbed on (A) silver nanostars and (B) nanospheres.

After the quality check, these nanoparticles were applied for SERS detection of neutral compounds: phenol, 2,4-dimethylphenol, catechol, and caffeine. Nanostars were washed with different solutions: HCl (1.0 mM), NaCl (10 mM), tetraethyl ammonium chloride (10 mM). Nanospheres were semi-aggregated in NaCl solution (20 mM). However, in all these experiments, no meaningful spectra for these compounds were observed. The measured spectra were varied with no consistent or characteristic features from spot to spot and scan to scan (Figure 6-2). This instability of the measured spectra can be a sign of photodegradation with graphitization of an analyte. Treatment of the nanostars with the NaCl solution simplified spectra of blanks because the organic species chemisorbed on the silver surface were removed at this washing step. However, this was not enough to give reproducible and meaningful SERS spectra for the analytes. All analytes, as organic matter, underwent intense photodegradation on the surface of silver nanoparticles.

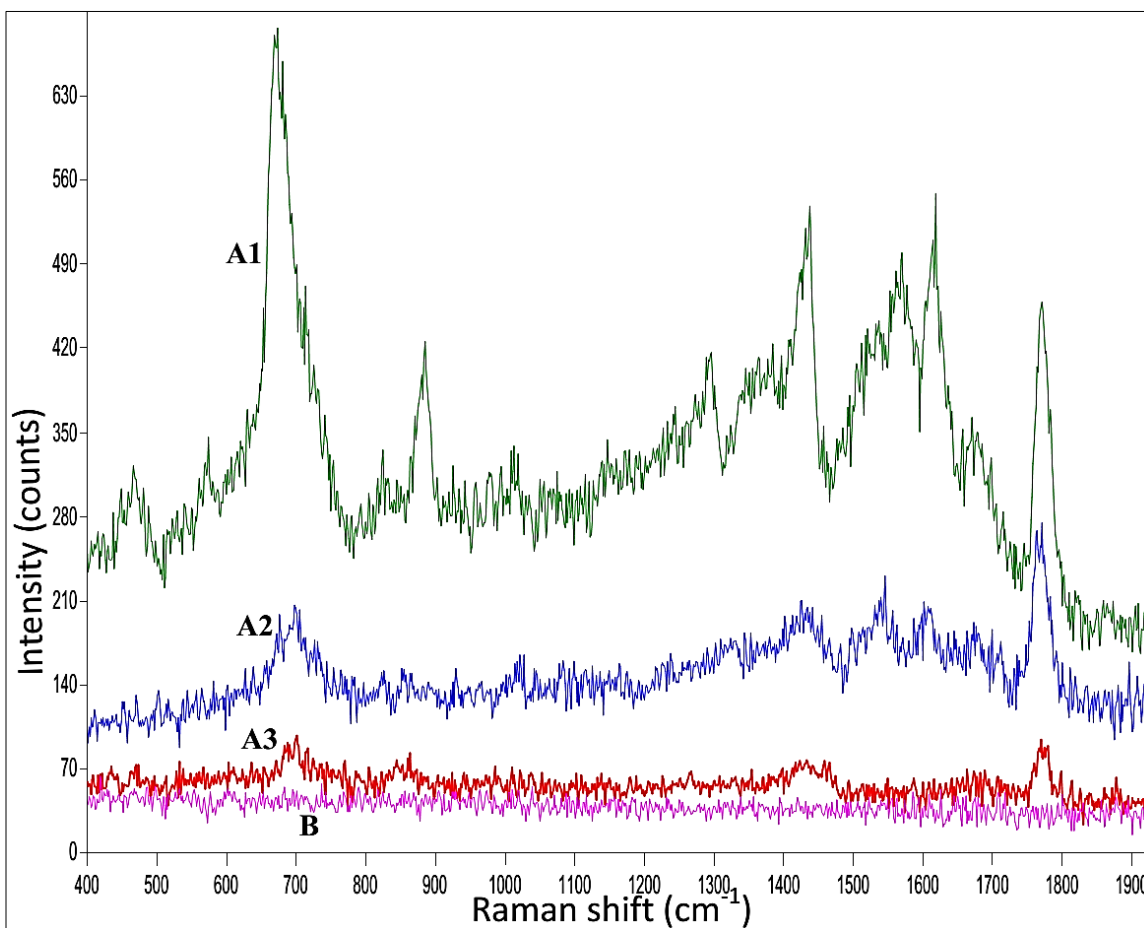


Figure 6-2. SERS spectra (532 nm laser) of phenol on nanostars (A), and (B) bare nanostars; A 1, 2, 3 – parallel scans.

Similar uncharacteristic SERS spectra have been observed by others and with other analytes such as aminoacids [7], sulfonamides, amino-, and nitropyrenes [23], when green lasers (532 and 514.5 nm) were used. These spectra showed broad peaks from the amorphous carbon. The “burning” problem can be related to the use of green lasers. The relatively high energy photons from the green lasers induce very strong local electrical field on the surface of nanoparticles. This causes the graphitization of analytes and other adsorbed species leading to the appearance of wide and tall “cathedral” peaks centered at

1360 and 1560 cm^{-1} . The shape and intensity of these peaks fluctuated from scan to scan [24]. The fact that amorphous carbon absorbs light over a wide range of wavelengths, including visible and IR regions, SERRS for amorphous carbon was observed when the green laser was employed. This explains why observed peaks were so intense.

Compared to phenol and other neutral analytes, very characteristic and reproducible SERS spectra were measured for Rhodamine 6G with 532 nm laser (Figure 6-1). Rhodamine 6G, with positively charged nitrogen, strongly interacts with the negatively charged silver surface replacing other adsorbed organic species that would produce anomalous and graphite peaks. Also, Rhodamine 6G absorbs light in the green region; therefore, SERS is enhanced even further because of this additional resonance component. Perhaps, because of a higher yield of SERRS, more laser energy is consumed by the Raman process rather than in graphitization.

The problem of photodegradation is a common problem for Raman microscopy and a number of approaches have been developed to diminish it: laser beam attenuation or defocusing, the use of objectives with lower numerical aperture values, the decrease of illumination time, and spinning or wetting a sample [23-26]. To solve the problem, all of these approaches were attempted, except spinning the sample; however, the “burning” effect could not be completely eliminated for phenols, or caffeine. The only positive result achieved was the reduction in the intensity of the graphite peaks. These methods only serve to reduce photon flux or heating per an exposed area or time. Another more fundamental solution is to use longer wavelength lasers, which emit less energetic photons, for example, near infra-red (NIR) lasers (785; 830; 1064 nm). Using a 830 nm laser Raman system, the similar set of experiments was completed.

6.3.3 SERS measurements with a 830 nm laser

In the second round of experiments, the same types of nanoparticles as in the previous section were used for SERS measurements with a 830 nm laser Raman microscope. Targeted analytes included an alkylphenol representative, 2,4,6-trimethylphenol, and dibenzothiophene as another important water pollutant from oil extraction. L-phenylalanine was used as a reference compound. SERS spectra of L-phenylalanine were already recorded with the use of the Lee-Meisel silver colloid [7]. In this work L-phenylalanine was used to check if tested nanoparticles could yield SERS in the new measurement conditions. L-phenylalanine had the same role as Rhodamine 6G in the experiments with 532 nm laser.

Compared to the SERS measurements with 532 nm laser, 830 nm laser made it possible to measure reproducible SERS spectra without many fluctuating features (Figure 6-3). No signs of photodecomposition were observed even at relatively high laser beam power (250 mW). Focusing with 20 × objectives was preferred because it provided less light power per illuminated area, which reduces the risk of sample heating and photodegradation. Another advantage to using this objective with the low numerical aperture value is an ease of focusing the laser beam. SERS spectra for both types of nanoparticles showed a presence of some anomalous bands (Figure 6-3) but they rarely overlapped with bands from the analytes (Figure 6-3, Spectrum 4). Raman spectra were measured exactly under the same conditions as SERS spectra for the same amount of an analyte but without any silver nanoparticles (Figure 6-3, Spectrum 2).

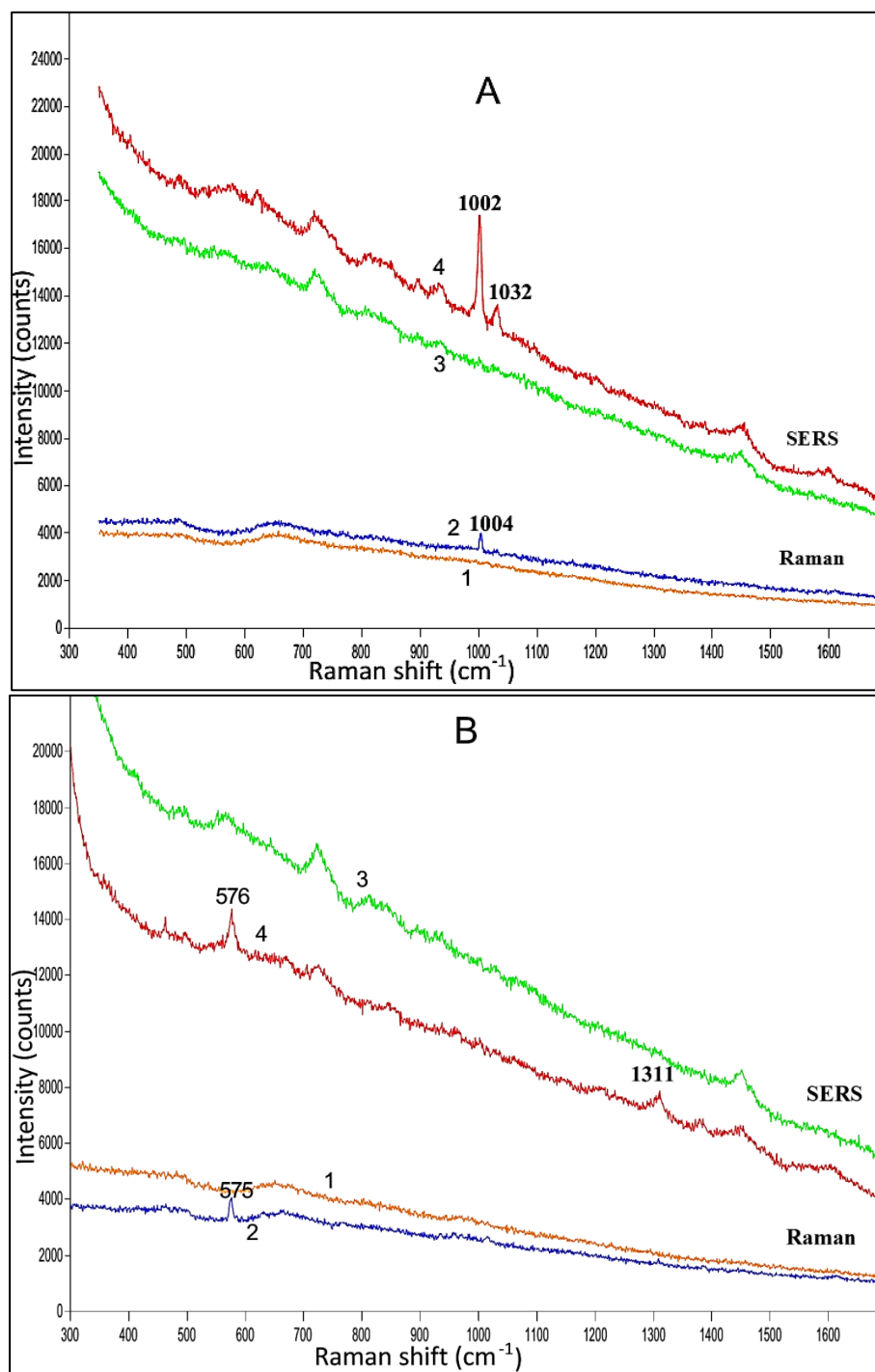


Figure 6-3. Raman and SERS spectra of (A) L-phenylalanine; (B) 2,4,6-trimethylphenol; (C) dibenzothiophene (~100 μg each) loaded on silica (cont. on the next page).

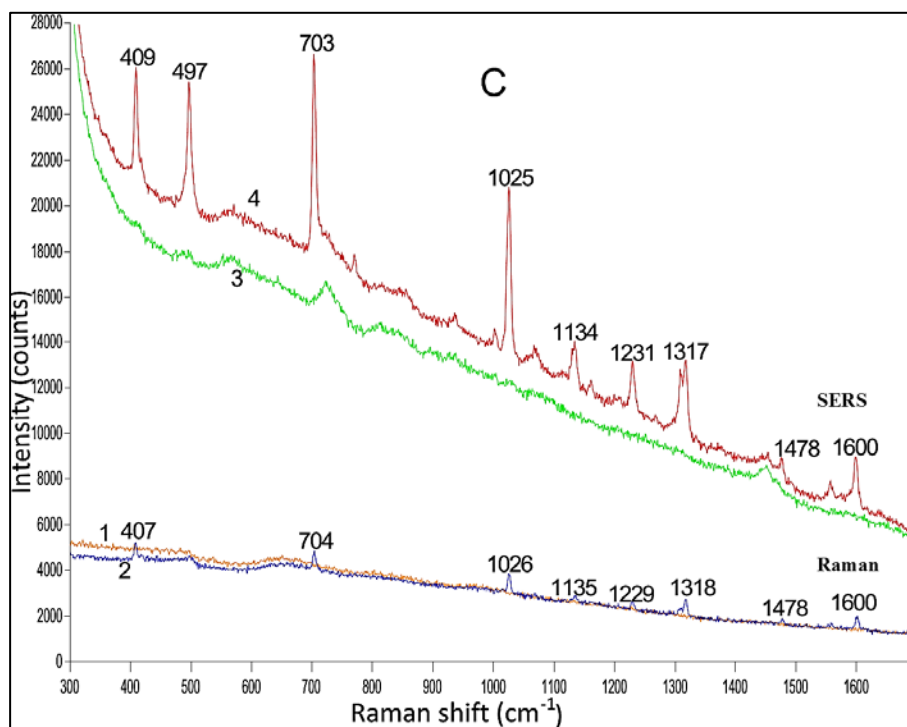


Figure 6-3 (cont). Raman and SERS spectra of (A) L-phenylalanine; (B) 2,4,6-trimethylphenol; (C) dibenzothiophene (~100 µg each) loaded on silica.

Note: 1 – Raman spectrum of bare silica; 2 – Raman spectrum of analyte on silica; 3 – SERS spectrum of semi-aggregated silver colloid; 4 – SERS spectrum of analyte on semi-aggregated silver colloid.

Initially, both Raman and SERS spectra were recorded for a high amount of analyte (~100 µg per spot) to make it easier to acquire interpretable and distinctive Raman spectra and to identify the most intense vibrational modes (Figure 6-3). In both Raman and SERS spectra, an intense band at 1002 cm^{-1} was observed for L-phenylalanine as in previous work [7]. The most intense peaks for 2,4,6-trimethylphenol appeared at 575 and 1311 cm^{-1} . Several strong peaks were observed for dibenzothiophene at 408, 702, 1026, 1600 cm^{-1} .

Silver nanospheres and nanostars were compared in terms of the SERS enhancement. Although there was variation in peak heights from sample to sample, comparison of average heights for the same band in Raman and SERS spectra gave an approximation of the extent of SERS enhancement. In this study, semi-aggregated silver nanospheres showed the highest enhancement for all analytes; the SERS spectra obtained with this substrate are shown in Figure 6-3. The nanostars without washing treatment and those washed with solutions of NaCl and tetraethyl ammonium chloride gave weaker SERS enhancement. Thus, the nanospheres treated by semi-aggregation show to be a more efficient SERS substrate than the nanostars. Semi-aggregation is a more crucial factor for the enhancement than the highly rough surface of nanostars.

A comparison of SERS enhancement for the analytes shows that the SERS enhancement for dibenzothiophene and L-phenylalanine was higher than for 2,4,6-trimethylphenol (Figure 6-3). This can be explained by the fact that these compounds can bind to colloidal silver, dibenzothiophene via the sulfur moiety and L-phenylalanine through a positive charge of its zwitter ion.

SERS spectra that were discussed so far were recorded for analytes present in large quantity on silica (Figure 6-3). In this case, these spectra probably also contain a significant portion of non-enhanced Raman scattering. SERS measurements were also completed for lower amounts of analytes ($\sim 1.33 \mu\text{g}$ per spot), which produced a negligible intensity of Raman scattering (Spectra 1 and 2 in Figure 6-4). The low analyte loading made it possible to estimate the SERS enhancement when the silver surface was not saturated with an analyte, which is appropriate for the estimation of sensitivity of

detection. Experiments at low analyte loading showed that only dibenzothiophene (Figure 6-4), but not L-phenylalanine or 2,4,6-trimethylphenol, produced SERS spectra discernible from the background. Thus, dibenzothiophene is promising for the detection with high sensitivity.

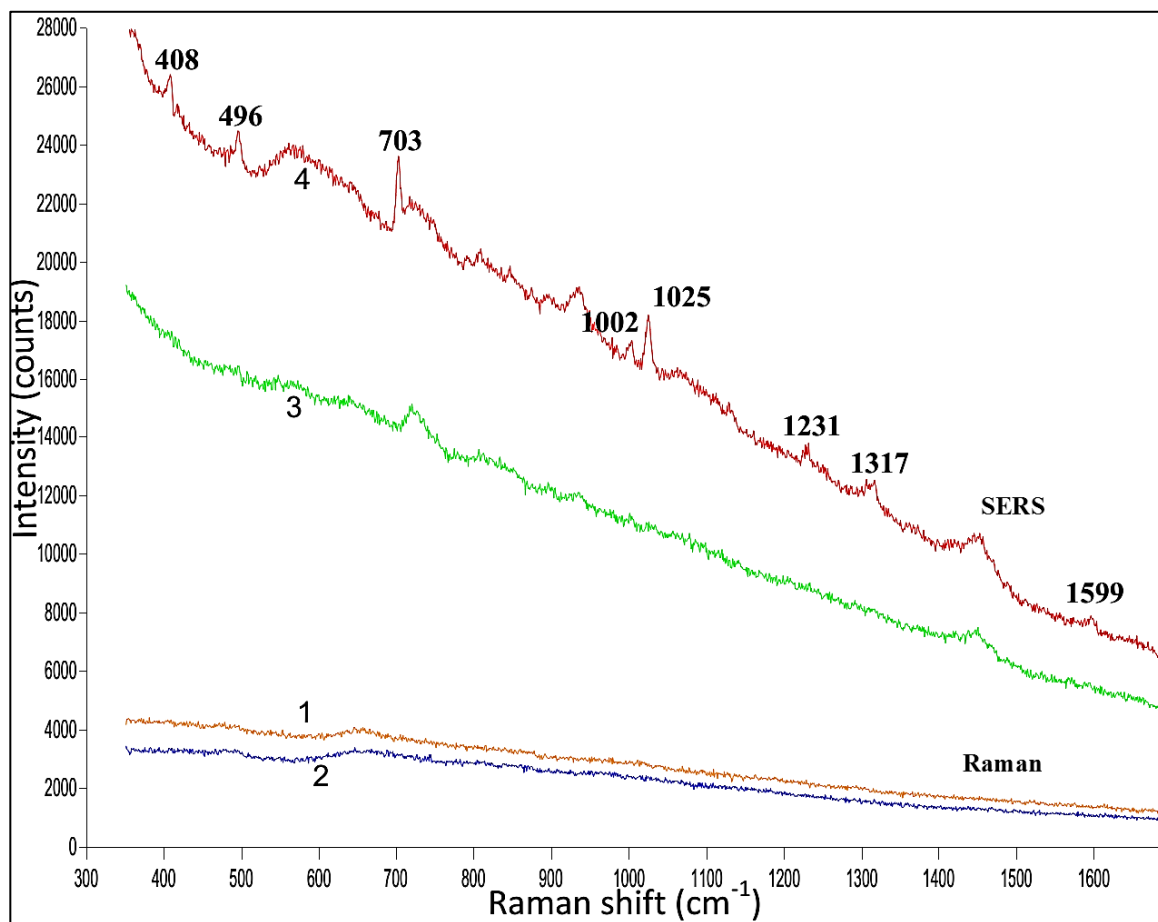


Figure 6-4. Raman and SERS spectra of dibenzothiophene ($\sim 1.33 \mu\text{g}$) loaded on silica; 1 – Raman spectrum of bare silica; 2 – Raman spectrum of dibenzothiophene on silica; 3 – SERS spectrum of semi-aggregated silver colloid; 4 – SERS spectrum of dibenzothiophene on semi-aggregated silver colloid.

Raman and SERS peaks of dibenzothiophene and 2,4,6-trimethylphenol mainly originate from ring breathing modes. According to previous work [27], some of the

observed bands for dibenzothiophene can be assigned (within the measurement error $\pm 4 \text{ cm}^{-1}$) to the following vibrational transitions: 703 cm^{-1} – one of “the CCC in-plane bending modes”; 1025 cm^{-1} – one of “the ring C–H in-plane bending modes of the aromatic systems combined with the C–C stretching modes⁴”; bands between $1300\text{--}1700 \text{ cm}^{-1}$ – “the C–C stretching modes in the aromatic system combined with the $\beta(\text{HCC})$ ”. It is not possible to see the 496 cm^{-1} band in the Raman spectrum of dibenzothiophene (Figure 6-4). This band is relatively much less intense than other assigned peaks in the Raman spectrum, e.g., 703 and 1025 cm^{-1} , according to Figure 6-3C and dibenzothiophene Raman spectrum measured by Frank et al. [27]. The situation becomes dramatically different with SERS where the peak at 496 cm^{-1} is one of the most intense. Thus, among all vibrational modes, the highest enhancement was observed for the 496 cm^{-1} peak, which corresponds to “the in-plane deformation mode of the thiophene ring, $\alpha(\text{CSC})$ ” [27]. The fact that the highest SERS enhancement was achieved for the moiety containing sulfur is indicative of strong interaction between the sulfur moiety and the silver surface. This interaction with the silver surface together with the high polarizability of dibenzothiophene can explain the high sensitivity of SERS for dibenzothiophene as compared to trimethylphenol and L-phenylalanine. The fact that dibenzothiophene can produce a SERS signal under conditions when other aromatics do not, demonstrates a distinct selectivity of SERS detection for thiophenes as water contaminants and components of oil.

⁴ this combined vibration is further indicated in the text as $\beta(\text{HCC})$

6.3.4 MIP as a matrix for SERS detection

A MIP has a complex composition consisting of cross-linked carbon chains, residual vinyl groups, and various monomer functionalities, which sometimes include aromatic moieties. All these moieties can result in vibrational bands in a SERS spectrum when MIP is used as a matrix to carry an analyte. Therefore, when SERS measurements are completed on a MIP film with an adsorbed analyte, the MIP can yield its own characteristic SERS spectrum, which will constitute the detection background. Although such a complex background is always undesirable, it can be used for an internal standardization in quantitative analysis. It is known that the heights of Raman and SERS peaks fluctuate from scan to scan because of variations in illumination and enhancement conditions. Analytical peaks could be normalized against a peak originating from the MIP matrix to achieve a more consistent quantitative analysis.

When a 830 nm laser was used to produce Raman scattering of the MIPs based on different functional monomers, the Raman spectra showed to be seriously distorted by fluorescence from the MIP matrices (Figure 6-5). This makes it impossible to further measure any Raman and SERS spectra on the MIPs with 830 nm laser wavelength, despite the fact that the “burning” problem is eliminated with this laser wavelength. Similar measurements of Raman spectra of the MIPs were completed with 532 nm laser (Figure 6-5). In this circumstance, vibrational bands of the MIPs were observed without a fluorescence background. The spectra of MIPs obtained at 830 nm have the same Raman peaks as in 532 nm spectra, but those peaks are superimposed on the broad fluorescence band. It is unusual to observe the excitation of fluorescence with 830 nm laser because traditionally near-IR lasers are specially designed not only to avoid photodegradation but

also fluorescence, e.g., for silica TLC plates [7]. Undesirable fluorescence is often observed for many samples when a green laser is employed [7, 23], which is not the case with the MIPs.

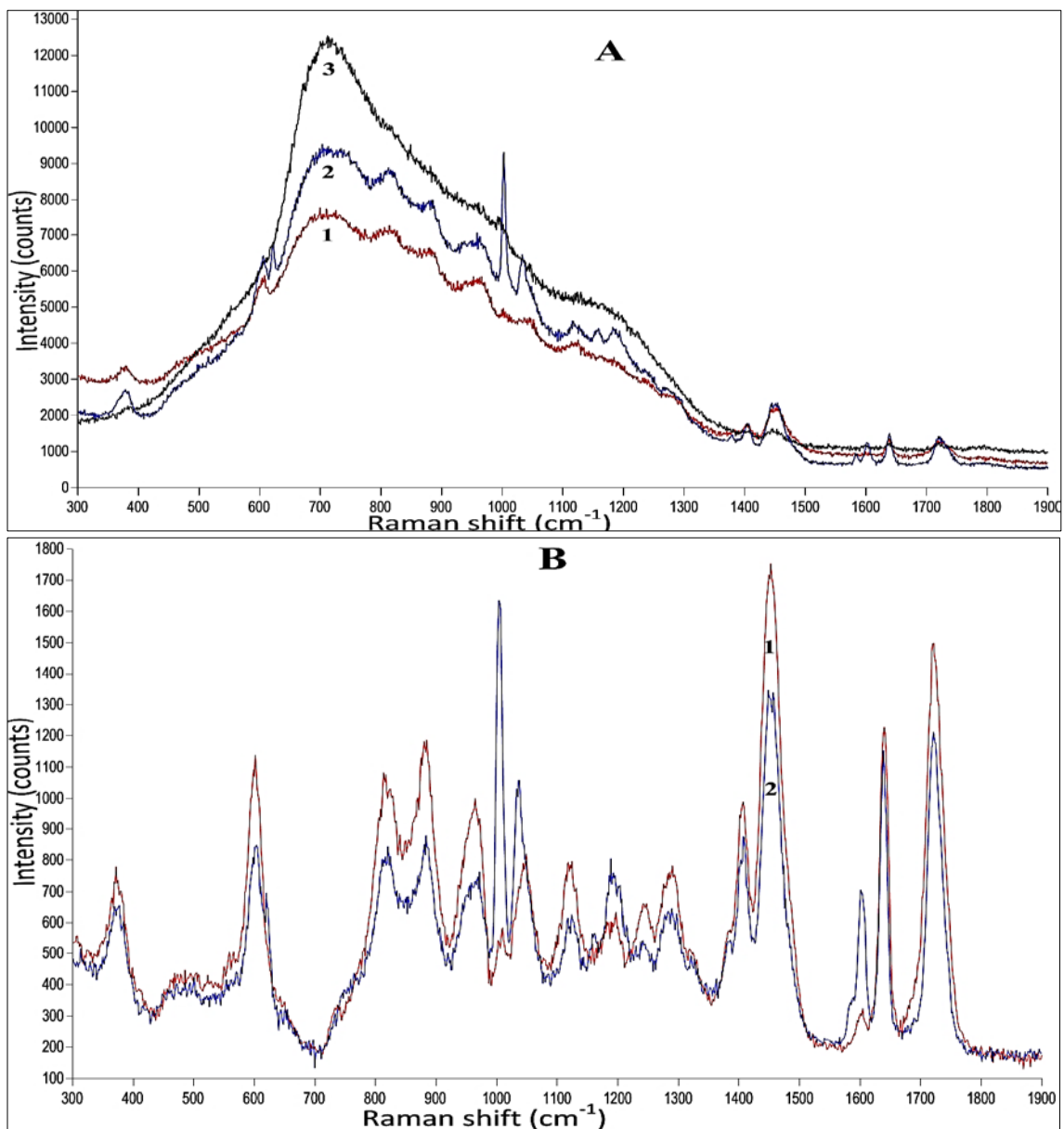


Figure 6-5. Raman spectra for MIP matrices based on EGDMA and different monomers: (1) itaconic acid; (2) styrene; (3) 4-vinylpyridine; scans with (A) 830 nm and (B) 532 nm lasers.

The interference by fluorescence can be eliminated with a time-resolved Raman spectrometer, though this equipment is very expensive, complex, and not widely-available. Another way to solve this problem may be to use a red laser (633 nm), which is another common laser source in Raman spectrometry. This wavelength maybe a compromise as it is between the near-IR region, where no photon induced damage occurs, but the fluorescence is observed, and the green region, where a sample is photo degraded but the fluorescence is not apparent. An even more dramatic and reliable way to solve the problem would be to use an MIP of completely different composition, for example, silica xerogels did not yield a background fluorescence when it was immobilized on a gold planar SERS substrate and a 785 nm laser was used [5].

6.4 Conclusions and future work

The idea of this research project was to develop an analytical test system based on SERS detection where silver nanoparticles are applied on a MIP film with an adsorbed analyte. An important feature of this detection approach is the direct contact between the nanoparticle surface and analyte, the preconcentration and separation of analyte, and the possibility to use a SERS peak originating from the MIP for internal standardization. The effect of different experimental parameters on the SERS detection, such as the type of nanoparticles, a laser wavelength, and the nature of an analyte were studied. Silver semi-aggregated nanospheres and nanostars were prepared and treated with “wet” chemistry methods to be used as SERS substrates. The semi-aggregated nanospheres induced more intense SERS than did the “chloride” activated nanostars, which points to a direction to improve the sensitivity of SERS detection, i.e., looking at different silver nanosphere

preparation and semi-aggregation procedures. Laser wavelength has been shown to have a dramatic effect on the quality of SERS measurements in terms of sample graphitization and excitation of fluorescence from MIPs. The green laser (532 nm) caused graphitization, while 830 nm-laser resulted in the abundant fluorescence background, seriously impeding the SERS detection on the MIPs. This project is not finished, and there is much work left to do to solve the problems encountered. The fluorescence from a MIP matrix should be eliminated; it is proposed that a red laser to be tested to avoid both the graphitization and fluorescence issues, or it may be necessary to use a MIP matrix of completely different composition. It is also reasonable to switch the targets of detection from phenol and alkylphenols to thiophenes, as another group of water contaminants from oil extraction and indicators of oil pollution. The reason for the change is that thiophenes are better suited for SERS detection due to the sulfur moiety, which can interact with the silver surface of nanoparticles.

6.5 References

1. Smith, E.; Dent, G., *Modern Raman Spectroscopy - A Practical Approach*. John Wiley & Sons Ltd: Great Britain, 2005; p 5.
2. Ru, E. L.; Etchegoin, P., *Principles of Surface-Enhanced Raman Spectroscopy and related plasmonic effects*. 1st ed.; Elsevier Science: Boston, 2009; p 15-17.
3. Ru, E. L.; Etchegoin, P., *Principles of Surface-Enhanced Raman Spectroscopy and related plasmonic effects*. 1st ed.; Elsevier Science: Boston, 2009; p 188, 294.
4. Kostrewa, S.; Emgenbroich, M.; Klockow, D.; Wulff, G., Surface-enhanced Raman scattering on molecularly imprinted polymers in water. *Macromolecular Chemistry and Physics* **2003**, *204* (3), 481-487.
5. Holthoff, E. L.; Stratis-Cullum, D. N.; Hankus, M. E., A nanosensor for TNT detection based on molecularly imprinted polymers and surface enhanced Raman scattering. *Sensors* **2011**, *11* (3), 2700-14.
6. Li, D.; Qu, L.; Zhai, W.; Xue, J.; Fossey, J. S.; Long, Y., Facile on-site detection of substituted aromatic pollutants in water using thin layer chromatography combined with surface-enhanced Raman spectroscopy. *Environmental science & technology* **2011**, *45* (9), 4046-52.
7. István, K.; Keresztury, G.; Szép, A., Normal Raman and surface enhanced Raman spectroscopic experiments with thin layer chromatography spots of essential amino acids using different laser excitation sources. *Spectrochimica Acta Part A: Molecular and Biomolecular Spectroscopy* **2003**, *59* (8), 1709-1723.
8. Peron, O.; Rinnert, E.; Toury, T.; Lamy de la Chapelle, M.; Compere, C., Quantitative SERS sensors for environmental analysis of naphthalene. *Analyst* **2011**, *136* (5), 1018-22.
9. Ru, E. L.; Etchegoin, P., *Principles of surface-enhanced Raman spectroscopy and related plasmonic effects*. 1st ed.; Elsevier Science: Boston, 2009; p 368.
10. Munro, C. H.; Smith, W. E.; Garner, M.; Clarkson, J.; White, P. C., Characterization of the surface of a citrate-reduced colloid optimized for use as a substrate for surface-enhanced resonance Raman scattering. *Langmuir* **1995**, *11* (10), 3712-3720.
11. Wang, Y.; Wang, E., Nanoparticle SERS substrate. In *Surface Enhanced Raman Spectroscopy: Analytical, Biophysical and Life Science Applications*, Schlucker, S., Ed. Wiley-VCH Verlag GmbH & Co. KGaA: Weinheim, Germany, 2011; pp 39-69.

12. Ru, E. L.; Etchegoin, P., *Principles of Surface-Enhanced Raman Spectroscopy and related plasmonic effects*. 1st ed.; Elsevier Science: Boston, 2009; p 374-408.
13. Smith, E.; Dent, G., *Modern Raman Spectroscopy - A Practical Approach*. John Wiley & Sons Ltd: Great Britain, 2005; p 24.
14. Smith, E.; Dent, G., *Modern Raman Spectroscopy - A Practical Approach*. John Wiley & Sons Ltd: Great Britain, 2005; p 126.
15. Shen, X. S.; Wang, G. Z.; Hong, X.; Zhu, W., Nanospheres of silver nanoparticles: agglomeration, surface morphology control and application as SERS substrates. *Physical chemistry chemical physics* **2009**, *11* (34), 7450-4.
16. Bruni, S.; Guglielmi, V.; Pozzi, F., Surface-enhanced Raman spectroscopy (SERS) on silver colloids for the identification of ancient textile dyes: Tyrian purple and madder. *Journal of Raman Spectroscopy* **2010**, *41* (2), 175-180.
17. Yaffe, N. R.; Blanch, E. W., Effects and anomalies that can occur in SERS spectra of biological molecules when using a wide range of aggregating agents for hydroxylamine-reduced and citrate-reduced silver colloids. *Vibrational Spectroscopy* **2008**, *48* (2), 196-201.
18. Faulds, K.; Smith, W. E.; Graham, D.; Lacey, R. J., Assessment of silver and gold substrates for the detection of amphetamine sulfate by surface enhanced Raman scattering (SERS). *The Analyst* **2002**, *127* (2), 282-286.
19. Bell, S. E.; Sirimuthu, N. M., Rapid, quantitative analysis of ppm/ppb nicotine using surface-enhanced Raman scattering from polymer-encapsulated Ag nanoparticles (gel-colls). *Analyst* **2004**, *129* (11), 1032-6.
20. Sánchez-Cortés, S.; García-Ramos, J. V., Anomalous Raman bands appearing in surface-enhanced Raman spectra. *Journal of Raman Spectroscopy* **1998**, *29* (5), 365-371.
21. Ru, E. L.; Etchegoin, P., *Principles of Surface-Enhanced Raman Spectroscopy and related plasmonic effects*. 1st ed.; Elsevier Science: Boston, 2009; p 405-407.
22. Wang, P.; Zhang, D.; Zhang, L.; Fang, Y., The SERS study of graphene deposited by gold nanoparticles with 785nm excitation. *Chemical Physics Letters* **2013**, *556*, 146-150.
23. Szabo, N. J.; Winefordner, J. D., Evaluation of two commercially available tlc materials as sers substrates. *Applied Spectroscopy* **1997**, *51* (7), 965-975.

24. Pieczonka, N. P.; Aroca, R. F., Inherent complexities of trace detection by surface-enhanced Raman scattering. *Chemphyschem: a European journal of chemical physics and physical chemistry* **2005**, *6* (12), 2473-84.
25. Yeo, B. S.; Schmid, T.; Zhang, W. H.; Zenobi, R., A strategy to prevent signal losses, analyte decomposition, and fluctuating carbon contamination bands in surface-enhanced Raman spectroscopy. *Applied Spectroscopy* **2008**, *62* (6), 708-713.
26. Lin, X. M.; Cui, Y.; Xu, Y. H.; Ren, B.; Tian, Z. Q., Surface-enhanced Raman spectroscopy: substrate-related issues. *Analytical and Bioanalytical Chemistry* **2009**, *394* (7), 1729-45.
27. Frank, O.; Jehlicka, J.; Edwards, H. G., Raman spectroscopy as tool for the characterization of thio-polyaromatic hydrocarbons in organic minerals. *Spectrochimica acta. Part A, Molecular and biomolecular spectroscopy* **2007**, *68* (4), 1065-9.

**Chapter 7. Application of Fluorimetry for Detection of
Water Contaminants on Molecularly Imprinted Polymeric Films**

7.1 Introduction

Fluorescence spectrometry, or fluorimetry, is one of the most sensitive methods of chemical analysis. It is based on the phenomenon of fluorescence. Fluorescence is a two photon process, which includes the following steps; first, a molecule absorbing a photon is excited from the ground singlet electronic state to an excited singlet electronic state, whose vibrational energy level can vary. Next, non-radiative vibrational relaxation brings the molecule into the lowest vibrational level within the same excited singlet electronic state. Following this, the energy transition to any vibrational level of the ground singlet electronic state yields a photon. Such photons constitute fluorescence, which has a longer wavelength than the exciting, or absorbed, radiation [1].

Fluorescence intensity (F , photon counts sec^{-1}) can be approximated at low analyte concentrations (C) when $\epsilon bc \leq 0.02$ as:

$$F = k \cdot \phi_F \cdot P_0 \cdot \epsilon \cdot b \cdot c \quad (7-1)$$

where k is the collection efficiency of fluorescence with fluorimeter optics; ϕ_F is the quantum yield of fluorescence; P_0 is the power of an excitation beam; ϵ is an absorption coefficient; b is the path length. Fluorescence can be a relatively efficient process where typical ϕ_F values for an average fluorophore are between 0.1 and up to unity. Fluorescence intensity can be raised by the increase of k and P_0 , which are related to fluorimeter optics, light source, and measurement settings. In favorable experimental conditions, the limit of the detection is mostly blank limited [2]. Compared to absorption spectrometry, fluorimetry has much lower detection limits and the linear range is wider [3]. The selectivity of fluorimetry is partially determined by the fact that not all species

can fluoresce. In addition, different fluorophores have different excitation spectra; therefore, the fluorophores can be excited in different wavelength regions. The same is true for the emission from different fluorophores, which can be detected at different wavelength regions. Thus, the excitation and emission collection can be performed with some measure of selectivity. However, the overlap of excitation and emission bands in a mixture of fluorophores, is common [3, 4].

Many water contaminants associated with oil extraction are aromatic, for example, alkylphenols, PAHs, and alkylbenzenes, and these can fluoresce. Fluorimetric detection of these analytes can be achieved directly in water [4], or the targets can be separated and preconcentrated on an adsorbent [5], which can be a MIP [6]. Fluorescence is susceptible to various matrix effects that usually quench but can also enhance the fluorescence signal, which can have negative consequences for quantitative fluorimetry [7]. To minimize these effects, the separation of an analyte from matrix interferences is very desirable. The separation results in the partition of analyte from water into a stationary phase with consistent composition. Once sequestered, the analyte can be detected directly on the MIP, which makes it possible to avoid the additional sources of error associated with sample handling such as the solvent extraction and reduction of extract volume. In addition, this simplification saves time and reagents. Coupling of MIPs or other adsorbent materials with fluorimetry has been completed before. In several examples, a polymeric adsorbent in the form of particles was packed in a flow-through cell with the light path of ~1 mm to accomplish the flow injection analysis [8] of aromatic hydrocarbons [9], naphthylamines [10], and PAHs [5] in water. A MIP film was incorporated into a microfluidic device for the detection of the dansyl derivatives of amino acids [11]. The

MIP film prepared by polyurethane polymerization [6, 12] and MIP particles by vinyl polymerization [13] were exploited for sensing PAHs. A fluorescence sensor for nitroaromatic explosives was developed based on a MIP with incorporated quantum dots. The inherent fluorescence of the quantum dots was quenched as a result of the binding event [14].

Because this work deals actively with the measurement of fluorescence from a solid, a MIP film, some background information about the nature of this type of measurement is given below. The measurement of fluorescence from solid materials is very common. In addition to the measurements in flow-injection analysis and chemical sensing exemplified above, fluorescence detection is also applied for thin layer chromatography and for in situ analysis of solid objects, e.g. tree leaves contaminated with PAHs [15]. Fluorimetry, applied to solid samples, is called “solid phase (or state) fluorimetry” due to some specificities of this kind of measurements. To observe fluorescence, an analyte can be spread on silica, paper, nylon, or salts, e.g., sodium acetate [15]. Compared to liquid samples, the movement of molecules is restricted in a solid matrix. This restriction can quench or, in reverse, enhance the fluorescence.

Since many solid samples, including polymers, are opaque or semi-opaque, fluorescence is measured as diffusely reflected emission. The excitation radiation is also diffusely reflected from samples and makes its way into the detector, leading to an intense Rayleigh scattering peak in a fluorescence spectrum. The tail of this peak cannot be removed with the emission monochromator and constitutes stray light in the measured fluorescence signal [16]. In opaque samples fluorescence is mostly induced and emitted at or near the surface. Thus, only a tiny volume of a solid sample is required for the

measurements. The excitation beam can be easily focused on a small spot of this sample. Therefore, solid-phase fluorimetry is very applicable in miniaturized analytical systems [11].

Solid phase fluorimetry suffers from the same problems as fluorescence spectrometry in general. These problems include different types of self-absorption, also called inner-filter effects. A primary inner-filter effect is observed when part of the incident or excitation radiation is absorbed by an analyte, diminishing the intensity of excitation radiation. A secondary inner-filter effect takes place when fluorescence is reabsorbed by an analyte due to the natural overlap of an analyte's absorption and emission bands. The inner-filter effects cause calibration lines to curve and the shapes of emission spectra to be distorted [17, 18]. The light path is shorter in opaque solids than in transparent liquids; therefore, the inner-filter effects are less pronounced for the opaque samples [17]. Another problem is background fluorescence [19] and Raman scattering [4], which both originate from a sample material. This is a factor that often limits the sensitivity of detection.

There are several types of spectral experiments where excitation and emission wavelengths are scanned or set. An emission spectrum is obtained when the emission output is scanned at a constant excitation wavelength. An emission spectrum is the most common and is used both for quantitative and qualitative analysis. An excitation spectrum is obtained when the intensity of emission at a single wavelength is measured, while an excitation monochromator scans a range of excitation wavelengths. An excitation spectrum is proportional to an absorption spectrum [17], and in this work, fluorescence was recorded in this measurement mode to find the optimal excitation wavelength.

Another mode of fluorescence measurement is the synchronous scan, or dual wavelength spectroscopy, which deserves special attention. Excitation (λ_{ex}) and emission (λ_{em}) wavelengths are scanned synchronously at a constant difference between them ($\Delta\lambda$).

$$\Delta\lambda = \lambda_{em} - \lambda_{ex} \quad (7-2)$$

The synchronous scan makes it possible to extend the capabilities of fluorimetry and to correct its weaknesses in a number of ways. First, the amount of stray light, which passes two monochromators, is reduced because excitation and emission monochromators scan at a fixed offset ($\Delta\lambda$) [7]. Second, in a synchronous scan spectrum a band for the particular transition is often narrower than the corresponding band in an emission spectrum [7, 20]. The effect of peak narrowing makes it possible to resolve and identify peaks from different analytes in a mixture. This deconvolution task is hardly possible in the emission scan mode even when excitation wavelengths are varied in an attempt to selectively excite certain analytes [7, 21, 20]. Third, synchronous scanning is widely used to record very characteristic “fingerprint” spectra, which can be used for identification of samples, e.g., of petroleum products [22].

In this work, an approach for direct fluorimetric detection of analytes adsorbed on a MIP film was developed to be used independently or as part of a sensor for on-line monitoring of water contaminants. Factors influencing the quality of fluorescence measurements were studied and the optimal conditions for such measurements were determined. Particular effort was given to the synchronous scan mode. Spectra of phenol, caffeine, and PAHs on MIP films were recorded and the possibility of direct detection of these analytes was assessed.

7.2 Materials and methods

Chlorosulfonic acid (99%), naphthalene (99%), phenanthrene ($\geq 99.5\%$), caffeine (Reagent Plus grade), and phenol (99%) were purchased from Sigma-Aldrich (Oakville, ON, Canada). Coumarin (98 %) was supplied by Alfa Aesar (Ward Hill, MA, USA). Potassium hydroxide of ACS reagent grade was purchased from ACP Chemicals (Montreal, QC, Canada).

7.2.1 Fluorimetric measurements

Measurements were made with a Photon Technology International Quanta Master 6000 spectrofluorimeter (Canada, ON, London) equipped as follows: 75W Usio Xenon arc lamp excitation source; Czerny-Turner $f/3.4$ grating excitation and emission monochromators; Hamamatsu R-928 five-stage photomultiplier tube. Excitation and emission spectra were corrected for the emission spectrum of the xenon lamp, the detector response, and light losses in optics with the correction curves supplied with Felix 32 (Photon Technology International, Version 1.42b). Slit widths of excitation and emission monochromators were set at 4 mm each. A metal holder⁵ was constructed to mount a quartz slide with a bound MIP film in a stable illumination position. The holder was mounted with double-sided adhesive tape on the rotating stage as a fluorimeter accessory to complete the illumination of the film at different angles. The holder was placed on the stage in the position where the excitation beam was focused on a $\sim 1 \times 5 \text{ mm}^2$ rectangular spot on the film surface.

⁵ A picture of a slide holder working by the same principle, but made from plastic is shown in Chapter 8.

7.2.2 Fabrication of MIP films and analyte adsorption to these films

Fabrication of 100 μm and 20 μm thick films is described in Chapter 2. In this work, a MIP was immobilized on a quartz slide instead of the glass slide because glass is fluorescent in UV light. Quartz slides $76 \times 25 \times 2 \text{ mm}^3$ (Chemglass Life Sciences, Vineland, NJ, USA) were cut into 3 pieces $25 \times 25 \text{ mm}^2$ and used as the substrates for MIP films. To load MIP films with an analyte, 250 mL of aqueous solution of the analyte (phenol, caffeine, naphthalene, or phenanthrene) was stirred in a beaker with a slide/MIP film for 4.5 hours. For Figure 7-10, the volume of the phenanthrene solutions was set at 750 mL to achieve the higher sensitivity of the detection. After analyte adsorption, the slide was removed, washed with water, and air dried. The composition of MIP films, the concentrations of analytes in the solutions for loading the MIP films, and measurement conditions used to obtain spectral data are given in Table 7-1.

Table 7-1. Measurement and experimental parameters to obtain data for Chapter 7.

	Composition of MIP with molar ratio of components	Film thickness, μm	Analyte, and its concentration in the aqueous solution	Illumination geometry and angle (α) as in Figure 7-2	Others
Figure 7-3	1(toluene):4(VP):20(EGDMA)		phenanthrene, $500 \mu\text{g L}^{-1}$	front face at 30° ; back surface at 60°	
Figure 7-4	1-4(Sty):20(EGDMA) 2-EGDMA 3-4(MAA):20(EGDMA) 4-4(VP):20(EGDMA) (non-imprinted)	100	N.A.	back surface at 60°	spectra were normalized at 370 nm
Figure 7-5	1(toluene):4(VP):20(EGDMA)		phenanthrene, $400 \mu\text{g L}^{-1}$	front face at 20°	
Figure 7-6	1(ph-l):4(IA):20(EGDMA)		phenol, 6.00 mg L^{-1}	front face at 30°	
Figure 7-7	1(ph-l):4(IA):20(EGDMA)	20	a drop of 1mM dye solution was deposited on the film and air dried	front face at 30°	excitation beam was focused on the visibly fluorescent spot
Figure 7-8	1(caffeine):4(MAA):20(EGDMA)		caffeine, 5.00 mg L^{-1}	front face at 20°	
Figure 7-9	1(ph-l):4(IA):20(EGDMA)		naphthalene, 1.00 mg L^{-1}	back surface at 60°	
Figure 7-10	1(toluene):4(VP):20(EGDMA)	100	phenanthrene, $500 \mu\text{g L}^{-1}$	front face at 20°	
Figure 7-11	1(toluene):4(VP):20(EGDMA)		phenanthrene: 2.0, 5.0, 10, 20, 40, 60, 100, 200, $400 \mu\text{g L}^{-1}$	front face at 20°	peak was integrated from 325 to 450 nm

Note: The data in figures 7-3, 7-5, 7-10, and 7-11 were obtained with the use of MIP for PAHs based on 4-vinylpyridine and EGDMA. The MIP prepolymerization mixture was donated by Stefana Egli, who developed this MIP in her research project [23].

7.2.3 Synthesis of coumarin-6-sulfonyl chloride and the derivatization of phenol

Coumarin-6-sulfonyl chloride was synthesized according to a published procedure (Figure 7-1A) [24]. Coumarin (1) was mixed with in a three-fold molar excess of chlorosulfonic acid, and the mixture was stirred at 100 °C for 2 h. The reaction product (2) was recrystallized three times from toluene, but not benzene as in the original work because benzene is highly carcinogenic according to the material safety data sheet. The procedure for derivatization of phenol (Figure 7-1B) on a MIP film was developed based on conditions recommended for derivatization in solution as the sample preparation for chromatographic analysis [24, 25]. Coumarin-6-sulfonyl chloride (2) (1.2 mg) was dissolved in 0.3 mL of acetonitrile and 2.5 mL of NaHCO₃/Na₂CO₃ aqueous buffer (pH=9.0). This solution was immediately sprayed on a 20 μm thick MIP film previously loaded with phenol to yield the dye precursor (3). The film was air dried, and 5% KOH aqueous was sprayed over the film to produce the fluorescing phenol-derivative (4); the film was air dried before fluorescence measurements.

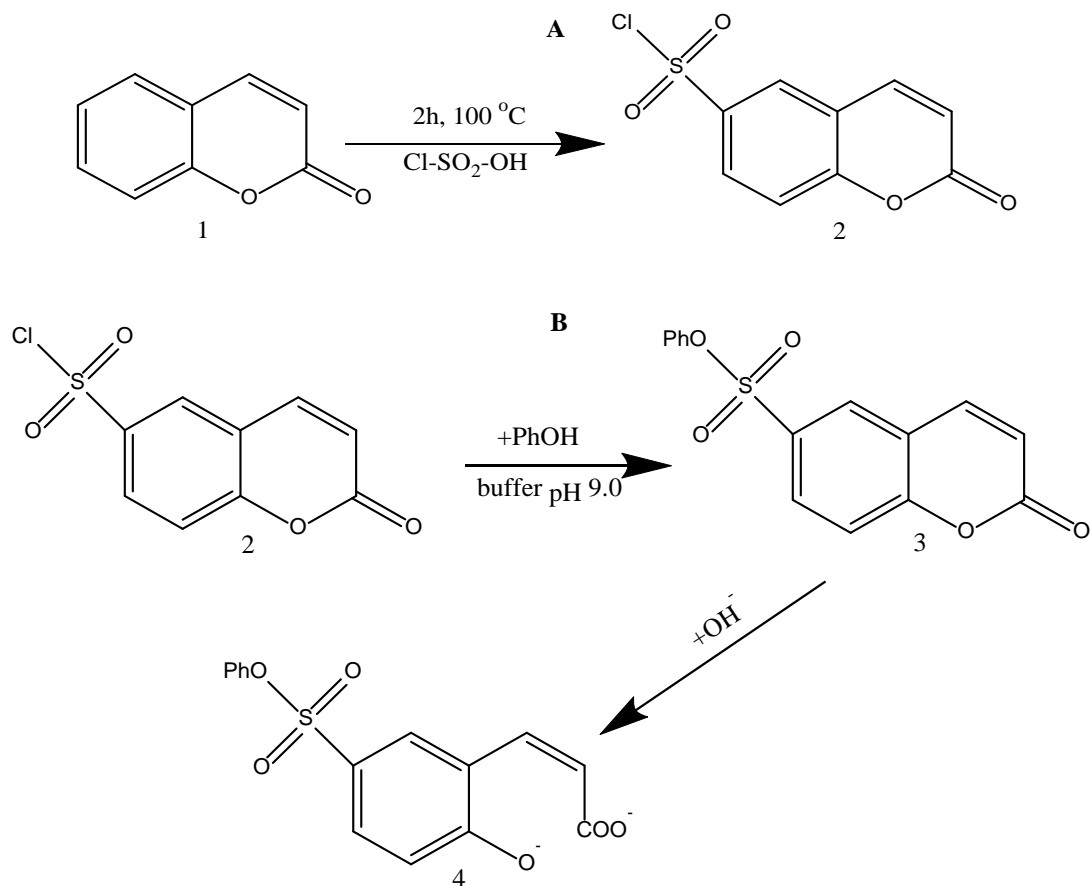


Figure 7-1. Reactions for synthesis of coumarin-6-sulfonyl chloride and derivatization of phenol.

7.3 Results and discussion

7.3.1 Illumination geometries to excite fluorescence

The immobilized MIP film can be illuminated by excitation from the front or back. Using back-surface excitation [26] (Figure 7-2), the rear side of the film was illuminated through the quartz slide and the emitted fluorescence was collected from the opposite side, or the front of the film. For front-face excitation, the incident beam illuminated the front side of the polymeric film and the emitted fluorescence was also collected from the

front side. The front-face is a basic illumination geometry in solid-phase fluorimetry [15, 17] and this approach was used when a MIP film was coated on a face of a waveguide to form a fluorimetric sensor [6].

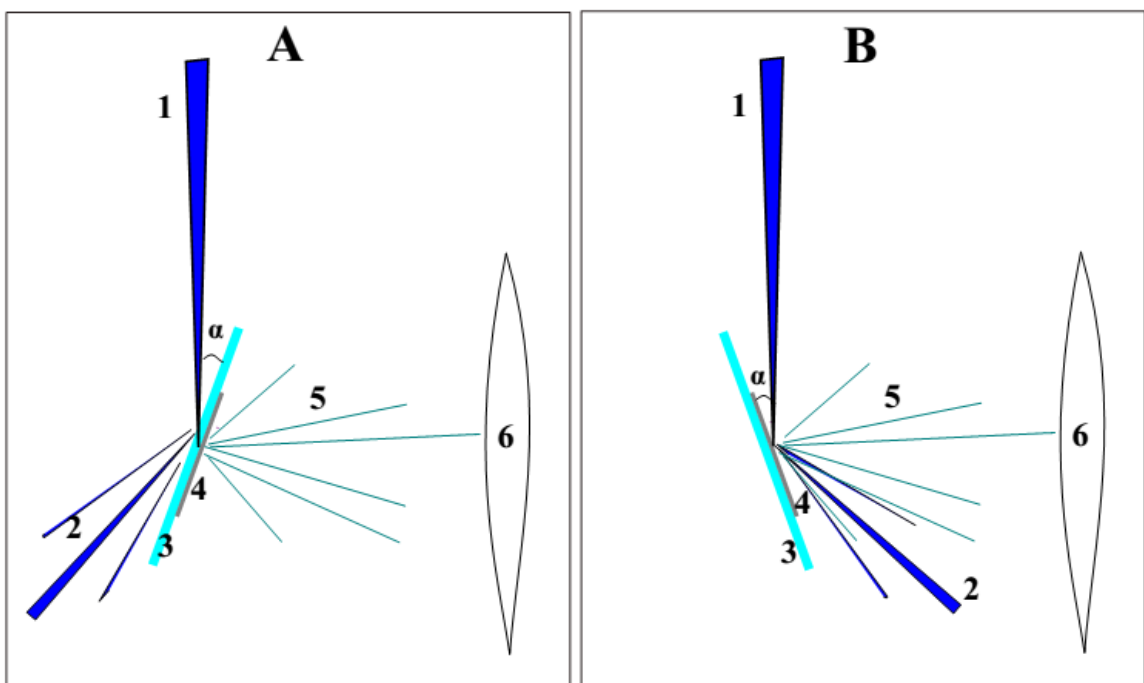


Figure 7-2. (A) Back-surface and (B) front-face illumination geometries to excite fluorescence from a polymeric film bound to the quartz slide.

Note: 1 – incident, or excitation, beam; 2 – the reflected and scattered light; 3 – quartz slide with (4) the bound MIP film; 5 – omni-directional fluorescence; 6 – collecting lense of an emission monochromator.

It was observed that the illumination geometries had a dramatic effect on the level of stray light, as well as the intensity of detected fluorescence, and the inner-filter effects. The main source of the stray light was the non-monochromatic light, which passed through the excitation monochromator. In the case of opaque samples such as the MIP film, the level of stray light was significant because a large fraction of the incident

radiation was not transmitted through the sample but reflected from the MIP film and, therefore, reached the detector. The stray light was observed in the emission spectrum as a broad tail at wavelengths longer than the excitation wavelength (Figure 7-3). The level of the stray light was much lower for the back-surface geometry: the tail ended at about 350 nm compared to 425 nm for the front-face geometry. This observation can be explained. The incident beam was mostly scattered and reflected from the rear surface of the slide, and much less collected by the lens of the emission monochromator. This rejection of the stray-light is an important advantage of the back-surface geometry [26]. However, the comparison of the intensities of fluorescence peaks for both geometries shows that the detected fluorescence was much weaker with the noisier spectrum for the back-surface geometry. When the rear side of the MIP film was illuminated, the emitted fluorescence had to pass through the full thickness of the MIP film to be detected. As a result, the fluorescence was also significantly scattered, which diminished the intensity of detected fluorescence. Self-absorption appeared in the phenanthrene spectrum (Spectrum 3 in Figure 7-3) as the lowering of the baseline below the zero line in the beginning of the spectrum. This depression of the baseline can be the result of absorbance of the stray light by phenanthrene, causing a background for the sample (Spectrum 1) to be lower than for the blank (Spectrum 2). The self-absorption effect was more pronounced for the back-surface geometry than for the front-face one because of the longer light path length [27].

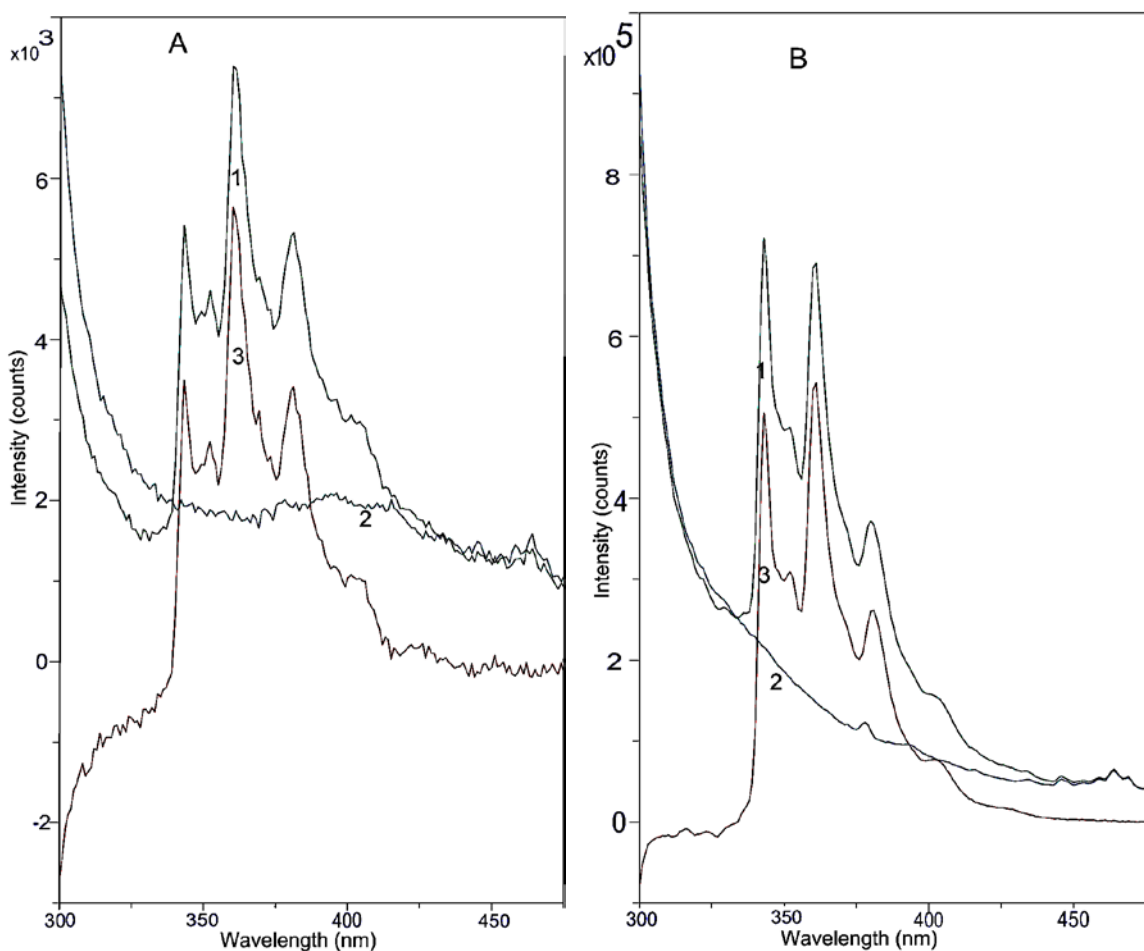


Figure 7-3. Effect of (A) back-surface and (B) front-face illumination geometries on emission spectrum ($\lambda_{\text{ex}}=298$ nm) of phenanthrene adsorbed on the MIP film.

Note: 1 – the spectrum of phenanthrene on MIP film (sample); 2 – the spectrum of MIP film (blank); 3 – the difference between 1 and 2: the spectrum from phenanthrene itself.

The level of stray light was reduced by varying the angle between the incident beam and the film surface (α in Figure 7-2). Different angles of illumination were tried for both geometries. In the case of the spectrofluorimeter used here, significant reduction of stray light was achieved at glazing angles of 20° and 60° for the front-face and back-surface geometries, respectively. At these angles, a significantly larger fraction of the reflected

and scattered light passed outside the collecting lens of the emission monochromator, which resulted in the much lower level of the stray light. The decrease in stray light level makes it possible to increase the intensity of the incident beam, e.g., by opening the lamp slit, in order to gain the detection sensitivity while still not overloading the detector. When changing the illumination geometries and angles, care must be taken to keep the incident beam sharply focused on the surface of the film by adjusting the distance between the slide and the focusing lens of the excitation monochromator.

An obvious way to reduce the level of stray-light is to introduce a short-pass filter after the excitation monochromator. The transfer function of the excitation beam will become much narrower, which will result in the depletion of the stray light. This method to reduce stray light, promises to be effective for the emission scan mode, though it requires an expensive set of filters to fit different excitation wavelengths.

7.3.2 Effect of MIP composition on the background of fluorescence spectra

The background of the fluorescence spectra originates not only from stray-light, but also from MIP network emission. This emission can be autofluorescence and/or Raman scattering. The emission spectra of pure MIPs, or blanks, based on EGDMA and different monomers (no monomer, MAA, Sty, and VP) were measured (Figure 7-4). Almost no difference was observed in the shape of the background spectra for MIPs based on EGDMA and EGDMA/MAA; they both had a peak at 310 nm with a rising baseline at longer wavelengths. The presence of styrene in the MIP greatly increased the intensity of the MIP background with the peak at 310 nm, probably because styrene is

naturally somewhat fluorescent. However, the addition of 4-vinylpyridine caused the suppression of the MIP emission, and a dip around 310 nm was observed.

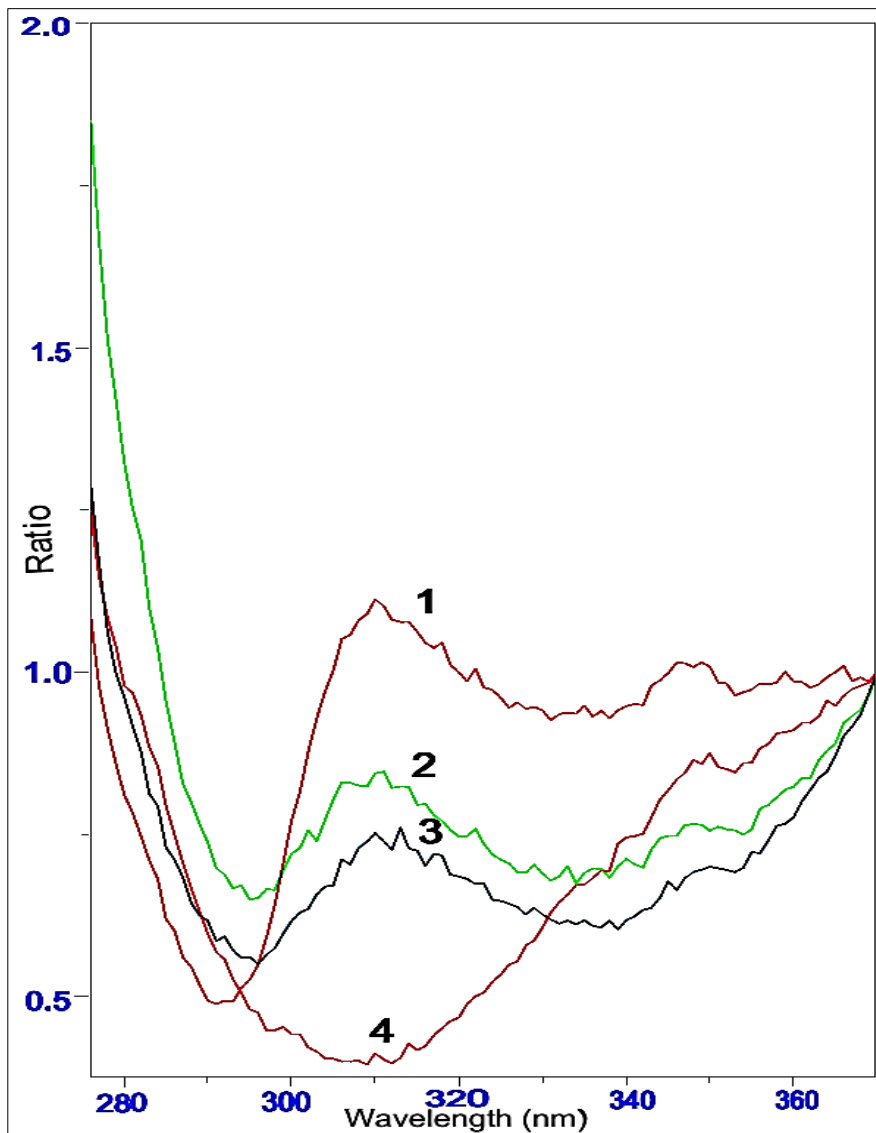


Figure 7-4. Background of fluorescence spectra ($\lambda_{\text{ex}}=270$ nm) originated from MIP matrices based on EGDMA and (1) styrene; (2) no monomer; (3) methacrylic acid; and (4) 4-vinylpyridine.

Since some components used to make the MIP are of an aromatic nature and may fluoresce, experiments were done to assess the contribution of the components to the

observed background. The functional monomers and EGDMA were purified from the stabilizer, monomethyl ether hydroquinone, and aromatic initiator, DMPA, was substituted on aliphatic azobisisobutyronitrile. However, the background was not reduced or changed. The emission background may be caused by unreacted vinyl groups left in the polymer networks. Furthermore, when the excitation wavelength was varied, the dominant background peak was not eliminated and the main background spectral features were preserved. This may be evidence of the Raman scattering in the background. Although the intense background was not beneficial for fluorimetric detection, the background appeared to be highly constant and reproducible in its spectral features and intensities. Thus, the emission background can be subtracted to obtain the spectrum of an analyte for a qualitative and quantitative analysis, for example, as was done for Spectrum 3 in Figure 7-3.

7.3.3 Effect of film thickness

MIP films were prepared with two average thicknesses: ~20 μm by the free standing polymerization and ~100 μm by polymerization in the membrane frame (Chapter 2). The terms “front-face” and “back surface” fluorimetry can imply that fluorescence is excited mostly from the sample surface. Therefore, it may seem that the film thickness should not have a dramatic effect on the intensity of excited fluorescence. However, significantly more intense fluorescence for caffeine and phenol was observed with front-face irradiation of the 100 μm MIP films than with the 20 μm films. This suggests that the incident beam penetrates relatively deeply into the opaque MIP network and the excited fluorescence can propagate within the film. In the case of the thicker

films, the light path length was much longer and a higher amount of an analyte can yield fluorescence. Thicker films, such as the 100 μm films, can be recommended for a gain in sensitivity.

7.3.4 Comparison of emission and synchronous scan measurement modes

Emission and synchronous scan spectra were acquired for phenanthrene loaded on a MIP film. Initially, the excitation spectrum of phenanthrene (Figure 7-10) was measured to find the excitation wavelength that yields the most intense fluorescent emission. In the excitation and emission spectra, maxima were located at 298 nm as excitation (Figure 7-10) and 361 nm as emission (Figures 7-5 and 7-10). The difference between these wavelengths was used as the spacing for the synchronous scan ($\Delta\lambda=63$ nm).

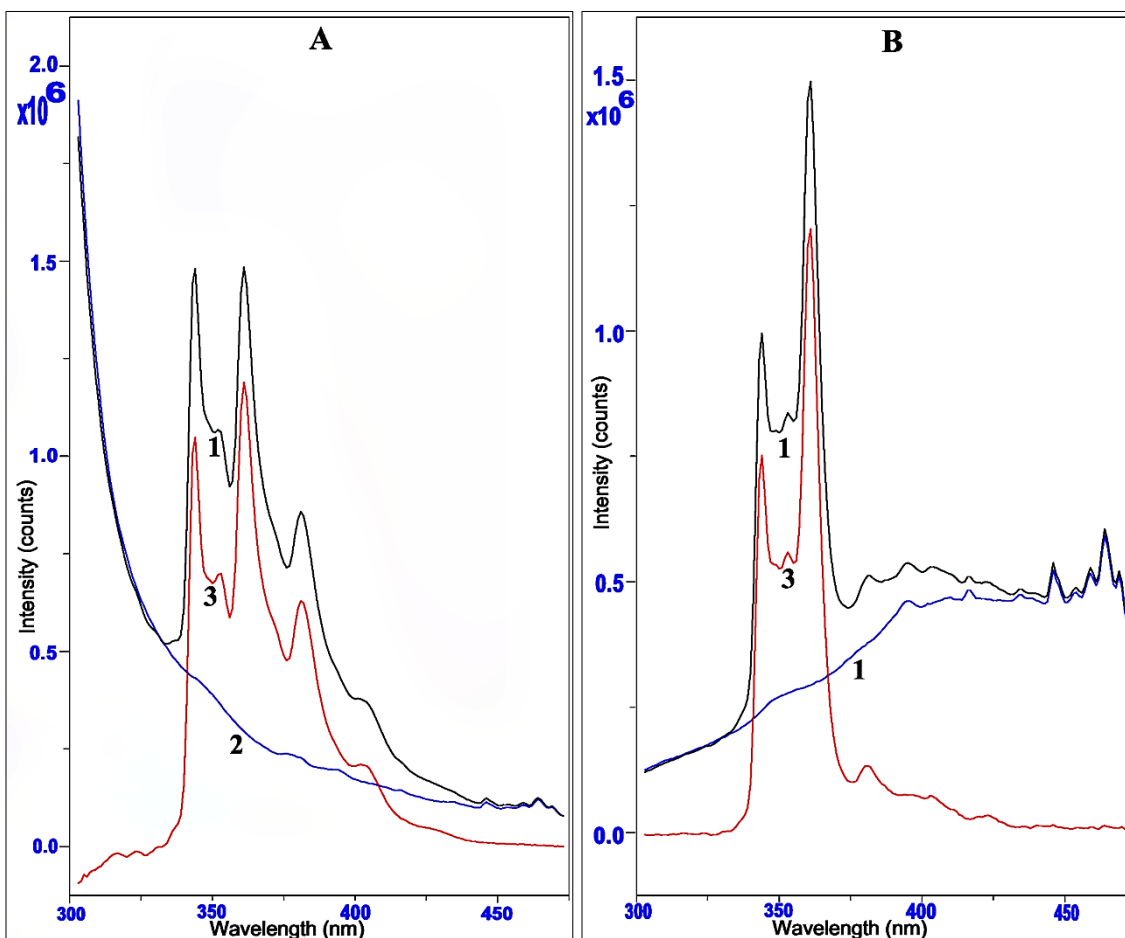


Figure 7-5. (A) Emission ($\lambda_{\text{ex}}=298$ nm) and (B) synchronous scan ($\Delta\lambda=63$ nm) spectra of phenanthrene adsorbed from $400 \mu\text{g L}^{-1}$ solution on the MIP film.

Note: 1 – the spectrum of phenanthrene on MIP film (sample); 2 – the spectrum of MIP film (blank); 3 – the difference between 1 and 2, as the spectrum from phenanthrene itself.

Both emission and synchronous spectra can be used for quantitative and qualitative analysis; however, these spectra have different features and quality. The comparison of the two spectra (Figure 7-5, Spectrum 3A and B) shows that they have different contours, though with similar features. The intensities of the highest peaks are the same (1.2×10^6); while the total transition band is almost two times narrower in the synchronous scan spectrum. The fact that peaks are often narrower when they are recorded at synchronous

scanning has been explained computationally [7, 20]. A very simplified explanation is the following. A synchronous scan spectrum can be presented as a sloping intersection of the emission-excitation matrix [3]. The peaks lying on the sloping intersection often appear to be narrower than on a horizontal intersection, or an emission spectrum for a single excitation wavelength. In practice, such $\Delta\lambda$ spacing is selected, so that the synchronous scan spectrum is the most intense for the analyte of interest or to make it possible to resolve peaks from different analytes in a mixture.

Because excitation and emission monochromators were scanned at a constant difference ($\Delta\lambda$), there was no tail in the beginning of the synchronous scan spectrum (Figure 7-5) such as in the emission spectrum. The ascending background in the synchronous scan spectrum at longer wavelengths was probably related to the rise of intensity of the xenon lamp with the increase of excitation wavelength. The absorption of stray light was observed in the emission scan mode as the depression of the baseline close to the excitation wavelength. This baseline depression can obscure a band close to the excitation wavelength and hinder the integration of peaks. For comparison, this depression was absent for the synchronous scan spectrum (Figure 7-5). The self-absorption did not greatly affect the synchronous scan spectrum because the constant difference between the excitation and emission wavelengths ($\Delta\lambda$) eliminates the part of the spectrum where emission and excitation wavelengths are close. The fact that the spectral baseline was much flatter is another advantage of the synchronous scan mode over the emission scan.

7.3.5 Fluorescence measurements for different analytes loaded on a MIP film

7.3.5.1 Phenol

Quantitation of phenol and alkylphenols has been performed by fluorimetry directly in water with detection limits in the low and sub mg L⁻¹ range [4]. Considering that such quantitation was successful, it was decided to attempt detection of phenol loaded on a MIP film. The extraction of phenols from water with the MIP film would separate phenol from possible interferences. At the same time, the preconcentration of phenols would add detection sensitivity. However, it was found that the phenol fluoresces only weakly when it is bound in the solid state, specifically when adsorbed on MIP (Figure 7-6), silica, and octadecyl-silica stationary phases.

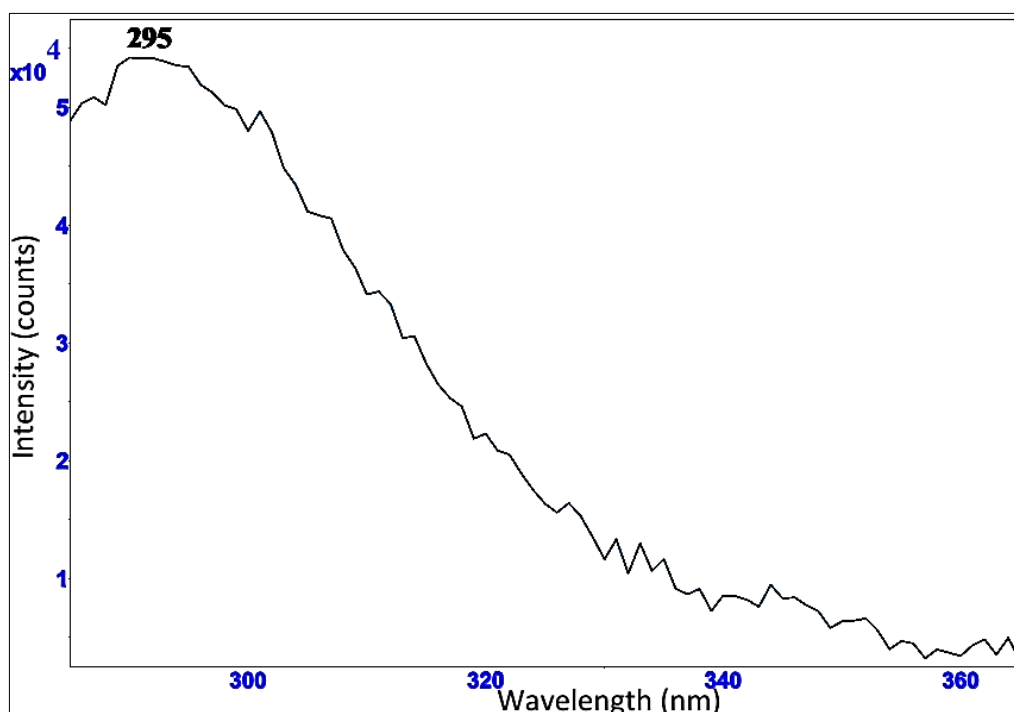


Figure 7-6. Emission spectrum of phenol ($\lambda_{\text{ex}}=269$ nm) adsorbed on the MIP film. Note: presented spectrum is the difference between the spectra for MIP with adsorbed phenol (sample) and bare MIP film (blank).

Another detection problem is a significant overlap between phenol absorption and emission bands, 270 and 295 nm, respectively. This caused a dramatic self-absorption effect with the observed cut-off of the emission band. The emission spectrum scanned close to the excitation wavelength was impacted by the presence of the stray-light from the excitation source. In addition, the weak and broad fluorescence from phenol was superimposed on the broad peak at 310 nm of the background originating from the MIP matrix (Figure 7-4), which made it difficult to reliably measure the fluorescence of phenol. Thus, to overcome all these issues, it seems to be reasonable to derivatize phenol with a strongly fluorescent moiety.

7.3.5.2 The derivatization of phenol by coumarin-6-sulfonyl chloride

The addition of a fluorescent tag to phenol is needed not only to enhance fluorescence, but to gain the selectivity over other aromatics such as PAHs that can occur in water along with phenols. Also, an increase of the difference between the excitation and emission peaks can be achieved. Similar to the derivatization of an analyte directly on a TLC plate for fluorimetric detection [28], the derivatization reaction can be completed on a MIP film with adsorbed phenol. Many reagents (Section 1.2.5.1) have been used for the derivatization of phenol. Among these, the esterification of phenol with coumarin-6-sulfonyl chloride has an advantage in that it can be completed quickly at room temperature. After derivatization, the treatment with potassium hydroxide cleaves the lactone ring, yielding the strongly fluorescent compound (Figure 7-1). This derivatization approach has been used to prepare aqueous samples for the analysis of phenolics by HPLC coupled with fluorescence detection [25, 29]. The derivatization reactions of

phenol bound to the MIP film yielded strong and characteristic fluorescence. However, the emission band was very broad and the self-absorption was pronounced (Figure 7-7). Some narrowing of the band was observed in the synchronous scan mode, though it was still broad.

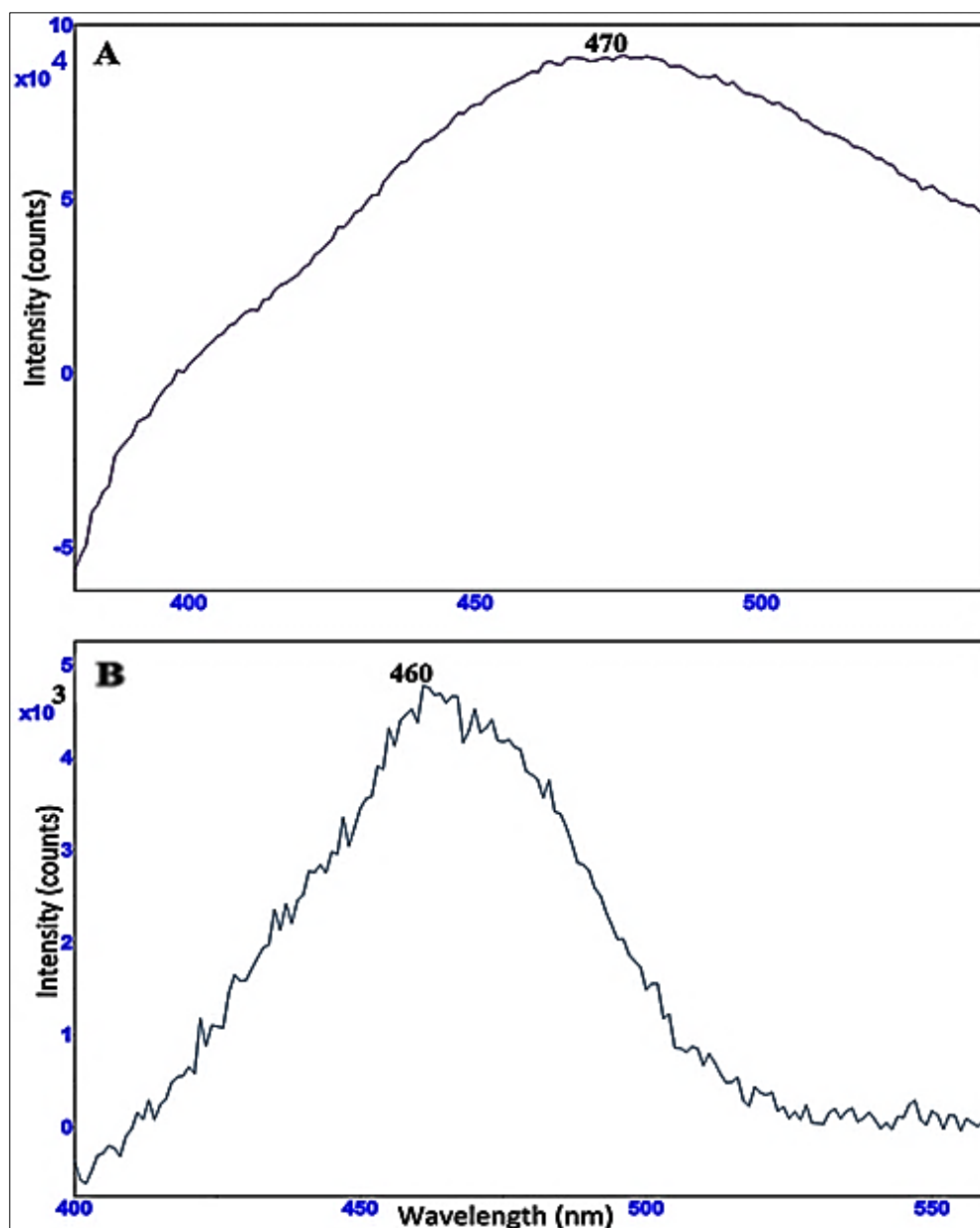


Figure 7-7. (A) Emission ($\lambda_{\text{ex}}=360$ nm) and (B) synchronous scan ($\Delta\lambda=100$ nm) spectra of phenol tagged with coumarin-6-sulfonyl chloride.

Note: presented spectrum is the difference between the sample and blank.

A significant drawback of this approach relates to issues associated with the homogeneity of the dye distribution. After spraying the potassium hydroxide solution on the MIP film, the dye diffused towards the edges of the polymeric film, which may have been worsened by the interactions of the ionic dye with the somewhat hydrophobic MIP matrix. The non-uniform distribution of the dye within the polymeric film makes difficult a precise quantitative detection. Another serious problem was the superimposition of the derivative dye fluorescence with the fluorescence from the reagent, which was present in the excess compared to the phenol derivative. Thus, the detection without derivatization on MIP films is preferred. This can be done with naturally strong fluorophores; among these are caffeine and PAHs, which also have been in the scope of the research interests of the Bottaro group.

7.3.5.3 Caffeine

Caffeine is an indicator of water contamination from domestic sewage. It is a stimulant drug that is consumed in large quantities in drinks and is eliminated in urine [30]. MIPs for caffeine have been developed and studied in our research group. Caffeine is a natural fluorophore due to the aromaticity of the xanthine substructure. Caffeine has been successfully quantified with fluorimetry in solid pharmaceutical formulations. To perform this detection, both synchronous scan [21] and the multivariate calibration [31] were applied to resolve the analytical signal of caffeine when in the mixture with other fluorophores. Although the multivariate analysis is more informative, the synchronous scan is a much simpler experimental approach. The fluorimetric detection of caffeine can be a better alternative to the MALDI detection on a MIP film as has been attempted

previously [30]. Direct fluorimetric detection on MIP films can be exploited to study MIPs for caffeine because the detection is a simpler and faster alternative to the extraction with HPLC-UV analysis that was applied in earlier work [30]. Furthermore, this detection approach could be adapted for an on-line fluorimetric sensor for environmental waters and beverages. Thus, it would be reasonable to apply the fluorimetric detection of caffeine on a MIP film and to measure the synchronous scan spectra of caffeine.

Excitation and emission spectra of caffeine loaded on the MIP (Figure 7-8) show that the most intense excitation and emission bands are centered around 338 and 391 nm, respectively, which gives the spacing of 53 nm for the synchronous scan mode. The synchronous scan spectrum had narrow and intense bands with a flat baseline, which can be suitable for the quantitative analysis (Figure 7-8C).

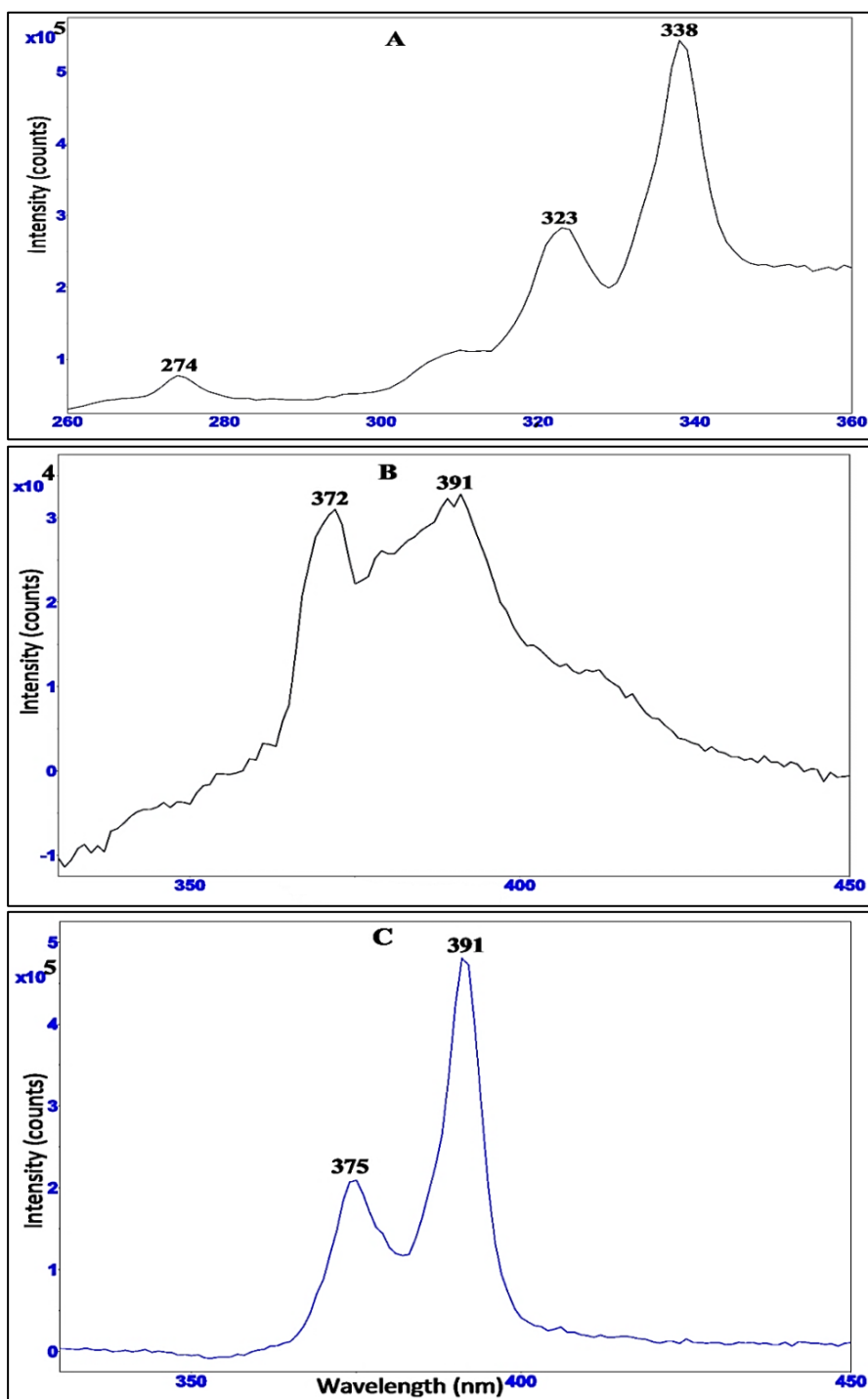


Figure 7-8. (A) Excitation ($\lambda_{em}=391$ nm), (B) emission ($\lambda_{ex}=275$ nm), and (C) synchronous scan ($\Delta\lambda=53$ nm) spectra of caffeine adsorbed on the MIP film. *Note: each spectrum is the difference between the sample and blank.*

7.3.5.4 Polycyclic aromatic hydrocarbons

Along with phenol and alkylphenols, polycyclic aromatic hydrocarbons (PAHs) form another group of water contaminants from petrogenic sources. PAHs are strongly fluorescent and their emission spectra are structured and complex. Fluorimetry has been used historically as the main analytical technique for their detection, including the detection in the solid phase [5]. PAHs with two and three aromatic rings, e.g., naphthalene and phenanthrene, constitute the largest fraction among naturally occurring PAHs, particularly in produced water [32]. Therefore, these low molecular weight PAHs were chosen as analytes for the fluorimetric detection on MIP films.

Both naphthalene and phenanthrene exhibited intense fluorescence when they were loaded in the MIP film from 0.50 – 1.0 mg L⁻¹ aqueous solution (Figures 7-9 and 7-10). Compared to the emission spectra, the synchronous scan spectra of naphthalene and phenanthrene had much narrower peaks and extra bands at 371 and 386 nm appeared for naphthalene in its synchronous scan spectrum. For comparison with naphthalene, the simplification of phenanthrene synchronous scan spectrum was observed; the broad “tail” spread over 370 nm was greatly diminished compared to the emission spectrum.

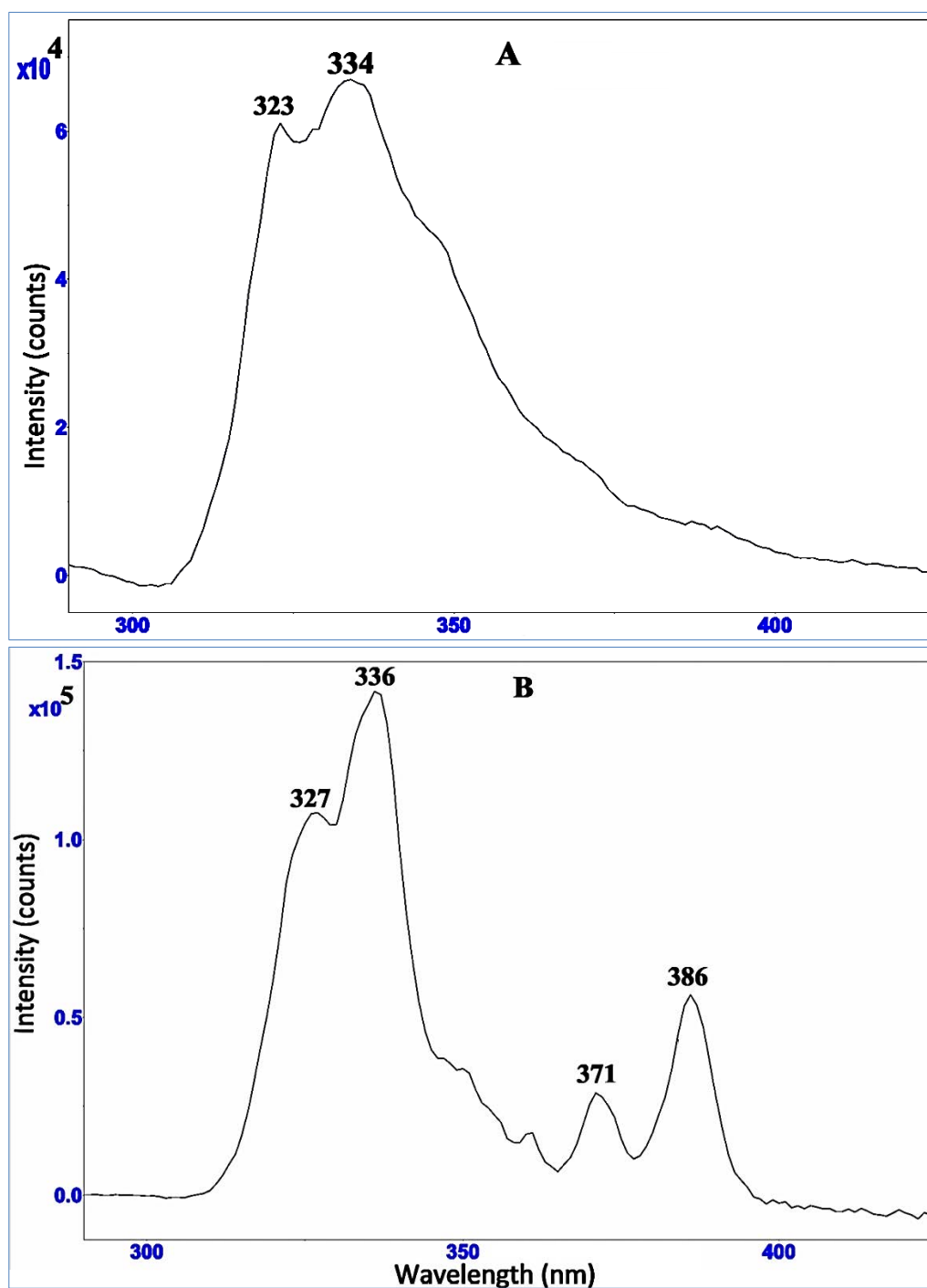


Figure 7-9. (A) Emission ($\lambda_{\text{ex}}=270$ nm) and (B) synchronous scan ($\Delta\lambda=50$ nm) spectra of naphthalene adsorbed on the MIP film.

Note: each spectrum is the difference between the sample and blank.

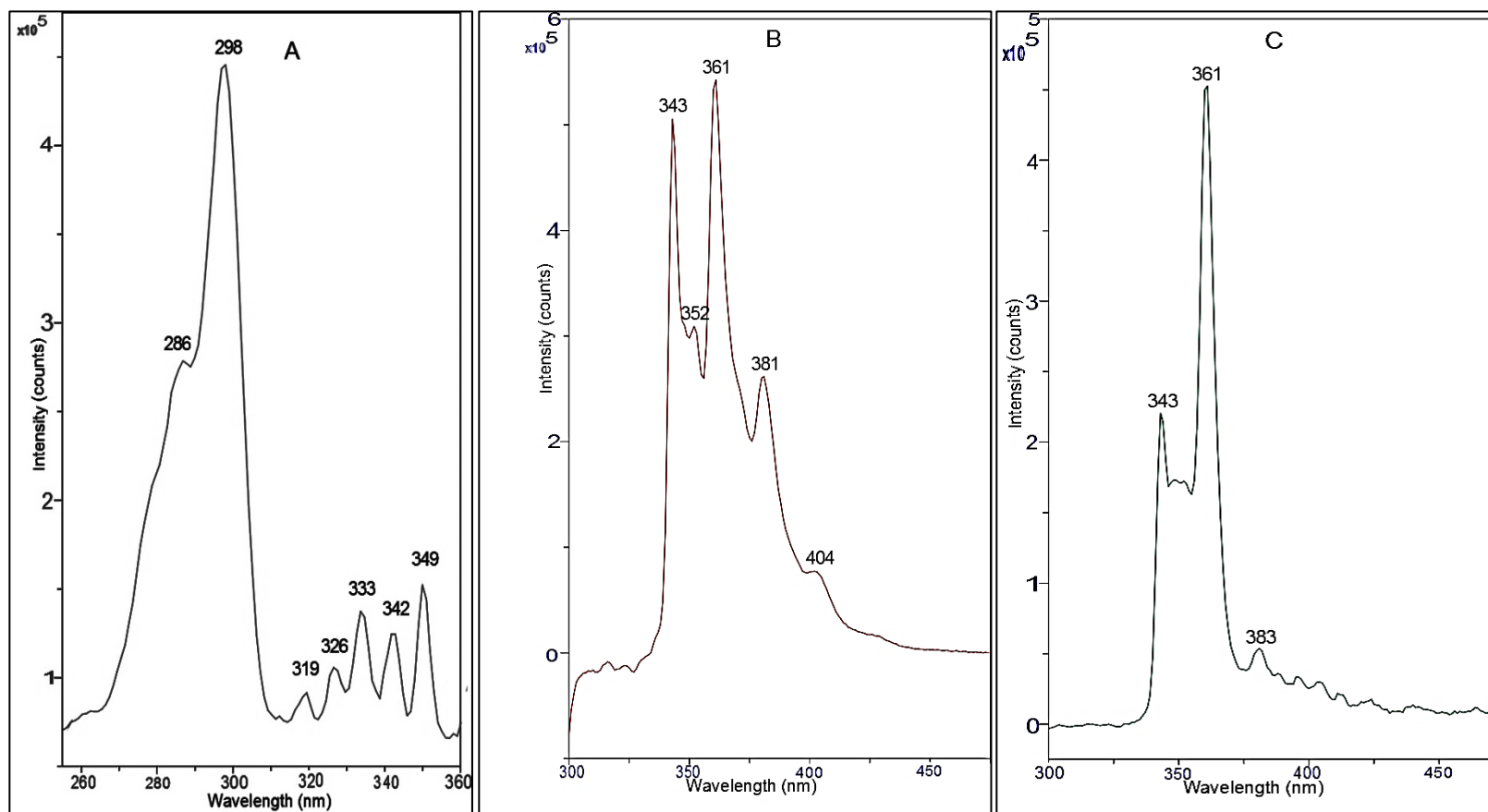


Figure 7-10. (A) Excitation ($\lambda_{em}=361$ nm), (B) emission ($\lambda_{ex}=298$ nm), and (C) synchronous scan ($\Delta\lambda=63$ nm) spectra of phenanthrene adsorbed on the MIP film.

Note: each spectrum is the difference between the sample and blank.

The relationship between fluorescence of MIP bound phenanthrene and the concentration of phenanthrene in the solutions used for loading the MIP films was studied (Figure 7-11). The observed graph is the result of two functions: the MIP adsorption isotherm towards phenanthrene and the relation of the fluorescence intensity to the amount of bound phenanthrene in the MIP. The function is curved with the fluorescence flattening at high phenanthrene concentrations. This flattening can be caused by either the saturation of the MIP binding capacity or by the inner-filter effects [33]. In any case, better linearity of the response should be expected at low concentration of the analyte, which is most environmentally relevant. The fluorescence could be easily quantified for low $\mu\text{g L}^{-1}$ phenanthrene, which suggests very low detection limits in the measurement conditions described here (more study in Chapter 8).

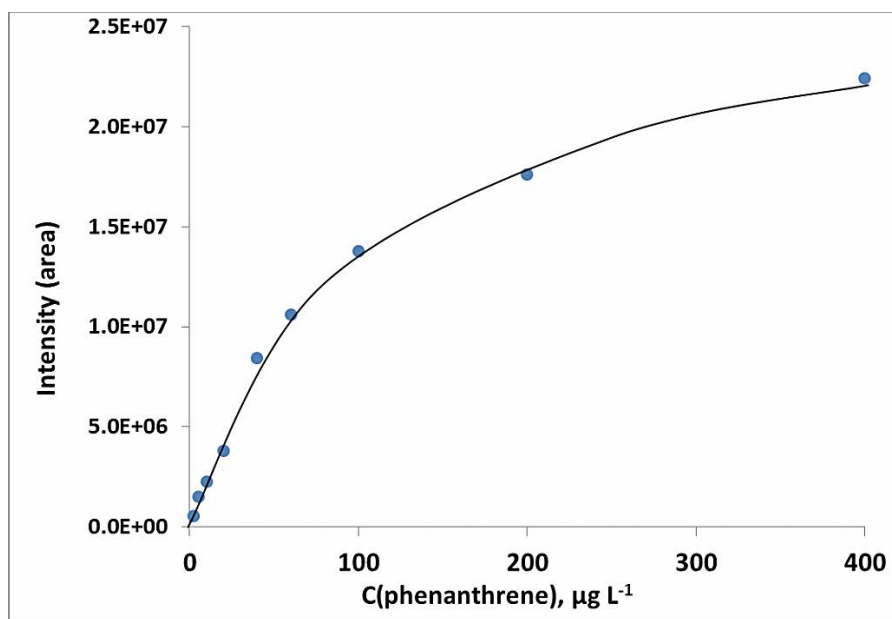


Figure 7-11. Function of fluorescence intensity from phenanthrene concentration in solutions for loading MIP films. The fluorescence was detected in synchronous scanning mode ($\Delta\lambda=63$ nm).

7.4 Conclusions

Direct fluorimetric detection for a solid phase and particularly for MIP films has many useful features and can be performed in a variety of ways. The quality of the spectra measured from MIP films is affected by the following factors: the high level of stray-light; the emission background from a MIP matrix; and inner-filter effects, which include the specific case where the stray-light is absorbed by an analyte. The effect of these factors depends on the measurement conditions. In the case of the front-face illumination geometry as compared to the back-surface geometry, the level of stray light is higher, but the inner-filter effects are less pronounced, and the detected fluorescence is more intense. Illumination with the excitation beam at glazing angles helps to reduce the stray-light. A thicker film gives more analyte to participate in the fluorescence process, which increases the signal intensity. MIPs synthesized by vinyl polymerization have their own emission background with characteristic bands. Although this background is intense, it is stable and can be subtracted for background correction.

Fluorescence can be measured in different types of spectral experiments, which were widely exploited in this project. The excitation spectrum was used to find the optimal excitation wavelengths to measure emission and synchronous scan spectra. Emission and synchronous scan spectra were moderately different in the shape and the number of bands. Both spectra can serve for qualitative and quantitative analysis. The comparison between emission and synchronous scan spectra showed that in the latter peaks were narrower, the background was less affected by the stray light, and the self-absorption affected the measured spectra to a smaller extent.

Initially, the fluorimetric detection on a MIP film was designed for phenol, but phenol bound to the MIP fluoresces only weakly. The derivatization of phenol with coumarin-6-sulfonyl chloride was limited by poor homogeneity of the dye on the MIP film and the fluorescence from the reagent. Naturally strong fluorophores, such as caffeine and PAHs, that were loaded on MIP films showed the intense and characteristic fluorescence. The quantitation of PAHs, e.g., phenanthrene, is suitable for the low concentrations (low $\mu\text{g L}^{-1}$), where the binding capacity is not saturated and the inner-filter effects are negligible.

7.5 References

1. Rendell, D., *Fluorescence and phosphorescence spectroscopy*. John Wiley & Sons: London, 1987; p 22-23.
2. Wehry, E. L., Chapter 26. Molecular fluorescence and phosphorescence spectrometry. In *Handbook of Instrumental Techniques for Analytical Chemistry*, 1st ed.; Settle, F. A., Ed. Prentice Hall PTR (ECS Professional): USA, 1997; p 519.
3. Skoog, D. A.; Holler, F. J. H.; Crouch, S. R., Chapter 15. Molecular luminescence spectrometry. In *Principles of Instrumental Analysis*, Brooks/Cole Pub Co.: Canada, 2007; pp 399-425.
4. Naley, A., Analysis of phenols in sea water by fluorometry: Direct analysis of the water phase. *Bulletin of Environmental Contamination and Toxicology* **1983**, *31* (4), 494-500.
5. Fernandezsanchez, J., The development of solid-surface fluorescence characterization of polycyclic aromatic hydrocarbons for potential screening tests in environmental samples. *Talanta* **2003**, *60* (2-3), 287-293.
6. Dickert, F. L.; Tortschanoff, M.; Bulst, W. E.; Fischerauer, G., Molecularly imprinted sensor layers for the detection of polycyclic aromatic hydrocarbons in water. *Analytical Chemistry* **1999**, *71* (20), 4559-4563.

7. Rendell, D., *Fluorescence and phosphorescence spectroscopy*. John Wiley & Sons: London, 1987; pp 196-205.
8. Molina-Díaz, A.; García-Reyes, J. F.; Gilbert-López, B., Solid-phase spectroscopy from the point of view of green analytical chemistry. *Trends in Analytical Chemistry* **2010**, *29* (7), 654-666.
9. Sainz-Gonzalo, F. J.; Medina-Castillo, A. L.; Fernandez-Sanchez, J. F.; Fernandez-Gutierrez, A., Synthesis and characterization of a molecularly imprinted polymer optosensor for TEXs-screening in drinking water. *Biosensors & Bioelectronics* **2011**, *26* (7), 3331-8.
10. Valero-Navarro, A.; Salinas-Castillo, A.; Fernandez-Sanchez, J. F.; Segura-Carretero, A.; Mallavia, R.; Fernandez-Gutierrez, A., The development of a MIP-optosensor for the detection of monoamine naphthalenes in drinking water. *Biosensors & Bioelectronics* **2009**, *24* (7), 2305-11.
11. Harz, S.; Schimmelpfennig, M.; Tse Sum Bui, B.; Marchyk, N.; Haupt, K.; Feller, K. H., Fluorescence optical spectrally resolved sensor based on molecularly imprinted polymers and microfluidics. *Engineering in Life Sciences* **2011**, *11* (6), 559-565.
12. Lieberzeit, P. A.; Halikias, K.; Afzal, A.; Dickert, F. L., Polymers imprinted with PAH mixtures – comparing fluorescence and QCM sensors. *Analytical and Bioanalytical Chemistry* **2008**, *392* (7-8), 1405-10.
13. Krupadam, R. J., An efficient fluorescent polymer sensing material for detection of traces of benzo[a]pyrene in environmental samples. *Environmental Chemistry Letters* **2010**, *9* (3), 389-395.
14. Stringer, R. C.; Gangopadhyay, S.; Grant, S. A., Detection of Nitroaromatic Explosives Using a Fluorescent-Labeled Imprinted Polymer. *Analytical Chemistry* **2010**, *82* (10), 4015-4019.
15. Hurtubise, R. J., Solid-surface luminescence spectrometry. *Analytical Chemistry* **1989**, *61* (15), 889A-895A.
16. Rendell, D., *Fluorescence and phosphorescence spectroscopy*. John Wiley & Sons: London, 1987; p 52.

17. Lagorio, M. G.; San Román, E., How Does Light Scattering Affect Luminescence? Fluorescence Spectra and Quantum Yields in the Solid Phase. *Journal of Chemical Education* **2002**, *79* (11), 1362.
18. Kubista, M.; Sjoback, R.; Eriksson, S.; Albinsson, B., Experimental correction for the inner-filter effect in fluorescence spectra. *The Analyst* **1994**, *119* (3), 417-419.
19. Piruska, A.; Nikcevic, I.; Lee, S. H.; Ahn, C.; Heineman, W. R.; Limbach, P. A.; Seliskar, C. J., The autofluorescence of plastic materials and chips measured under laser irradiation. *Lab on a chip* **2005**, *5* (12), 1348-54.
20. Tuan Vo, D., Multicomponent analysis by synchronous luminescence spectrometry. *Analytical Chemistry* **1978**, *50* (3), 396-401.
21. Karim, M. M.; Jeon, C. W.; Lee, H. S.; Alam, S. M.; Lee, S. H.; Choi, J. H.; Jin, S. O.; Das, A. K., Simultaneous determination of acetylsalicylic acid and caffeine in pharmaceutical formulation by first derivative synchronous fluorimetric method. *Journal of fluorescence* **2006**, *16* (5), 713-21.
22. Pharr, D. Y.; McKenzie, J. K.; Hickman, A. B., Fingerprinting Petroleum Contamination Using Synchronous Scanning Fluorescence Spectroscopy. *Ground Water* **1992**, *30* (4), 484-489.
23. Egli, S. N. Thin film molecularly imprinted polymers for detection systems targeted toward polycyclic aromatic hydrocarbons in water. Thesis. Memorial University of Newfoundland, St. John's, 2014.
24. Miller, J. N., Coumarin-6-sulphonyl chloride: a novel label in fluorimetry and phosphorimetry; Part 1. Synthesis and Luminescence Properties. *Analytica Chimica Acta* **1989**, *227* (0), 145-153.
25. Suliman, F. E.; Al-Kindi, S. S.; Al-Kindy, S. M.; Al-Lawati, H. A., Analysis of phenols in water by high-performance liquid chromatography using coumarin-6-sulfonyl chloride as a fluorogenic precolumn label. *Journal of Chromatography A* **2006**, *1101* (1-2), 179-84.
26. Spanggard, H. Introduction to fluorescence. The Danish Polymer Centre, Riso National Laboratory. http://www.risoe.dk.pol_fl920.ashx/ (accessed 10.12.2013).
27. Rendell, D., *Fluorescence and phosphorescence spectroscopy*. John Wiley & Sons: London, 1987; p 419.

28. Rochholz, G.; Mayr, A.; Schütz, H., TLC-screening of important pharmaceutical substances using fluorescence detection. *Fresenius Journal of Analytical Chemistry* **1993**, *346* (6-9), 819-827.
29. Al-Kind, S. M. Z.; Miller, J. N., Coumarin-6-sulphonyl chloride: a novel label in fluorimetry and phosphorimetry; Part 2. Chromatographic applications. *Analytica Chimica Acta* **1989**, *227* (0), 155-163.
30. Smith, J. W. Molecularly Imprinted Polymers for the Environmental Analysis of Caffeine. Thesis. Memorial University of Newfoundland, St. John's, 2010.
31. Moreira, A. B.; Dias, I. L. T.; Neto, G. O.; Zagatto, E. A. G.; Kubota, L. T., Simultaneous spectrofluorimetric determination of paracetamol and caffeine in pharmaceutical preparations in solid-phase using partial least squares multivariate calibration. *Analytical Letters* **2006**, *39* (2), 349-360.
32. *Report 1.20/324. Aromatics in produced water - occurrence, fate and effects, and treatment*; International Oil and Gas Producers Association: London, UK, 2002; p 30.
33. Rendell, D., *Fluorescence and phosphorescence spectroscopy*. John Wiley & Sons: London, 1987; p 105-112.

Chapter 8. Fluorimetric Detection of PAHs on Molecularly Imprinted Polymeric Films

8.1 Introduction

In the previous chapter, the methodology of the direct fluorimetric detection on a MIP film was described, and different experimental conditions, which determine the quality of the fluorimetric measurements, were studied. The effect of the illumination geometry, the chemical composition of MIP films along with the types of spectral experiments and analytes were studied, and the optimal measurement conditions were derived. This chapter can be considered as the continuation of the previous work in Chapter 7. The focus of the current chapter is the application of the methodology of the fluorimetric measurements to estimate the basic performances of the quantitation of PAHs and achieve the selectivity of the detection of PAHs in a mixture. This work supports efforts to develop simple and fast techniques for the analysis of natural waters, which can be applied for the on-line and remote sensing of PAHs. The targets were two and three ring PAHs exemplified with naphthalene, fluorene, phenanthrene, and anthracene, as common water pollutants from crude oil. They also constitute the largest fraction of PAHs found in produced water and oil [1].

In early work to develop a fluorescence sensor towards PAHs based on MIP films, Dickert et al. [2, 3] coated polyurethane imprinted films on a waveguide. This device was used to study the selectivity of the MIPs, and some basic characteristics of detection, such as linear range along with the limit of the detection, were determined. The targets for the detection were mostly large PAHs with 4-5 rings. As far as light PAHs are concerned, in work by Prahl et al. [4], a polyurethane based MIP layer was coated on the bottom of a glass vial to be used to study the fluorimetric detection of anthracene. The effect of the

nature of the MIP layer on the fluorimetric detection was studied both experimentally and theoretically. It was found that the limit of detection of anthracene was not better than 15 mg L^{-1} . This relatively poor sensitivity of the detection was explained by the significant absorption of the excitation light by the polyurethane MIP and background fluorescence from the MIP. Analysis of “heavy” PAHs with MIPs and fluorimetric detection promises to be more sensitive than for the 2-3 ring PAHs because the preconcentration factors of the “heavy” PAHs are higher [3] and they fluoresce much more intensely. However, the light PAHs were chosen as targets because they present special environmental concern.

In this work, the fluorimetric detection was used with MIP films based on pentaerythritol triacrylate (PETA), styrene, and xylene, which served as cross-linker, functional monomer, and template, respectively. These MIP films have the advantage of water compatibility along with the high binding capacity towards hydrophobic species, and some imprinting effect towards PAHs (Chapter 5). Results presented in the previous chapter (Chapter 7) showed that the most intense fluorescence could be measured at the front-face illumination geometry, which also gave the least pronounced inner-filter effects. The synchronous scanning mode was especially suitable for fluorimetric detection on the polymeric films because the level of the stray light could be significantly reduced. This measurement mode is also one of the most effective and simplest means to improve the selectivity of the fluorimetric detection [5, 6], particularly, since this principle works without complex instrumental systems. Synchronous scanning and emission measurement modes were compared for the identification of the PAHs in a mixture adsorbed on a MIP

film. The quantitative detection of PAHs was assessed in terms of the limits of detection/quantitation and the precision of the measurements.

8.2 Materials and methods

Naphthalene (99%), phenanthrene (99.5%), fluorene (99%), and anthracene (99.0%, Fluka Analytical), a slide mailer for 5 microscope slides ($75 \times 25 \text{ mm}^2$) were purchased from Sigma-Aldrich (Oakville, ON, Canada). The MIP films were prepared using a prepolymerization mixture containing PETA, styrene, and xylene (MIP 8 in Chapter 5); the fabrication technique for 100 μm -thick films was used on quartz slides (Chapter 7).

8.2.1 Loading of MIP films with PAHs

The slide/MIP films were placed in 1100 mL beaker containing 750.0 mL of aqueous solution of individual PAH or a mixture of PAHs, and the beaker was sealed with Parafilm ®. The solutions had the following concentrations of PAHs: naphthalene – $60.0 \mu\text{g L}^{-1}$, fluorene – $8.00 \mu\text{g L}^{-1}$, phenanthrene – $4.00 \mu\text{g L}^{-1}$, and anthracene – $4.00 \mu\text{g L}^{-1}$, unless otherwise indicated. The content of the beaker was stirred for 4 h 30 min at 150 rpm and $20.0 \text{ }^\circ\text{C}$ in an Innova 4230 Incubator Shaker (New Brunswick Scientific, Enfield, CT, USA). The slide/MIP film was then removed, washed with water, and air dried. A MIP/slide was exposed to pure water in the same loading conditions and used as a blank.

8.2.2 Fluorescence measurement from a MIP film

A PTI Quanta Master 6000 spectrofluorimeter was used in this work, as in Chapter 7. Slit widths of the excitation and emission monochromators were set at 4 nm each, except 8 nm each for experiments illustrated in Figure 8-5 to achieve a higher sensitivity of detection. To accomplish the front-face illumination, a slide holder (Figure 8-1, 4) was constructed from a plastic box for microscope slides. The box was cut in half, and the bottom section was cut again in half, leaving a section that served as the socket for the slides/MIP films. The socket was mounted with a double-sided adhesive tape on the rotating stage (Figure 8-1, 3). Microtweezers with pulled apart ends (Figure 8-1, 6) served as a plate spring to press the MIP film/slide in the socket to fix the slide in a stable and reproducible position.

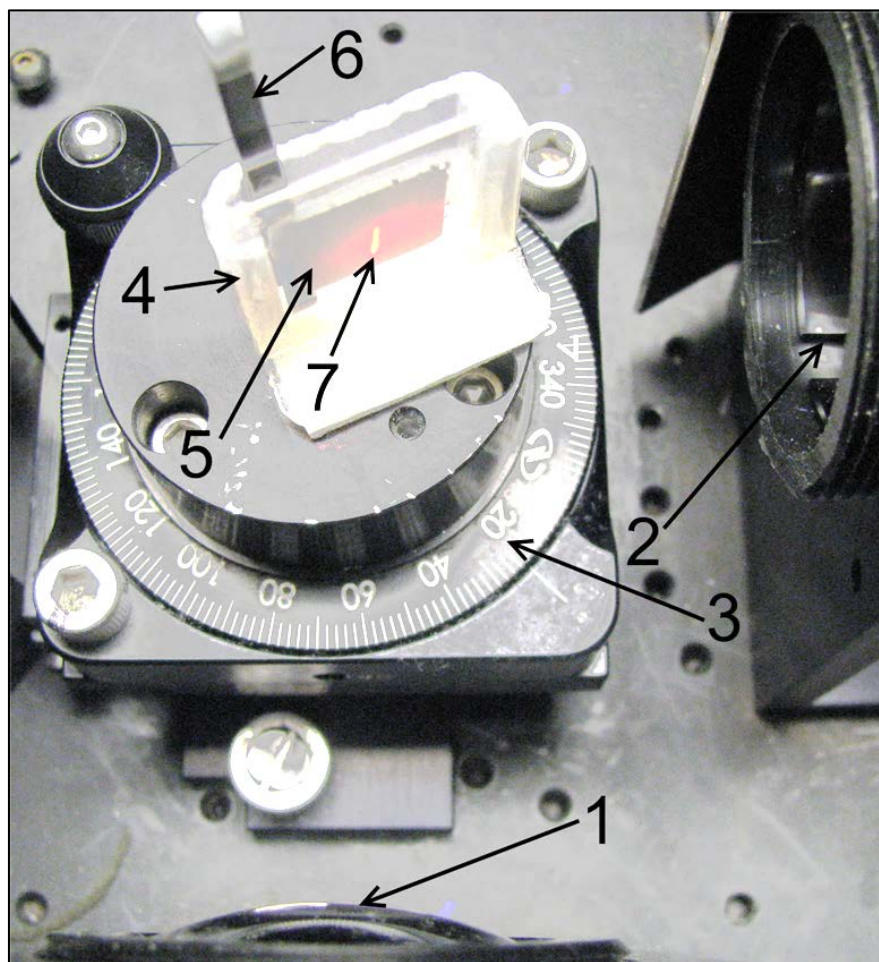


Figure 8-1. Experimental set-up for front-face illumination of MIP films to excite fluorescence.

Note: 1 – the collecting lens of the emission monochromator; 2 – the focussing lens of the excitation monochromator; 3 – the rotating stage; 4 – the socket for (5) the MIP film/slide; 6 – the plate spring; 7 – the focused spot of the excitation beam.

To improve the precision of the measurement of the fluorescence intensity, small variations in the spectral baseline were corrected by normalization of spectra. Recorded spectra were normalized against a wavelength beyond the band of interest: 370 nm for naphthalene, 466 nm for phenanthrene, and 418 nm for both fluorene and anthracene. The

spectra of the blank, or the MIP films, were subtracted from the spectra of the MIP films with PAHs to obtain the pure PAH spectra. The intensity of the PAH emissions were measured at 335 nm for naphthalene, 319 nm for fluorene, 363 nm for phenanthrene, and 379 nm for anthracene. For each slide, the fluorescence was measured at least for two different locations on the film, and their average was taken.

8.2.3 Estimation of performances of quantitative detection

The limit of detection was estimated by the visual comparison [7] of the difference between the spectra of the MIP film with phenanthrene and the blank, taking into account the repeatability of the spectral scans and instrumental noise. The limit of quantitation (LoQ) was calculated using the standard deviation of y-intercepts (S_a) and slope (b) for regression line [7]:

$$LoQ = 10 \frac{S_a}{b} \quad (8-1)$$

The precision of detection, in terms of standard deviation (S), was estimated based on the differences between duplicates (x_{i1} , x_{i2}), which were fluorescence intensities for the two MIP/slides loaded with the same amount of PAHs and measured in the same conditions. A set of pairs of the duplicates (n=5) measured at different days was adapted to calculate the coefficient of variance (S_r , %), using the method of estimation of standard deviation (SD) from paired results [8]. The average relative percentage difference (RPD) between match pairs was also calculated as an alternative figure of merit to S_r , which is convenient for the prompt control of the precision.

$$SD = \sqrt{\frac{\sum_{i=1}^n (x_{i1} - x_{i2})^2}{2n}} \quad (8-2)$$

$$S_r, \% = 100 \frac{SD}{\bar{x}} \quad (8-3)$$

$$RPD = \frac{\sum_{i=1}^n \left(100 \frac{x_{i1} - x_{i2}}{\bar{x}_i} \right)}{n} \quad (8-4)$$

8.3 Results and discussion

8.3.1 Comparison of fluorescence measurement modes to identify PAHs in their mixture

8.3.1.1 Emission measurement mode

Compared to measurements by synchronous scanning, the measurement of emission spectra is simpler in terms of the principle and required equipment. Therefore, the measurement of emission spectra should be tried first. To begin, the excitation and emission spectra of the PAHs, individually loaded on the MIP, were measured (Figure 8-2). The excitation spectra of the PAHs overlap to a significant extent while some parts of the emission spectra do not overlap. For example, the excitation spectrum of fluorene is superimposed on its emission spectrum around 300 nm. Thus, it is not possible to excite a PAH individually and not excite other PAHs in the mixture. As a compromise, excitation at 290 nm can be used for naphthalene, fluorene, and

phenanthrene and at 358 nm for anthracene (Figure 8-2). The emission spectra of the mixture of the PAHs were compared with the spectra of the individual PAHs (Figure 8-3, 1 and 3) to identify peaks for the mixture of PAHs (Figure 8-3, 2 and 4). It can be seen that only phenanthrene at the excitation wavelength of 290 nm and anthracene at 358 nm can be clearly distinguished in the mixture.

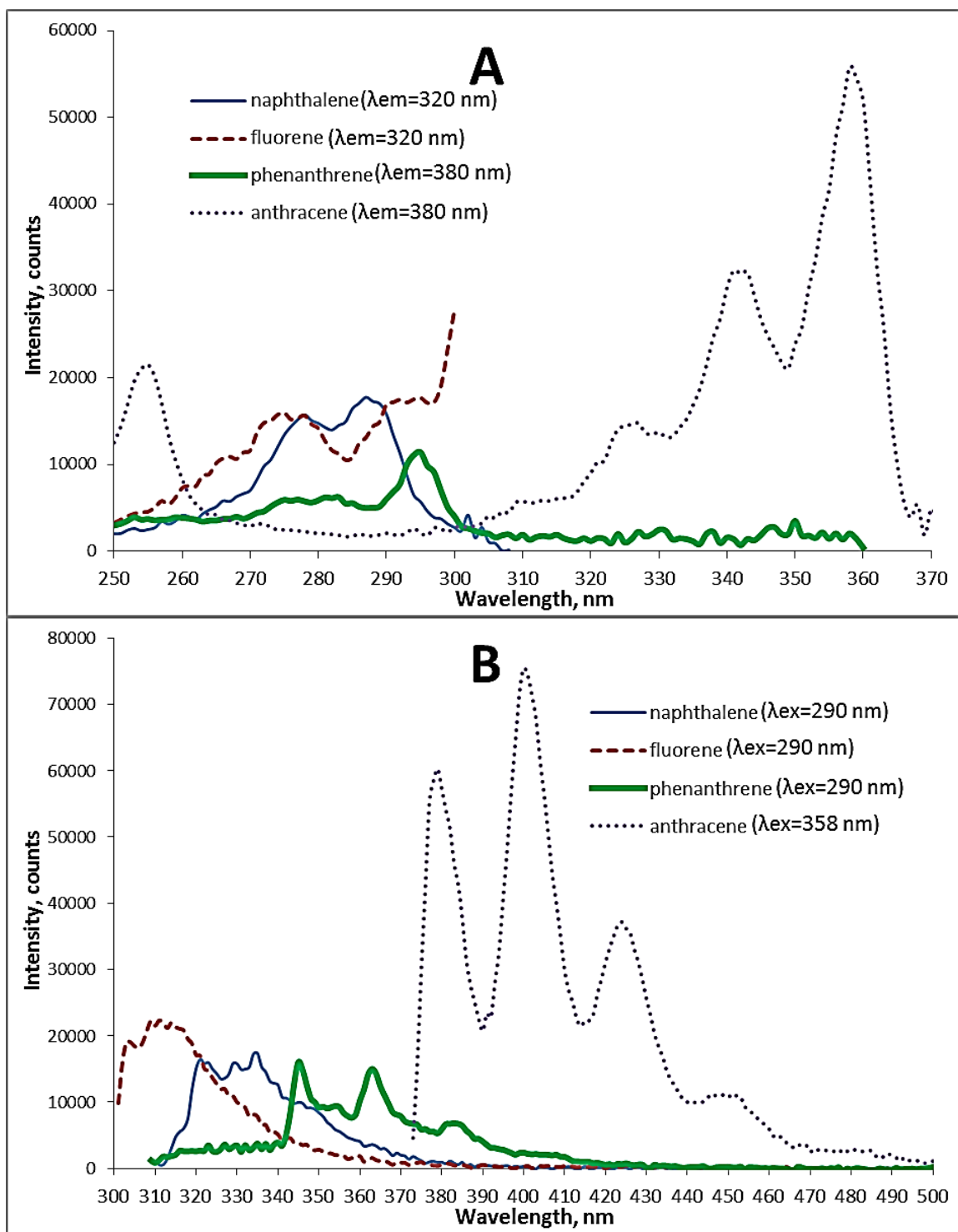


Figure 8-2. (A) Excitation and (B) emission spectra of naphthalene, phenanthrene, fluorene, and anthracene individually loaded on the MIP film.

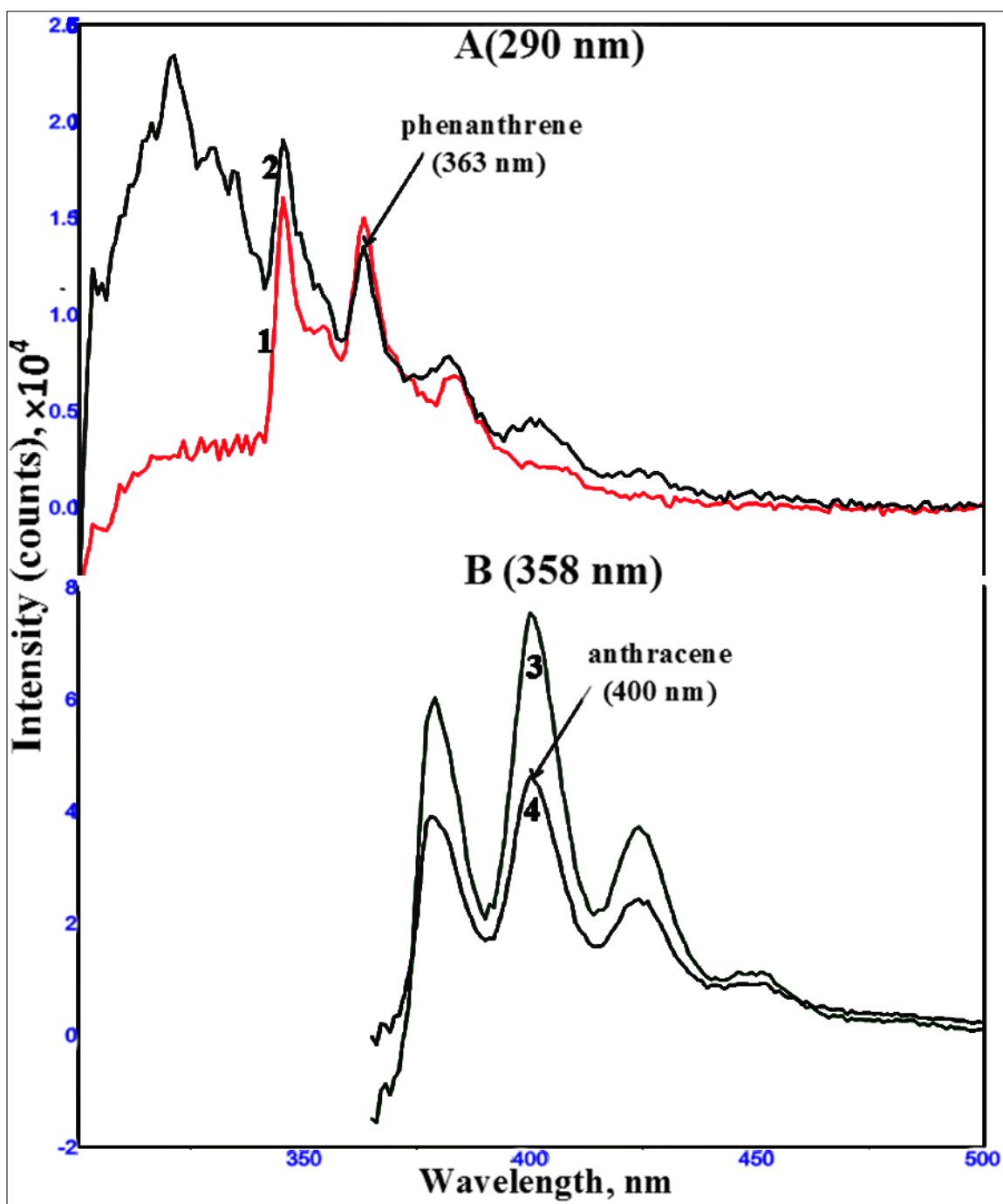


Figure 8-3. Emission spectra for the mixture of naphthalene, phenanthrene, fluorene, and anthracene loaded on the MIP film at (A) $\lambda_{\text{ex}} = 290 \text{ nm}$ and (B) $\lambda_{\text{ex}} = 358 \text{ nm}$.

Note: 2, 4 – the spectra for the mixture of PAHs and 1, 3 – the spectra for phenanthrene and anthracene, respectively, loaded individually on the MIP.

8.3.1.2 Synchronous scanning measurement mode

To find the spacing ($\Delta\lambda$) at which each PAH can be identified in the mixture with other PAHs, the following approach was applied [9]. Synchronous scanning spectra of naphthalene, fluorene, phenanthrene, anthracene, and their mixture were recorded at a number of the spacings from 10 – 70 nm at 10 nm increment. Chosen spacing ($\Delta\lambda$) allowed the differentiation of the peaks of each PAH among the peaks of other PAHs (Figure 8-4). To prove the identification, the spectra of PAHs loaded individually on the MIP films were also acquired. The PAHs can be identified at three $\Delta\lambda$: 60 nm for naphthalene, 20 nm for fluorene and anthracene, and 70 nm for phenanthrene. Although anthracene can be distinguished based on its characteristic triplet emission band almost at any $\Delta\lambda$, a significant simplification and narrowing of anthracene peaks can be observed at 20 nm.

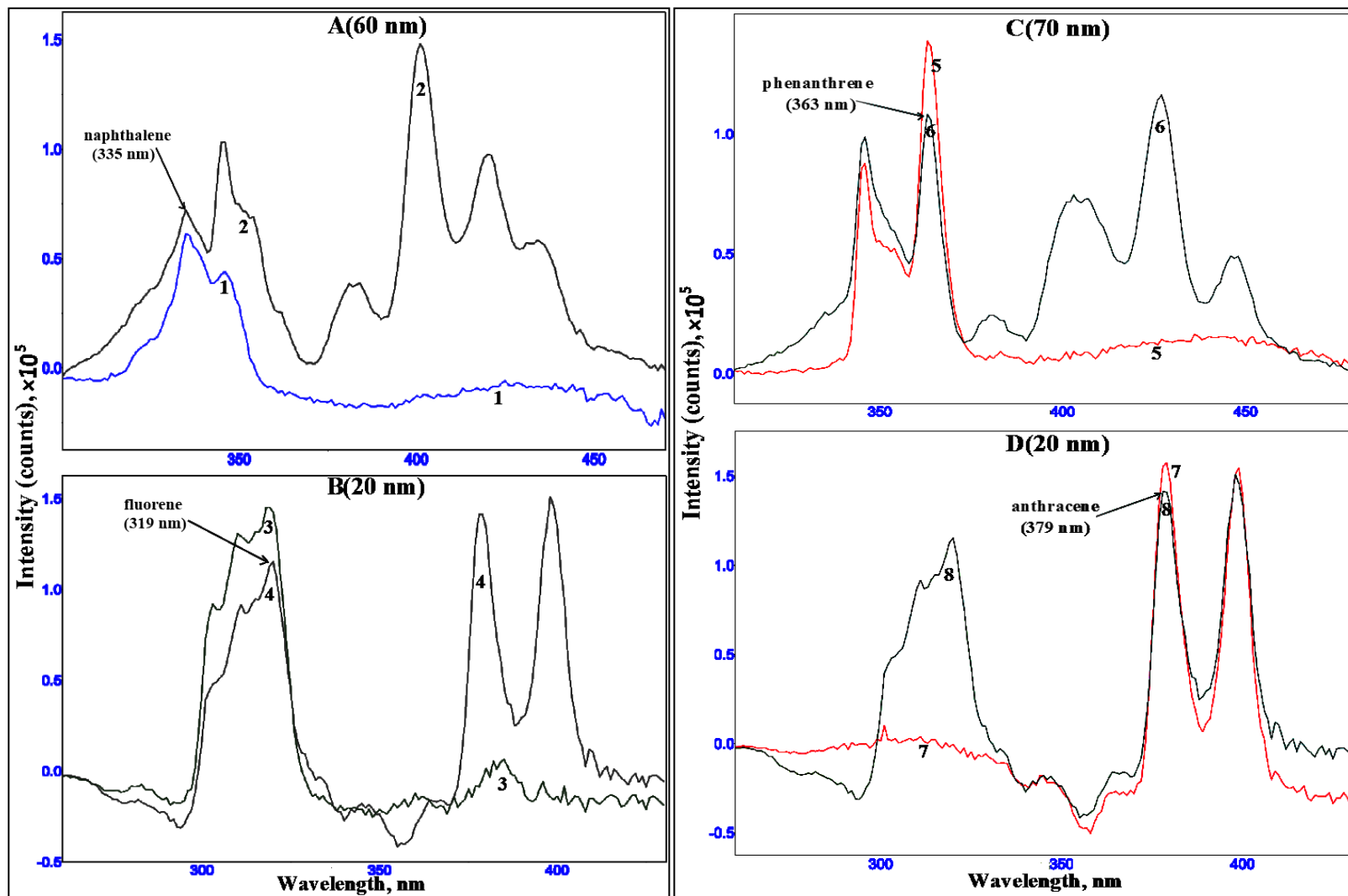


Figure 8-4. Synchronous scan spectra at different $\Delta\lambda$ for individual PAHs (Spectra 1, 3, 5, 7) and their mixture (Spectra 2, 4, 6, 8) loaded on the MIP films: (A) naphthalene ($\Delta\lambda=60$ nm), (B) fluorene ($\Delta\lambda=20$ nm), (C) phenanthrene ($\Delta\lambda=60$ nm), and (D) anthracene ($\Delta\lambda=20$ nm).

8.3.2 Preliminary characterization of quantitative fluorimetric detection

Fluorescence was measured for MIP films loaded with phenanthrene from 0.200, 0.500, 1.00, 2.00, 4.00, 6.00, 10.0 $\mu\text{g L}^{-1}$ aqueous solutions (Figure 8-5) to estimate the limit of detection (LoD) and the limit of quantitation (LoQ) (Table 8-1). The response relative to phenanthrene concentration can be considered linear over the narrow range of concentrations (0.200 – 10.0 $\mu\text{g L}^{-1}$). The value of LoQ is mostly determined and limited by the scatter of points along the regression line (Figure 8-5 A). The linearity of response is greatly improved when the fluorescence intensity and phenanthrene concentration are plotted on a logarithmic scale (Figure 8-5 B). It is probable that the logarithmic function compensates non-linear dependence of MIP binding capacity from phenanthrene concentration.

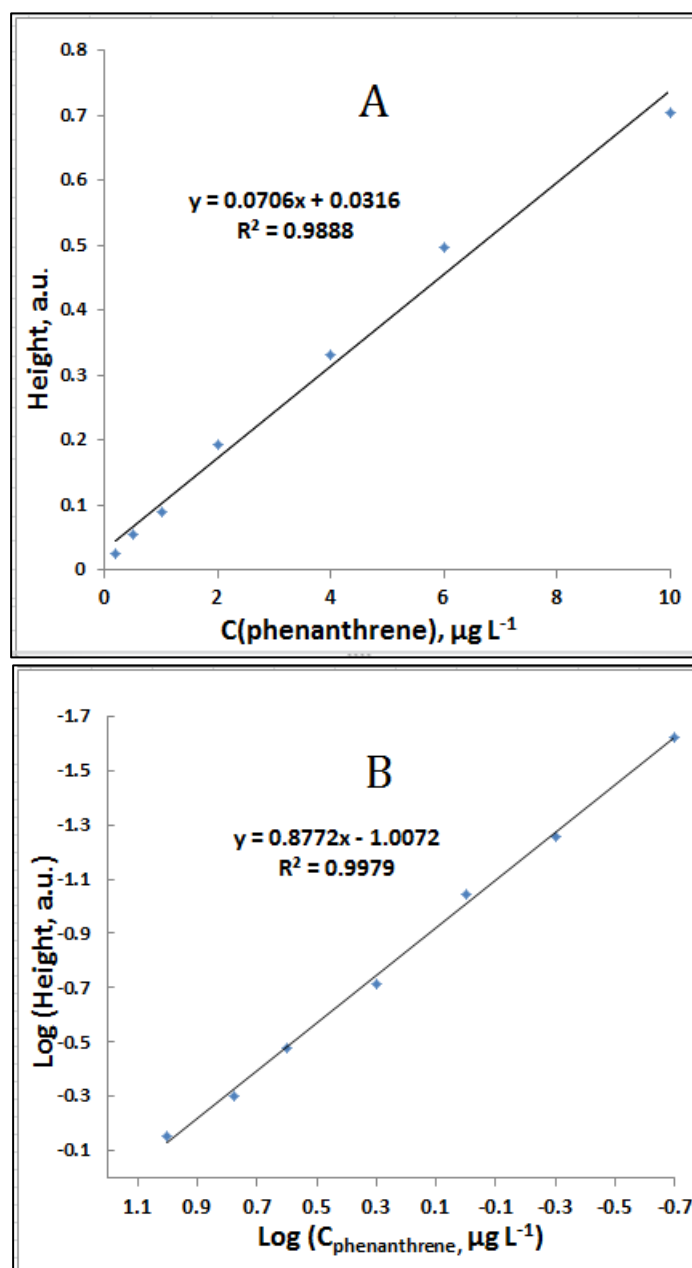


Figure 8-5. Function of fluorescence intensity (A) from phenanthrene concentration in solutions for loading MIP films and Log-Log plot of this function (B). Fluorescence was detected in synchronous scanning mode ($\Delta\lambda=69$ nm).

The spectral features of phenanthrene, based upon which phenanthrene can be unambiguously identified, can be clearly observed at $0.200 \mu\text{g L}^{-1}$. Therefore, the LoD of phenanthrene for the current experimental conditions can be considered to be better than $0.200 \mu\text{g L}^{-1}$. The LoD achieved by this measurement scheme can be compared to the LoD by complex analytical procedures, for example, $0.64 \mu\text{g L}^{-1}$ of phenanthrene can be determined by solvent extraction with HPLC/fluorescence detection [10].

The precision of the measurement of fluorescence is presented as the coefficient of variance (S_r , %) and the average relative percentage difference (RPD) between duplicates. The latter is a quick and convenient estimate of the repeatability of the measurements (Table 8-1); the observed RPD is mostly less than 5%. The merit of this repeatability can be considered as relatively good, taking into account that trace concentrations of the PAHs were detected. The high precision of the measurements can be explained by the overall simplicity of the procedure, which includes only two steps: the adsorption and measurement.

Table 8-1. Estimation of fluorimetric quantitative detection of PAHs on MIP films in the synchronous scanning mode.

Parameter	Merit
R ² for the function of fluorescence intensity vs concentration	0.9888
R ² for log-log plot of the function	0.9979
Limit of Detection (LoD) (visual comparison)	<0.2 µg L ⁻¹
Limit of Quantitation (LoQ) (Equation 8.1)	2.3 µg L ⁻¹
Precision (S _r , %, f=10; RPD, %, n=5, Equations 8.2 – 8.4) for:	
naphthalene	2.9, 3.4
fluorene	2.8, 3.6
phenanthrene	4.8, 4.2
anthracene	4.3, 3.6

Note: the precision of the measurements was assessed for the MIP films loaded with the mixture of PAHs as for Figure 8-4: naphthalene – 60.0 µg L⁻¹, fluorene – 8.00 µg L⁻¹, phenanthrene – 4.00 µg L⁻¹, and anthracene – 4.00 µg L⁻¹.

It can be seen that peak heights for PAHs in the mixture are only slightly lower than the heights for same peaks when PAHs were loaded individually, except naphthalene (Figure 8-4 A). In the case of naphthalene, its peak (335 nm) is slightly higher because it overlaps with the peak of fluorene that was also present in the mixture. The fact that the presence of other PAHs did not dramatically affect the individual fluorescence of each PAH shows that the adsorption of the PAHs on the MIP film may not be competitive at

these concentrations. This observation holds promise for the simplification of the methods for quantitative analysis of the mixtures of light PAHs. Under any circumstances, the moderate effect of PAHs on each other's analytical signal can be compensated for with the method of standard addition or multivariate calibration.

8.4 Conclusions

The developed approach of the direct fluorimetric detection of light PAHs on MIP films has a potential to be applied for the rapid analysis of natural waters and development of systems for on-line and remote sensing of PAHs. The detection scheme is simple, consisting of only two steps: loading of PAHs on MIP films and the direct measurement of fluorescence, using widely available and inexpensive equipment. The detection is characterized with low LoD in the sub $\mu\text{g L}^{-1}$ range as estimated for phenanthrene and with satisfactory precision of the fluorescence measurements ($S_r < 5\%$). The fluorescence of different PAHs was superimposed when the measurements were completed in the emission measurement mode, whereas the identification of the PAHs in their mixture was completed in the synchronous scanning mode by the selection of specific spacings for each PAH. The exploitation of the resolving power of the synchronous scanning measurement mode gives good grounds for the effective analysis of the mixtures of PAHs.

8.5 References

1. Report 1.20/324. *Aromatics in produced water - occurrence, fate and effects, and treatment*; International Oil and Gas Producers Association: London, UK, 2002; p 30.
2. Lieberzeit, P. A.; Halikias, K.; Afzal, A.; Dickert, F. L., Polymers imprinted with PAH mixtures—comparing fluorescence and QCM sensors. *Analytical and Bioanalytical Chemistry* **2008**, 392 (7-8), 1405-10.
3. Dickert, F. L.; Tortschanoff, M.; Bulst, W. E.; Fischerauer, G., Molecularly imprinted sensor layers for the detection of polycyclic aromatic hydrocarbons in water. *Analytical Chemistry* **1999**, 71 (20), 4559-4563.
4. Chen, Y. C.; Brazier, J. J.; Yan, M.; Bargo, P. R.; Prahl, S. A., Fluorescence-based optical sensor design for molecularly imprinted polymers. *Sensors and Actuators B: Chemical* **2004**, 102 (1), 107-116.
5. Patra, D.; Mishra, A. K., Recent developments in multi-component synchronous fluorescence scan analysis. *Trends in Analytical Chemistry* **2002**, 21 (12), 787-798.
6. Wehry, E. L., Molecular fluorescence, phosphorescence, and chemiluminescence spectrometry. *Analytical Chemistry* **1986**, 58 (5), 13R-33R.
7. Shrivastava, A.; Gupta, V., Methods for the determination of limit of detection and limit of quantitation of the analytical methods. *Chronicles of Young Scientists* **2011**, 2 (1), 21.
8. Synek, V., Evaluation of the standard deviation from duplicate results. *Accreditation and Quality Assurance* **2008**, 13 (6), 335-337.
9. Andrade Eiroa, A.; Vazquez Blanco, E.; Lopez Mahia, P.; Muniategui Lorenzo, S.; Prada Rodriguez, D., Simultaneous determination of 11 polycyclic aromatic hydrocarbons (PAHs) by second-derivative synchronous spectrofluorimetry considering the possibility of quenching by some PAHs in the mixture. *The Analyst* **1998**, 123 (10), 2113-2117.
10. Method 8310. Polynuclear Aromatic Hydrocarbons. US Environmental Protection Agency. 1986; pp 13.

Chapter 9. Conclusions and Future Work

The research achievements of this research project can be grouped in three main categories. The first one unites the procedures to fabricate MIP films along with the characterization of the fabrication process (Chapter 2) and morphology of the MIP films (Chapters 4). The synthesis of various MIPs and study of their binding properties constitute the second category (Chapters 4 and 5). The third group of results relates to the development of direct detection of phenol and PAHs using various analytical techniques (Chapters 6 – 8). In order to develop an effective MIP film and to use it for direct detection, it was crucial to have optimized all stages of the development process: the choice of MIP components, the fabrication of MIP films, methodology to study MIP properties, and the application of an analytical technique for direct detection. This complex concurrence was challenging to achieve, and the various kinds of incompatibilities were encountered. For example, not all components that benefit binding of phenol could be easily used for the fabrication of MIP films, e.g., styrene and divinylbenzene (Chapter 2). Films had to be fabricated to be uniform, porous, and mechanically stable; otherwise, the repeatability of the binding studies would be seriously affected. Despite the fact that a MIP film had good binding and morphological properties, the MIP chemical composition could cause an intense background when a spectral analytical technique was hyphenated with the MIP film (Chapter 6). Thus, in order to find a compromise between the steps of the development process and to achieve these project goals, a large diversity of MIP compositions and experimental methods were used.

To be incorporated into analytical test systems, MIP films have to be fabricated as porous films. The principle of the polymerization between two glass surfaces, or

sandwiching, was put into the development of procedures to fabricate various MIP films to suit different applications (Chapters 4 and 8). The UV-curing of a free-standing layer of prepolymerization mixture produced ~20 μm thick MIP films. A MIP prepared in this format was studied for phenol binding and morphology. Thicker films (100 μm) were fabricated with a porous membrane frame, and used to achieve a higher sensitivity of fluorimetric detection. MIP-divinylbenzene particles were adapted for the fabrication of films by their “gluing” in a polymer network.

The factors influencing the fabrication process were derived (Chapter 2). The morphology, thickness, and porosity of MIP films were studied with scanning electron microscopy and gravimetric analysis (Chapter 4). To fabricate a polymeric film without physical defects, a prepolymerization mixture must be sufficiently viscous and its layer between two planar surfaces must not be restricted at glass sides with solid spacers. The mechanical stability of the films and the extensive surface of MIPs available for the adsorption of phenol are linked to the granular morphology of the films. Such morphology was rendered with the use of “poor” solvents and linear polymers. Alcohol-water mixtures (MeOH/H₂O, PrOH/EG/H₂O, PrOH/EG) were used as these “poor” solvents. Apolar (DMF) and low-polar (CHCl₃) solvents were adapted to form the granular structure by the addition of linear polymers (PEG, PVA), which also helped to adjust the viscosity of the prepolymerization mixtures. The procedures and principles of the fabrication of films described in this project can be employed to prepare MIP films from a wide variety of prepolymerization mixtures and MIP particles. Films can be

fabricated in situ or on any other planar surfaces, e.g., on the substrates of microfluidic and sensing devices.

A large variety of MIP films were systematically studied in order to develop efficient MIPs towards phenol and to formulate principles of their synthesis. MIPs were synthesized through non-covalent imprinting, varying all main MIP components: template, functional monomer, solvent, and cross-linker. Precise procedures to determine the adsorption capacities of MIP films towards phenol were developed (Chapter 4 and Appendix A). The efficacy of MIP binding and imprinting performances were determined based on analysis of a set of adsorption capacities along and adsorption isotherms, and cross-binding of other phenolics and PAHs.

Initially, phenol, as a template, was used for synthesis of MIPs based on functional monomers acting by hydrogen bonding (itaconic acid and 4-vinylpyridine) or hydrophobic interactions (styrene) (Chapter 4). For each functional monomer, a solvent was matched to promote the interaction between phenol and monomers: dimethylformamide for the formation of itaconic acid anion that can bind phenol, CHCl_3 for hydrogen bonding with 4-vinylpyridine, alcohol-water mixtures for hydrophobic interactions with styrene. Based on spectroscopic studies of monomer-phenol interactions (UV absorbance and Raman spectroscopies, Chapter 3) and the fact that low imprinting factors were observed (Chapter 4), the following barriers to achieve a high imprinting effect towards phenol can be concluded. Phenol as the template probably does not imprint highly selective binding sites because it has only single and low acidic hydroxyl group that cannot form a strong prepolymerization complex with the functional monomers

acting by hydrogen bonding. In addition, the selective recognition of phenol by hydrogen bonding is suppressed in water. Binding of phenol by hydrophobic interactions also did not show selectivity, possibly, because phenol is a small molecule with no remarkable shape to form structurally specific binding sites. Nevertheless, both selective and non-selective binding by hydrophobic interactions was compatible with the practically important condition for the adsorption of phenol from water.

Since MIPs for phenols based on hydrophobic interactions had not been studied previously in detail, further work in this area was done in efforts to increase imprinting effects and binding capacities. The first work in this direction was to test cross-linkers in addition to ethylene glycol dimethacrylate, such as triethylene glycol dimethacrylate and pentaerythritol triacrylate (PETA) (Chapter 4). A significant improvement of the imprinting effect was achieved for the MIP based on PETA, whose binding was described by a Freundlich isotherm model, with an imprinting factor that was higher for lower phenol concentrations, 1.16 at 0.5 mg L^{-1} phenol. The better imprinting effect for the PETA-MIP probably can be attributed to the formation of a tighter polymer network with smaller sized binding sites, which can better fit small sized phenol. The second phase of experiments was completed to improve the phenol binding capacity (Chapter 5). The MIP with increased styrene content and xylene, as a template, was synthesized. A film made of a copolymer of divinylbenzene and PETA, as non-imprinted polymer, acting as a simple adsorbent, was also prepared. These two polymeric adsorbents can be recommended for the practical application because they exhibited the highest binding capacities towards phenol. These films had a homogeneous and porous morphology combined with water

compatibility. The fact that these two binding media do not contain a residual phenol, which will eliminate the false positive response of a detector, meets the condition for the application in chemical analysis.

The characteristic feature of any MIP is the imprinting effect, which is determined by the presence of selective binding sites over non-selective ones. A high imprinting effect towards phenol was a MIP property that was being targeted throughout this project. However, the observed imprinting effect for the MIPs appeared to be modest. The limited number of selective binding sites probably will not produce selectivity for phenol binding by these MIPs when phenol is in a mixture with other hydrophobic and aromatic species. Therefore, the overall selectivity of direct detection of phenol will be solely determined by the selectivity of an analytical technique itself, e.g., mass spectrometry. The fact that both selective and non-selective binding was observed not only for phenol, but also for alkylphenols, resorcinol and PAHs, suggests that the MIPs can be used as universal adsorbents towards simple aromatics, e.g, alkylated benzenes. Instead of providing the outstanding binding selectivity, the modest imprinting effect that was achieved can be considered as another tool to increase the binding capacity. For example, addition of xylene into a prepolymerization mixture, similar to the increase in the content of styrene in the polymer network, led to an increase in the phenol binding capacity (Chapter 5).

Another important property of MIPs that was targeted for improvement, the same as imprinting effect, was the overall binding capacity towards phenol. This binding capacity consists of both selective and non-selective components, and it determines the efficiency of MIPs as adsorbents and the sensitivity of direct detection. Unfortunately, because of

the dramatic difference in experimental conditions, it was difficult to compare the binding performances of the MIPs studied in this project (Chapters 4 and 5) with similar characteristics of other adsorbents and MIPs for phenol studied by other scientists. However, some comparison can be done. Testing different MIP/NIP compositions showed that an improvement of adsorption capacity towards phenol was achieved, as compared to the MIP acting by hydrogen bonding. For example, the adsorption capacity of DVB-PETA copolymer (Ads) is higher than that for MIP 1 based on itaconic acid by 1.75 times. Also, the assessed adsorption capacities for MIPs/NIPs in this project can be used for comparison with other binding materials for phenol, which will be developed in the future.

Together with imprinting effect, selectivity, and binding capacity, other practically important aspects of MIPs and their synthesis were taken into consideration during the development process. The MIP/NIP films were prepared to be water-compatible; the quality of fabricated films was good; widely-available and inexpensive reagents were used; and the film fabrication process was economical. The author believes that because of all these useful characteristics, the MIP/NIP films have a considerable potential to be used as adsorbent layers for a wide variety of applications in analytical chemistry. In addition to the film format required for analytical applications, the MIP formulations could be prepared in other physical forms, e.g. beads [1, 2], to be used for industrial separations.

Having time and resources, even more advanced MIPs or adsorbents [3] for phenol could be developed using the methodology and principles derived from this project.

Particularly, it was found that the use of a higher content of styrene and/or more hydrophobic monomers such as divinylbenzene and ethylvinylbenzene enriches the binding capacity. The imprinting effect benefited from a tighter polymer network formed by PETA and the use of a more hydrophobic template, such as xylene, compared to phenol. In addition, PETA made another significant contribution to the quality of films; the hydrophilic nature of PETA compensated the water repelling effect from styrene or divinylbenzene moieties, keeping the polymer water compatible. The use of mixtures of highly polar alcohols as solvents, e.g., 1-propanol and ethylene glycol, has a positive dual role. Protic nature of these solvents promotes the formation of a prepolymerization complex by hydrophobic interactions. At the same time, such solvents render the porosity to the films. One possible effort to develop a more effective MIP for phenol is to imprint the divinylbenzene-PETA co-polymer (Chapter 5) with xylene, varying the ratio of components for this new MIP to optimize binding and imprinting properties. The experimental methodology developed in this thesis can be employed for development of MIPs towards other simply shaped aromatic compounds without distinctive functionalities, which are also of environmental concern as phenol, for example, light PAHs, alkylated benzenes (BTEX), and chlorobenzenes [4].

Many analytical techniques using a variety of measurement conditions (Chapters 6-8 and Appendix D) were attempted for application in the direct detection of phenol adsorbed on a MIP film, aiming to benefit from preconcentration of phenol and to avoid the extraction with solvent. However, the direct detection appeared to be problematic because of the low intensity of the analytical signal or its absence (fluorimetry, MALDI-

MS, RRS), complications associated with the derivatization reactions, and the obstructive effect from the MIP matrix (SERS and fluorimetry).

For SERS detection, the suspension of silver nanoparticles was deposited on the MIP film after phenol adsorption (Chapter 6). Nanoparticles of different types and post-treatments along with various measurement conditions, including the laser wavelength, were tested for their ability to produce SERS. However, the severe interference from the MIP matrix made the detection impossible. To overcome the interference, another laser wavelength or even a polymer of different composition should be applied. The studies about the applicability of SERS detection to different analytes showed that, compared to phenol, much more intense SERS was produced from dibenzothiophene, which can bind to the silver surface. Therefore, if SERS detection on MIP films is to be developed further, a change of targets to thiophenes would be reasonable. More intensive SERS was measured for dibenzothiophene compared to phenol. Similar to phenols, thiophenes are also of the interest of Bottaro group because they constitute a fraction of water pollutants from produced water and oil extraction.

Taking into account that little success was achieved with optical spectroscopic techniques for the detection of phenol, probably, the only analytical techniques applicable for this purpose are atmospheric pressure ionization-mass spectrometry. Particularly, DESI-MS and DAPCI-MS should be able to ionize phenol, and these techniques are well compatible with film format [5]. The preliminary experiments with ESI of phenol (Appendix C) demonstrated that phenol gave the intense phenolate ion peak under the

action of alkaline reagents such as ammonia and TMAH. ESI of phenol suggests the possibility of DESI detection with a basic spray solvent.

The approach to measure fluorescence directly from MIP films, initially employed for phenol, was applied and developed for the detection of light PAHs. Two and three ring PAHs, altogether with thiophenes, phenol and alkylphenols are major water pollutants from produced water and oil extraction, and they are all targeted by Bottaro group. Fluorimetric detection suffered from problems intrinsic both to general fluorimetry and solid-phase fluorimetry: inner-filter effects, the emission background from a MIP matrix, and the high level of stray-light due to light scattering with opaque films. The effect of these problems was reduced by selection of measurement conditions connected with film format altogether with the type and parameters of fluorescence measurements. The combination of the front-face illumination geometry, 100 μm thick films as samples, and synchronous scanning made it possible to achieve a compromise between a high detection sensitivity, the reduction of self-absorption, and the stray-light background. The suggested design for fluorimetric detection of light PAHs demonstrated linear response and good repeatability of the measurements along with the ability to differentiate PAHs in a mixture, exemplified with naphthalene, fluorene, phenanthrene, and anthracene. The author believes that this design can be used as a platform for the development of quantitative procedures for analysis of light PAHs in real water samples and for construction of sensors for on-line monitoring of light PAHs in natural waters [6, 7].

References

1. Shen, X.; Xu, C.; Ye, L., Molecularly imprinted polymers for clean water: analysis and purification. *Industrial & Engineering Chemistry Research* **2013**, *52* (39), 13890-99.
2. Murray, A.; Ormeci, B., Application of molecularly imprinted and non-imprinted polymers for removal of emerging contaminants in water and wastewater treatment: a review. *Environmental Science and Pollution Research International* **2012**, *19* (9), 3820-30.
3. Lin, S. H.; Juang, R. S., Adsorption of phenol and its derivatives from water using synthetic resins and low-cost natural adsorbents: a review. *Journal of Environmental Management* **2009**, *90* (3), 1336-49.
4. Chapter 1. Potential pollutants, their sources and their impacts. Food and Agriculture Organization of the United Nations.
<http://www.fao.org/docrep/x5624e/x5624e04.htm#1.8.6%20benzenes>
(accessed 09.05.2014).
5. Van Biesen, G.; Wiseman, J. M.; Li, J.; Bottaro, C. S., Desorption electrospray ionization-mass spectrometry for the detection of analytes extracted by thin-film molecularly imprinted polymers. *The Analyst* **2010**, *135* (9), 2237-40.
6. Ko, E.-J.; Kwak, J.; Kim, J.-Y.; Park, K.; Hamm, S. Y.; Kim, K. W., Application of laser based spectroscopic monitoring into soil remediation process of PAH-contaminated soil. *Geosystem Engineering* **2011**, *14* (1), 15-22.
7. Locke, J. Protecting our oceans, one polymer at a time. Faculty of Engineering and Applied Science. <http://www.engr.mun.ca/news.php?id=1226> (accessed 05.09.2014).

Appendix A

Procedures to Determine Adsorption Capacities of MIPs to bind Phenol

In this project, MIP binding properties were estimated as part of the study of adsorption of phenol from water by a MIP, which yields the simplest and independent characteristic of the MIP binding—adsorption or binding capacity. The set of adsorption capacities at different concentrations can be used to construct MIP binding isotherms [1]. In this project, procedures to determine MIP binding capacities were adapted based on the “extraction” and “by difference” approaches [2, 3]. Procedures take into account the specificity related to the film format of the MIP and the volatility of phenol and simple alkylphenols. High precision of the measurements is needed to study a weak imprinting effect, which is generally attributed to the MIPs for phenols. The applicability and limitations of the procedures are discussed.

A.1 Procedures to determine MIP adsorption capacities

Phenol (99%), 4-methylphenol (99%), 2,4-dimethylphenol (98%) were purchased from Sigma-Aldrich (Oakville, ON, Canada). Methanol, acetonitrile, acetic acid, aqueous ammonium hydroxide (28-30%) were of ACS reagent grade and were purchased from ACP Chemicals (Montreal, QC, Canada).

A.1.1. Extraction of phenols with methanol:ammonia for HPLC-UV analysis

First, phenol was loaded on a MIP film by stirring 100 mL of their aqueous solution with a magnetic stirring bar over the MIP film/slide in a 250 mL beaker. Next, the slide/MIP film with the loaded phenol was placed in a 50 mL beaker filled with 10.0 mL of methanol:ammonium hydroxide solution (25:1, v/v) and sealed with Parafilm wrap. The solvent was stirred with a magnetic microbar (5 mm) for 3 h. The extract of the phenol was evaporated under a nitrogen stream in a 100 mL-tube with a narrow sprout at the bottom until 0.5 mL of the extract remained. Next, the sample for HPLC analysis was made by reconstitution of the extract with water in a 2.00 mL volumetric flask and the solution was filtrated with nylon syringe filters (0.2 μm , 25 mm) from Canadian Life Science (Montreal, QC, Canada) before HPLC analysis. The quantitation of phenol in the extract was completed with HPLC-UV (Chapter 4)

A.1.2 Extraction of phenols with methanol:ammonia:water for HPLC-UV analysis

Phenol and alkylphenols were loaded on a MIP/film using the same procedure as in the previous section. The extraction solvent was prepared in the following way: 1.00 mL of ammonium hydroxide solution and 20.00 mL of methanol were diluted with water in a 50.00 mL-volumetric flask. A slide/MIP film with loaded phenol was covered with 2.50 mL of the prepared solvent in a 50 mL-beaker. The beaker was sealed with Parafilm wrap, and the solvent was stirred with a magnetic microbar (5 mm) for 3 h to extract phenols. After the extraction step, 36.0 μL of acetic acid was pipetted into the extract to neutralize the solution. The neutralization was controlled with pH universal indicator paper (Hydrion® Brilliant) for a small portion of the solution. The neutral solutions were

filtrated with nylon syringe filters (0.2 μm , 25 mm) from Canadian Life Science (Montreal, QC, Canada) for the HPLC-UV analysis (Chapter 4).

A.1.3 Extraction of phenols with acetonitrile:acetic acid for UV-absorbance spectrometry

To complete the adsorption of phenol on a MIP film, a slide/MIP film was placed in a 250 mL-beaker filled with 100 mL of a phenol solution. The beaker was sealed with Parafilm wrap and placed in an Innova 4230 Incubator Shaker (New Brunswick Scientific, Enfield, USA) and shaken at 150 rpm (rotations per minute) at 20.0 $^{\circ}\text{C}$ for 4 h 30 min. The incubator-shaker can provide more reproducible adsorption conditions, e.g., the temperature and stirring rate, rather than a hot plate with magnetic stirring as in the previous section. After the adsorption step, drops of the phenol solution were gently wiped from the film surface and the MIP film/glass slide was immersed in 10.00 mL of acetonitrile/acetic acid mixture (99:1, v/v) [4] in a beaker. The beaker was sealed with Parafilm wrap and the extraction solvent was magnetically stirred for 3 h. The absorbance of phenol in the final extract was measured at 272 nm with a Thermo Scientific Evolution 600 UV-Vis Spectrophotometer (Thermo Scientific, Ottawa, ON, Canada) against the extraction solvent in the reference cuvette to calculate a concentration of phenol in the extract (C , mg L^{-1}). Taking into account the volume of the extract (V , 0.01000 L), the binding capacity (Q , mg g^{-1}) was calculated as:

$$Q = \frac{V \cdot C}{m(\text{MIP})} \quad (\text{A-1})$$

A.2 Discussion of procedures to determine MIP adsorption capacities

A.2.1 The determination of adsorption capacities based on extraction step coupled with HPLC-UV

Initially, some serious incompatibilities were encountered when phenols were extracted from MIP films for chromatographic analysis (LC or GC). The phenol and simple alkylphenols (cresols, xylenols, and 2,4,6-trimethylphenol) can be extracted from the MIP network only into an organic solvent of a high elution strength, e.g., acetonitrile or methanol with the addition of ammonia or acetic acid [4-6]. The purpose of the additives, acetic acid and ammonia, is to disrupt hydrogen bonding between phenols and a MIP matrix. These solvent systems, as matrices of samples for HPLC, have an elution strength higher than the mobile phases, e.g., acetonitrile/water (1:1), which seriously affected the separation. Also, these protic solvents interfere with the derivatization with N,O-bis(trimethylsilyl) trifluoroacetamide for GC-MS analysis [7]. The presence of acetic acid and ammonia in the final extract greatly distorted the baseline of HPLC chromatograms with C18/SiO₂ packed columns.

A common way to eliminate a solvent effect is the following: evaporation of the solvent and dissolution of the dry substrate in another suitable solvent [3]. In relation to phenol and simple alkylphenols, this method cannot be applied because a significant loss of phenols was observed due to their volatility. Therefore, it was decided to extract phenols from MIPs with a methanol:ammonia solution. Then, a large portion of methanol together with ammonia were evaporated by purging the extract with nitrogen, leaving an aliquot of phenols solution in methanol that was free of ammonia (neutral by indicator paper). Next, the aliquot was diluted with water to make a sample for HPLC.

An extraction procedure without the evaporation step was also tested. Phenols were extracted from MIP films with an ammonia solution in methanol:water. A volume of this solvent (2.50 mL) was set to cover the slide/film in the beaker. After the extraction, the solvent was simply neutralized with an aliquot of acetic acid and directly used for HPLC analysis; thus, the evaporation step could be avoided.

These two extraction procedures work well and can be used for the analysis of phenols based on solid-phase extraction. However, the uncertainty by these procedures was still too high (10 – 30% as S_r) to be used to probe the differences in MIP (NIP) adsorption capacities of ~5%, which were common in this research project. The accuracy and precision of the extraction procedures are limited by the following factors: incomplete extraction of phenols; losses of phenols at the evaporation step; and baseline fluctuations in HPLC chromatograms when a sample contains organic solvents and ammonia/ammonium and/or acetic acid/acetate.

These two extraction procedures were applied to estimate an imprinting factor for many other MIP films of different composition listed in Table A1, but not studied in details as has been given in Chapter 4. Although the uncertainty of these measurements was relatively high for the accurate measurements of the imprinting effect, it was possible to conclude that the imprinting effect of the MIP formulations studied was either very modest or absent. This conclusion conforms to discussions on the effect of monomer-phenol interactions on the MIPs imprinting effect towards phenol (Chapter 4).

Table A-1. Compositions of prepolymerization mixtures for MIP films studied for imprinting effect

1(TMP):4(4-VP):20(EGDMA)/acetonitrile
 1(TMP):4(4-VP):20(EGDMA)/CHCl₃
 1(TMP):4(4-VP):30(EGDMA)/acetonitrile
 1(TMP):4(4-VP):20(EGDMA)/MeOH:H₂O (4:1)
 1(TMP):6(4-VP):6(EGDMA)/MeOH:H₂O (4:1)
 1(phenol):4(4-VP):20(EGDMA)/6% PVA in DMSO
 1(TMP):4(MAA):20(EGDMA)/MeOH:H₂O (4:1)
 1(phenol):2(IA):20(EGDMA)/MeOH:H₂O (4:1)
 1(phenol):4(IA):20(EGDMA)/MeOH:H₂O (4:1)
 2(phenol):4(IA):20(EGDMA)/20% (w/w) PEG in MeOH:H₂O (4:1)
 2(phenol):4(IA):20(EGDMA)/10% (w/w) PVA in diglyme
 2(phenol):4(IA):20(EGDMA)/10% (w/w) PVA in DMF
 2(resorcinol):4(IA):20(EGDMA)/15% (w/w) PEG in DMF
 2(phenol):4(Sty):20(EGDMA)/6% PVA (w/w) in DMSO
 1(phenol):2(IA):2(Sty):20(EGDMA)/MeOH:H₂O (4:1)

Note 1: The MIP (NIP) films were prepared by the sandwich technique (Chapter 4) and were studied in terms of an imprinting factor at rebinding phenol, cresol, and xylene. The ratio of a template to monomer and cross-linker is presented in moles. The ratio of DMPA (initiator):EGDMA (cross-linker): a solvent was 15.0mg:740μL:1000μL, respectively.

Note 2: TMP – 2,4,6-trimethylphenol; DMPA – 2,2-dimethoxy-2-phenylacetophenone; EGDMA – ethyleneglycol dimethacrylate; Sty – styrene; IA – itaconic acid; 4-VP – 4-vinylpyridine; MAA – methacrylic acid; DMF – dimethylformamide; DMSO – dimethyl sulfoxide; PEG – polyethylene glycol; PVA – polyvinyl acetate.

A.2.2 The determination of adsorption capacities based on extraction step coupled with UV-absorbance spectrometry

To avoid some of the aforementioned experimental drawbacks of the common extraction procedures, the extraction of phenol from MIPs/NIPs with acetonitrile:acetic acid (1%, v/v) was carried out, and UV-absorbance spectrometry was used for the

quantification of phenol in the extract were applied. Acetonitrile:acetic acid (1%, v/v) exhibited high extraction efficiency for phenols when they were desorbed from a MIP [4]. The advantage of UV-absorbance spectrometry is that it is robust and is not affected by the solvent composition of a sample such as the LC and GC methods. Thus, it was possible to achieve the quantitative extraction of phenol from a MIP matrix and to skip the extract evaporation step. However, this procedure suits only MIP films with a high loading of phenol. Binding capacities obtained for phenol solutions over 300 mg L^{-1} were high enough to make a phenol absorbance value for the extract lying in the optimal range (0.4 – 1.5). Much lower concentrations can be targeted screening the E2 band at 220 nm, which is about 3 times more intense than B band at 270 nm. The disadvantage of UV-absorbance spectrometry is that only a single phenolic can be probed because the UV absorbance spectra of phenol and the alkylphenols are not significantly different.

This procedure was applied to study the binding behavior of MIPs (NIPs) 1–5 (Chapter 4) in the flattening region of the phenol binding isotherms, which was observed at high phenol concentrations, over 200 mg L^{-1} (Table A-2). These experiments were used to build the MIP (NIP) adsorption isotherms over the wide range of phenol concentrations up to 2000 mg L^{-1} . Also, the imprinting factors in this concentration region, over 1000 mg L^{-1} , were compared with the imprinting factors between 100 and 300 mg L^{-1} for the same MIPs (Figure 4-3 and Table 4-4). It can be seen that for all five MIPs the imprinting factors towards phenol are about the same. Therefore, it is possible to expect that over 100 mg L^{-1} up to the saturation of the binding capacities at $1000 - 2000 \text{ mg L}^{-1}$ the imprinting behavior follows the same pattern.

Table A-2. The determination of binding capacities of MIPs (NIPs) 1–5 (Chapter 4) at the high phenol concentrations with procedure based on extraction and UV-absorbance spectrometry

C(phenol), mg L⁻¹	1000	1500	2000
MIP 1 – ph-l:IA:EGDMA			
Q(NIP), mg g ⁻¹	N.A.	N.A.	74.5
Q(MIP), mg g ⁻¹	N.A.	N.A.	73.5
IF	N.A.	N.A.	0.99
MIP 2 – ph-l:VP:EGDMA			
Q(NIP), mg g ⁻¹	N.A.	102.4	N.A.
Q(MIP), mg g ⁻¹	N.A.	103.3	N.A.
IF	N.A.	1.01	N.A.
MIP 3 – ph-l:Sty:EGDMA			
Q(NIP), mg g ⁻¹	51.1	N.A.	76.4
Q(MIP), mg g ⁻¹	52.8	N.A.	79.3
IF	1.03	N.A.	1.04
MIP 4 – ph-l:Sty:TEGDMA			
Q(NIP), mg g ⁻¹	N.A.	76.6	N.A.
Q(MIP), mg g ⁻¹	N.A.	81.2	N.A.
IF	N.A.	1.06	N.A.
MIP 5 – ph-l:Sty:PETA			
Q(NIP), mg g ⁻¹	48.1	54.8	61.6
Q(MIP), mg g ⁻¹	52.3	62.4	68.2
IF	1.09	1.14	1.11

Note: the average difference between two parallel measurements of binding capacities is 2.0%.

A.2.3 The determination of adsorption capacities based on “by difference” approach

The main reason for determining the amount of MIP bound phenol indirectly by measuring the phenol concentration before and after adsorption is to avoid the extraction step and the associated steps such as evaporation, neutralization, and dilution. By doing so, the analysis is less laborious and more accurate because many common sources of

error are eliminated: incomplete extraction of phenols and loss of phenols during the treatment of extract. Also, this method is highly compatible with reversed phase HPLC because phenol concentration is quantified in pure aqueous solutions, which is a favorable circumstance for peak shape, baseline, and repeatability of retention times and peak areas. Therefore, this method was considered to be the main in the study of MIP adsorption in this project, particularly, in Chapters 4 and 5. The precision of the indirect procedure appears to be very satisfactory. The difference between two parallel measurements was often less than 3.0 %. To achieve this precision it is important to have sufficient difference between the initial and final phenol concentrations (20 – 80%), which can be adjusted using the ratio of the volume of a phenolic solution to the mass of MIP film, e.g., 0.714 mL mg⁻¹. The difference drops, e.g. to 10 %, when working with relatively hydrophilic species such as resorcinol, or at the high adsorbate concentrations such as 200 – 300 mg L⁻¹ of phenol. In the latter, it is more appropriate to use the extraction procedure. There are two other important factors that appeared to be crucial for the quality of the measurements when working with polymer films. One is that it is necessary is to have a completely uniform MIP film, which can be achieved by careful trimming of the damaged spots; the second is to adjust the volume of adsorbate solution according to the mass of the film keeping the ratio strictly constant.

A.3 Summary

MIP adsorption and imprinting properties were studied on the basis of MIP (NIP) binding capacities determined at the rebinding of phenol and simple alkylphenols from their aqueous solutions. In order to determine these binding capacities, procedures were developed based on the “extraction” and “by difference” approaches with the HPLC and UV-absorbance quantification methods. The extraction was attempted with an organic solvent (methanol, acetonitrile, methanol:water) with the additives of ammonia or acetic acid. The extraction steps have the following specific features: incomplete drying of the extract due to the volatility of phenols and the elimination of the presence of free ammonia in the final sample by either blowing off ammonia out with the stream of nitrogen or by neutralization. However, the extraction procedures suffered from incomplete extraction of phenols, losses at the evaporation step, and fluctuations of the baseline during HPLC runs. Although these drawbacks limit the applicability of the extraction procedures for the precise and reliable assessment of the phenol binding capacities, the extraction procedures, coupled with HPLC, can be used for the analytical solid-phase extraction with the MIP films.

Based on the “by difference” approach, a more specialized procedure was developed to study the binding properties of the MIP films. It has the advantage that it contains only two steps: phenol loading on a MIP film from aqueous solution and quantification of phenol with reversed phase HPLC, which is well compatible with pure aqueous solutions. To ensure the precision of the measurements, it is important to have a homogeneous high quality film, to normalize the bound amount of adsorbate to the mass

of the polymer, and to precisely adjust the volume of the solution for the uptake according to the film mass. This “by difference” procedure works well for relatively low and moderate concentrations of adsorbate, e.g., phenol, when the drop of the concentration is enough significant. To extend the range of the studied concentrations up to the saturation region of the binding isotherms, which is observed at high adsorbate concentrations, extraction with acetonitrile:acetic acid coupled with UV-absorbance spectrometry can be used. Compared to HPLC separations, UV-absorbance spectrometry is able to be coupled with solvents of high elution strength. However, UV-absorbance spectrometry cannot be used for the simultaneous quantification of a group of phenolics.

A.4 References

1. Toth, B.; Pap, T.; Horvath, V.; Horvai, G., Which molecularly imprinted polymer is better? *Analytica Chimica Acta* **2007**, *591* (1), 17-21.
2. Volesky, B., Equilibrium (bio-)Sorption. In *Sorption and Biosorption*, BV-Sorbex, Inc.; Montreal, Canada, 2004; pp 103-116.
3. Van Biesen, G.; Wiseman, J. M.; Li, J.; Bottaro, C. S., Desorption electrospray ionization-mass spectrometry for the detection of analytes extracted by thin-film molecularly imprinted polymers. *The Analyst* **2010**, *135* (9), 2237-40.
4. Feng, Q.; Zhao, L.; Lin, J. M., Molecularly imprinted polymer as micro-solid phase extraction combined with high performance liquid chromatography to determine phenolic compounds in environmental water samples. *Analytica Chimica Acta* **2009**, *650* (1), 70-6.
5. Qi, P.; Wang, J.; Jin, J.; Su, F.; Chen, J., 2,4-Dimethylphenol imprinted polymers as a solid-phase extraction sorbent for class-selective extraction of phenolic compounds from environmental water. *Talanta* **2010**, *81* (4-5), 1630-5.
6. Feng, Q. Z.; Zhao, L. X.; Yan, W.; Lin, J. M.; Zheng, Z. X., Molecularly imprinted solid-phase extraction combined with high performance liquid chromatography for

analysis of phenolic compounds from environmental water samples. *Journal of Hazardous Materials* **2009**, 167 (1-3), 282-8.

7. Szyrwińska, K.; Kołodziejczak, A.; Rykowska, I.; Wasiak, W.; Lulek, J., Derivatization and gas chromatography-low-resolution mass spectrometry of Bisphenol A. *Acta Chromatographica* **2007**, (18), 48-58.

Chapter B

Supporting Information for Chapter 4

In this appendix, more information is presented on MIP film morphology (Figure B1), the data for isotherm figures (Tables B1 and B2), fitting experimental isotherms to Langmuir binding model (Figure B2), Freundlich isotherm affinity distribution (Figure B3), and formulas to calculate binding parameters according to Freundlich isotherm binding model.

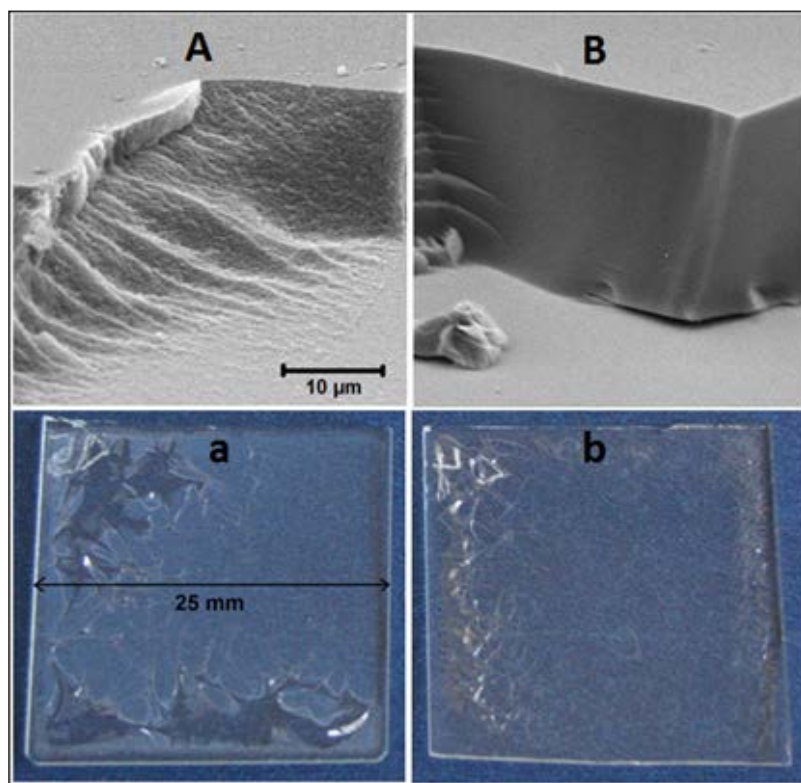


Figure B1. Morphology of MIP films prepared without polyethylene glycol (PEG) and polyvinylacetate (PVA). MIP 1 (no PEG): (A) SEM image, (a) photo; composition of prepolymerization mixture: 2(ph-l):4(IA):20(EGDMA)/pure DMF; MIP 2 (no PVA): (B) SEM image, (b) photo; composition of prepolymerization mixture: 2(ph-l):4(VP):20(EGDMA)/pure CHCl_3 .

Table B1. Data for binding isotherms for Sty-based MIP/NIP on different cross-linkers for Figure 4-3.

$C_i(\text{phenol}), \text{mg}\cdot\text{L}^{-1}$	15	40	100	150	200	250	300
MIP 3 (EGDMA)							
$Q(\text{MIP}), \text{mg}\cdot\text{g}^{-1}$	2.60	6.30	13.0	17.0	21.7	23.7	26.2
$Q(\text{NIP}), \text{mg}\cdot\text{g}^{-1}$	2.60	6.51	13.7	17.3	22.4	24.6	27.2
IF	1.00	1.03	1.05	1.02	1.03	1.04	1.04
MIP 4 (TEGDMA)							
$Q(\text{MIP}), \text{mg}\cdot\text{g}^{-1}$	1.79	4.91	10.1	14.9	18.4	22.3	27.1
$Q(\text{NIP}), \text{mg}\cdot\text{g}^{-1}$	1.72	4.76	9.7	14.2	17.4	21.2	25.6
IF	1.04	1.03	1.04	1.05	1.06	1.05	1.06
MIP 5 (PETA)							
$Q(\text{MIP}), \text{mg}\cdot\text{g}^{-1}$	2.52	5.41	11.5	15.4	18.2	21.9	24.6
$Q(\text{NIP}), \text{mg}\cdot\text{g}^{-1}$	2.31	5.20	10.7	14.2	16.9	19.8	22.1
IF	1.09	1.04	1.07	1.09	1.08	1.11	1.12

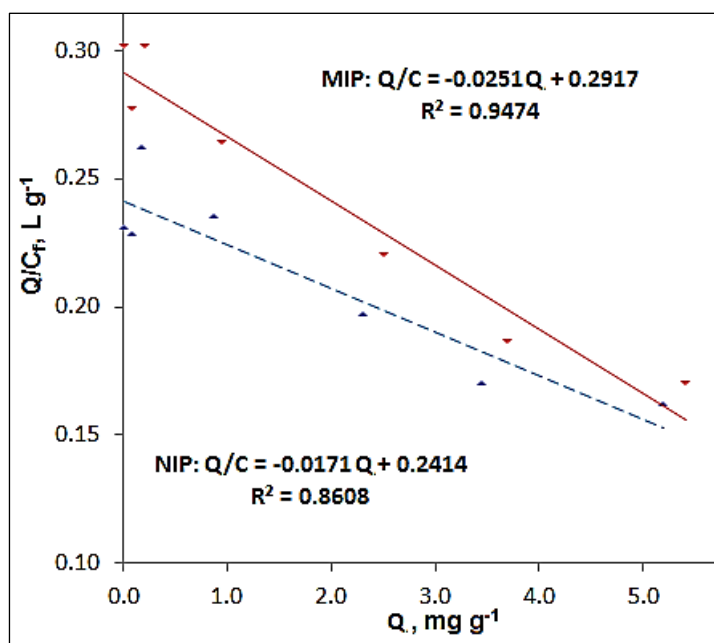


Figure B2. Phenol binding isotherms for MIP 5 and corresponding NIP (PETA) in $Q/C_f - Q$ format and Langmuir binding model fits [1] to them: ( MIP,  NIP). Note: Q – binding capacity, C_f – phenol concentration at adsorption equilibrium.

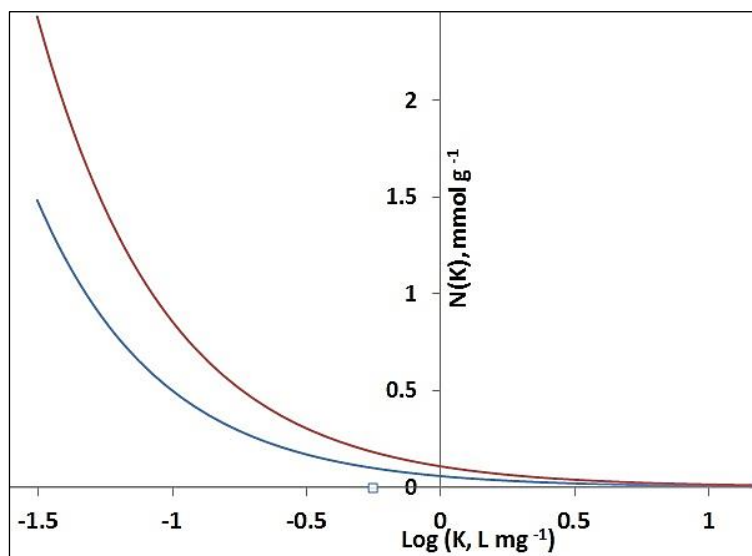


Figure B3. Affinity distributions corresponding to Freundlich Isotherm binding model for MIP 5 on PETA (top curve) and corresponding NIP (bottom curve) calculated based on binding parameters (Formula B3).

Calculation of binding parameters and affinity distribution based on Freundlich isotherm fitting parameters [2].

$$N_{K_1-K_2} = a(1 - m^2)(K_1^{-m} - K_2^{-m}) / M, \text{mmol} \cdot \text{g}^{-1} \quad (\text{B1})$$

$$K_{K_1-K_2} = \left(\frac{m}{m-1} \right) \left(\frac{K_1^{1-m} - K_2^{1-m}}{K_1^{-m} - K_2^{-m}} \right), \text{L} \cdot \text{mg}^{-1} \quad (\text{B2})$$

$$N(K) = [2.303am(1 - m^2)e^{-2.303m \text{Log}K}] / M, \text{mmol} \cdot \text{g}^{-1} \quad (\text{B3})$$

m and a – Freundlich Isotherm fitting parameters; K – affinity constant at phenol concentration (C): $K=I/C$, $\text{L} \cdot \text{mg}^{-1}$; M – phenol molar mass; $N_{K_1-K_2}$ – apparent number of binding sites; $K_{K_1-K_2}$ – apparent weighted average affinity, $N(K)$ – affinity distribution function: a relation between the number of binding sites (N) with a certain affinity constant and this constant value (K).

References

1. Lulinski, P.; Maciejewska, D., Examination of imprinting process with molsidomine as a template. *Molecules* **2009**, *14* (6), 2212-25.
2. Rampey, A. M.; Umpleby, R. J.; Rushton, G. T.; Iseman, J. C.; Shah, R. N.; Shimizu, K. D., Characterization of the imprint effect and the influence of imprinting conditions on affinity, capacity, and heterogeneity in molecularly imprinted polymers using the freundlich isotherm-affinity distribution analysis. *Analytical Chemistry* **2004**, *76* (4), 1123-1133.

Appendix C

Electrospray Ionization of Phenol facilitated with Basic Reagents

Though PAHs and dibenzothione are within the scope of the research interests of the Bottaro group to detect various contaminants from oil, there is a demand to develop the detection technique for phenol and alkylphenols despite the fact that such detection appeared problematic (Chapters 6 and 7). DESI-MS can be a promising tool for phenol detection because phenols can be extracted from a MIP film with solvents based on methanol. In addition, phenols can be ionized in ESI (-) [1-4] and APCI (-) [5-7] conditions. In this appendix, it will be shown which spray solvent in ESI conditions, or possible DESI, can be used to efficiently ionize phenol.

C.1 Experimental

Phenol (99%), 4-methylphenol (99%), 2,4-dimethylphenol (98%), pyrrolidine (Fluka, $\geq 99.5\%$), triethylamine ($\geq 99.5\%$), tetramethylammonia hydroxide (25% by weight in water) were purchased from Sigma-Aldrich (Oakville, ON, Canada). Acetic acid, aqueous ammonium hydroxide (28-30%), methanol were of ACS reagent grade and were purchased from ACP Chemicals (Montreal, QC, Canada).

Solutions tested were 1.00 μM phenol or a mix of phenol, m-cresol, and 2,4-dimethylphenol (1.00 μM each) in methanol with the addition of various agents: acetic acid, pyrrolidine, triethylamine at 5.0 mM level except ammonia hydroxide at 5.0 and 100 mM and tetramethylammonia hydroxide at 0.10, 0.50, 1.0, 5.0 mM. An Agilent 1100

Series LC (Agilent Technologies Canada Inc., Mississauga, ON, Canada) equipped with an electrospray ionization mass detector (ESI-MSD) (1100 series MSD, quadrupole) was operated in the flow injection analysis mode. A 100 μL -plug of the samples was injected into a mobile phase, water:methanol (3:2, v/v), flowing at 0.60 mL min^{-1} . The ESI-MSD was operated with the following parameters: negative mode; capillary current (13 nA) was set in “smart” mode; nebulizer gas (N_2) at 60.0 psi, drying gas (N_2) at 11 L min^{-1} ; drying temperature $350 \text{ }^\circ\text{C}$, the ions scanned from 85 to 130 m/z. The ions of interest were observed with the ion extraction tool at 93.11, 107.14, 121.16 Da for phenolate, methylphenolate, dimethylphenolate ions, respectively.

C.2 The choice of solvent for ESI-MS of phenol

The DESI process uses an electrospray emitter to form the jet of charged droplets, gas phase ions and their clusters. These ionized species impact an analyte deposited on a surface, causing the ionization and desorption of the analyte [8]. Thus, ESI-MS experiments can be used, at first approximation, to study the ionization process in DESI conditions. Phenol and alkylphenols are still very weak electrolytes to be ionized independently in ESI conditions when a neutral or acidic solvent is applied (Figure C-1). This explains why phenols did not produce an intense signal under the ESI conditions [5]. Thus, it is possible to assume that bases should be used to facilitate the deprotonation of phenols. ESI-MS was used to study the effect of the solvent composition on the yield of phenolate ions in order to suggest a spray composition for the DESI analysis. A range of reagents with the potential to ionize phenol was studied (Figure 6). These included typical amines (pyrrolidine, triethylamine), ammonium hydroxide, as a common basic additive

for DESI [3, 9] spray solvents, and the very strong base, tetramethylammonia hydroxide (TMAH).

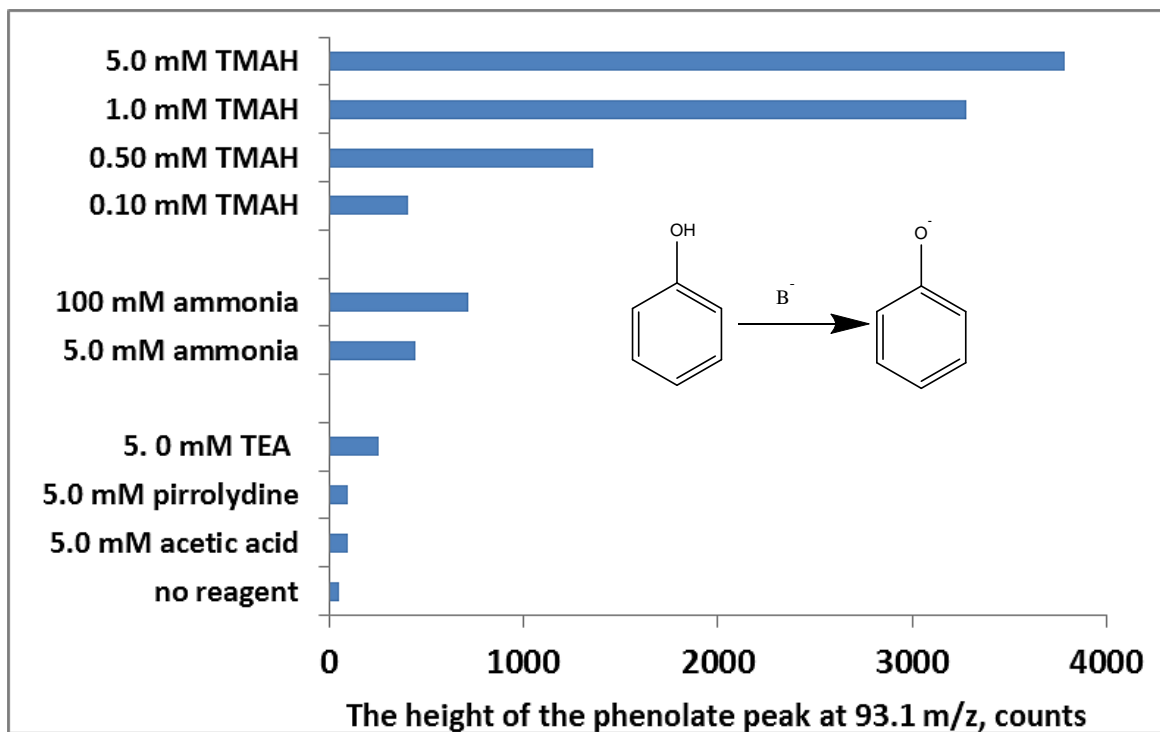


Figure C-1. The effect of different reagents on ionization efficiency of phenol (1.00 μ M) in methanol solution in ESI (-) mode.

Note: TMAH – tetramethylammonium hydroxide; TEA – triethylamine.

TMAH was used to enhance ESI of weakly acidic compounds in a crude oil [2]. It is well known that ions from strong electrolytes can compete for sites on the surface of the charged microdrops and can form a too high abundance of gas phase ions, suppressing the analytical signal from an analyte [2]. Thus, in addition to the nature of the reagents, the effect of their concentrations in the spray solvent was also studied. The comparison of phenolate abundances, produced by different reagents, shows that 1.0 mM TMAH

concentration is the most optimal. Thus, this medium should be considered as a starting spray solvent for DESI-MS of phenol and alkylphenols.

C.3 References

1. Henriksen, T.; Juhler, R. K.; Svensmark, B.; Cech, N. B., The relative influences of acidity and polarity on responsiveness of small organic molecules to analysis with negative ion electrospray ionization mass spectrometry (ESI-MS). *Journal of the American Society for Mass Spectrometry* **2005**, *16* (4), 446-55.
2. Lobodin, V. V.; Juyal, P.; McKenna, A. M.; Rodgers, R. P.; Marshall, A. G., Tetramethylammonium hydroxide as a reagent for complex mixture analysis by negative ion electrospray ionization mass spectrometry. *Anal Chem* **2013**, *85* (16), 7803-8.
3. Shao, B.; Han, H.; Hu, J.; Zhao, J.; Wu, G.; Xue, Y.; Ma, Y.; Zhang, S., Determination of alkylphenol and bisphenol A in beverages using liquid chromatography/electrospray ionization tandem mass spectrometry. *Analytica Chimica Acta* **2005**, *530* (2), 245-252.
4. Jahnke, A.; Gandrass, J.; Ruck, W., Simultaneous determination of alkylphenol ethoxylates and their biotransformation products by liquid chromatography/electrospray ionisation tandem mass spectrometry. *Journal of Chromatography A* **2004**, *1035* (1), 115-122.
5. Martinez Vidal, J. L.; Belmonte Vega, A.; Garrido Frenich, A.; Egea Gonzalez, F. J.; Arrebola Liebanas, F. J., Determination of fifteen priority phenolic compounds in environmental samples from Andalusia (Spain) by liquid chromatography-mass spectrometry. *Analytical and Bioanalytical Chemistry* **2004**, *379* (1), 125-30.
6. Jauregui, O.; Moyano, E.; Galceran, M. T., Liquid chromatography-atmospheric pressure ionization mass spectrometry for the determination of chloro- and nitrophenolic compounds in tap water and sea water. *Journal of Chromatography A* **1997**, *787* (1-2), 79-89.
7. Puig, D.; Silgoner, I.; Grasserbauer, M.; Barceló, D., Part-per-Trillion Level Determination of Priority Methyl-, Nitro-, and Chlorophenols in River Water Samples by Automated On-Line Liquid/Solid Extraction Followed by Liquid Chromatography/Mass

Spectrometry Using Atmospheric Pressure Chemical Ionization and Ion Spray Interfaces. *Analytical Chemistry* **1997**, *69* (14), 2756-2761.

8. Takats, Z.; Wiseman, J. M.; Cooks, R. G., Ambient mass spectrometry using desorption electrospray ionization (DESI): instrumentation, mechanisms and applications in forensics, chemistry, and biology. *Journal of mass spectrometry* **2005**, *40* (10), 1261-75.

9. Kauppila, T. J.; Wiseman, J. M.; Ketola, R. A.; Kotiaho, T.; Cooks, R. G.; Kostiainen, R., Desorption electrospray ionization mass spectrometry for the analysis of pharmaceuticals and metabolites. *Rapid communications in mass spectrometry* **2006**, *20* (3), 387-92.

Appendix D

Attempts for Direct Detection of Phenol on MIP Films using Colorimetry, Resonance Raman Spectroscopy, and Matrix-Assisted Laser Desorption/Ionization-Mass Spectrometry

A technique for the direct detection on a MIP film can be a convenient alternative to traditional procedures involving the extraction step of phenols from a water sample and chromatographic analysis of the extract [1, 2]. In addition, the direct detection can be used to study binding properties of different MIP formulations [3]. Many analytical techniques, using equipment available on the campus, were attempted to be adapted for the direct detection of phenols loaded on a MIP film. The facilities of the MUN Chemistry department made possible the exploitation of colorimetry, Raman and fluorescence spectrometries, and MALDI. Fluorimetry was attempted for the direct detection of phenol (Chapter 7). Fluorimetry is probably the most convenient for on-line detection and the solid-phase version of fluorimetry can be easily adapted for the detection on a MIP film. Phenols appeared to produce a weak fluorescence and the labelling of phenols with a fluorescent tag broke the uniform distribution of the dye on MIP film. Therefore, polycyclic hydrocarbons, which are naturally very strong fluorophores, were attempted to be detected instead of phenols. Another technique which was unsuccessfully applied for the direct detection of phenol was surface-

enhanced Raman spectroscopy (SERS) (Chapter 6). It was attempted to do the SERS detection by the application of silver nanoparticles onto phenol prior loaded on a MIP film. Although it was possible to find the conditions for SERS measurements to avoid the graphitization process and a working SERS substrate, it appeared that an insignificant SERS enhancement was observed for phenol. A much higher enhancement was observed for another contaminant from the oil extraction—dibenzothiophene, which has a sulfur moiety to interact with the silver surface, which suggests that the SERS detection should be designed for the detection of thiophenes. Colorimetry along with Resonance Raman Spectroscopy (RRS) with phenol derivatization, Matrix-Assisted Laser Desorption/Ionization-Mass Spectrometry (MALDI-MS) were also attempted for the phenol detection in this research project but they were not described in the main body of this thesis. In this appendix, these experimental approaches will be described briefly altogether with the problems that made the detection impossible.

D.1 Colorimetry

In this work, phenol loaded on a MIP film was derivatized via the Emerson reaction [3]. The MIP film was sprayed with 2% 4-aminoantipyrine solution in 10% (v/v) aqueous ammonia and 2% $K_3[Fe(CN)_6]$ aqueous solution to form the red dye [3]. It was observed that the dye formed did not spread uniformly on the film, partitioning close to the edges of the MIP film. The non-uniform distribution of the dye hindered the quantitative analysis. This effect was especially pronounced when thin $\sim 20 \mu\text{m}$

films were sprayed. The droplets of the reagent solutions could not be absorbed completely by that thin film. The droplets dried from the edges with the diffusion of the liquid from the droplet to its edges. As a result, the dye naturally partitions to the edges.

D.2 Resonance Raman Spectroscopy

The red dye formed by the Emerson reaction [3] absorbs around 500 nm, or the green light. Thus, it is possible to complete measurements of Raman scattering when the absorption of incident radiation takes place, for example, with the application of a 532 nm-Raman system (Chapter 6). It is a well-known phenomenon that when the Raman scattering occurs at an electronic transition, or at the resonance, the Raman scattering is enhanced by $10^3 - 10^4$ times [4]. As a result, a much higher sensitivity of detection can be achieved. Outstanding selectivity is promised by the high resolution of the Raman spectra, together with the specificity of this derivatization reaction. However, the dye appeared to degrade under the illumination with the green laser even when it was defocused and attenuated. To succeed in this kind of detection it would be useful to test other dyes as phenol derivatives, for example, that one obtained via a diazotization reaction with 4-nitroaniline. In a study of RRS of phenol derivatives [5], the diazo-derivative of phenol appeared to be stable and not to fluoresce under the action of 488 and 514.5 nm lasers when resonance Raman scattering was measured for the aqueous solutions.

D.3 Matrix-Assisted Laser Desorption/Ionization-Mass Spectrometry

For the ionization of phenols loaded on a MIP film, a MALDI matrix solution in acetonitrile was pipetted and dried to form spots on the film of the following reagents: 2,5-dihydroxybenzoic acid, anthracene, 2-aminofluorene, tetramethylammonium hydroxide. However, the phenol ions, particularly from 2,4,6-trimethylphenol, were hidden in an intense ion current from the matrix in both positive and negative modes.

No phenolic ions were observed when 4-vinylpyridine and styrene based MIPs acted as the matrix for the laser desorption in the absence of any reagents. Thus, phenols have to be labelled with a high molar mass and easily ionized tag to follow the reactive MALDI approach [6]. For example, 4-(4,5-diphenyl¹H-imidazol-2-yl)benzoyl chloride [7] can be used, which absorbs the wavelength of the nitrogen MALDI laser (337 nm). However, in this case, the MALDI detection will become very complex and cumbersome due to the derivatization reaction, the effect of a matrix, the very limited applicability for quantitative analysis, and the use of an expensive and not widely available MALDI-MS system. Thus, this approach is not suitable for affordable and rapid chemical analysis of phenols and preference should be given to other techniques.

D.4 Concluding remarks

Taking into account that the detection of phenol with colorimetry, fluorimetry, SERS, resonance Raman spectrometry, MALDI-MS appeared to be problematic, it would be reasonable to use these technique for the detection of other analytes, such as PAHs and thiophenes, which also in the scope of Bottaro group. Fluorimetry should be used for PAHs, and SERS for thiophenes. As far as phenol and alkylphenols are in concern, it would be prospective to use desorption electrospray ionization-mass spectrometry (DESI-MS) because it has been used for the detection on MIP film before [8] and phenol has a potential to be ionized in ESI conditions (Appendix C).

D.4 References

1. Jauregui, O.; Moyano, E.; Galceran, M. T., Liquid chromatography-atmospheric pressure ionization mass spectrometry for the determination of chloro- and nitrophenolic compounds in tap water and sea water. *Journal of Chromatography A* **1997**, 787 (1-2), 79-89.
2. Martinez Vidal, J. L.; Belmonte Vega, A.; Garrido Frenich, A.; Egea Gonzalez, F. J.; Arrebola Liebanas, F. J., Determination of fifteen priority phenolic compounds in environmental samples from Andalusia (Spain) by liquid chromatography-mass spectrometry. *Analytical and Bioanalytical Chemistry* **2004**, 379 (1), 125-30.
3. Sergeyeva, T. A.; Gorbach, L. A.; Slinchenko, O. A.; Goncharova, L. A.; Piletska, O. V.; Brovko, O. O.; Sergeeva, L. M.; Elska, G. V., Towards development of colorimetric test-systems for phenols detection based on computationally-designed molecularly imprinted polymer membranes. *Materials Science and Engineering: C* **2010**, 30 (3), 431-436.

4. Smith, E.; Dent, G., *Modern Raman Spectroscopy – A Practical Approach*. John Wiley & Sons: 2005; p 93-112.
5. Van Haverbeke, L.; Herman, M. A., Determination of three phenolic compounds in water by laser excited resonance Raman spectrometry. *Analytical Chemistry* **1979**, *51* (7), 932-936.
6. Mugo, S. M.; Bottaro, C. S., Rapid on-plate and one-pot derivatization of carbonyl compounds for enhanced detection by reactive matrix LDI-TOF MS using the tailor-made reactive matrix, 4-dimethylamino-6-(4-methoxy-1-naphthyl)-1,3,5-triazine-2-hydrazine (DMNTH). *Journal of Mass Spectrometry* **2007**, *42* (2), 206-17.
7. Nakashima, K.; Kinoshita, S.; Wada, M.; Kuroda, N.; R. G. Baeyens, W., HPLC with fluorescence detection of urinary phenol, cresols and xylenols using 4-(4,5-diphenyl-H-imidazol-2-yl)benzoyl chloride as a fluorescence labeling reagent. *The Analyst* **1998**, *123* (11), 2281-2284.
8. Van Biesen, G.; Wiseman, J. M.; Li, J.; Bottaro, C. S., Desorption electrospray ionization-mass spectrometry for the detection of analytes extracted by thin-film molecularly imprinted polymers. *The Analyst* **2010**, *135* (9), 2237-40.